DESIGN AND ANALYSIS STUDY OF A SPACECRAFT OPTICAL TRANSCEIVER PACKAGE

FINAL REPORT

19 AUGUST, 1985

JPL CONTRACT NO. 957061

S. G. LAMBERT, ET AL

This work was performed for the Jet Propulsion Laboratory, California Institute of Technology, sponsored by the National Aeronautics and Space Administration.

MCDONNELL DOUGLAS ASTRONAUTICS COMPANY-ST. LOUIS DIVISION
Box 516, Saint Louis, Missouri 63166 (314) 232-0232

MCDONNELL DOUGLAS CORPORATION

TABLE OF CONTENTS

TABLE OF CONTENTS

TABLE OF CONTENTS

THIS PAGE INTENTIONALLY LEFT BLANK

ABSTRACT

This study produced a detailed system level design of an Optical Transceiver Package (OPTRANSPAC) for a deep space vehicle whose mission is outer planet exploration. In addition to the terminal design, this study provides estimates of the dynamic environments to be encountered by the transceiver throughout its mission life. Optical communication link analysis, optical thin lens design, electronic functional design and mechanical layout and packaging are employed in the terminal design. Results of the study describe an Optical Transceiver Package capable of communicating to an Earth Orbiting Relay Station at a distance of 10 Astronomical Units (AU) and data rates up to 100 KBPS. The transceiver is also capable of receiving 1 KBPS of command data from the Earth Relay. The physical dimensions of the terminal are contained within a 3.5' x 1.5' x 2.0' envelope and the transceiver weight and power are estimated at 52.2 Kg (115 pounds) and 57 watts, respectively.

THIS PAGE INTENTIONALLY LEFT BLANK

NEW TECHNOLOGY

The design of the OPTRANSPAC has required the development of the following New Technology. The development of the Offset Dichroic Optical Boresight Alignment Device provides for continuous alignment of the transmit and receive paths (refer to Appendix E-1 for details). The Offset Dichroic Optical Boresight Alignment Device was conceived by W. L. Casey and first reported in the monthly review for OPTRANSPAC (JPL Contract #957061) dated 15 February 1985. It was also reported in the OPTRANSPAC Midterm Review on 2-3 April 1985, Pages 41, 47, 48 and 65 and is included in this report on Pages 47, 48, 49, 57, 58, 60, 72, 75, 76, 116, 117, 118, 120, 126, 127, C-31 through C-81, D-5, D-6 and D-7.

THIS PAGE INTENTIONALLY LEFT BLANK

1.0 INTRODUCTION

The objective of this study was to produce a detailed design of an Optical Transceiver Package (OPTRANSPAC) for a deep space vehicle whose mission is outer planet exploration. The optical communication system must be capable of transmitting up to 100KBPS of data to a relay station located in low earth orbit. The transceiver design must provide accurate estimates of the OPTRANSPAC size, weight and power as well as a definition of the overall operational characteristics. Operationally, the OPTRANSPAC must be capable of communicating at the desired data rate from a distance of Saturn and beyond. Figure 1-1 illustrates the operational OPTRANSPAC scenario.

In addition to the terminal design, the study was to provide estimates of the dynamic environments (see Figure 1-2) to be encountered by the transceiver package throughout its mission life.

Results of the study indicate a transceiver design capable of performance meeting the specified requirements. The physical envelope of the OPTRANSPAC is illustrated in Figure 1-3. The transceiver consists of an eleven inch aperture telescope fixed mounted to an optical baseplate. Imaging optics provide relay paths to and from the telescope, laser and detectors. Three separate electronic boxes provide for power regulation, transceiver control and communication functions. The detailed weight and power estimates, outlined in Figure 1-4, indicate a transceiver weight of 115.0 pounds and power consumption of 57 watts.

OPTRANSPAC SCENARIO

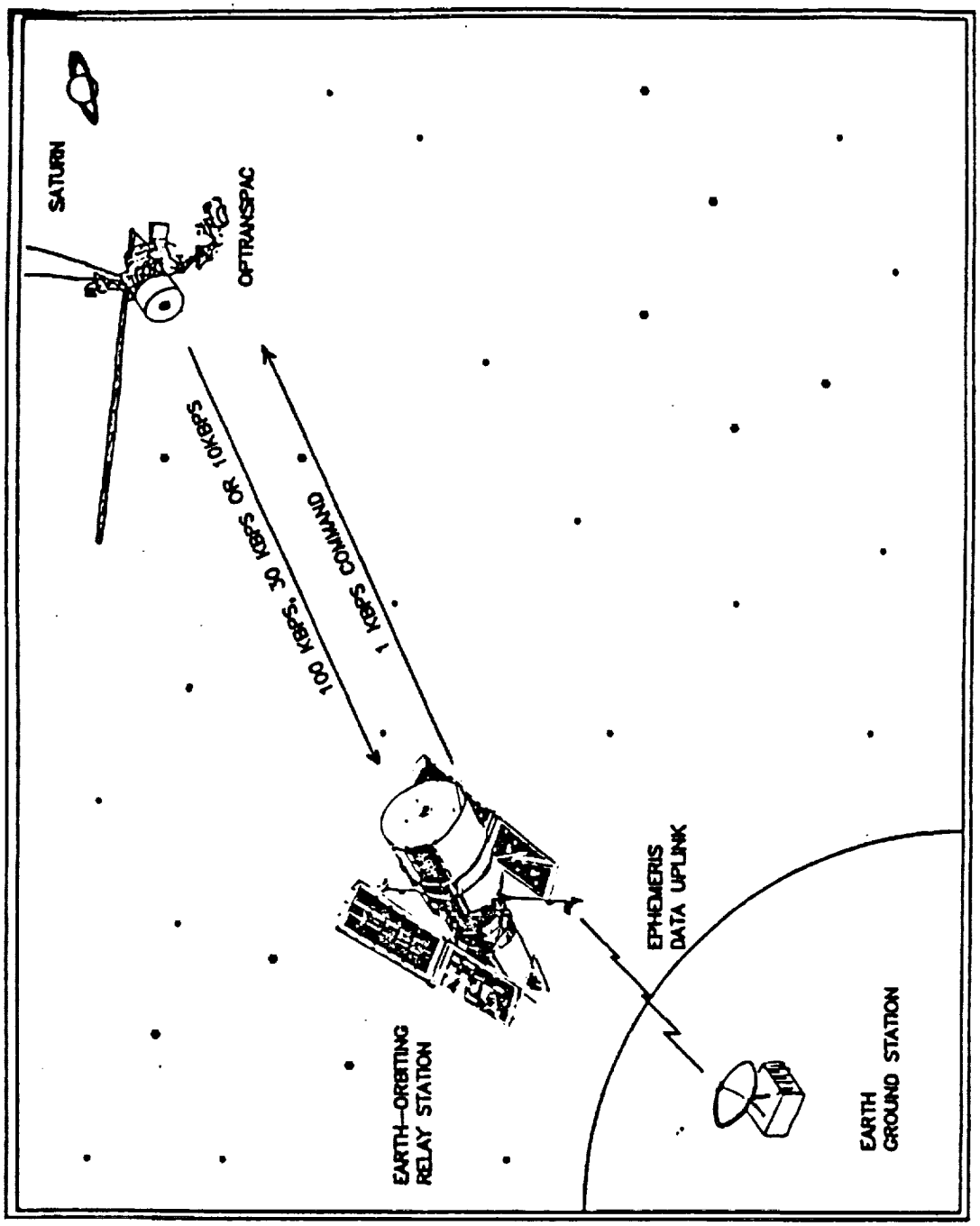

FIGURE 1–1

DYNAMIC ENVIRONMENTS

- ORBITAL DYNAMICS
- POINT AHEAD AND DOPPLER
- METERORIOD ENVIRONMENT
- GRAVITATIONAL, MAGNETIC, ELECTRICAL AND THERMAL RADIATION
- VIBRATION ENVIRONMENT
- ACOUSTIC ENVIRONMENT
- PYROTECHNIC SHOCK
- SATURNIAN RADIATION ENVIRONMENT
- OPTICAL BACKGROUND RADIATION

FIGURE 1-2

OPTRANSPAC
ISOMETRIC VIEW

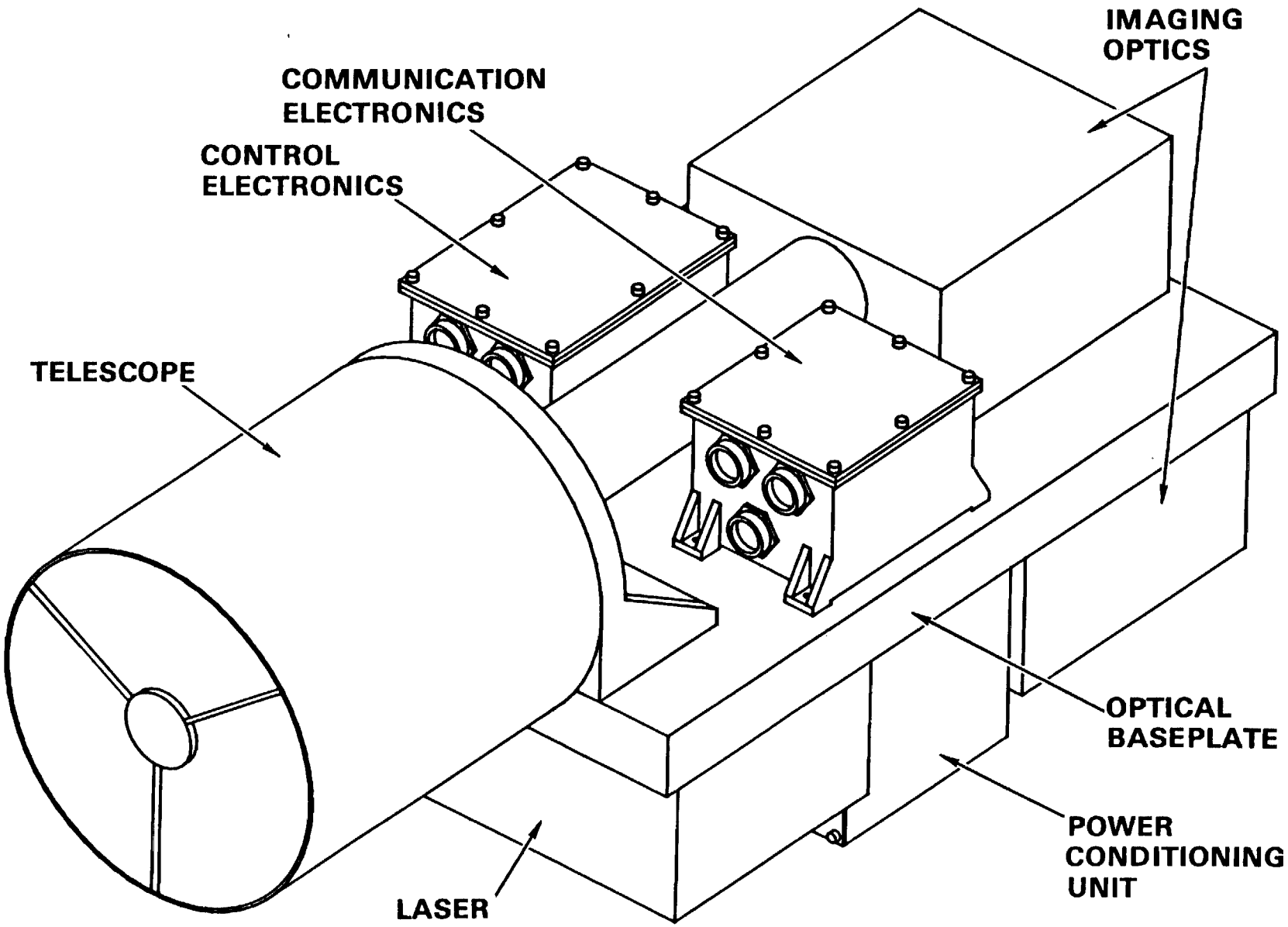

FIGURE 1–3

WEIGHT AND POWER SUMMARY

ITEM	WEIGHT (LBS.)	POWER (WATTS)
• ELECTRO-OPTICS ASSEMBLY	(57.0)	(11.0)
TELESCOPE (11 IN)	18.0	-
IMAGING OPTICS ASSEMBLY	13.5	2.0
LASER ASSEMBLY	20.0	4.0
DETECTOR ASSEMBLY	1.0	.4
EARTH TRACKER	4.5	4.6
• ELECTRONICS	(41.0)	(39.3)
COMMUNICATIONS ELECTRONICS	9.0	7.7
CONTROL ELECTRONICS	12.5	14.5
POWER CONDITIONER UNIT	19.5	17.1
• STRUCTURE/WIRE/MISC	(17.0)	(6.7)
TOTAL	115.0	57.0

FIGURE 1-4

2.0 SYSTEMS OVERVIEW

2.1 REQUIREMENTS - The specified system level requirements for the OPTRANSPAC are outlined in Figure 2-1. The OPTRANSPAC is required to communicate with an Earth-Orbiting Relay Station (EORS) at a maximum distance of 10 Astronomical Units. Downlinking of data from the OPTRANSPAC to the EORS at discrete rates of 10KBPS, 30KBPS and 100KBPS at a bit error probability of 10^{-3} is required. The OPTRANSPAC must also be capable of receiving command data on an optical uplink from the EORS at a 1KBPS data rate (10^{-3} BER).

Choice of useful wavelengths were set by the statement of work requirements. The downlink wavelength could not exceed 1.0 micron while the uplink wavelength was limited to under 2.0 microns. Outages, attributed to all factors excluding earth blockage, were required to be less than 10%. This resulted in an availability requirement of 90 percent and accounts for outages when the sun is in close proximity to the OPTRANSPAC or EORS optical boresights.

Maximum Weight and Power Requirements for the OPTRANSPAC were set at 50 kilograms and 50 watts, respectively. Technology to be employed in the OPTRANSPAC design was restricted to that "reasonable by 1988". Where the term "reasonable by 1988" means laboratory demonstrated feasible, but not necessarily space qualified by 1988.

2.2 EORS CHARACTERISTICS - While not specifically part of the OPTRANSPAC design, the EORS characteristics directly affect the terminal design. The major characteristics that contribute to OPTRANSPAC design considerations are outlined in Figure 2-2. The EORS transmits a 10 watt average power, 5 microradian laser beam at the wavelength less than 2 microns. The EORS platform stability and other dynamic instabilities were assumed controlled such that open loop pointing of the transmit beam at the OPTRANSPAC is accomplished with zero pointing loss. As a receiver, the EORS consist of a 10 meter effective clear aperture with a 1 microradian field-of-view. The receiver consists of a photomultiplier based direct detection system. The quantum efficiency of the detector at a nominal wavelength of 532nm was assumed to be 30 percent.

2.3 MAJOR DESIGN ASSUMPTIONS - The major assumptions made in the design of the OPTRANSPAC terminal are outlined in Figure 2-3. The assumptions specify certain design aspects of the OPTRANSPAC that should be carefully, noted. Any change in these assumptions may affect the completed design of the transceiver terminal.

Spacecraft attitude control to within ±2 milliradians is assumed. This criteria provides for accurate pointing of the OPTRANSPAC telescope viewfield towards the Earth. Without this accurate knowledge, much larger telescope viewfields would have to be employed or a system design which included a gimballed telescope would have to be implemented. In the former this would require a large and bulky optical system causing added system weight and complexity. In the latter decreased pointing accuracy (due to gimbal jitter effects) would require a larger beam divergence resulting in an increase in system power in addition to weight and complexity increases associated with including the gimbal. Thus, this assumption provides for an OPTRANSPAC design which minimizes weight, power and complexity of the transceiver terminal.

OPTRANSPAC SYSTEM REQUIREMENTS

MAXIMUM OPERATIONAL RANGE	10 AU*
DATA RATES	
DOWNLINK	10, 30 & 100KBPS
UPLINK	1KBPS
BIT ERROR RATE (BOTH CHANNELS)	$<10^{-3}$
WAVELENGTH	
DOWNLINK	$<1.0\ \mu M$
UPLINK	$<2.0\ \mu M$
AVAILABILITY (EXCLUDING EARTH BLOCKAGE)	$\geq$90%
MASS	$\leq$50KG
POWER	$\leq$50 WATTS
TECHNOLOGY RESTRICTION	REASONABLE BY 1988
COMMUNICATION BETWEEN	EORS**

* AU = ASTRONOMICAL UNIT = 1.496×10^{11} METERS

** EORS = EARTH ORBITING RELAY STATION

FIGURE 2-1

EARTH ORBITING RELAY STATION (EORS)
CHARACTERISTICS

APERTURE SIZE	10 METERS EFFECTIVE
DETECTOR FIELD-OF-VIEW	1 μRAD
BACKGROUND REQUIREMENT	SATURNIAN
RECEIVER	PHOTOMULTIPLIER BASED DIRECT DETECTION QUANTUM EFFICIENCY 30%
TRANSMIT POWER	10 WATTS, AVERAGE
TRANSMIT DIVERGENCE	5 μRAD DIAMETER
POINTING LOSS	ZERO
POINTING	CAPABLE OF OPEN LOOP POINTING 5 μRAD BEAM AT OPTRANSPAC

FIGURE 2-2

MAJOR ASSUMPTIONS

- OPEN LOOP S/C ATTITUDE CONTROL TO WITHIN ±2 MRAD IS AVAILABLE
- OPTRANSPAC COMMANDS ARE PROCESSED BY THE S/C
- EMERGENCY COMMAND DATA IS AVAILABLE TO MAINTAIN THE ±2 MRAD KNOWLEDGE AND POINT THE S/C TO EARTH
- ACQUISITION TIME OF THE OPTICAL LINK IS NOT CRITICAL TO S/C FUNCTIONS AND WILL NOT BE A MAJOR DESIGN DRIVER
- ALL NECESSARY ATTITUDE REFERENCE SYSTEM DATA WILL BE PROVIDED IN A FORM DESIRABLE TO THE OPTRANSPAC
- ALL SENSOR DATA INPUTS FROM THE S/C WILL BE SERIAL DIGITAL WITH ASSOCIATED CLOCK INPUTS
- ALL DATA OUTPUTS TO THE S/C WILL BE VIA A SERIAL DIGITAL INTERFACE
- THE SYSTEM REDUNDANCY PHILOSOPHY WILL PUT THE BURDEN ON THE SOURCE

FIGURE 2-3

In the event of attitude control disruption (outside of the ±2 milliradian knowledge) and associated break-lock of the optical links, it is assumed emergency command data is available to reestablish the ±2 milliradian knowledge and restore the pointing of the OPTRANSPAC boresight towards the Earth. The OPTRANSPAC system relies on this emergency control to reestablish communication after a disturbance to the spacecraft attitude control accuracy.

The electrical interface between the spacecraft and the OPTRANSPAC is assumed serial digital for all data transfer to and from each side of the interface. Data, including the spacecraft sensor inputs, spacecraft telemetry, and spacecraft attitude reference system data will be transferred to the transceiver along these serial data ports. The redundancy philosophy is assumed to put the burden on the source to handle all redundancy switching. That is, signal flow from the source (be it the transceiver or the spacecraft) will determine which side of the load (prime or redundant) will be passed the signal. This technique is employed in current Lasercom systems.

All command data sent via the optical uplink is assumed passed to the spacecraft command decoder for processing. Commands pertinent to OPTRANSPAC operation are decoded by the spacecraft and returned to the transceiver via the serial interface. This simplifies the command data format and allows for command decoding at only one location.

A final assumption deals with system acquisition time. It was assumed that transceiver acquisition time was not a critical system parameter and was not critical to spacecraft functions. For this reason it was not considered a major system driver to the transceiver design. Later, analysis indicated that this was true and average acquisition times were calculated to be less than three seconds.

2.4 SYSTEM DESIGN RATIONALE - For purposes of this transceiver design study, the following rationale outlined in Figure 2-4 was chosen. The environmental factors that are prime system design drivers were identified. These included optical backgrounds, orbital dynamics, point-ahead angles, Doppler, vibration and range to name a few. Mission specific constraints such as the lack of a continuous track beacon from EORS were also identified.

Candidate system designs were selected for consideration based upon the environmental effects, mission constraints and system requirements. Preliminary link analysis was performed to verify the validity of the designs. Initial size, weight, power and complexity comparisons were then made. One or more designs were then chosen and the link analysis was refined and components defined (lasers, detectors, telescopes, etc). Finally, a baseline configuration was selected for its performance, size, weight, power, reliability and design simplicity. Detailed mechanical, optical and electrical component design was then performed to yield the final OPTRANSPAC terminal design.

SYSTEM DESIGN RATIONALE

- IDENTIFY ENVIRONMENTAL EFFECTS THAT ARE PRIME SYSTEM DESIGN DRIVERS
- IDENTIFY ANY SPECIFIC MISSION CONSTRAINTS
- SELECT CANDIDATE DESIGNS FOR CONSIDERATION BASED UPON ABOVE POINTS AND SYSTEM REQUIREMENTS
- PERFORM PRELIMINARY LINK ANALYSIS TO VERIFY VALIDITY OF DESIGNS (FIRST ORDER)
- MAKE INITIAL SIZE, WEIGHT, POWER AND COMPLEXITY ESTIMATES
- SETTLE ON ONE OR MORE DESIGNS OR RECONFIGURE TO ACCOMMODATE VALIDITY OF DESIGN
- REFINE LINK ANALYSIS OF SELECTED DESIGN(S) DEFINING COMPONENTS (I.E., LASER, DETECTORS, POINTING REQUIREMENTS, ETC.)
- SETTLE ON BASELINE CONFIGURATION SELECTED FOR ITS PERFORMANCE, SIZE, WEIGHT, AND POWER, RELIABILITY AND DESIGN SIMPLICITY
- PERFORM DETAILED OPTICAL, MECHANICAL AND ELECTRICAL DESIGN ON BASELINE SYSTEM MAKING MINOR MODIFICATIONS TO SYSTEM AS NECESSARY

FIGURE 2-4

3.0 DYNAMIC ENVIRONMENTS

The dynamic environments assumed to be encountered by the OPTRANSPAC on its mission are analyzed and defined herein. A complete dynamic environment specification is included in Appendix A.

3.1 ORBITAL DYNAMICS - A generic transfer orbit was generated for a deep space probe from Earth to Saturn. The orbit pictured in Figure 3-1 is a Hohmann transfer, which is the minimum energy orbit for transfer. Transit time is 1827 days (details of the orbit are given in Figure 3-1 and Appendix A). This orbit was used to calculate the relative velocities between the Earth Orbiting Relay Station and the OPTRANSPAC spacecraft for use in the Doppler and point-ahead calculations. Figure 3-2 illustrates the range versus time between the earth and the OPTRANSPAC spacecraft using the Hohmann transfer orbit. The range increases rapidly at first as the spacecraft is on the closest part of the orbit to the Sun and the Earth is also swinging away from the spacecraft's orbit. The Earth's orbital motion is the most obvious feature of the range, with oscillations of 2 AU superimposed upon the distance of the spacecraft from the Sun. After one year, the range to the spacecraft is almost 5 AU, or nearly half the distance to Saturn.

3.2 POINT-AHEAD AND DOPPLER - The Doppler shift of the light transmitted between the OPTRANSPAC and the Earth Orbiting Relay Station and the point-ahead angle necessary for correct illumination were determined by the relative velocity between the two platforms. The four contributors to this velocity when the spacecraft is encountering Saturn are 1) Earth's orbital rate around the Sun; 2) Saturn's orbital rate around the Sun; 3) The EORS orbital rate around the Earth; and 4) The spacecraft's flyby or orbital rate around Saturn. A flyby was assumed because it results in higher relative velocities than does a Saturn orbit. A flyby with a periapse of twice the radius of Saturn and an EORS altitude of 300 nautical miles were assumed. The contributing velocities of each of these in the directions defined are given in Figure 3-3.

Figure 3-4 shows the maximum contributions to Doppler shift and point-ahead angles from the velocities noted in Figure 3-3. For point-ahead, all four contributors may have their total velocity perpendicular to the line-of-sight and, thus, apply to point-ahead. However, the maximum angle contribution from the EORS is limited by the extremes of where it can be in its orbit around the Earth. As the OPTRANSPAC range increases, the effective angle traversed by the Relay Station back and forth around the Earth is inversely proportional to the range. The maximum point-ahead angle which the OPTRANSPAC must use is 440 microradians. Because the contribution of Saturn's velocity is only in one direction, the maximum point-ahead angle in the opposite direction is 312 microradians.

The Doppler shift is caused by the instantaneous velocity along the line of sight. The contribution of the EORS was therefore, not limited as it was for point-ahead. Saturn's velocity, however, only contributes through the sine of the minimum angle of itself with respect to the line-of-sight. Defined by the minimum distance from the Earth to Saturn and the maximum crossrange of the Earth's position. The Earth and spacecraft flyby contributing velocities are the same as for the point-ahead case. The four contributions were summed to get a maximum Doppler shift at 1064 nanometers of 2.3 Angstroms and at 532 nanometers of 1.15 Angstroms.

EARTH TO SATURN TRANSFER ORBIT

- HOHMANN TRANSFER
- SEMI-MAJOR AXIS 5.67 AU
- ECCENTRICITY 0.826

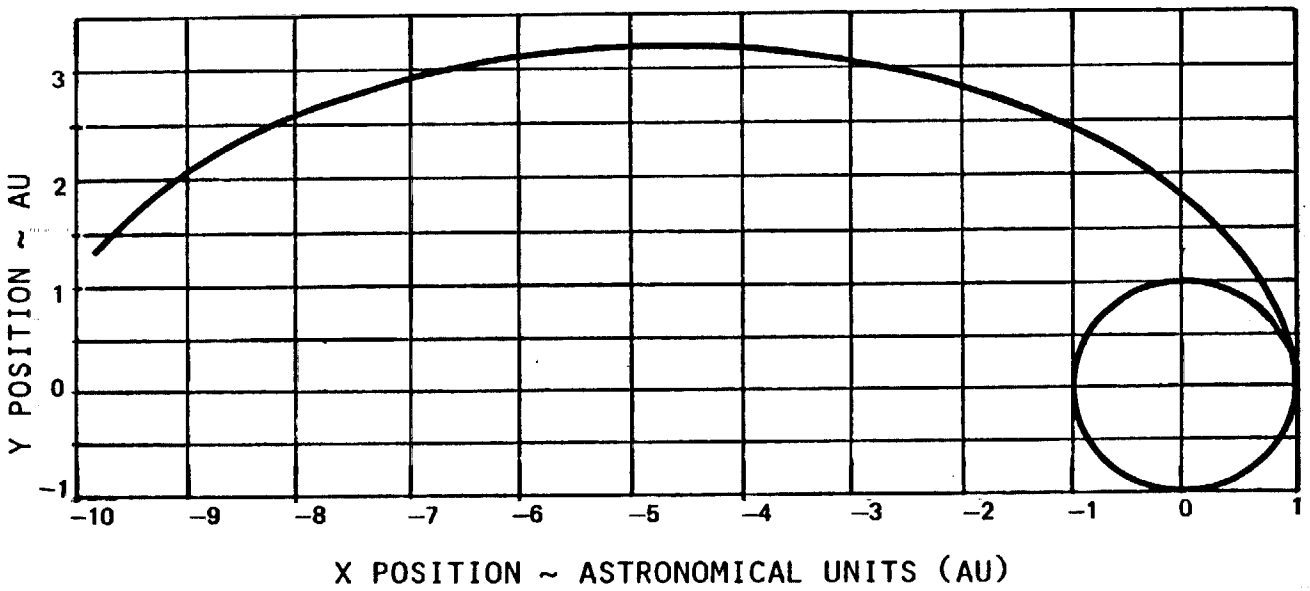

FIGURE 3–1

EARTH TO SPACECRAFT RANGE

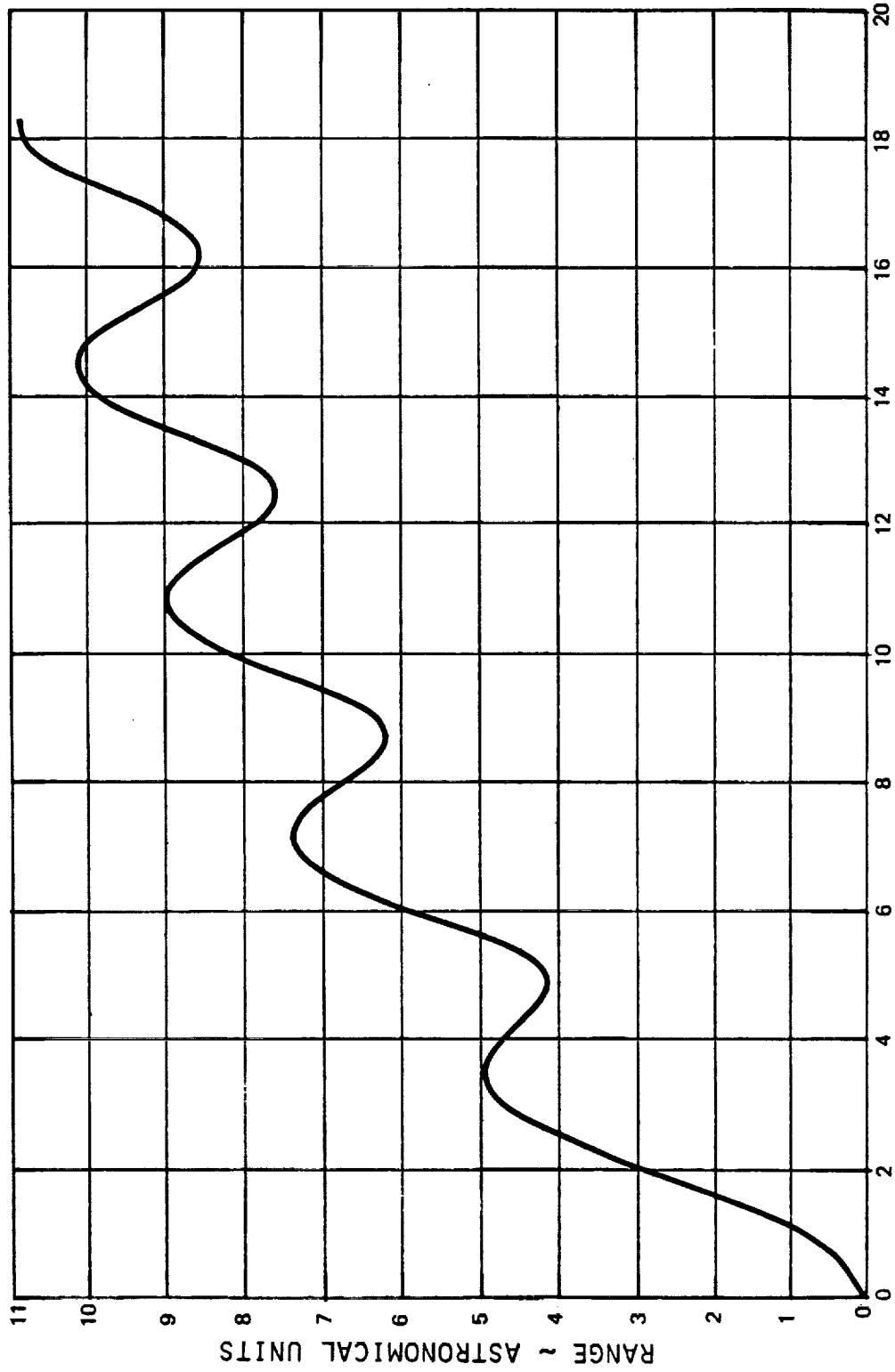

FIGURE 3–2

POINT AHEAD AND DOPPLER CONTRIBUTORS

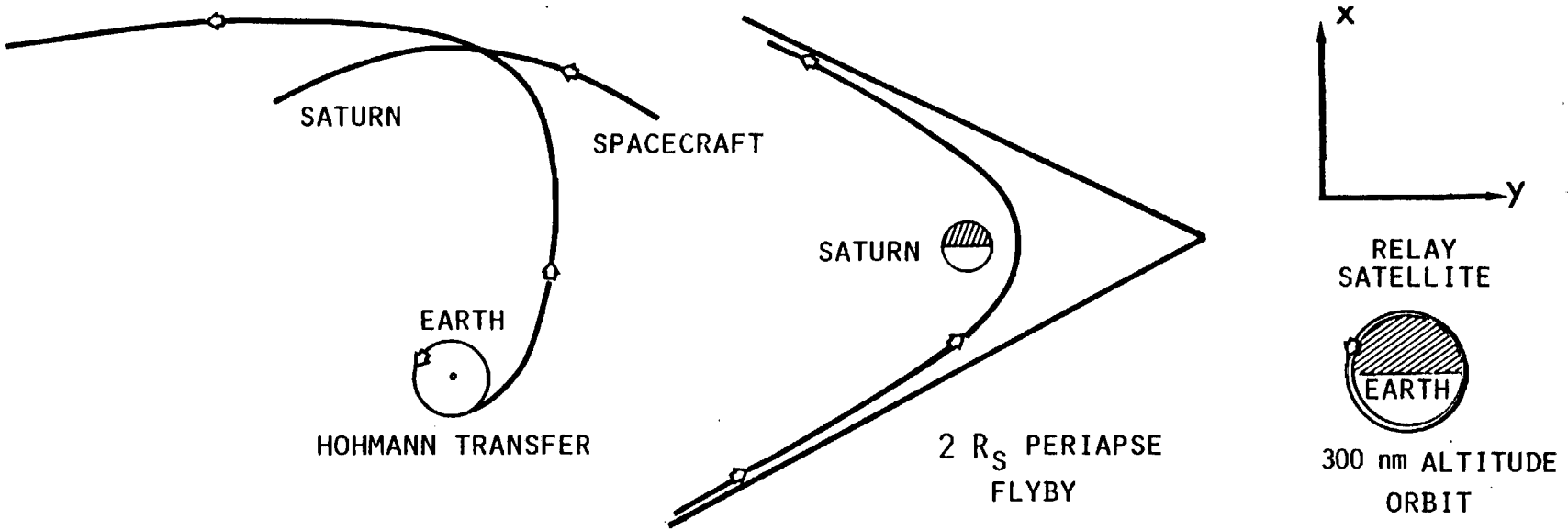

MAXIMUM VELOCITIES

	DIRECTION	
	X (KM/SEC)	Y (KM/SEC)
EARTH	±29.8	±29.8
RELAY	± 7.6	± 7.6
SATURN	SMALL	- 9.6
FLYBY	±25.1	±25.1

FIGURE 3-3

MAXIMUM POINT AHEAD AND DOPPLER

POINT AHEAD MAXIMUM CONTRIBUTIONS (μRAD)

EARTH	199
RELAY SATELLITE	51, RANGE $\leq$ 1.8 AU
	92.7/R, RANGE $\geq$ 1.8 AU
SATURN	64
SPACECRAFT FLYBY	167
	440, RANGE = 9.5 AU

DOPPLER MAXIMUM CONTRIBUTIONS (A) (λ = 1.064 UM)

EARTH	1.06	
RELAY SATELLITE	.27	
SATURN	.08,	SIN (ARC TAN (2/8.5)) FACTOR
SPACECRAFT FLYBY	.89	
	2.3	

FIGURE 3—4

Figure 3-5 through 3-8 analyze Doppler and point-ahead. Prior to the Saturn encounter, only the Earth, the EORS, and the spacecraft transfer orbit motion apply. Figure 3-5 shows the velocities of the Earth and spacecraft in the directions of the axes of the transfer orbit. The spacecraft has an original velocity of about 10Km/second more than the Earth's in the minor axis direction and a velocity the same as the Earth's in the major axis direction. As the spacecraft travels farther from the Sun, its velocity decreases as potential energy increases. The Earth's velocity follows the expected sinewave pattern as it orbits the Sun.

The velocities of Figure 3-5 were rotated into the line-of-sight direction between the Earth and the spacecraft. The relative velocities between the Earth and spacecraft in this coordinate system, parallel to and perpendicular to the line of sight are plotted versus flight time (See Figure 3-6). These, when combined with the Earth-Orbiting Relay Station maximum velocity contribution, noted previously, determine the necessary point-ahead angles and expected doppler shift during the Earth to Saturn transfer.

Figure 3-7 shows the necessary point-ahead angles for the OPTRANSPAC during the Hohmann transfer between the Earth and Saturn due to the relative velocities shown in Figure 3-6. Adding the point-ahead angle needed to compensate for the EORS motion (51 microradians maximum) creates a total point-ahead angle of 322 microradians during the transfer as compared to 440 microradians during the Saturn encounter.

The maximum Doppler shift expected during the Hohmann transfer without the Relay Station contribution is plotted versus flight time (See Figure 3-8). Adding in the maximum velocity contribution of the Relay Station yields an expected Doppler shift of approximately 1.7 Angstroms (λ = 1064 nanometers) during the Hohmann transfer from Earth to Saturn. This value is less than the maximum expected during the Saturn encounter.

Figures 3-5 through 3-8 illustrate the effects of Doppler and point-ahead during the Hohmann transfer are less than those during the Saturn encounter. Thus, the OPTRANSPAC design must accommodate the maximum Doppler and point-ahead effects defined by the Saturn encounter and in doing so will also accommodate any Doppler or point-ahead contributions during transfer.

3.3 METEOROID ENVIRONMENT - Figure 3-9 tabulates the meteoroid environment design requirement for travel to Saturn. This data was derived from the Galileo Orbiter environmental design requirements, GLL-3-240 Rev. A, JPL, 1982. The integral fluence numbers from the Galileo environment were increased by the ratio of relative transit times to Saturn instead of Jupiter. This ratio calculation assumes 90% of the Galileo environment fluence was attributed to the asteroid belt and did not change. The mean relative speed was increased by one-half the velocity change difference from transfer to Saturn instead of Jupiter.

Contact with the meteoroids occurs when the spacecraft collides with the slower moving particles. Upon encountering the micrometeoroids the spacecraft's velocity vector is assumed normal to the meteoroids' velocity vectors. Nominal spacecraft velocity (approximately 15 km/sec) is orders of magnitude greater than the velocities of the micrometeorites. Vector algebra will show the contribution from the particles' velocities are negligible when compared to the

EARTH AND SPACECRAFT VELOCITIES

- HOHMANN TRANSFER TO SATURN

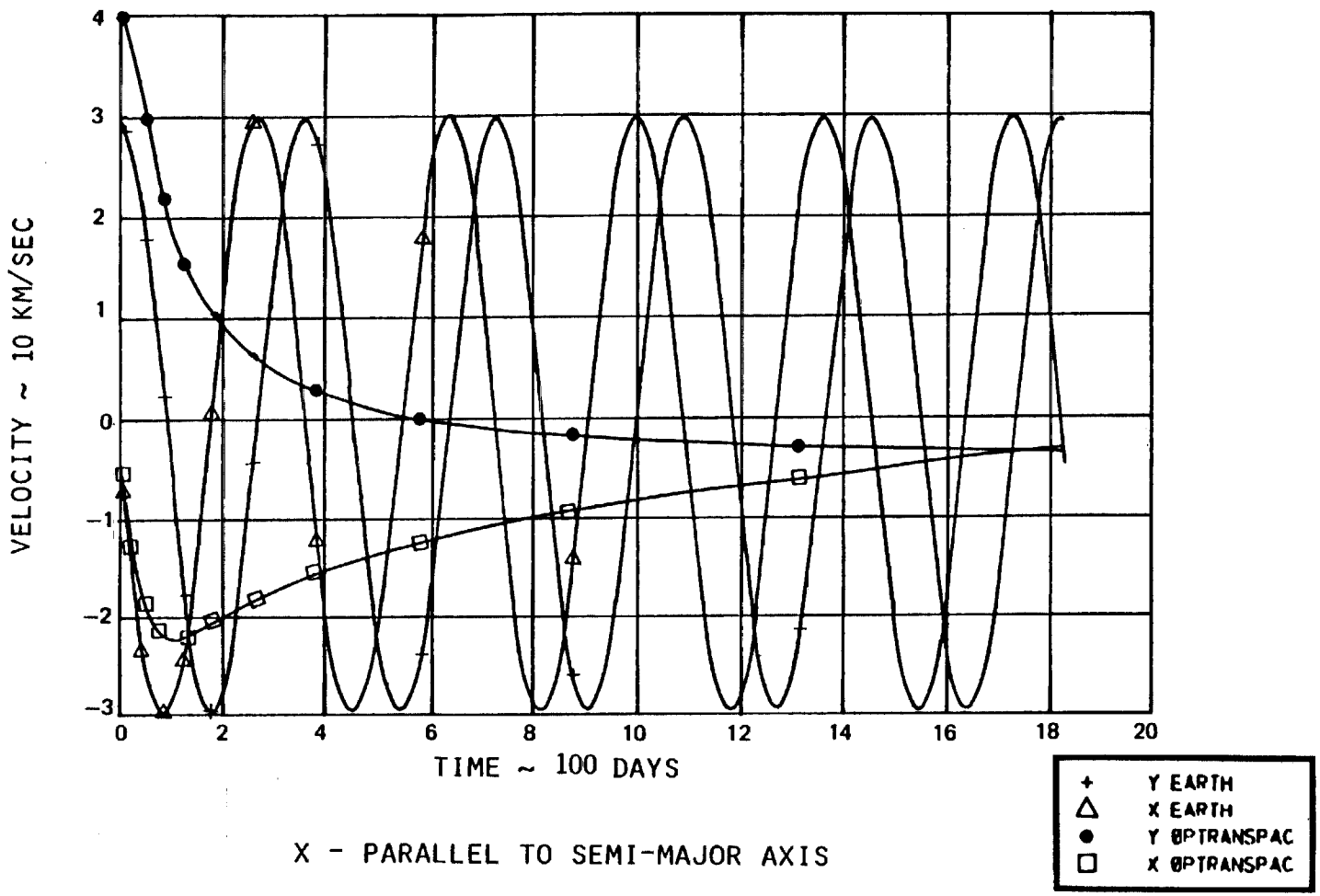

X - PARALLEL TO SEMI-MAJOR AXIS

Y - PARALLEL TO SEMI-MINOR AXIS

FIGURE 3-5

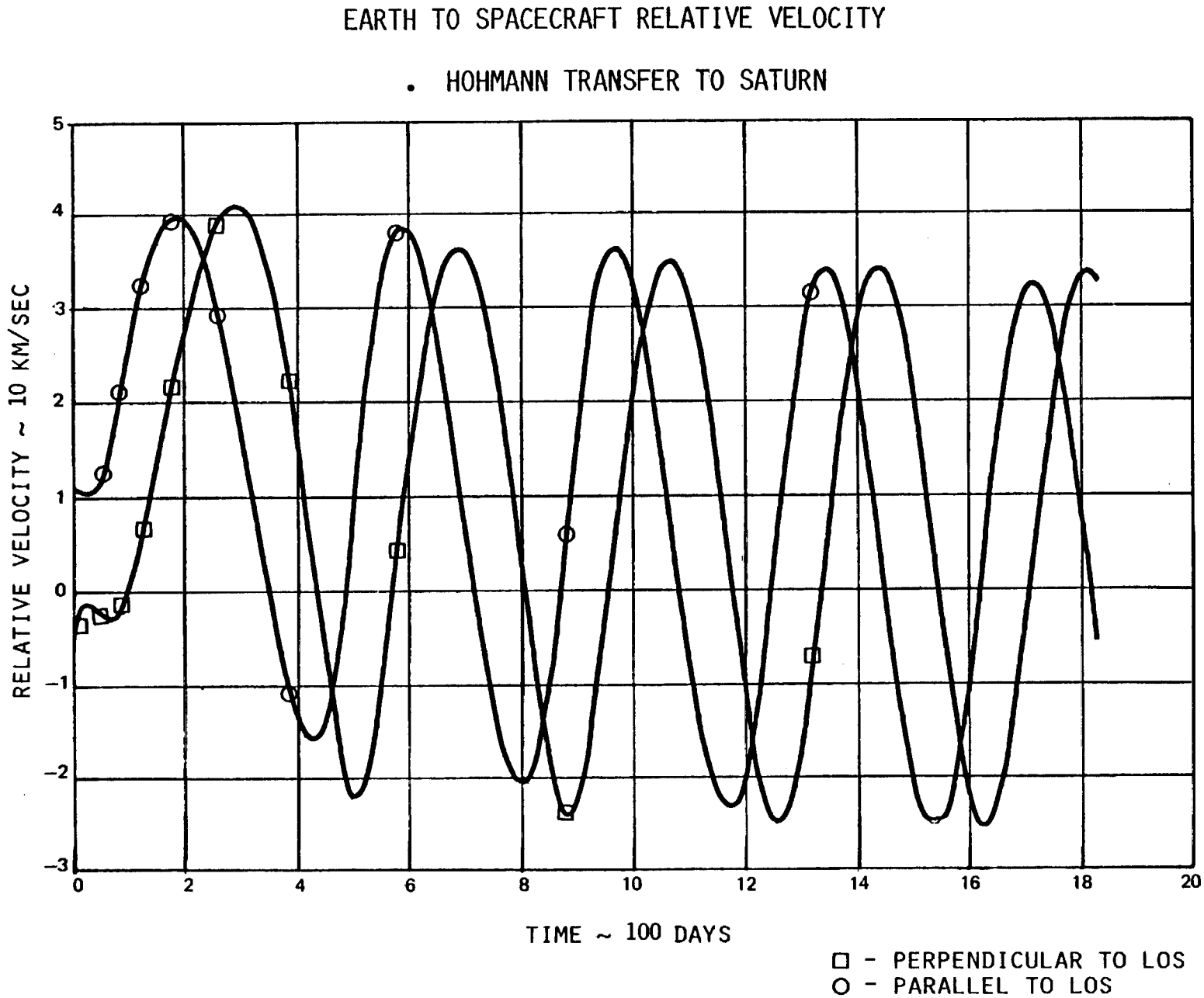
EARTH TO SPACECRAFT RELATIVE VELOCITY
• HOHMANN TRANSFER TO SATURN
RELATIVE VELOCITY ~ 10 KM/SEC
5
4
3
2
1
0
−1
−2
−3
0
2
4
6
8
10
12
14
16
18
20
TIME ~ 100 DAYS
□ - PERPENDICULAR TO LOS
○ - PARALLEL TO LOS

FIGURE 3-6

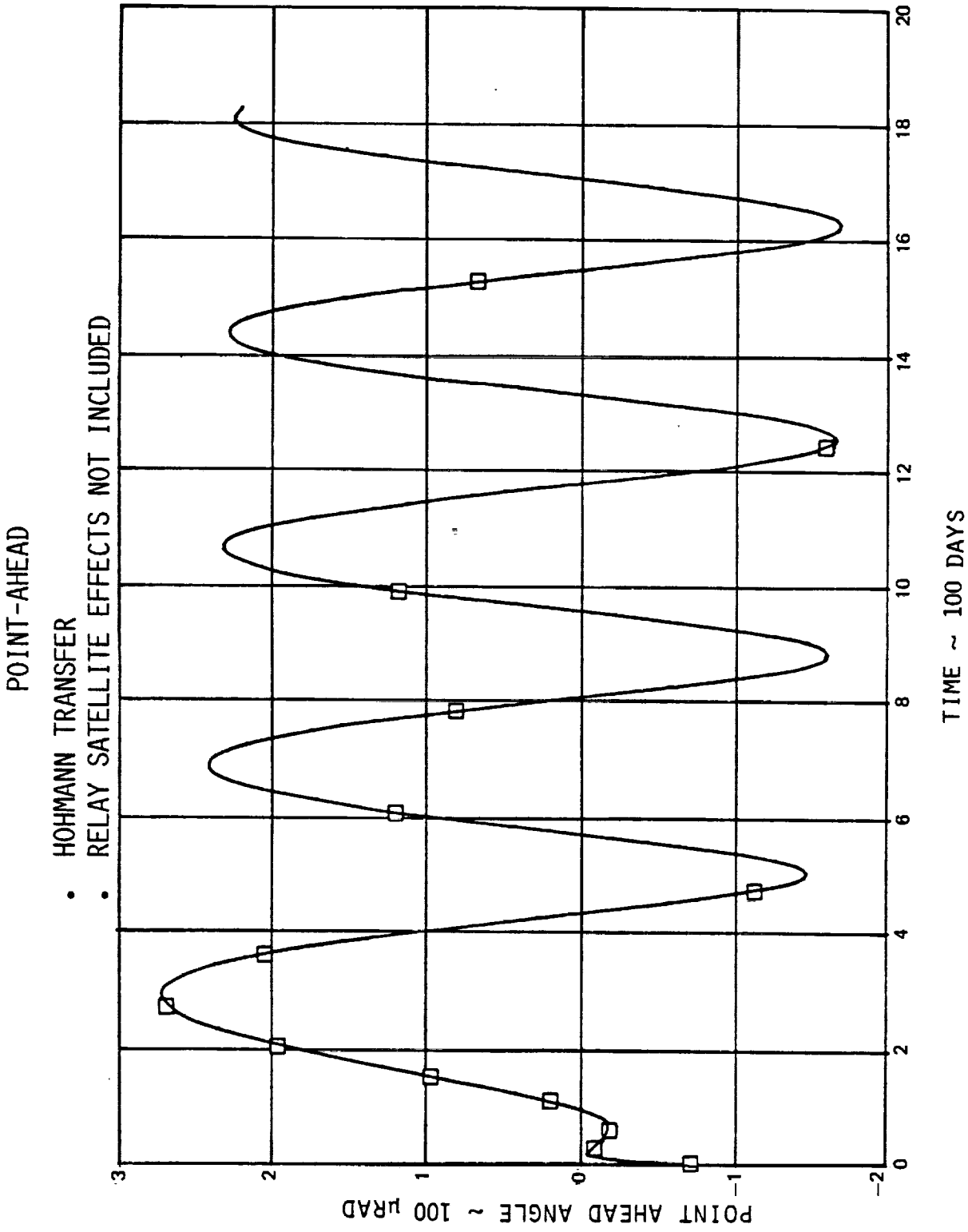
POINT-AHEAD
• HOHMANN TRANSFER
• RELAY SATELLITE EFFECTS NOT INCLUDED
POINT AHEAD ANGLE ~ 100 μRAD
TIME ~ 100 DAYS
3
2
1
0
−1
−2
0
2
4
6
8
10
12
14
16
18
20

FIGURE 3–7

DOPPLER SHIFT

- HOHMANN TRANSFER TO SATURN
- NO RELAY SATELLITE EFFECTS
- $\lambda = 1.064\ \mu M$

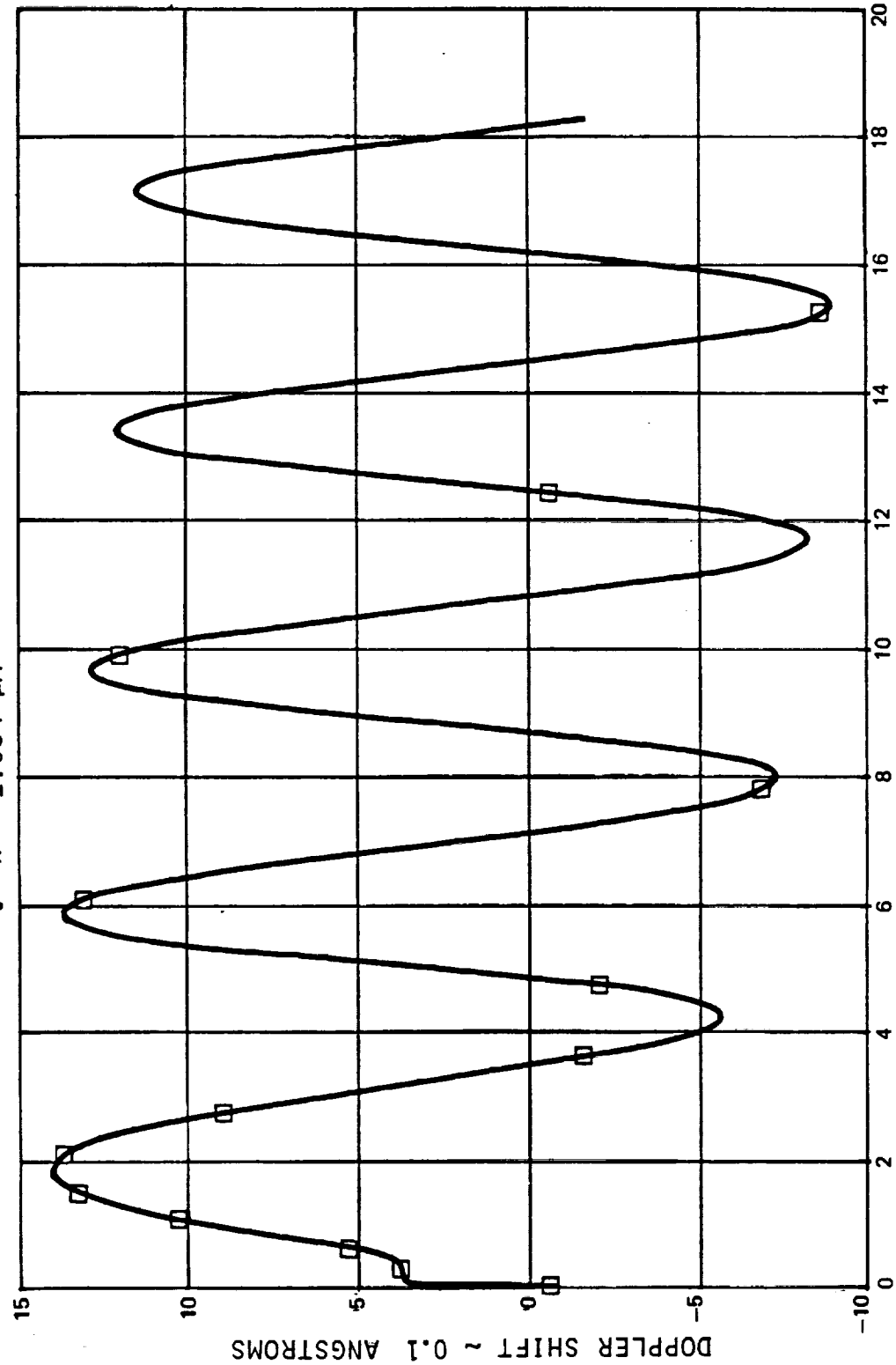

FIGURE 3–8

METEOROID ENVIRONMENT DESIGN REQUIREMENT

INTEGRAL FLUENCE DURING TRANSIT

PARTICLE MASS (G)	FLUENCE (PARTICLES/M^2)
10^{-12}	2.2×10^{5}
10^{-10}	1.8×10^{3}
10^{-8}	2.3×10^{2}
10^{-6}	9.2
10^{-5}	5.7×10^{-1}
10^{-4}	3.5×10^{-2}
10^{-3}	2.1×10^{-3}
10^{-2}	1.2×10^{-4}
10^{-1}	7.7×10^{-5}
10^{0}	4.8×10^{-7}

MEAN RELATIVE SPEED

15 KM/SEC

PARTICLE MASS DENSITY

0.5 G/CM^3

FIGURE 3-9

spacecraft velocity. Thus, it is concluded that the collisions occurs along the direction of the velocity vector.

The critical component in the OPTRANSPAC system when considering the micrometeoroid environment is the telescope mirror. Since the primary mirror is not shielded it could possibly be exposed to the incident meteoroids. However, the OPTRANSPAC telescope boresight is assumed to be pointed towards the Earth (approximately directly opposite the velocity vector). Due to this reasoning, shielding requirements for the OPTRANSPAC terminal are assumed no larger than the nominal shielding required for the entire spacecraft.

3.4 GRAVITATIONAL, MAGNETIC, ELECTRICAL AND THERMAL RADIATION - The data given in Figure 3-10 was collected from several sources. They are given below.

A) Galileo Orbiter Environmental Design Requirements, GLL-3-240 Rev. A, JPL, 1982.
B) Space Vehicle Design Criteria (Environment), The Planet Saturn, NASA SP-8091, 1970.
C) Space and Planetary Environment Criteria Guidelines for use in Space Vehicle Development, NASA TM-82501, 1982.
D) Space Shuttle System Payload Accommodations, NASA JSC-07700, Volume XIV, Rev. H, 1983.

The maximum gravitational, magnetic, electrical and thermal radiation environments are within present Lasercom capabilities. the Earth, the shuttle and near-Earth orbit provide the largest values of these environments to be encountered by the OPTRANSPAC. Saturn's environments are less than these because encounter is assumed at a distance of twice the Saturnian radius from the planet's surface. Minimum thermal radiation at 10 AU may require a thermal design that includes heaters to keep the components within specified operating limits.

3.5 VIBRATION ENVIRONMENT - The Space Shuttle vibration environment during launch is illustrated in Figure 3-11. This data was taken from Space Shuttle System Payload Accommodations, NASA JSC-07700, Volume XIV, Rev. H, 1983. This environment is within present Lasercom system capability. Current Lasercom systems are designed and tested to withstand the Space Shuttle vibration environments.

3.6 ACOUSTIC ENVIRONMENT - Figure 3-12 illustrates the Space Shuttle acoustic environment during launch. The data was also taken from Space Shuttle System Payload Accommodations, NASA JSC-07700, Volume XIV, Rev. H, 1983. This environment is also within present Lasercom system capability. Current Lasercom systems are designed and tested to withstand the Space Shuttle acoustic environment.

3.7 PYROTECHNIC SHOCK - Figure 3-13 depicts the spectrum of the expected pyrotechnic shock environment. This is the maximum spectrum during spacecraft launch/separation. It will be attenuated by intervening spacecraft structure. The data was taken from the Galileo Orbiter Environment Design Requirement, GLL-3-240, Rev. A, JPL, 1982. Present Lasercom design capability for pyrotechnic shock is a factor of 10 less at the spacecraft/Lasercom interface. If the attenuation of the spacecraft structure (which is as yet undefined) is

GRAVITATIONAL, MAGNETIC, ELECTRICAL, AND THERMAL RADIATION ENVIRONMENTS

MAGNETIC FIELD (MAX)

EARTH	5×10^4 NT @ SURFACE
INTERPLANETARY	25 NT
SATURN	8×10^3 NT @ 2 R_S
SHUTTLE (NON-OPERATING)	32 MT

GRAVITATIONAL FIELD DIFFERENTIAL ACCELERATION

EARTH	3.0×10^{-6}	$M/SEC/_M$ @ SURFACE
SUN	7.9×10^{-14}	$M/SEC/_M$ @ 1 AU
SATURN	4.3×10^{-8}	$M/SEC/_M$ @ 2 R_S

THERMAL RADIATION

EARTH REFLECTED	57.3 MW/CM^2 @ R_E
SOLAR	163.0 MW/CM^2 @ 1 AU
SATURN REFLECTED	1.1 MW/CM^2 @ R_S

ELECTRICAL FIELD

SATURN	116 V/M @ 2 R_S

FIGURE 3-10

SPACE SHUTTLE VIBRATION ENVIRONMENT

• LAUNCH

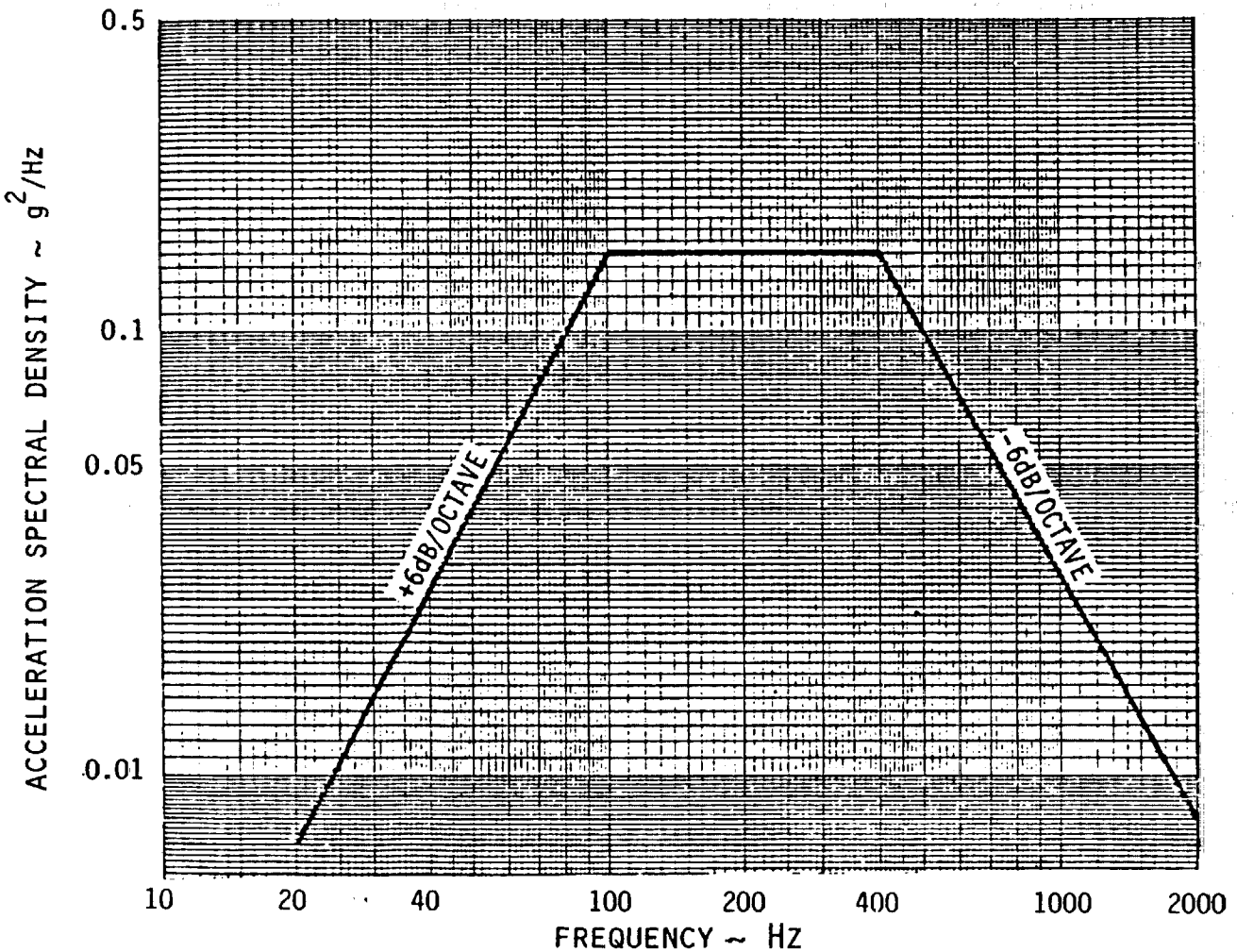

FIGURE 3-11

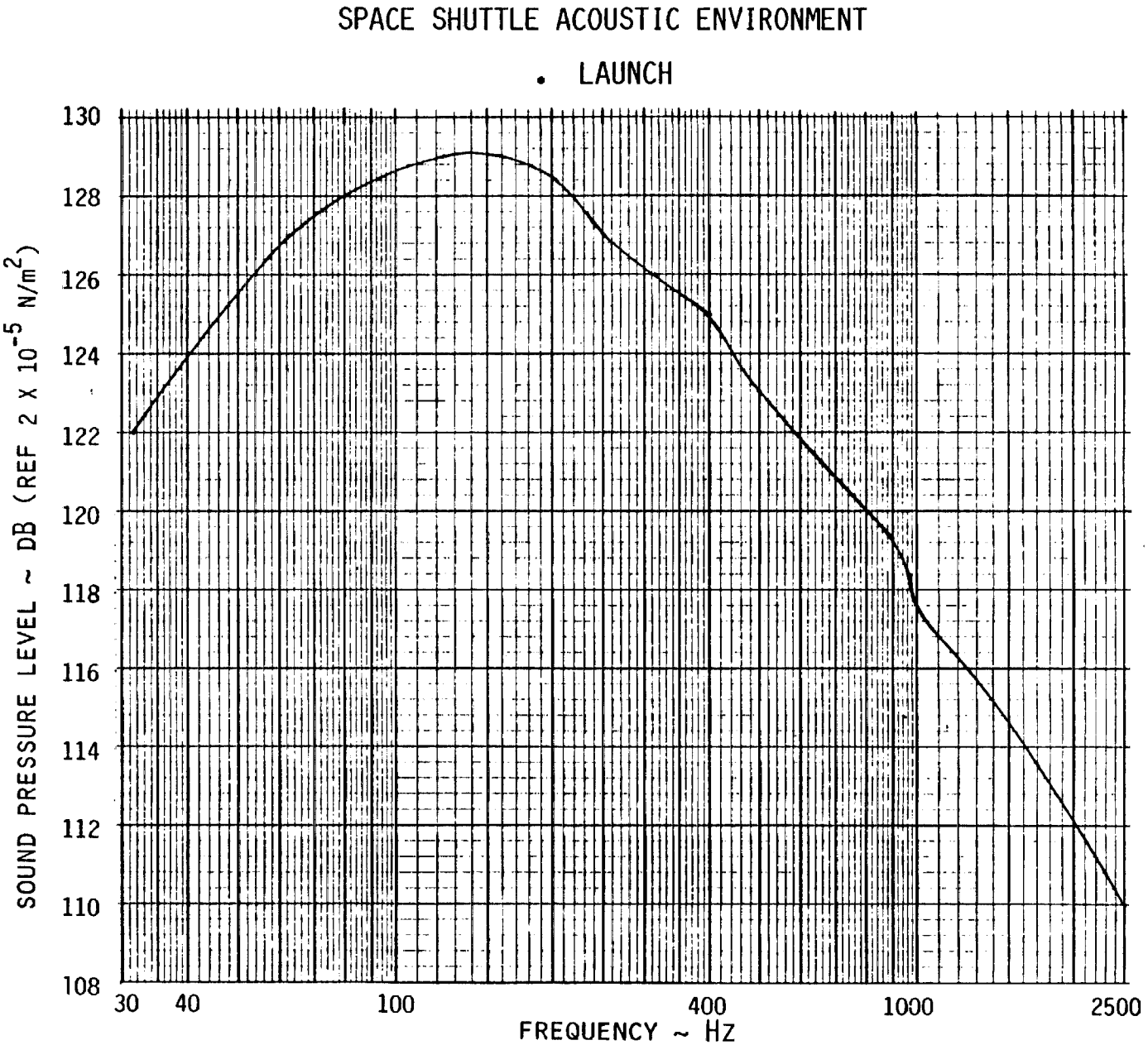
SPACE SHUTTLE ACOUSTIC ENVIRONMENT
• LAUNCH
SOUND PRESSURE LEVEL ~ DB (REF 2 X 10^-5 N/m^2)
130
128
126
124
122
120
118
116
114
112
110
108
30
40
100
400
1000
2500
FREQUENCY ~ HZ

FIGURE 3-12

PYROTECHNIC SHOCK

- SPACECRAFT/LAUNCH VEHICLE SEPARATION

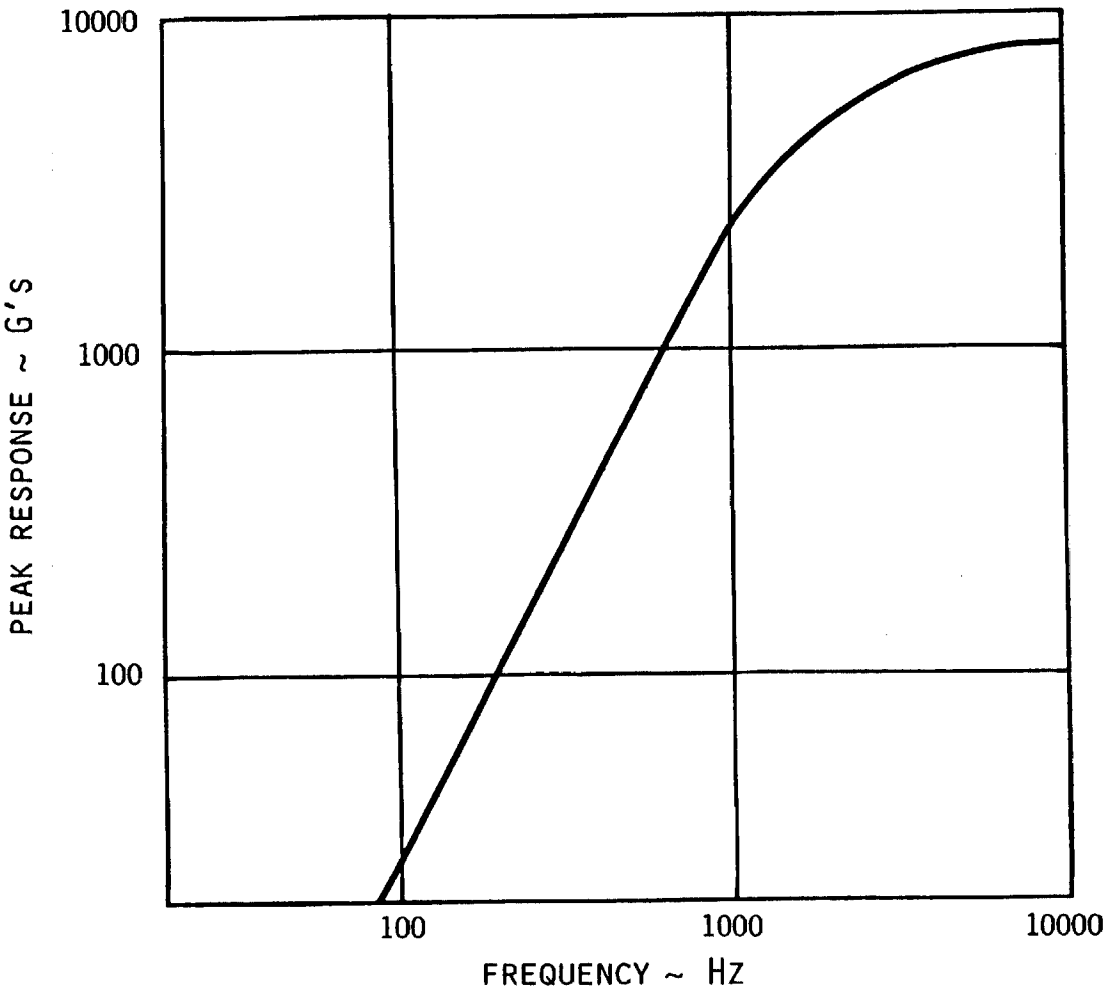

FIGURE 3-13

greater than a factor of ten, the design will be within present Lasercom capability. If not, shock isolation must be provided between the spacecraft and the OPTRANSPAC system.

3.8 SATURNIAN RADIATION ENVIRONMENTS - The OPTRANSPAC radiation environments associated with the charged particle and radioisotope thermoelectric generator are given in Figure 3-14. The trapped proton and electron environments were taken from the Pioneer 11 and Voyager missions. Electron and proton doses are representative of a Jovian flyby environment. From the data it was determined that this environment was worst case for Saturn, and therefore, representative radiation levels for the OPTRANSPAC system were chosen as 100 KRADS total dose and 1×10^{14} (1 MeV damage equivalent) neutrons/cm^2 displacement damage.

The OPTRANSPAC can expect to see a Galactic particle environment on the order of that shown in Figure 3-15. This environment interacts with the system electronics introducing soft errors in the LSI/VLSI devices. Hard errors or single event latch-up of devices will be eliminated by device selection.

Mitigation of the single event upset environment can be handled by system circumvention (i.e., redundant storage of critical data, error detection/correction, watchdog timer, reasonableness of data checks, etc.). Appropriate device selection can reduce the probability of soft errors and aid in the mitigation of these effects.

The mission environments contributing to total dose include the interplanetary electrons, protons and solar flare particles plus the Saturn electron and proton Van Allen belts. Figure 3-16 illustrates that under nominal spacecraft shielding of one gram per cm^2 (Al), the total dose experienced by semiconductor electronics will be 60 KRADS (Si).

The major contributing environments to displacement damage in semiconductor electronics are the protons trapped in Saturn's Van Allen belt and the interplanetary cosmic ray protons. Minor contributions are made by the nuclear power source and mission electron environments. Figure 3-17 indicates under nominal spacecraft shielding (1 gram/cm^2 (Al)) the electronics will experience 2.5×10^{13} neutrons/cm^2 (1 MeV neutron equivalent damage in silicon).

The total dose level of 100 KRADS as determined from the electron/proton data is currently within the capability of Lasercom systems. Development data and hardness assurance results from Lasercom hardware programs on electronic, electro-optic and optical piece parts support this conclusion. The required radiation design margin for the system can be accommodated with a hardness assurance test program during the production phase of the program.

The displacement damage fluence is currently higher than Lasercom design levels, however, within the capability of selected electronics. Care in device selection and appropriate development testing may be necessary.

3.9 OPTICAL BACKGROUND RADIATION - Five specific background noise source scenarios were defined for the OPTRANSPAC design. Figure 3-18 outlines the five scenarios. On the uplink to the OPTRANSPAC from the EORS, background radiation from the Earth as well as off-axis scattering of sunlight onto the detector must be considered. The earth tracker must also deal with off-axis

SATURNIAN RADIATION ENVIRONMENTS

- CHARGED PARTICLE TOTAL DOSE WITH NOMINAL SHIELD (1 GM/CM^2 AL)
  - ELECTRONS: 48×10^3 RADS (SI)
  - PROTONS
    - TRAPPED: 12.8×10^3 RADS (SI)
    - INTERPLANETARY: 4.4×10^3 RADS (SI)

  TOTAL CALCULATED DOSE = 65.2×10^3 RADS (SI)

- CHARGED PARTICLE AND NEUTRON EQUIVALENT DISPLACEMENT DAMAGE (1 MEV EQUIVALENT NEUTRONS) BEHIND NOMINAL SHIELDS (1 GM/CM^2 AL)
  - RTG NEUTRONS: 2×10^{11} N/CM^2 (1 METER)
  - PROTONS
    - TRAPPED: 2.87×10^{13} N/CM^2
    - INTERPLANETARY: 4.18×10^{12} N/CM^2
  - ELECTRONS: 1.5×10^{11} N/CM^2

  TOTAL DISPLACEMENT DAMAGE = 3.3×10^{13} N/CM^2

- REPRESENTATIVE LEVELS FOR OPTRANSPAC
  - TOTAL DOSE: 100×10^3 RADS (SI)
  - DISPLACEMENT DAMAGE: 1×10^{14} N/CM^2 (1 MEV EQ.)

FIGURE 3-14

SATURNIAN RADIATION ENVIRONMENTS

- GALACTIC PARTICLES

ATOMIC NUMBER		PARTICLES/CM^2-SEC
1.	(PROTON)	4
2.	(ALPHA PARTICLE)	0.5
8.	(OXYGEN)	3×10^{-2}
14.	(SILICON)	7×10^{-3}
26.	(IRON)	3×10^{-4}

- SINGLE EVENT UPSET
  - EFFECTS SYSTEM ELECTRONICS

FIGURE 3-15

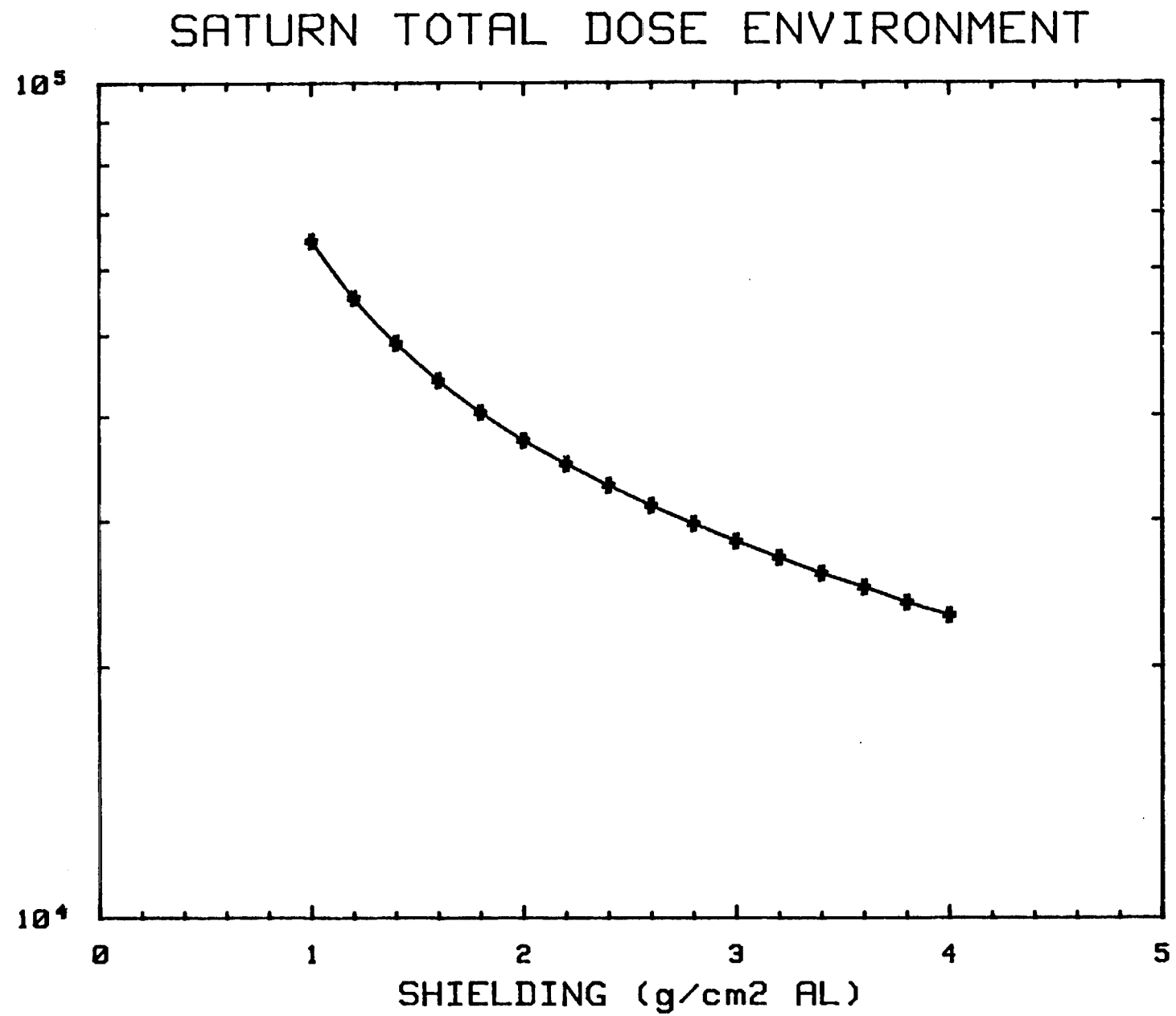
SATURN TOTAL DOSE ENVIRONMENT
TOTAL DOSE RADS (SI)
10^5
10^4
0
1
2
3
4
5
SHIELDING (g/cm2 AL)

FIGURE 3-16

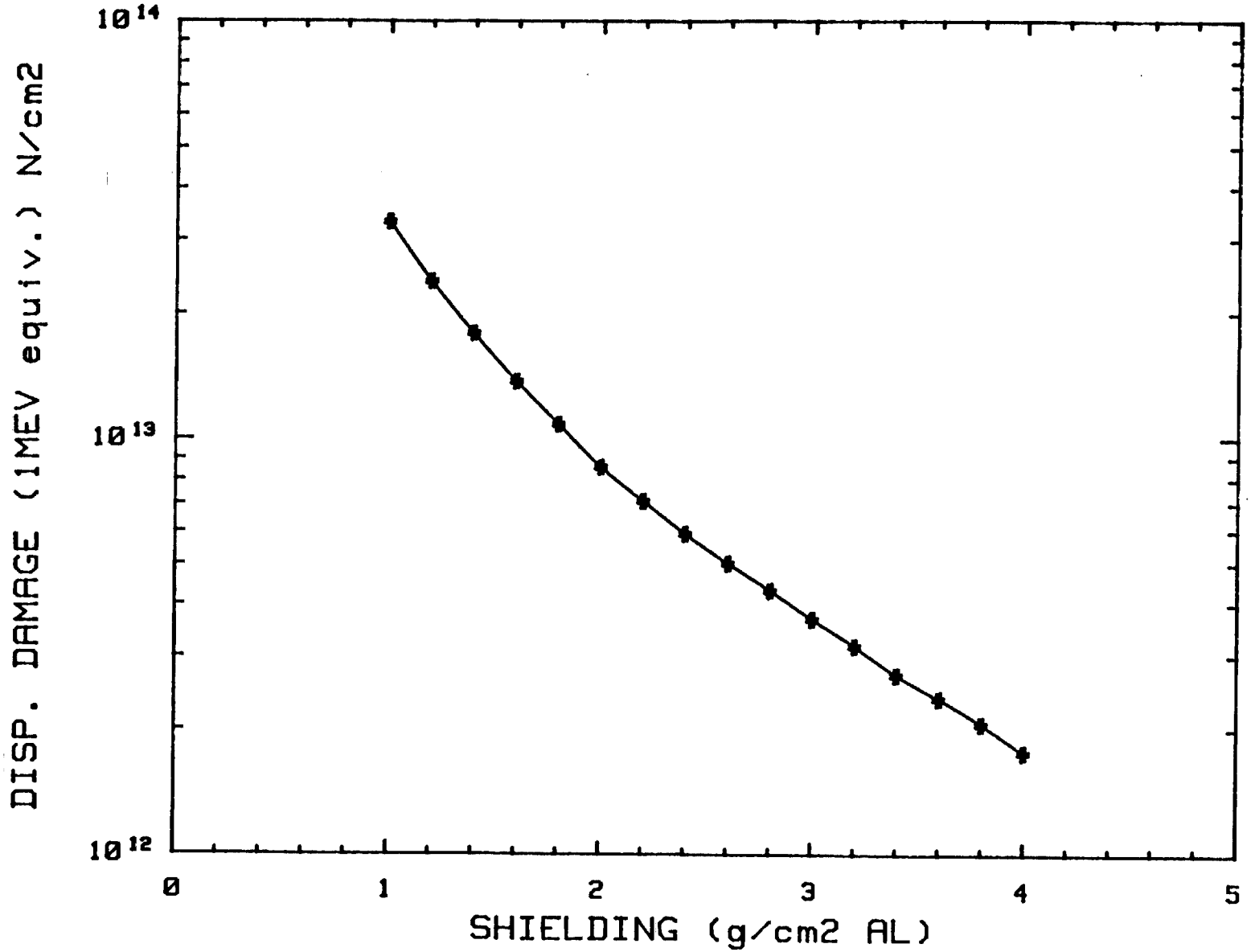
SATURN TOTAL DISPLACEMENT DAMAGE ENVIRONMENT
DISP. DAMAGE (1MEV equiv.) N/cm2
10 14
10 13
10 12
0
1
2
3
4
5
SHIELDING (g/cm2 AL)

FIGURE 3-17

OPTICAL BACKGROUND POWER

UPLINK

- EARTH BACKGROUND AT OPTRANSPAC
  - FUNCTION OF WAVELENGTH, RANGE, APERTURE, AND FOV AS WELL AS EARTH PHASE

- OFF-AXIS SCATTERING OF SUNLIGHT
  - FUNCTION OF WAVELENGTH, RANGE, APERTURE, FOV, AND OFF-AXIS SUN ANGLE

DOWNLINK

- SATURN BACKGROUND AT EORS
  - FUNCTION OF WAVELENGTH, APERTURE SIZE, AND FOV

- OFF-AXIS SCATTERING OF SUNLIGHT
  - FUNCTION OF WAVELENGTH, APERTURE SIZE, FOV, AND OFF-AXIS SUN ANGLE

EARTH TRACKER

- OFF-AXIS SCATTERING OF SUNLIGHT
  - FUNCTION OF WAVELENGTH BAND, APERTURE SIZE, FOV AND OFF-AXIS SUN ANGLE

FIGURE 3-18

scattering of light onto the array detector. On the downlink, the EORS receiver must concern itself with the radiation from Saturn and also off-axis scattering of solar radiation.

3.9.1 EARTH BACKGROUND AT OPTRANSPAC - The calculation of the Earth background at the OPTRANSPAC follows from the following analysis. The energy incident upon the Earth in a particular wavelength band was reduced by the albedo factor. The albedo factor of the Earth was taken to be approximately 30%. [Ref. 1]. The Earth was then assumed to re-radiate this energy into a 2π steradian half sphere. The energy flux at the OPTRANSPAC is then simply a function of the range from the OPTRANSPAC to the Earth. Figure 3-19 shows the range relationship on Earth background flux at the OPTRANSPAC for three distinct wavelengths of interest. Note, although the Earth moves through phases as viewed from the OPTRANSPAC, the radiant background energy was calculated on a "full Earth" assumption.

3.9.2 SOLAR BACKGROUND AT OPTRANSPAC - The amount of solar background incident upon the OPTRANSPAC detectors is a function of the Sun angle geometry, the off-axis solar rejection function and the wavelength of interest. For the OPTRANSPAC, the Sun angle geometry is sketched in Figure 3-20. The 90% availability requirement set forth in the statement of work defines the Sun angle requirement. As is seen in Figure 3-20, the Earth orbit has two places in each half orbit where the OPTRANSPAC to Sun Angle, α, is identical. Simple geometric algebra yields the expression of α as a function of link distance, D. Figure 3-21 shows the minimum Sun angle is given as approximately one degree off of boresight.

To determine the amount of solar energy that reaches the detectors, an off-axis stray light model was defined for the optical system. The off-axis stray light rejection model is pictured in Figure 3-22 and was taken from previous analysis performed for a similar telescope design on another Lasercom project. The rejection function, $S(\Theta)$, was obtained from a complex modeling of the stray light rejection properties of anti-reflective coatings, aperture, stops, telescope cleanliness levels, and baffle designs for specific telescopes. The assumption made here, with high confidence, was extrapolation to similar telescope designs with differing aperture sizes and viewfields was valid. The optical background power on the detector was readily obtained from this model.

The effective background radiance at the OPTRANSPAC due to the off-axis solar scattering is plotted versus link distance. The worst case angle (i.e. smallest off-axis angle) occurs at the maximum range from the Earth (smallest solar intensity). The two phenomenon, range loss and scatter function, tend to offset each other. As can be seen by the curves in Figure 3-23, the solar scattering background flux can be modeled as a constant over all range. To this end, the background radiant flux was modeled as the constant levels illustrated in Figure 3-23 for each of the three wavelengths.

3.9.3 SATURN BACKGROUND AT EORS - The background flux at the EORS platform due to Saturn was taken from recorded Earth orbit measurements of Saturn's irradiance [Ref. 2]. Since the EORS characteristics specify a one microradian viewfield and Saturn subtends approximately 95 Microradians when viewed from the Earth, the Saturn background flux must be expressed in terms of a radiance function (i.e. only a fraction of Saturn, about one ninetieth is viewed by the EORS). Figure 3-24 tabulates the effective Saturn background available at the

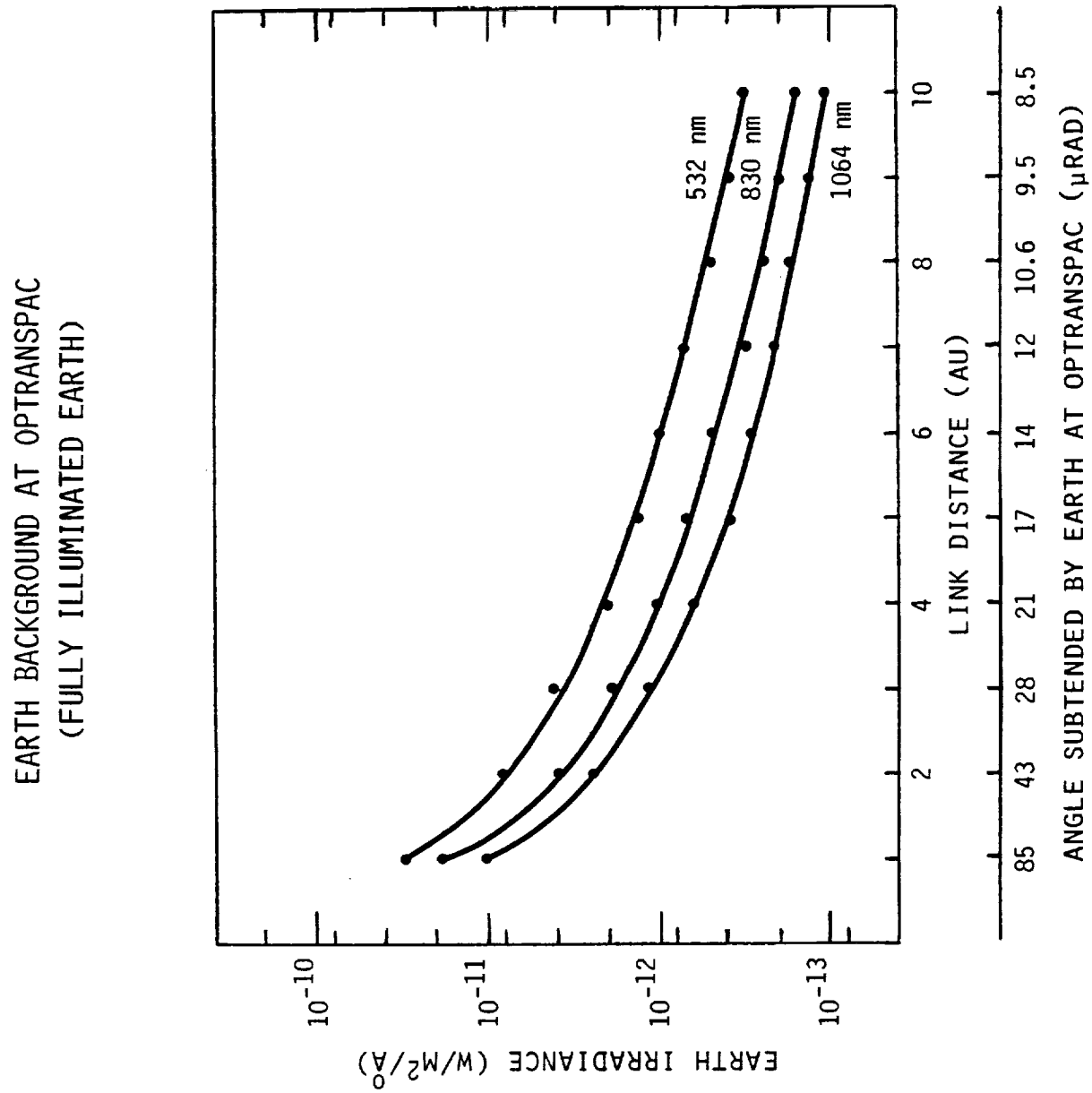
EARTH BACKGROUND AT OPTRANSPAC
(FULLY ILLUMINATED EARTH)
EARTH IRRADIANCE (W/M²/Å)
10⁻¹⁰
10⁻¹¹
10⁻¹²
10⁻¹³
532 nm
830 nm
1064 nm
2
4
6
8
10
LINK DISTANCE (AU)
85
43
28
21
17
14
12
10.6
9.5
8.5
ANGLE SUBTENDED BY EARTH AT OPTRANSPAC (μRAD)

FIGURE 3–19

SUN ANGLE GEOMETRY
(OPTRANSPAC)

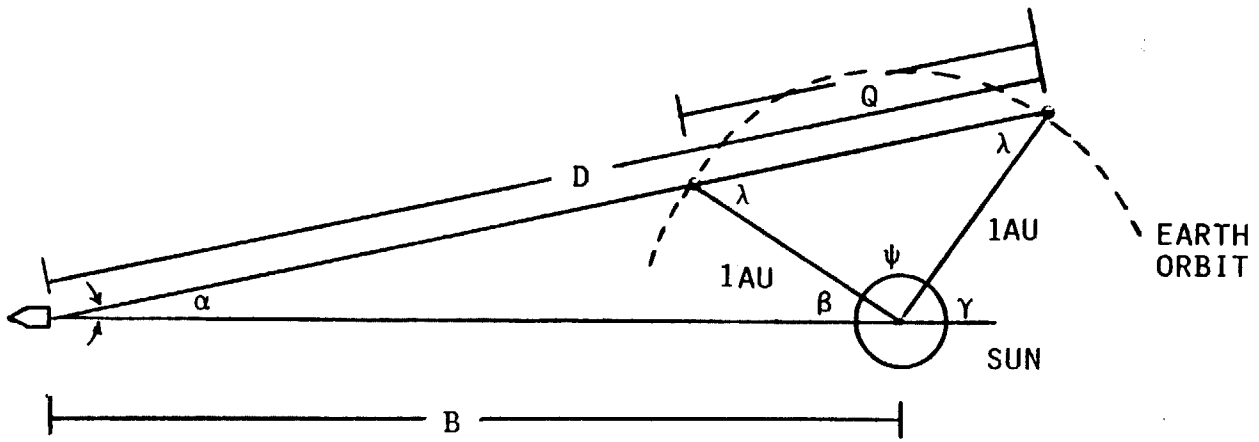

α = SUN ANGLE FROM OPTRANSPAC
SUN OUTAGES CAN OCCUR 10% OF THE TIME
THUS,

$\gamma + \beta = (180^{o})\ (.1) = 18^{o}$ $\qquad \psi = 162^{o}$

$\lambda = (180^{o} - 162^{o})/2 = 9^{o}$

$B = [D^{2} - 2D\ \cos\ (9^{o}) + 1]^{1/2}$

$\alpha = \sin^{-1} [\frac{\sin\ (9^{o})}{B}]$

FIGURE 3-20

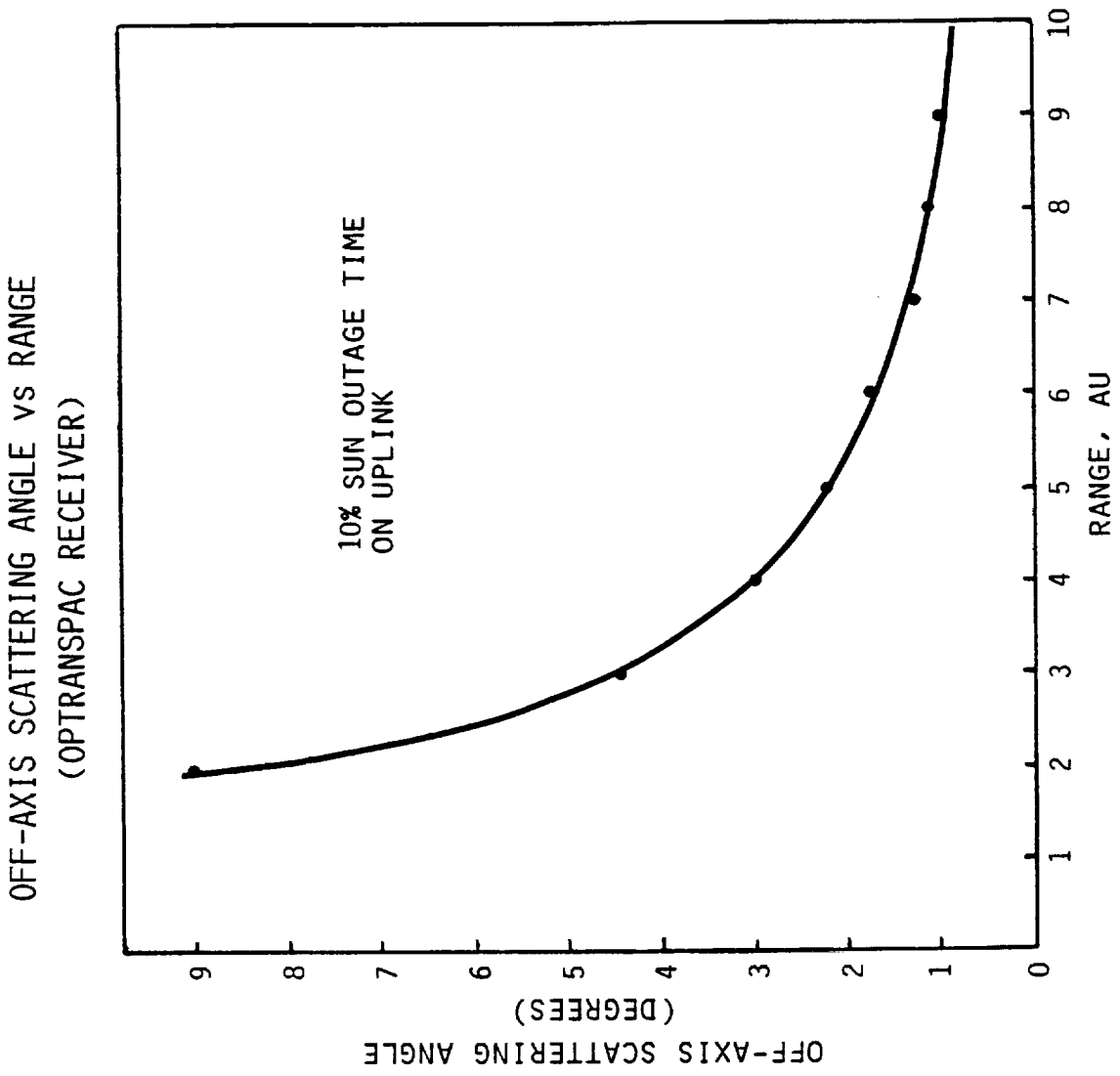
OFF-AXIS SCATTERING ANGLE vs RANGE
(OPTRANSPAC RECEIVER)
10% SUN OUTAGE TIME
ON UPLINK
OFF-AXIS SCATTERING ANGLE
(DEGREES)
0
1
2
3
4
5
6
7
8
9
RANGE, AU
1
2
3
4
5
6
7
8
9
10

FIGURE 3–21

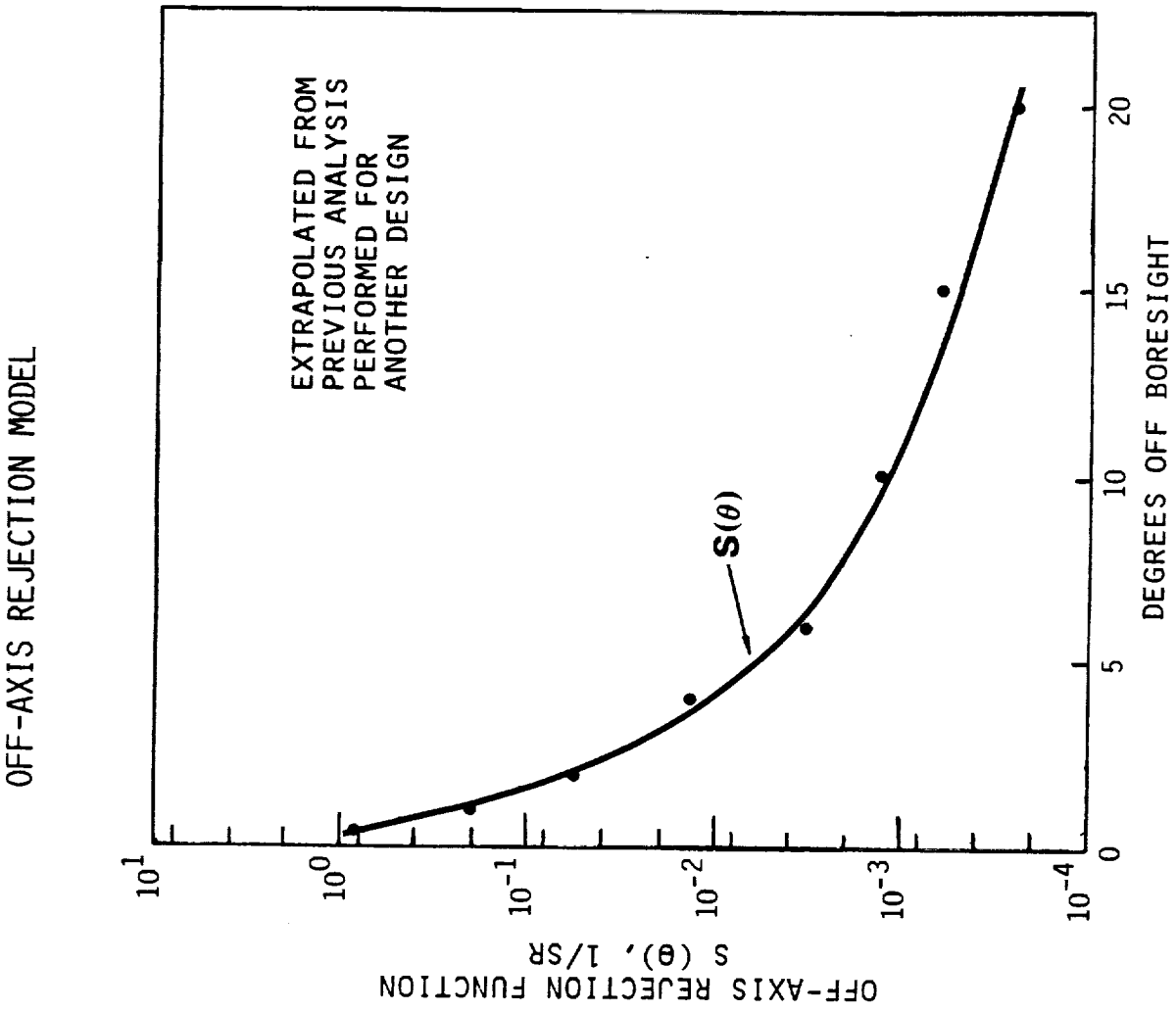
OFF-AXIS REJECTION MODEL
EXTRAPOLATED FROM
PREVIOUS ANALYSIS
PERFORMED FOR
ANOTHER DESIGN
S(θ)
OFF-AXIS REJECTION FUNCTION
S (θ), 1/SR
DEGREES OFF BORESIGHT
10^1
10^0
10^-1
10^-2
10^-3
10^-4
0
5
10
15
20

FIGURE 3–22

SOLAR BACKGROUND RADIANCE AT OPTRANSPAC
DUE TO OFF-AXIS SCATTERING

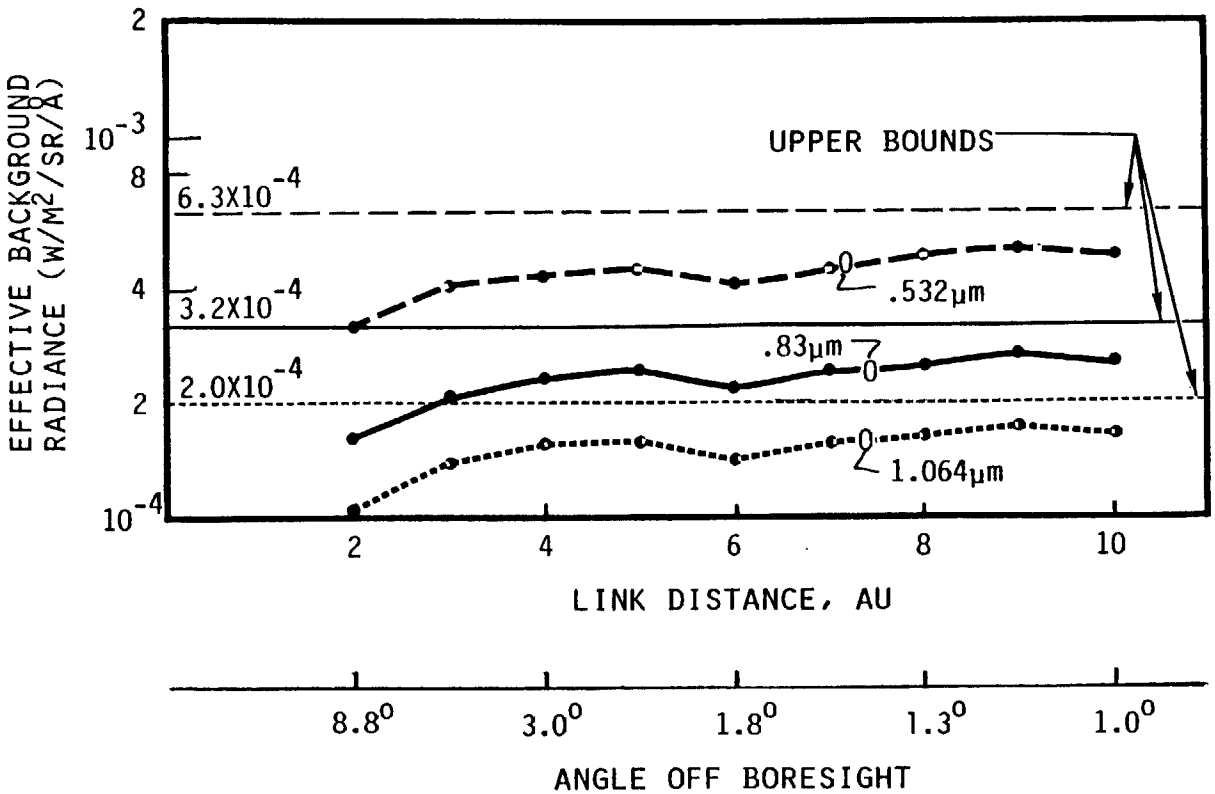

FIGURE 3-23

SATURN BACKGROUND AT EORS

λ NM	IRRADIANCE $W/M^2/A^o$	RADIANCE* $W/M^2/SR/A^o$
532	$8X10^{-12}$	$1.14X10^{-3}$
830	$3.2X10^{-12}$	$4.55X10^{-4}$
1064	$2X10^{-12}$	$2.85X10^{-4}$

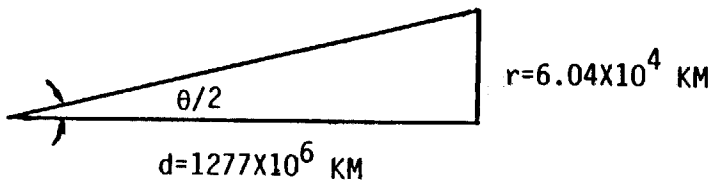

$\theta = 2.\text{ARC TAN } (\frac{r}{d})$

$\theta = 94.6\ \mu\text{RAD}$

* VALID FOR FIELD-OF-VIEWS LESS THAN θ

FIGURE 3-24

EORS. The radiance function was used directly with the field-of-view, aperture size, optical filter bandwidth and optics transmission, to obtain the background optical power on the EORS detector.

3.9.4 SOLAR BACKGROUND AT EORS - Once again the amount of solar background radiation is a function of the Sun angle geometry and off-axis solar rejection. The EORS Sun angle geometry (See Figure 3-25) was calculated similar to the OPTRANSPAC geometry (See Section 3.9.2) except the 90% availability requirement encompasses only the "backside" EORS position. The angle γ was fixed at 18 degrees and the off-axis angle, β, was given by the range between the EORS and the OPTRANSPAC. The off-axis scattering angle versus range for the EORS receiver boresight is illustrated in Figure 3-26.

The scatter function, $S(\Theta)$, defined in Figure 3-22, was used in conjunction with the solar radiance measured in the Earth's atmosphere to define the background radiance. Figure 3-27 shows the effective background radiance as a function of the link distance for the EORS. The background radiant flux is larger at close range and becomes less at long ranges (i.e., the off-axis angle increases). The link margin close in was sufficiently large to offset the increase in background power. Thus, the links were designed to accommodate maximum range background.

SUN ANGLE GEOMETRY
(EORS)

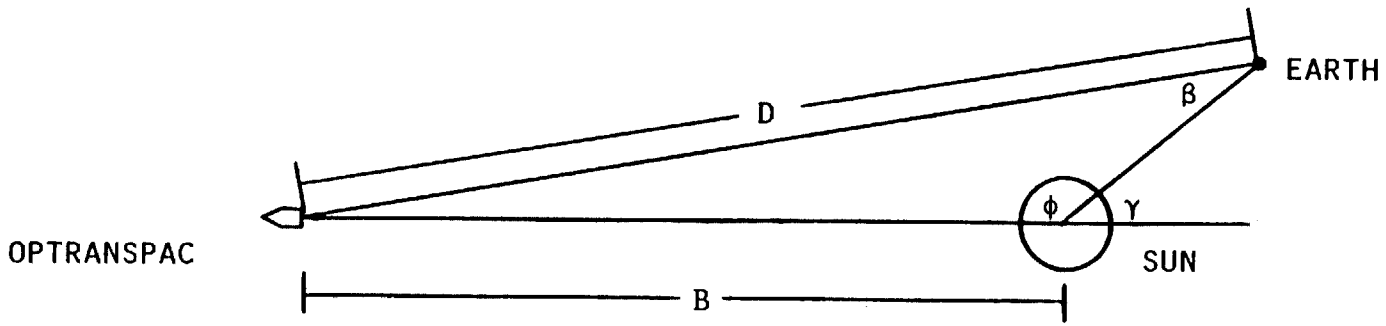

β = OFF-AXIS SUN ANGLE AT EORS
WITH 90% ORBITAL AVAILABILITY REQUIRED

$\gamma = (180^{o})\ (.1) = 18^{o}$

$\phi = 180^{o} - 18^{o} = 162^{o}$

$B = \cos\ (162^{o}) + [\cos^{2}\ (162^{o}) + (D^{2} + 1)]^{1/2}$

$\beta = \sin^{-1}\ [\frac{B\ \sin\ \phi}{D}\ ]$

FIGURE 3-25

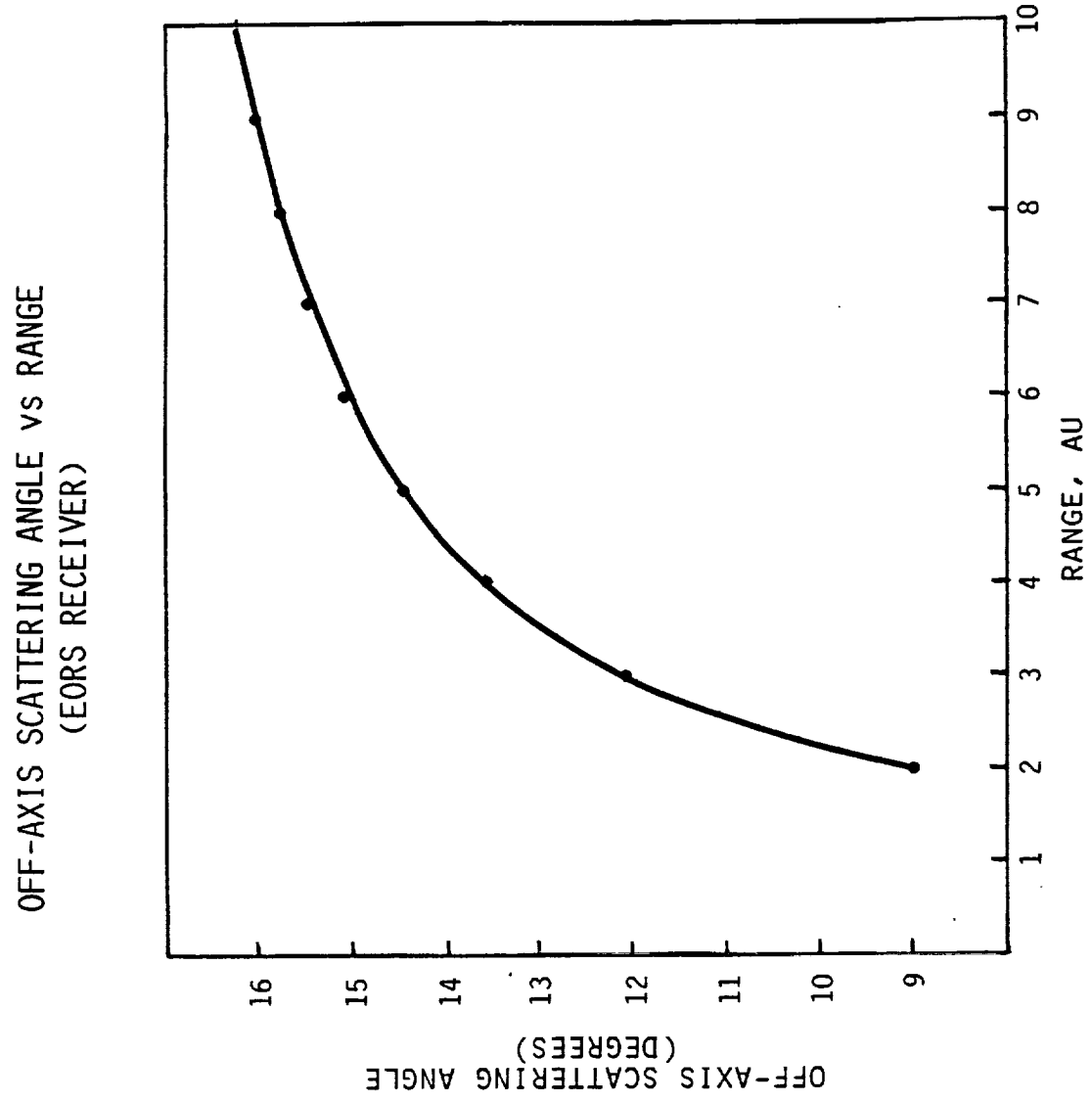
OFF-AXIS SCATTERING ANGLE vs RANGE
(EORS RECEIVER)
OFF-AXIS SCATTERING ANGLE
(DEGREES)
16
15
14
13
12
11
10
9
1
2
3
4
5
6
7
8
9
10
RANGE, AU

FIGURE 3–26

SOLAR BACKGROUND RADIANCE
AT EORS
(DUE TO OFF-AXIS SCATTERING)

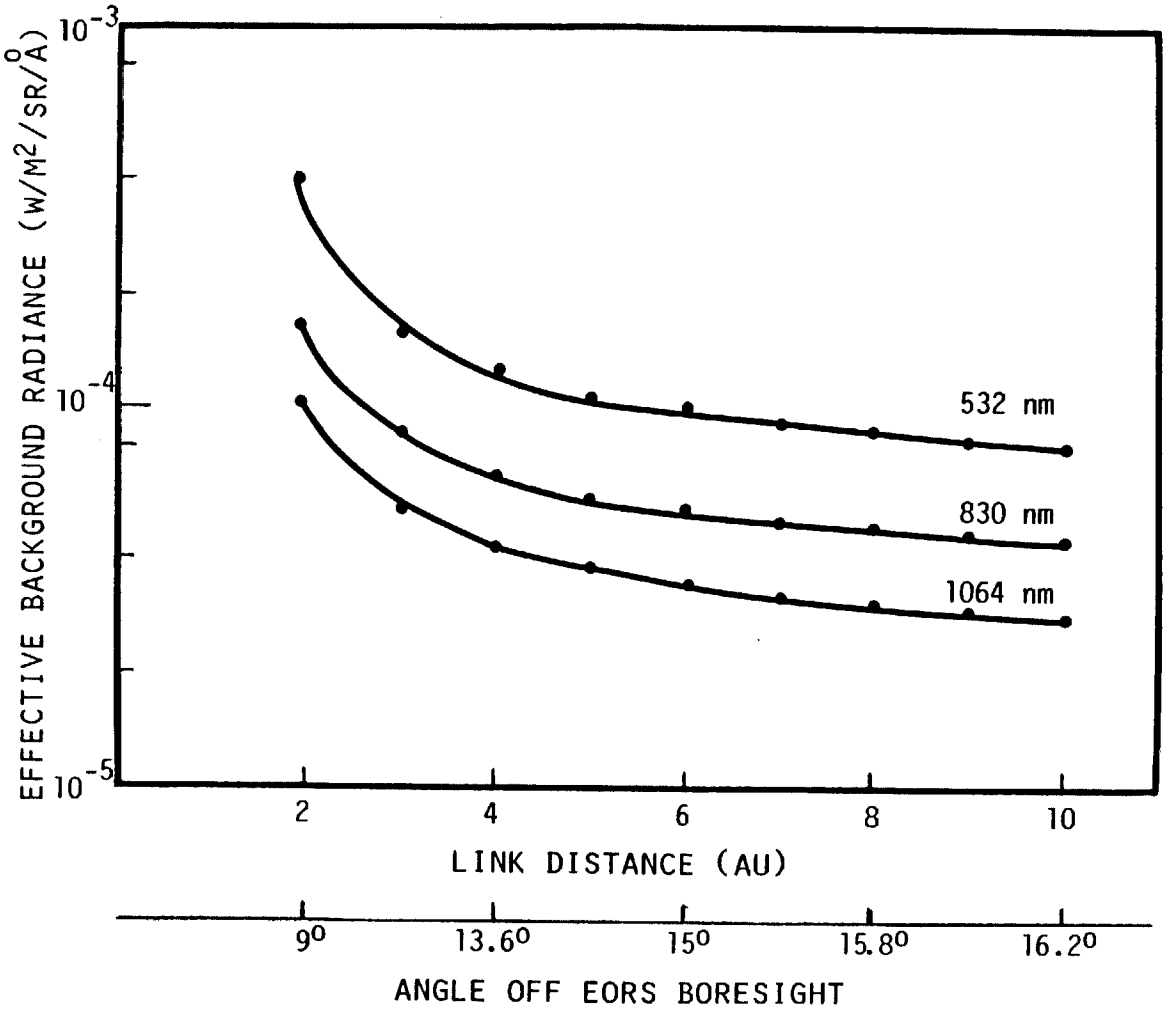

FIGURE 3-27

4.0 FUNCTIONAL ORGANIZATION

Various system configurations were envisioned as possible solutions to the OPTRANSPAC design. From these, one configuration was selected as the baseline design. A detailed system block diagram and functional description was also generated for the baseline design. A detailed optical layout was then generated based on the configuration selected.

4.1 BASELINE SELECTION RATIONALE - Eight possible system configurations were considered for the OPTRANSPAC terminal design. Five major functions were identified as trade space. The design rationale was to minimize system complexity and weight. Continuous or static alignment was necessary to maintain transmit/receive path alignment during OPTRANSPAC lifetime. Point-ahead compensation was necessary to correct for line-of-sight variations due to platform velocity aberrations. Earth tracking was considered as necessary to provide track capability when no beacon is present (i.e., the EORS disappears behind the Earth). Beacon track existed as a trade parameter or option. Beacon communications was required by the statement of work.

Figure 4-1 shows the baseline configuration selection rationale trade matrix. Figures 4-2 through 4-9 illustrate the optical systems associated with each of the eight systems configurations. The baseline selection process quickly eliminated options B,C,E,F, and G since no beacon communication was possible. Option H was ruled out because the wide viewfields required severely taxed the quadrant detector Earth tracker option. Options A and D became the only viable solutions out of the original eight. Option A was chosen over option D because it offered a lighter weight and less complex (fewer mechanisms) solution to the OPTRANSPAC design.

4.2 SYSTEM CONFIGURATION - The top level OPTRANSPAC terminal configuration is shown in Figure 4-10. The OPTRANSPAC system at the box level consists of an Electronics Assembly and Electro-Optics Assembly. The Electronics Assembly consist of a Power Conditioner Unit, a Communications Electronics Assembly and a Control Electronics Assembly. The Electro-Optics Assembly contains a telescope, imaging optics, downlink laser, Earth tracker head assembly, and beacon communication detector. Figure 4-11 illustrates the OPTRANSPAC signal flow from, and to, each of the subassemblies. The functional description of each subassembly is listed below:

Fixed Mounted Telescope:
- The uncertainty area of the platform is within its viewfield.
- Allows diffraction limited transmit operation.
- Collects beacon and Earth radiation and relays it to the imaging optics.

Imaging Optics:
- Provides for dichroic separation of transmit and receive paths.
- Allows for co-alignment of transmit and receive paths.
- Transfers optical energy from laser to telescope and from telescope to appropriate detectors.
- Contains tracking mirrors for vernier tracking function and viewfield scan.

Downlink Laser:
- Generates 532 nm laser radiation in a pulsed format encoded with information from the communication electronics.

BASELINE CONFIGURATION SELECTION RATIONALE

CONSIDERATIONS	OPTIONS								COMMENTS
	A	B	C	D	E	F	G	H	
ALIGNMENT									NECESSARY FOR LONG LIFE STABILITY, AT LEAST IN STATIC FORM
STATIC	YES	YES	YES	YES	YES	YES	YES	YES	
CONTINUOUS	YES	YES	YES	NO	NO	NO	NO	NO	
POINT-AHEAD									NO MECHANICAL DEVICES WOULD BE BEST, ESPECIALLY IF NO ADDITIONAL WEIGHT PENALTY IS INCURRED
DETECTOR OFFSET	YES	YES	YES	NO	NO	NO	NO	NO	
MECHANICAL	NO	NO	NO	YES	YES	YES	YES	YES	
EARTH TRACKER									QUADRANT TRACKER LIMITED BY BACKGROUND - PROBLEMS WHEN USED WITH WIDE VIEWFIELDS
ARRAY TRACKER	YES	YES	YES	YES	YES	YES	NO	NO	
QUADRANT DETECTOR	NO	NO	NO	NO	NO	NO	YES	YES	
BEACON TRACK	NO	YES	NO	NO	YES	NO	NO	YES	NOT NECESSARY WITH EARTH TRACKER
BEACON COMMUNICATION									BEACON COM REQUIRED BY SOW - - NOT FEASIBLE AT 10 AU WITH QAPD
WITH DEDICATED APD	YES	NO	NO	YES	NO	NO	NO	YES	
WITH BEACON QAPD	NO	YES	NO	NO	YES	NO	NO	NO	

FIGURE 4-1

OPTRANSPAC OPTICAL CONFIGURATION
OPTION A

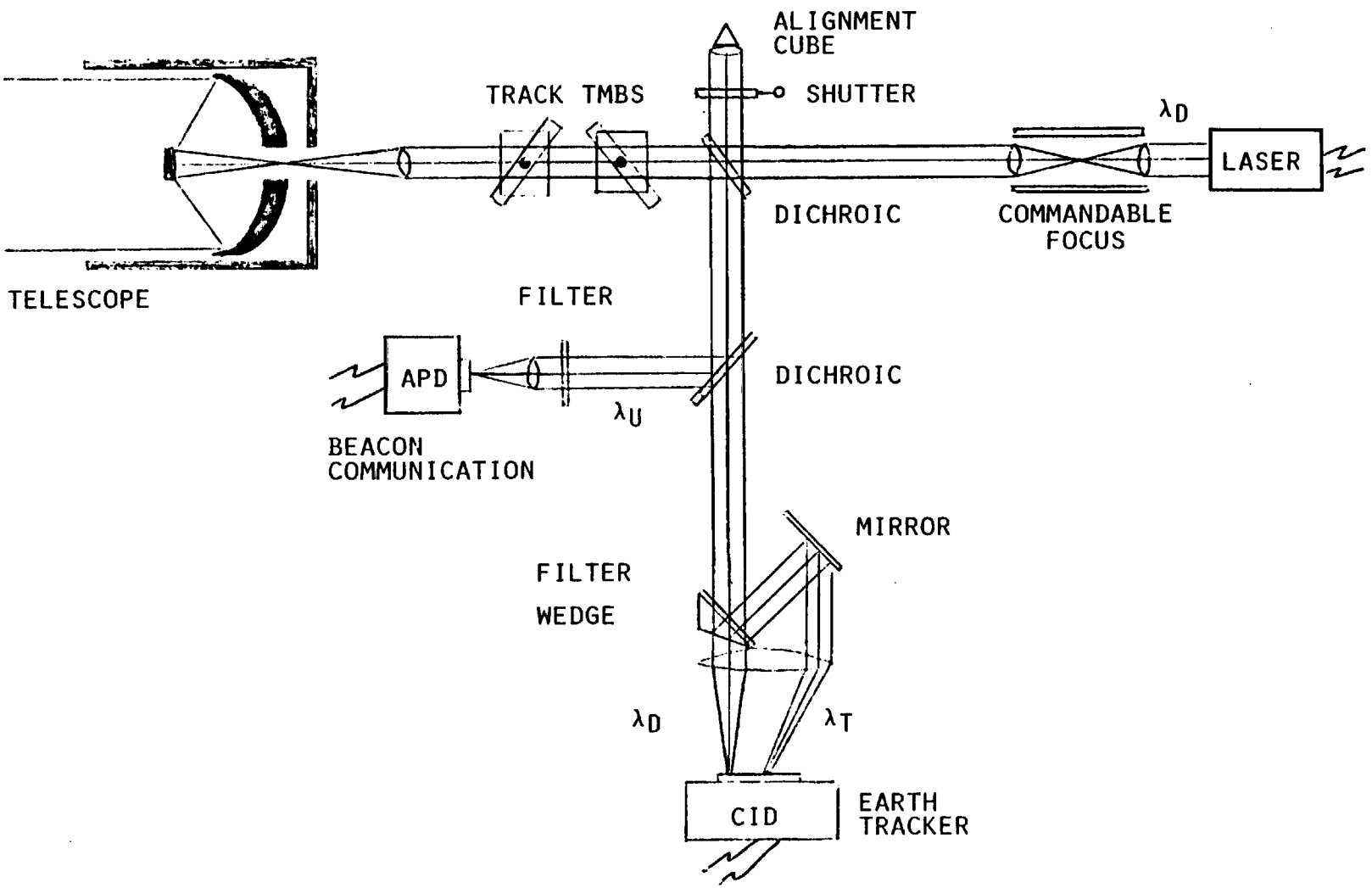

FIGURE 4-2

OPTRANSPAC OPTICAL CONFIGURATION
OPTION B

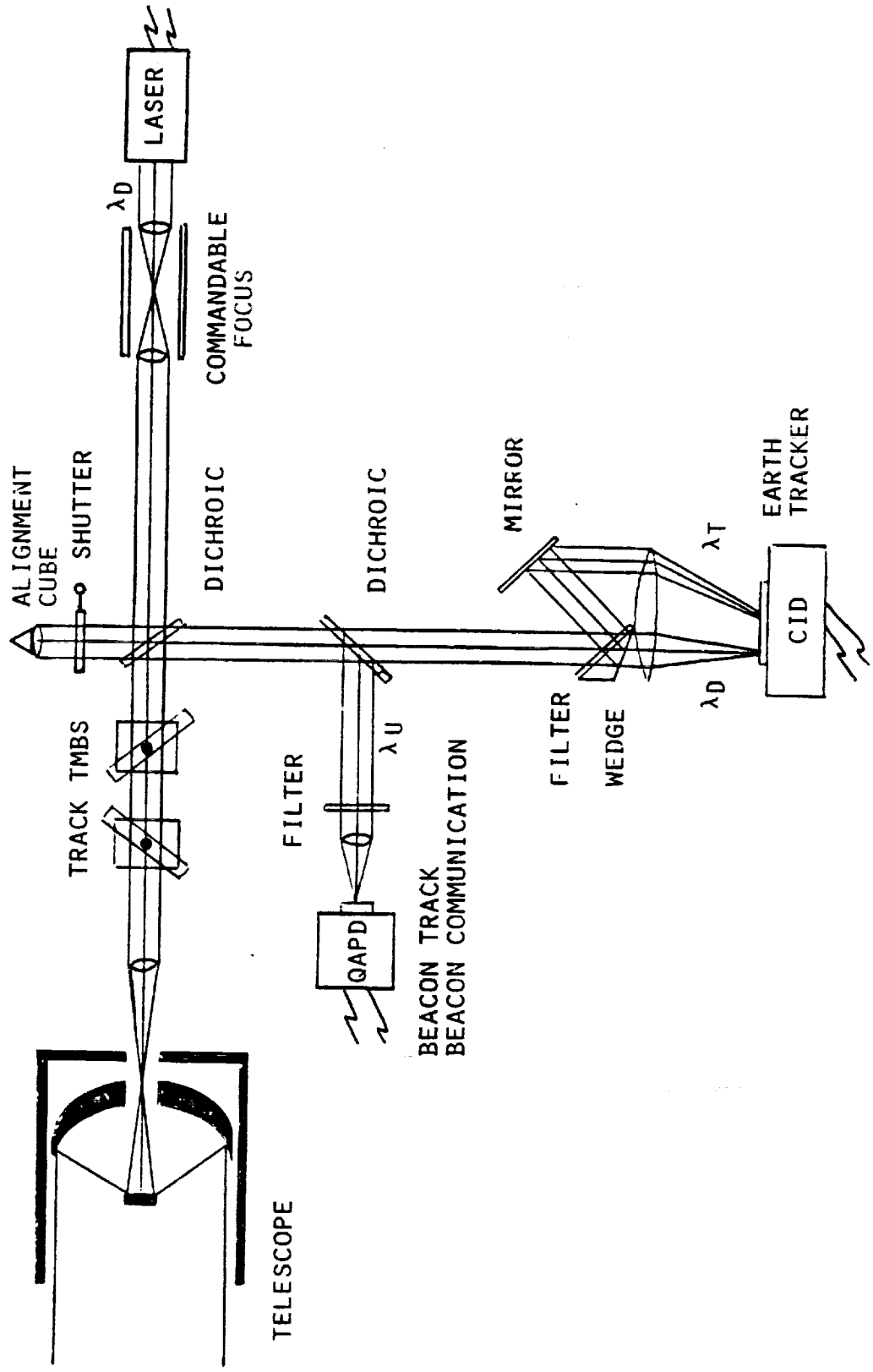

FIGURE 4–3

OPTRANSPAC OPTICAL CONFIGURATION
OPTION C

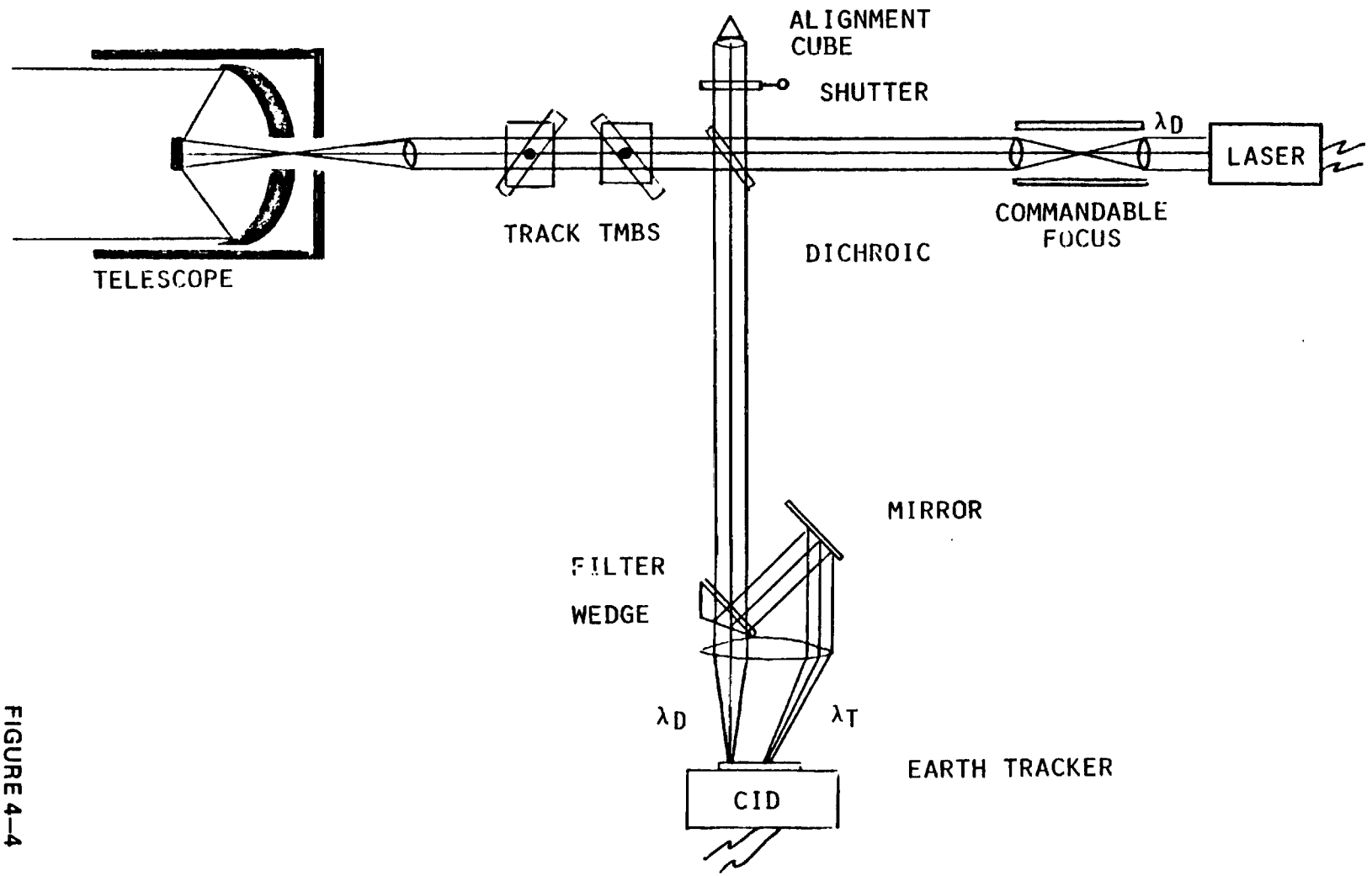

FIGURE 4-4

OPTRANSPAC OPTICAL CONFIGURATION
OPTION D

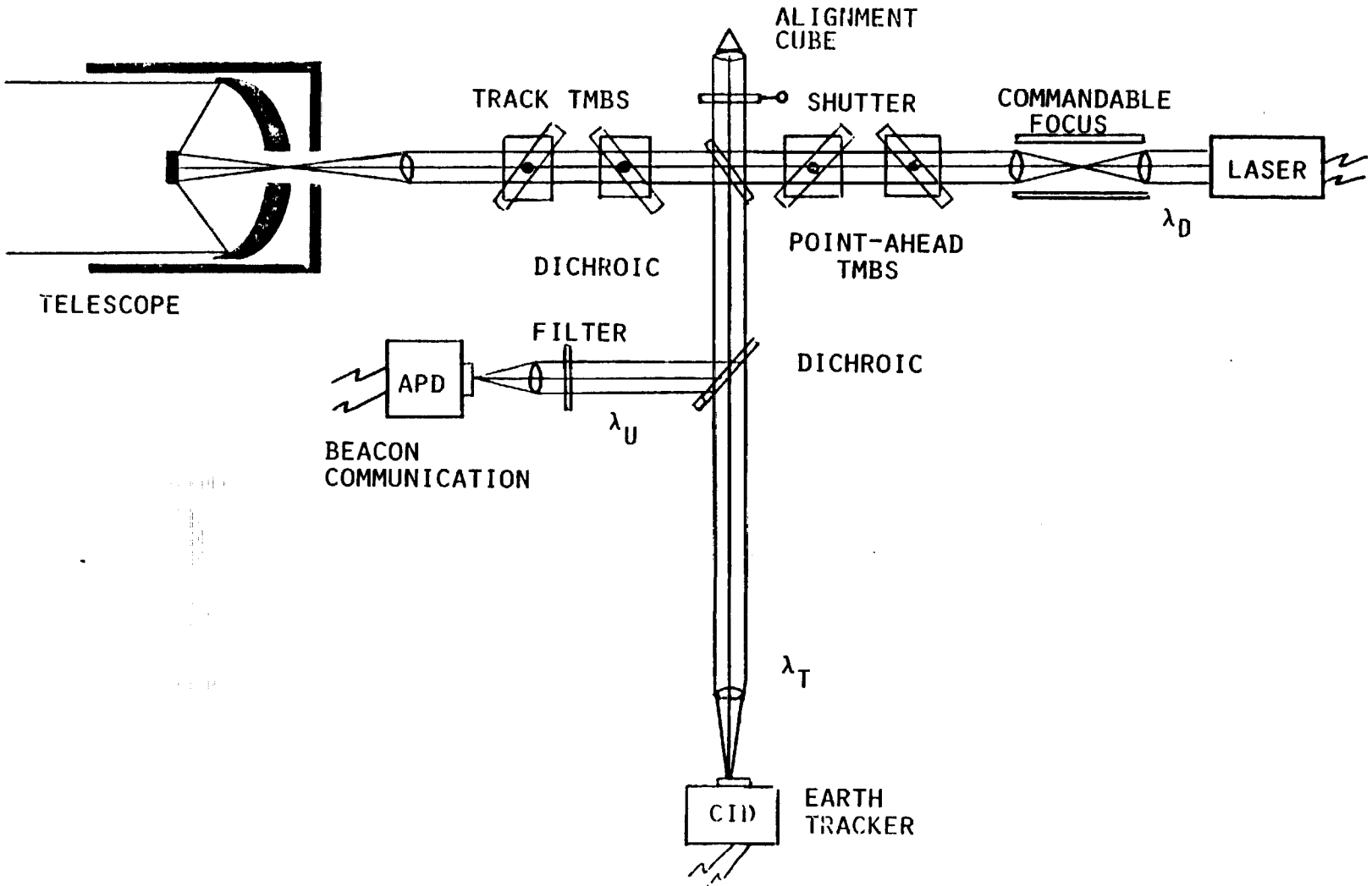

FIGURE 4-5

OPTRANSPAC OPTICAL CONFIGURATION
OPTION E

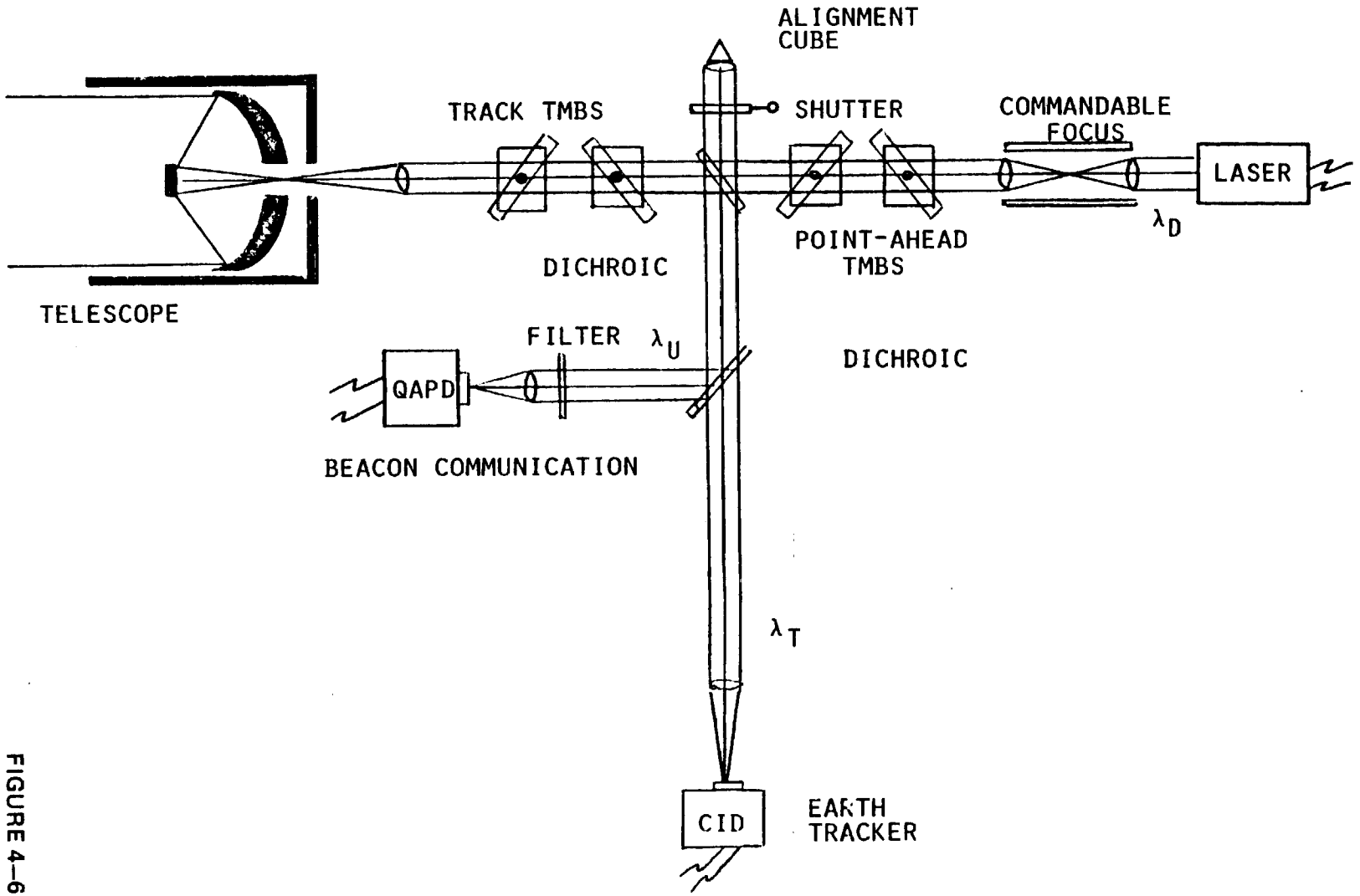

FIGURE 4-6

OPTRANSPAC OPTICAL CONFIGURATION
OPTION F

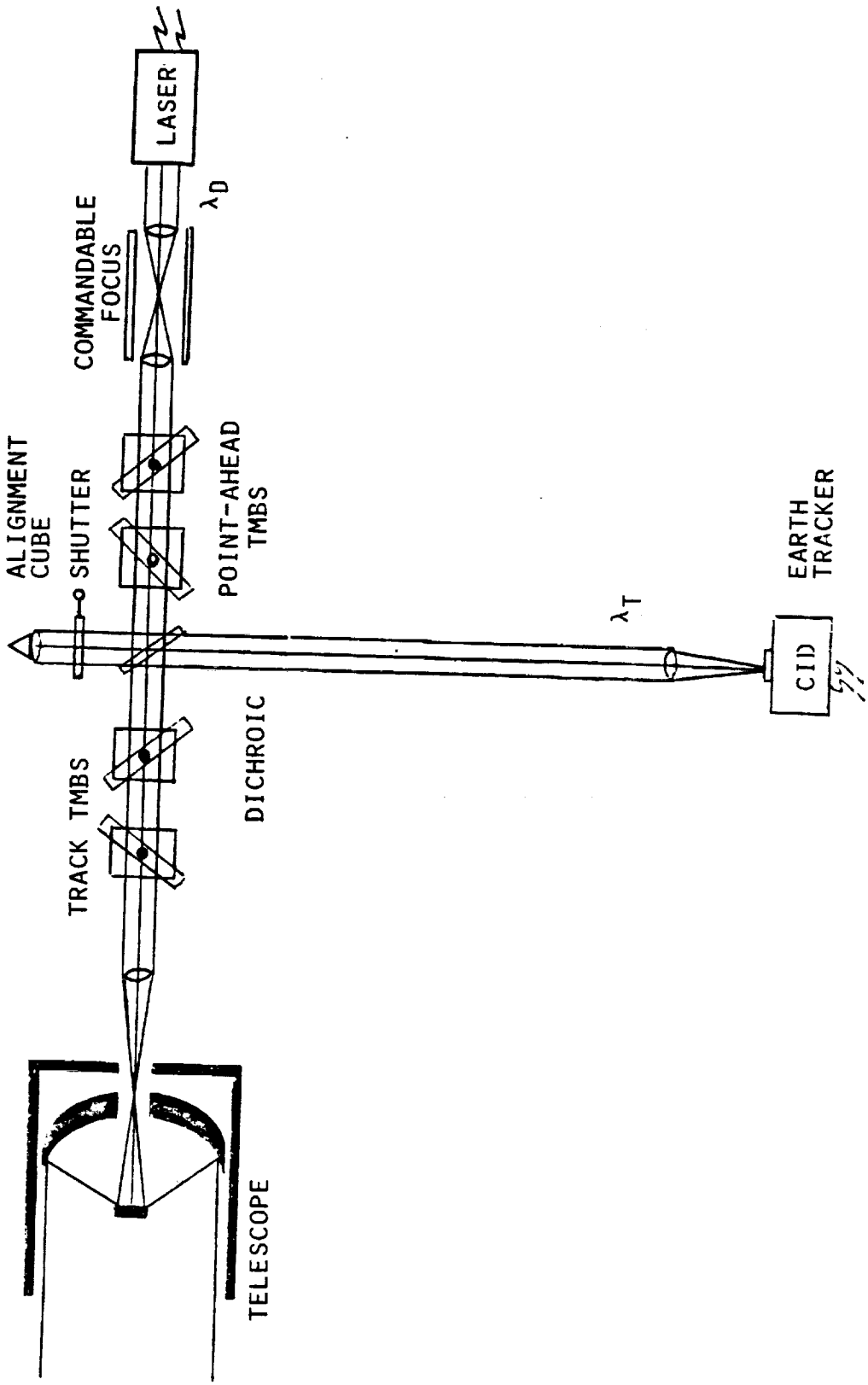

FIGURE 4–7

OPTRANSPAC OPTICAL CONFIGURATION
OPTION G

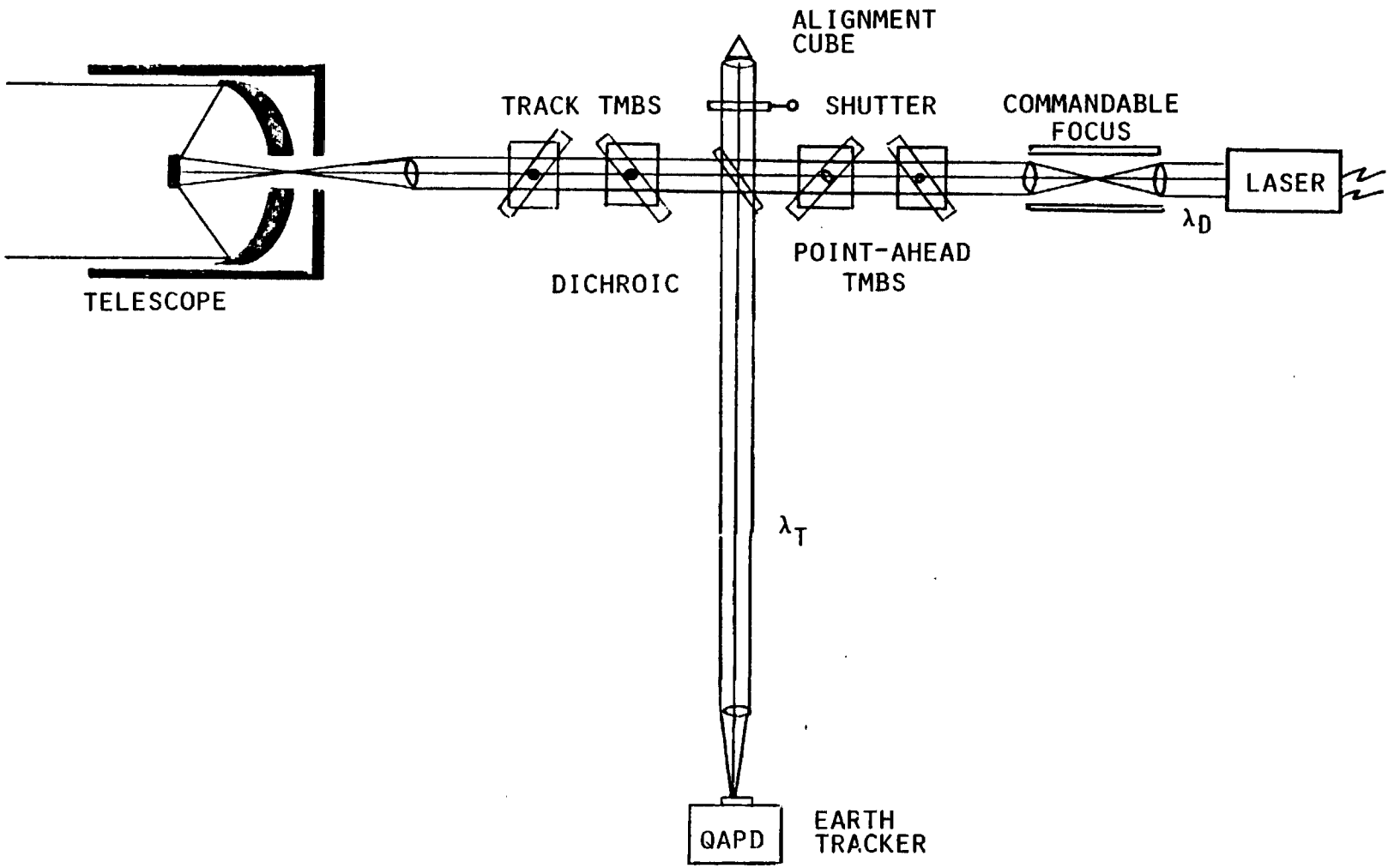

FIGURE 4-8

OPTRANSPAC OPTICAL CONFIGURATION
OPTION H

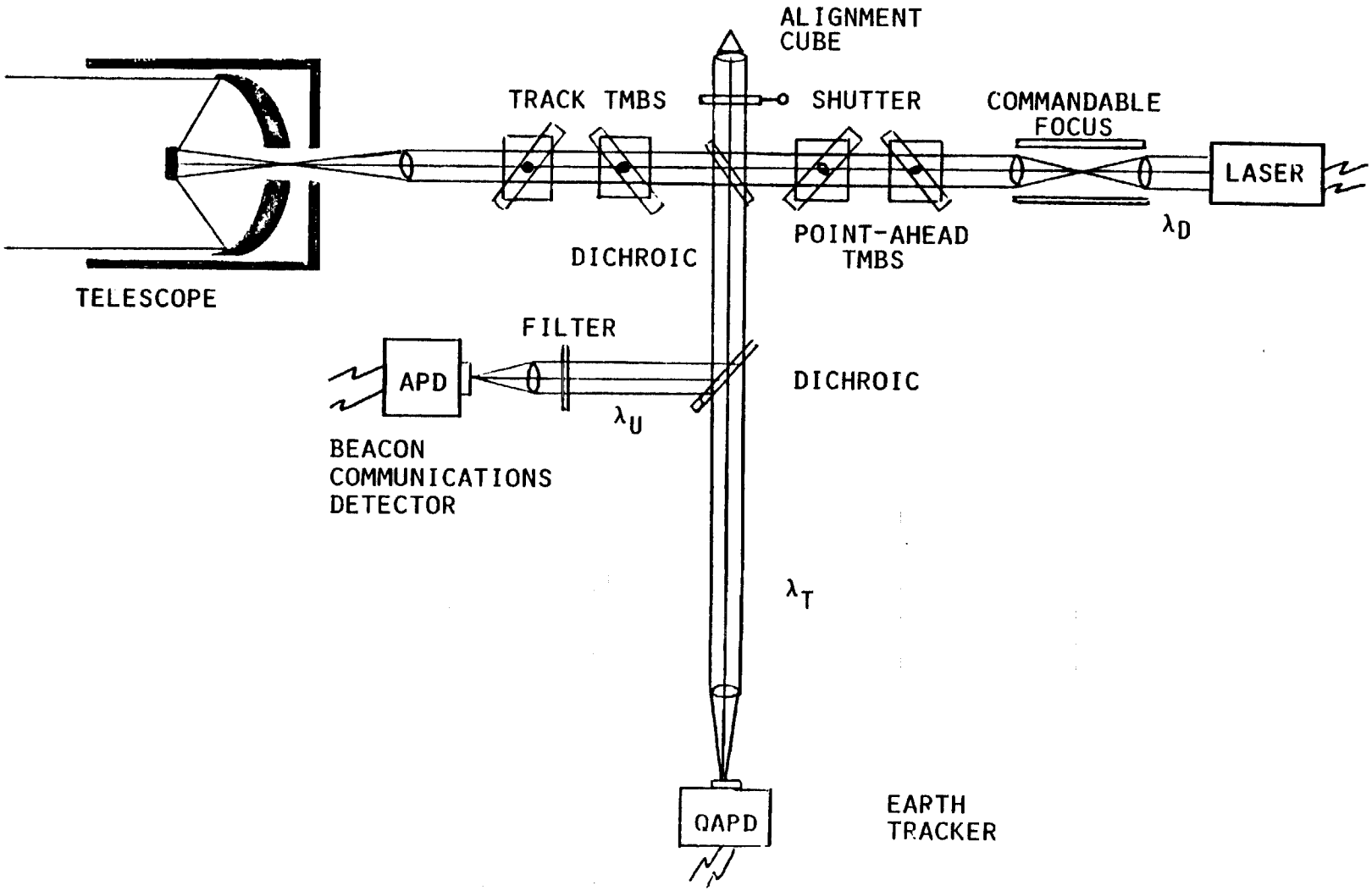

FIGURE 4-9

OPTRANSPAC TOP LEVEL DESCRIPTION

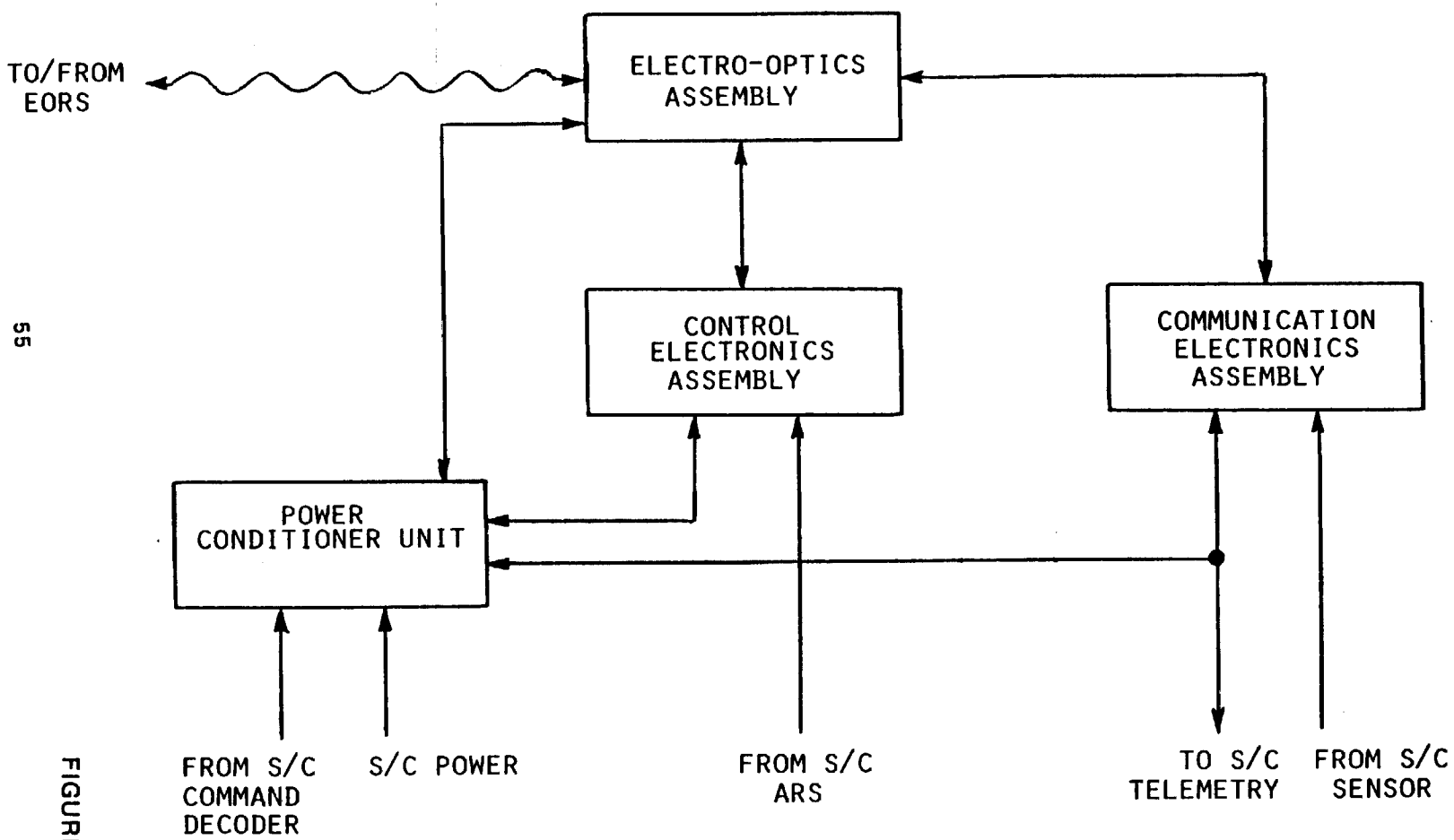

FIGURE 4-10

OPTRANSPAC SYSTEM CONFIGURATION

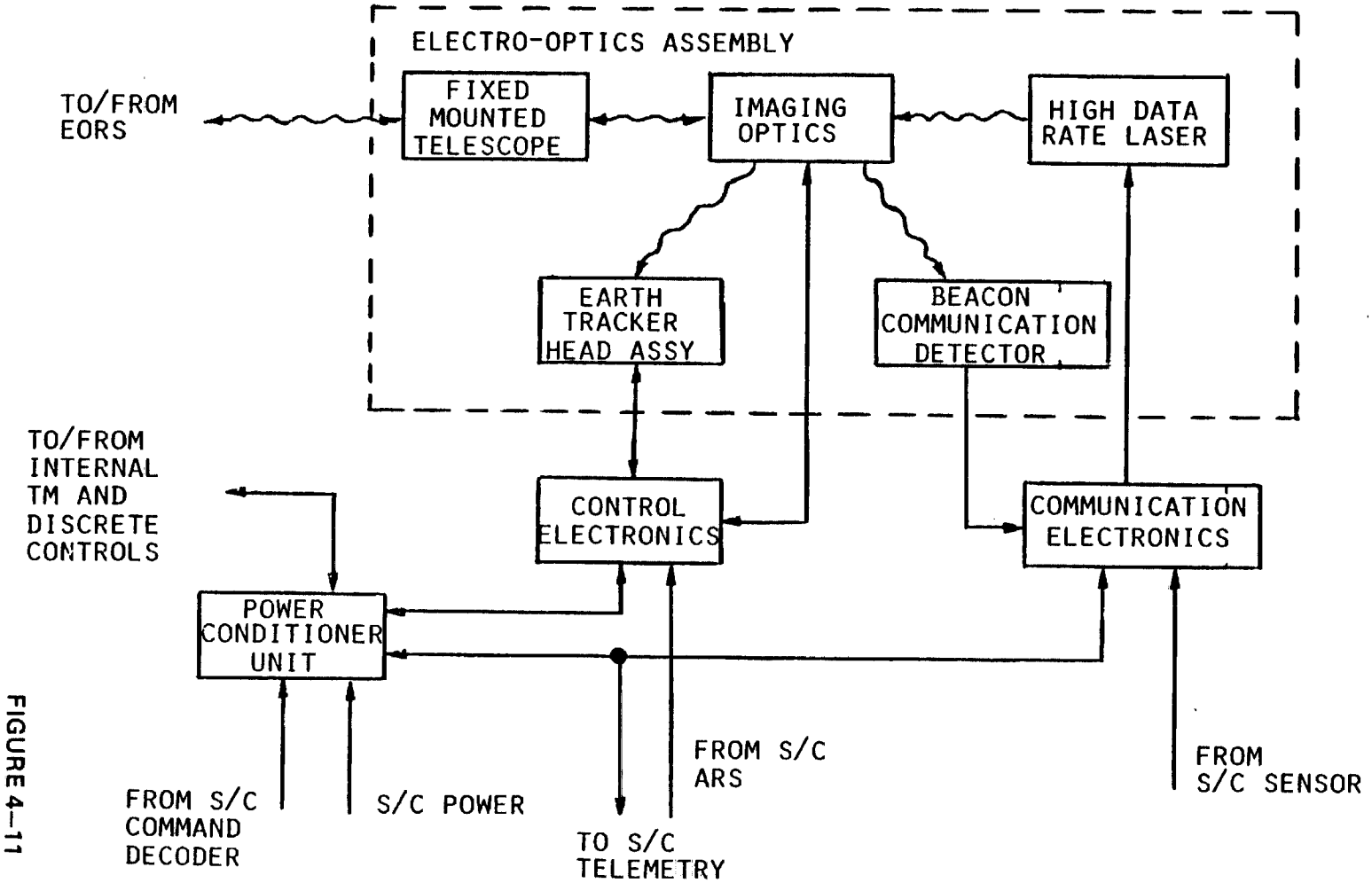

FIGURE 4-11

Earth Tracker Head Assembly:
- An array detector used for point-ahead and Earth tracking functions.

Beacon Communication Detector:
- An avalanche photodiode used for beacon communication

Communication Electronics:
- Provides for pulse position modulation conversion of input data from the spacecraft.
- Encodes input data from spacecraft into a rate 7/8 Reed-Solomon code word.
- Decodes rate 7/8 Reed-Solomon data from beacon link.
- Demodulates the pulse position modulated signal in a "greatest-of" format.

Control Electronics:
- Provides for Earth track capability.
- Controls all OPTRANSPAC modes of operation.
- Controls alignment function.
- Interfaces with spacecraft attitude reference system and Earth tracker error signals to provide TMBS track commands.
- Calculates point-ahead angle offsets to be used by the Earth tracker.
- Communicates with spacecraft control processor for time of day and orbital information.

Power Conditioner Unit:
- Provides all prime power conditioning for the various OPTRANSPAC components.
- Provides telemetry multiplexing of monitor signals for telemetry link.
- Controls all OPTRANSPAC redundancy switching

4.3 OPTICAL SYSTEM DESCRIPTION - The system level layout of the optical train is given in Figure 4-12. Descriptions of the optical elements employed in the OPTRANSPAC system are given in Figure 4-13. The optical design consists of a diffraction limited eleven inch modified Cassegrain Telescope coupled into an imaging optics assembly. The telescope maintains an image quality of at least $\lambda/20$ RMS at the transmit wavelength of 532 nanometers over a $\pm$ 2.5 milliradian transmit viewfield.

The imaging optics contains beam steering mirrors for vernier tracking and optical relay elements that transfer the transmit laser energy to the telescope as well as transfer the received energy to the appropriate detectors. Dichroic filters were used to differentiate between the transmit and receive paths which allowed use of common path optics. Redundant paths around active elements were used to eliminate single point failures. Redundant switching of active elements, such as lasers and detectors was accomplished through use of solenoid driven "pop" mirrors. The Earth track optics path offset dichroic boresight alignment device allowed for Earth track, continuous alignment, and electrical point-ahead functions to be implemented in one optics path design.

OPTRANSPAC OPTICAL SCHEMATIC

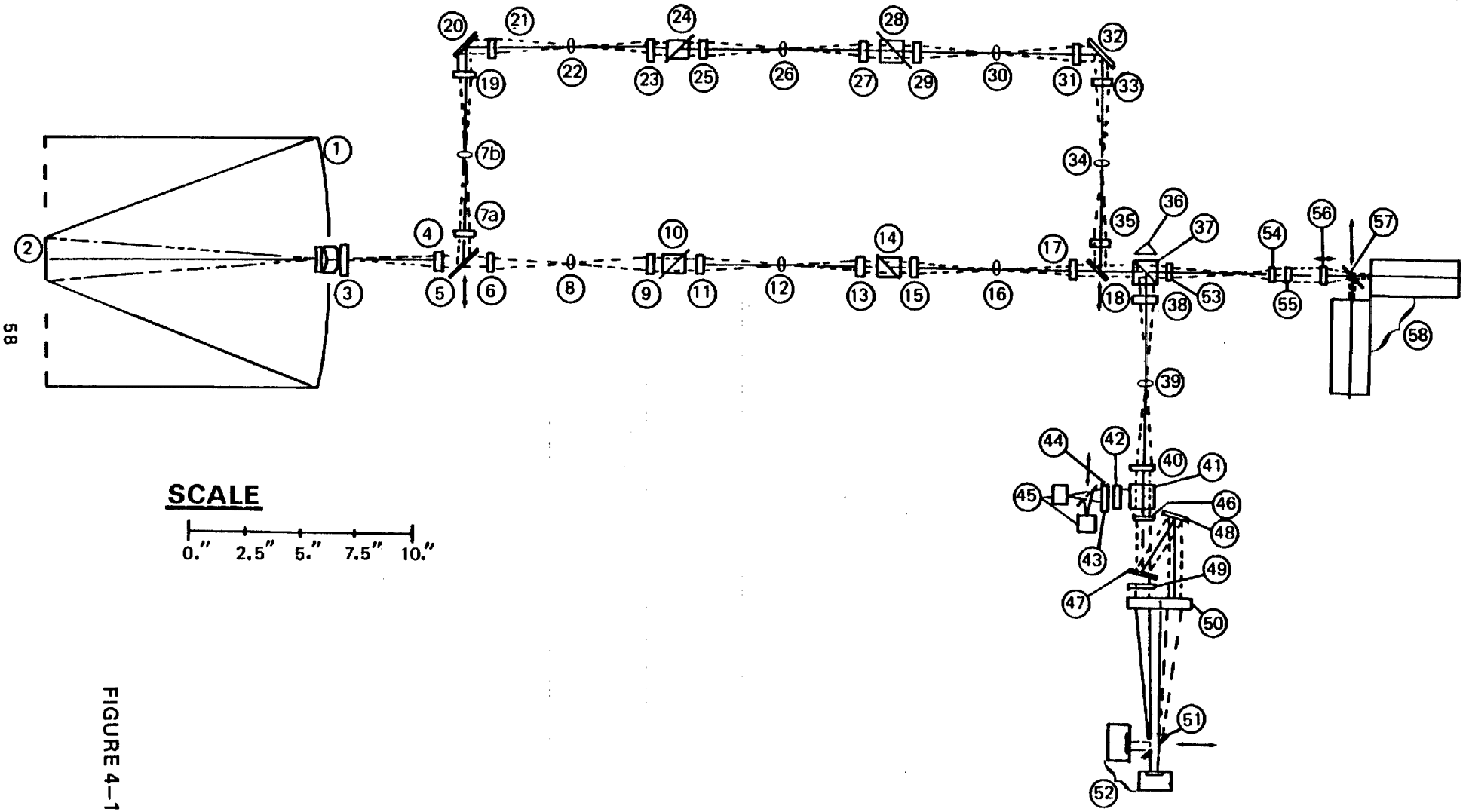

FIGURE 4–12

OPTICAL SCHEMATIC KEY

NUMBER	OPTICAL PATH	COMPONENT DESCRIPTION
1	TELESCOPE	CASSEGRAIN PRIMARY MIRROR
2	TELESCOPE	CASSEGRAIN SECONDARY MIRROR
3	TELESCOPE	FIELD CORRECTION GROUP
4	COMMON (PRIME & REDUNDANT)	COLLIMATOR
5	COMMON (PRIME & REDUNDANT)	REDUNDANT SELECT MECHANISM ("POP MIRROR")
6, 8, 9	COMMON (PRIME)	COLLIMATOR-FIELD LENS-COLLIMATOR GROUP ("CFC")
10	COMMON (PRIME)	TORQUE MOTOR BEAM STEERER (TMBS)
11, 12, 13	COMMON (PRIME)	CFC GROUP
14	COMMON (PRIME)	TMBS
15, 16, 17	COMMON (PRIME)	CFC GROUP
18	COMMON (PRIME & REDUNDANT)	REDUNDANT SELECT MECHANISM ("POP MIRROR")
7A, 7B, 19	COMMON (REDUNDANT)	CFC GROUP
20	COMMON (REDUNDANT)	TYPICAL FOLD MIRROR
21,22,23	COMMON (REDUNDANT)	CFC GROUP
24	COMMON (REDUNDANT)	TMBS
25, 26, 27	COMMON (REDUNDANT)	CFC GROUP
28	COMMON (REDUNDANT)	TMBS
29, 30, 31	COMMON (REDUNDANT)	CFC GROUP
32	COMMON (REDUNDANT)	TYPICAL FOLD MIRROR

FIGURE 4-13

OPTICAL SCHEMATIC KEY
(CONTINUED)

NUMBER	OPTICAL PATH	COMPONENT DESCRIPTION
33, 34, 35	COMMON (REDUNDANT)	CFC GROUP
37	COMMON PATH (PRIME & REDUNDANT)	TRANSMIT/RECEIVE BEAMSPLITTER (DICHROIC) CUBE (TRANSMITS 532 NM)
36	STATIC ALIGNMENT	STATIC ALIGNMENT RETROREFLECTOR
38, 39, 40	RECEIVE	CFC GROUP
41	RECEIVE	TRACKING/COMMUNICATION BEAMS SPLITTER (DICHROIC) CUBE (REFLECTS 1064 NM)
42	COMMUNICATION	1064 NM BANDPASS FILTER
43	COMMUNICATION	COMMUNICATION DETECTOR FOCUSSING LENS
44	COMMUNICATION	PRIME/REDUNDANT COMM DETECTOR SELECT MECHANISM ("POP MIRROR")
45	COMMUNICATION	COMMUNICATION DETECTOR (APD)
46	TRACKING	VARIABLE ATTENUATION FILTER (INCLUDES SELECTION MECHANISM)
47	TRACKING (AND STATIC ALIGNMENT)	532 NM BANDPASS FILTER (PASS 532 NM AND REFLECT OUTSIDE PASSBAND)
48	TRACKING	MIRROR FOR EARTH TRACKING CHANNEL
49	STATIC ALIGNMENT	WEDGE (DEVIATES RETROREFLECTED TRANSMIT BEAM TO OFFSET POSITION OR TRACKING DETECTOR
50	TRACKING	TRACKING FOCUSSING LENS
51	TRACKING	PRIME/REDUNDANT TRACKING DETECTOR SELECT MECHANISM ("POP MIRROR")

FIGURE 4-13

OPTICAL SCHEMATIC KEY
(CONTINUED)

NUMBER	OPTICAL PATH	COMPONENT DESCRIPTION
52	TRACKING	TRACKING DETECTOR
53, 54	TRANSMIT	TRANSMIT BEAM EXPANDER
55, 56	TRANSMIT	ACTIVE FOCUS UNIT
57	TRANSMIT	PRIME/REDUNDANT LASER SELECT MECHANISM ("POP MIRROR")
58	TRANSMIT	LASER

FIGURE 4-13

5.0 COMPONENT SELECTION RATIONALE

The rationale behind selection for each major OPTRANSPAC component is outlined below. Also, rationale for selection of modulation type and coding is given. Specifications for major components (laser, telescope, optics, detector/ preamplifier and Earth tracker) are detailed in Appendices B-1 through B-5.

5.1 LASER SOURCES - Laser source selection for the OPTRANSPAC encompassed comparisons of a variety of laser sources. Three types of lasers were considered; gas, solid-state, and semiconductor. Figure 5-1 outlines the laser sources considered as candidates for the OPTRANSPAC terminal. The figure illustrates the lasers' operational wavelengths and defines their typical operational characteristics. The selection of the downlink and uplink laser sources was made simple by the reduced trade space set forth by the system requirements. It was determined through preliminary link analysis that the Gallium Arsenide sources could not provide enough power to sufficiently operate at a range of 10 AU. The Helium Neon source provided low reliability in meeting the lifetime needed. The Carbon Dioxide laser did not fall within the wavelength requirements. The only viable sources found to close the OPTRANSPAC links were the Nd:YAG and frequency doubled Nd:YAG sources. The doubled Nd:YAG laser was chosen as the downlink source as it met the wavelength requirement and the PMT receiver provided an adequate quantum efficiency at 532 nanometers. The Nd:YAG source was then selected as the uplink source. In addition, high quantum efficiency APD's enabled good uplink operation at the Nd:YAG frequency.

5.1.1 DOWNLINK LASER - The downlink laser on-board the OPTRANSPAC terminal was specified as a frequency doubled Nd:YAG (532 nm) source in a diode pumped slab configuration. The diode pumped slab design enables high efficiency laser operation effectively reducing the required prime pump drive power. A functional specification for the downlink laser is given in Appendix B-1.

The downlink laser was specified to operate at three distinct pulse rates corresponding to the three distinct data rates. The nominal pulse rates of operation are 14.285 KPPS, 4.285 KPPS and 1.429 KPPS. The laser pulsewidth was specified at 10 nanoseconds (FWHM) and the average output power was specified to be 400 milliwatts. An isometric view of an external cavity frequency doubled diode pumped slab laser is illustrated in Figure 5-2. For high efficiency, the laser is pumped by laser diode bar arrays matched in wavelength to the absorption band of the Nd:YAG material. The frequency doubling can either be internal or external to the laser cavity. Figure 5-3 outlines the specific design considerations associated with each device. A specific choice of cavity design was left as a design choice further into actual hardware implementation.

5.1.2 UPLINK LASER - While not a part of the OPTRANSPAC design, the characteristics of the uplink laser are governed by the OPTRANSPAC command receiver implementation. To that end, the uplink laser shall transmit 10 nsec FWHM pulses at a nominal rate of 142.86 PPS. The transmitted wavelength shall be 1064 $\pm$ 0.5 nm. The energy per pulse, referenced to the nominal wavelength, shall be 70 millijoules and the interpulse period shall be 70 msec $\pm$ 25.6 μsecond.

LASER COMPARISONS

LASER TYPE	WAVELENGTH RANGE	CHARACTERISTICS	DOWNLINK	UPLINK	SUFFICIENT POWER	RELIABILITY	COMMENTS
GaAs Laser Diode (Single Heterostructure)	790-910 NM 790-910 NM	DUTY CYCLE LIMITED; PEAK POWER LIMITED; CAN BE SPATIALLY AND SPECTRALLY COMBINED	λ OK	λ OK	NO	-	DOES NOT PROVIDE SUFFICIENT PEAK POWER EVEN IN COMBINED ORIENTATIONS
GaAlAs Laser Diodes (Single Heterostructure)	790-910 NM	SAME AS ABOVE	λ OK	λ OK	NO	-	DOES NOT PROVIDE SUFFICIENT PEAK POWER EVEN IN COMBINED ORIENTATIONS
GaAlAs Laser Diodes (Double Heterostructure)	790-910 NM	TYPICALLY 50% DUTY CYCLE, BUT CAN POSSIBLY OPERATE AT DUTY CYCLES APPROACHING 12%. AVERAGE POWER AT 50-100 MW. CAN BE COMBINED AS ABOVE.	λ OK	λ OK	NO	-	DOES NOT LEND ITSELF TO HIGH PEAK POWER OPERATION. POSSIBLY USEFUL IN M-ARY OPERATION BUT NOT LARGE M (I.E., NOT GOOD FOR M >8)
GaAlAs Phased Arrays (Double Heterostructure)	790-910 NM	OPERATE LIKE DOUBLE HETS ABOVE AT AVERAGE POWERS OF 500-1000 MW PER DEVICE. CAN ALSO BE COMBINED AS ABOVE.	λ OK	λ OK	NO	-	SAME AS DOUBLE HETEROSTRUCTURE ABOVE.
Helium Neon (HeNe)	632.8 NM	GAS LASER	λ OK	NO	-	NO	RELIABILITY OVER LONG LIFE IS LOW
Carbon Dioxide (CO_2)	10.6 μM	GAS LASER	NO	NO	-	-	DOES NOT MEET WAVELENGTH REQUIREMENT
Nd:Yag	1064 NM	DIODE PUMPED WITH 300-500 MW AVERAGE POWER ACHEIVABLE	NO	λ OK	YES	OK	APPEARS TO BE VIABLE UPLINK LASER SOURCE IN Q-SWITCH OPERATION
Doubled Nd:Yag	532 NM	FREQUENCY DOUBLED VERSION OF ABOVE.	λ OK	λ OK	YES	OK	APPEARS TO BE VIABLE UPLINK OR DOWNLINK SOURCE IN CAVITY DUMP OPERATION

FIGURE 5-1

DIODE PUMPED SLAB LASER

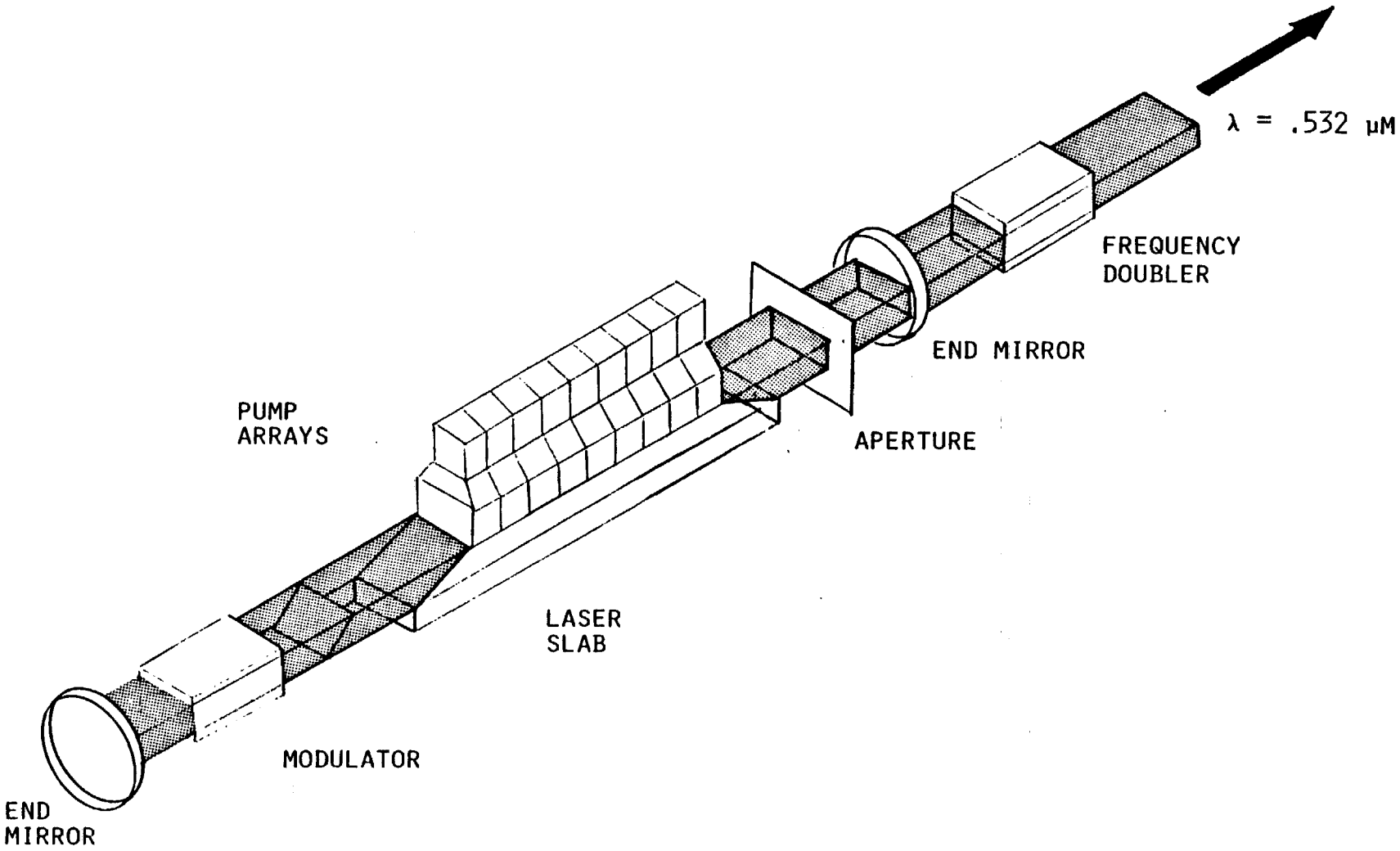

FIGURE 5-2

LASER DESIGN CONSIDERATIONS

- INTERCAVITY DEVICE
  - FREQUENCY DOUBLING IN CAVITY
  - QUADRATIC GAIN CURVE DESIGN
  - ALLOWS FOR NARROW PULSE Q-SWITCHING AT FAIRLY HIGH PRF
  - HIGH EFFICIENCY LASER
  - HIGHER RISK DESIGN THAN EXTERNAL CAVITY

- EXTERNAL CAVITY
  - FREQUENCY DOUBLING EXTERNAL TO CAVITY
  - LINEAR GAIN CURVE DESIGN
  - OPERATES IN CAVITY DUMP CONFIGURATION TO ACHIEVE HIGH PRF AND NARROW PULSE WIDTH
  - LESS EFFICIENT THAN INTERCAVITY DEVICE
  - LOWER RISK DESIGN THAN INTERCAVITY DEVICE

FIGURE 5-3

5.2 TELESCOPE SELECTION - To meet the specified requirements outlined in Appendix B-2, a mirror based reflective telescope was chosen over a refractive system. An 11" aperture refractor would likely require several lens elements to meet the image quality requirements over the viewfield and, and a result, would be heavy. A refractive design would also be too prone to thermal gradients, which adversely affect transmitted wavefront by the large temperature dependence of the glass refractive indices .

Figure 5-4 illustrates the wide variety of reflective telescopes available. The image quality requirements over the viewfield limit the choice of telescopes. The Newtonian form was unacceptable over this field due to the coma inherent in the base paraboloid mirror. The Gregorian form was too long and bulky. The Maksoutoff arrangement tended to be either too long (with a thin corrector plate) or too heavy (the corrector plate thickness increases as telescope length is reduced to maintain the required correction). The Cassegrain design form, in one of its many variants, offered the best approach to meeting the diffraction limited performance requirements over the viewfield with a compact, light weight, stable package.

The "Classical Cassegrain" consists of a paraboloid primary mirror with a hyperboloid secondary mirror. This arrangement can cover a larger viewfield than the single paraboloid mirror with substantially better imaging performance. It will, however, not be able to cover the full ± 2.5 milliradian field with the required near diffraction limited performance.

Several variants to the "Classical Cassegrain" offer improved image quality over the field at a cost in complexity. One variant is the Ritchey Chretien which consist of aspheric primary and secondary mirrors whose zonal curvatures are slightly weakened with respect to the paraboloid/hyperboloid mirrors of the Classical Cassegrain. Another variant is the Schmidt Cassegrain which incorporates a full aperture aspherized reflective plate to correct the resulting spherical aberration. This plate covers the full aperture and is prone to thermal gradients perturbing the wavefront quality. A final variant is to incorporate small refractive correcting elements in the converging beam after the secondary. This allows additional aberration correction. It was this final variant that offered the best approach to meeting the image quality over the full telescope viewfield.

5.3 OPTICAL MECHANISMS - The use of optical mechanisms should be minimized to provide a design with the fewest possible moving parts. However, gimbals, beam steerers, and optical mechanisms (select mirrors, shutters, adjustable, field stops, etc.) are usually needed (in some combination) to accommodate dynamic system fluctuations and provide for redundancy switching.

The OPTRANSPAC system design accommodates pointing and tracking with a single set of beam steerers. Gimbal pointing was determined as not being necessary. Many types of beam steering mechanisms were considered; piezoelectric deflectors, torque motor types and acousto-optic deflectors. One and two axis deflector mechanisms were considered. Piezoelectric steerers require high voltage drivers for the crystal. They also exhibit an inherent mechanical weakness of the crystal to the mechanical deflection inputs at the structural resonant frequency. Acousto-optical deflectors, although widely used commercially, exhibit optical transmissions of about 70% for a single axis and about 50% for both axes. It was this loss in optical signal power that made AO deflectors undesirable for the OPTRANSPAC design.

TELESCOPE CONFIGURATIONS

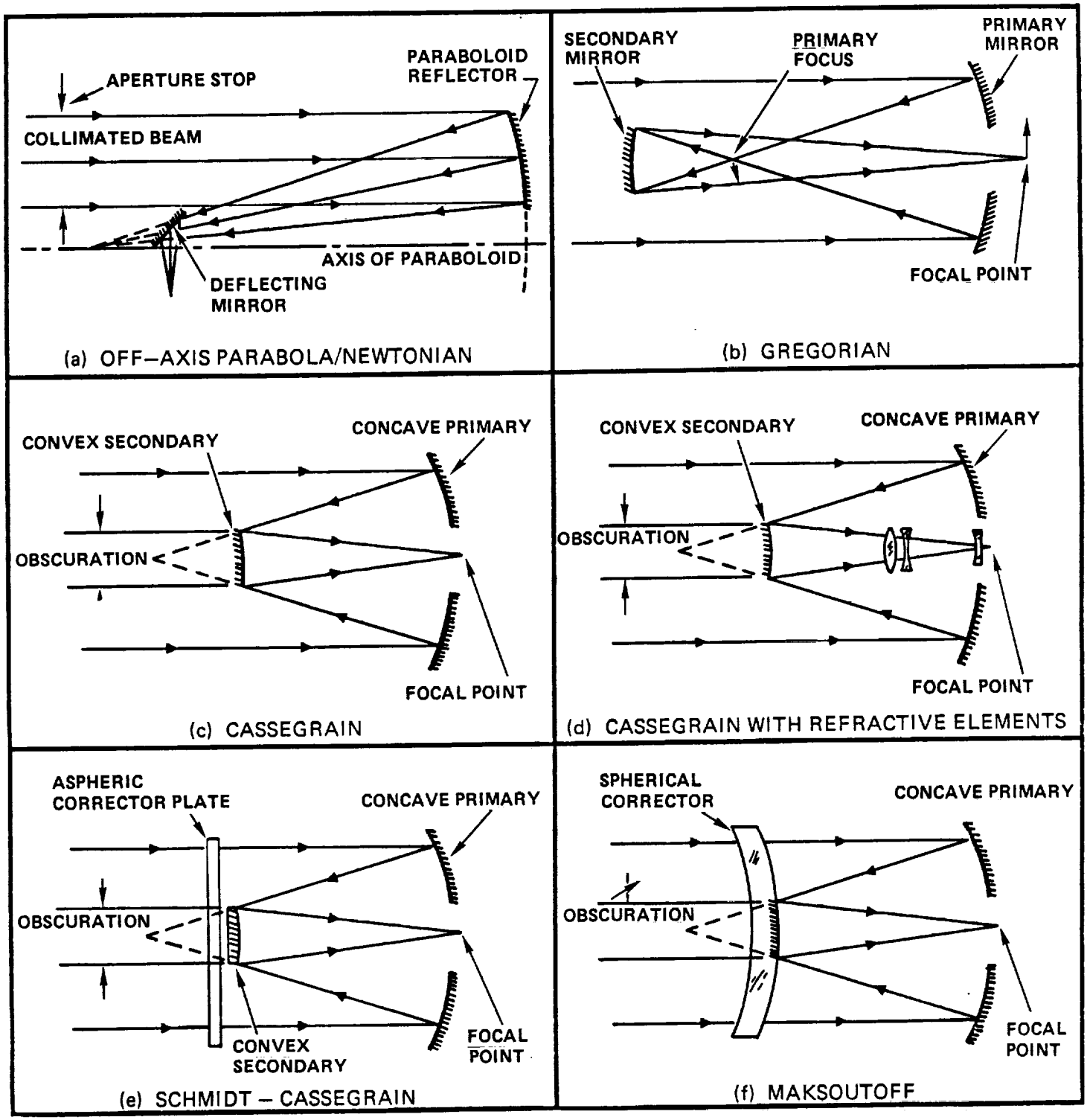

FIGURE 5–4

The OPTRANSPAC design employs two single axis torque motor beam steerers in an X-Y configuration. The torque motor devices were chosen because of their long development heritage and low risk design. Space qualified torque motor beam steerers already exist and are being integrated into a spaceborne optical communication terminal.

Other mechanisms required in the OPTRANSPAC design include a commandable focus drive to ensure diffraction limited beam quality over the design life and redundancy select flip mirrors that allow selection of redundant optical paths or electro-optic devices (detectors, laser). The use of solenoid and motor driven select mirrors for redundancy switching is a proven method for redundancy management. Redundant drives were associated with each mechanism to ensure reliable switching.

5.4 MODULATION FORMAT SELECTION - Laser sources cannot be modulated in all possible modulation formats. Because of this fact, the choice of a particular laser affects the selection of an applicable modulation type. The selection of the Nd:YAG lasers and the high peak powers needed to communicate from deep space, yield a short pulse, high peak power laser source.

The most efficient pulsed modulation format to use with a narrow pulse laser is an M-ary pulse position format. M-ary Pulse Position Modulation (PPM) with "greatest-of" detection provides the most sensitive receiver in terms of bits of information per photons transmitted. The PPM format employed in the OPTRANSPAC system is illustrated in Figure 5-5. Electronic speeds as well as hardware maturity drove the design to a 256-ary (8 bits/pulse) pulse position format. Compatibility with eight bit Reed-Solomon encoders and decoders made 8 bit PPM an attractive solution to the OPTRANSPAC design.

5.5 DETECTOR-PREAMPLIFIER SELECTION - The command uplink communication detector selection involved comparisons of five applicable optical detectors. The detector types chosen for comparison are listed along with their important characteristics in Figure 5-6. Front end detector gain, quantum efficiency, internal noise mechanisms (i.e. dark current, ionization coefficient) and reliability are listed for each detector. The selection criteria for the uplink communication detector are listed in Figure 5-7. Moderate to high front end gain is necessary to partly offset the effects of the preamplifier noise contributions; high quantum efficiency is necessary to provide high efficiency conversion of optical to electrical energy; low internal noise yields good receiver sensitivity; and high reliability is necessary for the long life required. As is seen (Figure 5-7), the silicon APD provides the best fit to the selected criteria. The low-k device with dimpled design provides good quantum efficiency and low noise operation. An avalanche gain on the order of 200 helps to reduce the effective preamplifier noise contributions and the proven reliability of the silicon APD offers the desired lifetime operation.

Low noise transimpedance preamplifiers were interfaced with the command uplink receiver avalanche photodiode to provide good overall system sensitivity. The noise current effects of the preamplifier were reduced by the front-end avalanche gain of the APD. The increased gain, however, increases the internal APD noise as well as the received background noise. An optimum APD gain was found when the contributions of the preamplifier noise and detector noise (includes background) were equal. Thus, low noise preamplifiers are important in achieving the greatest possible receiver sensitivity.

PPM DATA FORMATS

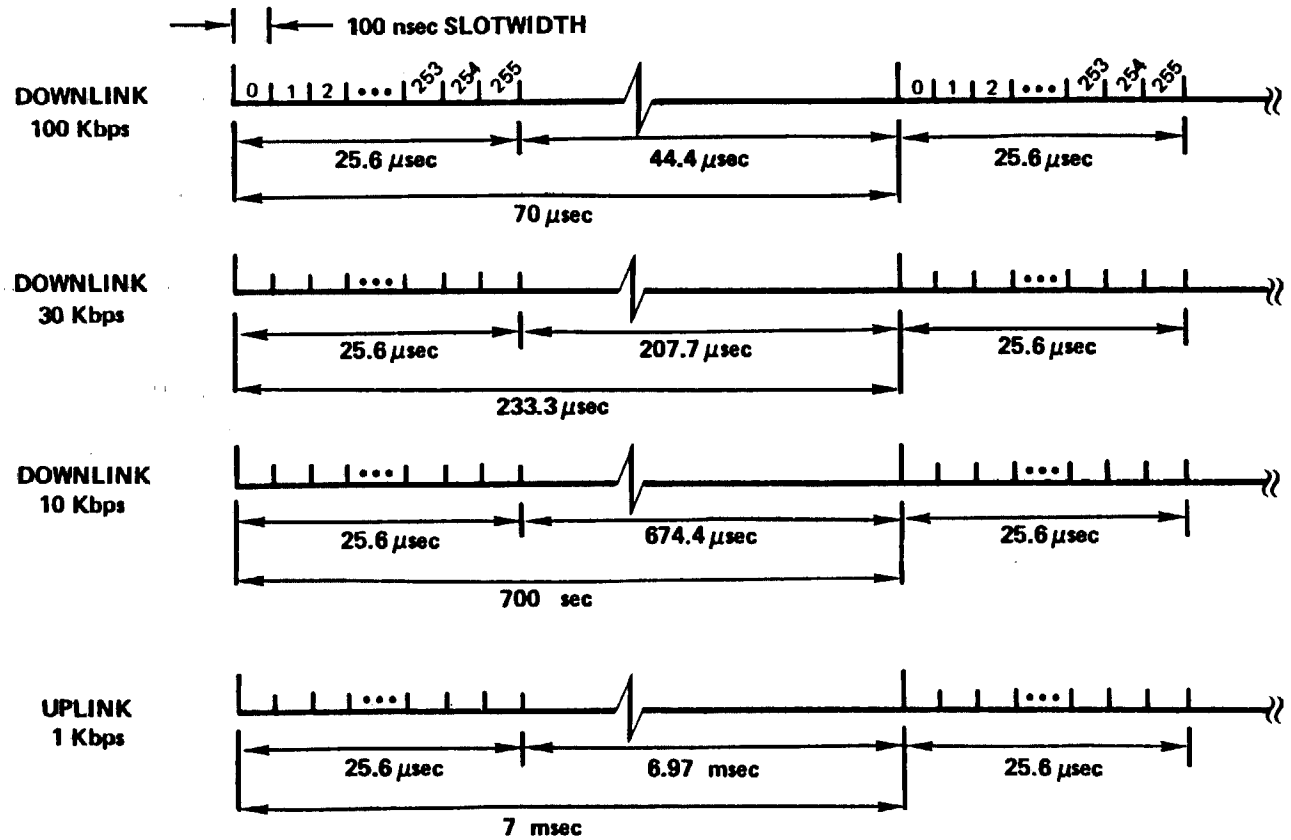

FIGURE 5–5

UPLINK DETECTOR TRADE MATRIX

DETECTOR TYPE	DETECTOR GAIN	QUANTUM EFFICIENCY @ 1064 NM	IONIZATION COEFFICIENT	RELIABILITY	COMMENTS
SI-APD	UP TO 300	40% DIMPLED	LOW K K=.007	HIGH	BEST POSSIBLE CONFIGURATION, HIGH QE, LOW K
INGAAS APD	UP TO 50	80-90%	VERY HIGH K K=.1	HIGH	HIGH INTERNAL NOISE UNACCEPTABLE
SI-QAPD	UP TO 150	20%	HIGH K K=.02	HIGH	CANNOT BE DIMPLED LOW K NOT DEVELOPED
PIN	UNITY	40% DIMPLED	N/A	HIGH	LACK OF AVALANCHE GAIN CAUSES PREAMP TO DOMINATE
PMT	VERY LARGE 10^5 TO 10^6	< 1%	N/A	MODERATE TO LOW	LOW QE AND RELIABILITY MAKES PMT UNSATISFACTORY FOR OPTRANSPAC @ 1064 NM

FIGURE 5-6

DETECTOR SELECTION

- DETECTOR SELECTION CRITERIA
  - A) MODERATE TO HIGH GAIN DEVICE TO PARTLY OFFSET THE EFFECTS OF PREAMPLIFIER NOISE CONTRIBUTIONS
  - B) HIGH QUANTUM EFFICIENCY TO PROVIDE HIGH EFFICIENCY CONVERSION OF OPTICAL TO ELECTRICAL ENERGY
  - C) LOW INTERNAL NOISE GENERATION
  - D) HIGH RELIABILITY

- SELECTION MATRIX

	CRITERIA			
DETECTOR	A	B	C	D
SI-APD	YES	YES!	YES	YES
INGAAS-APD	YES	YES!	NO	YES
SI-QAPD	YES	NO	NO	YES
PIN	NO	YES!	YES	YES
PMT	YES!	NO	YES	NO

FIGURE 5-7

For the OPTRANSPAC system, the selection of an appropriate preamplifier with low noise occurred from the extrapolation of present measured device values to the system technology time frame. The preamplifier noise current is bandwidth dependent and Figure 5-8 shows this relationship for a few low noise devices manufactured by MERET, Inc. Extrapolation to the 50MHz preamplifier bandwidth required to pass the received 10 nsec pulsewidth resulted in a selection of a preamplifier with a noise equivalent current of approximately 1.4 picoamps per root Hertz. Figure 5-9 illustrates the effect on uplink margin sensitivity resulting from an increase or decrease in the preamplifier noise current. The OPTRANSPAC detector and preamplifier design parameters are specified in Appendix B-4.

5.6 EARTH TRACKER DETECTOR SELECTION - In order to provide track capability by the OPTRANSPAC such that a narrow divergence beam can be transmitted back to the Earth, a method of beacon tracking had to be devised. Most narrow divergence optical communication systems cooperatively track each others transmissions. However, the OPTRANSPAC scenario required communication with an EORS that disappeared every 45 minutes. With round trip transmit times to Saturn of approximately 2.75 hours, tracking the EORS command beacon was not feasible.

A solution to this problem involved tracking the Earth with a quadrant or an array detector. Quadrant detectors did not provide the sensitivity (due to insufficient background rejection) necessary to track the Earth under the specified availability requirements. An array tracker implementation provided the best background rejection available due to the small pixel angular viewfields. Random readout and access techniques offered multiple target tracking. This multiple target tracking enabled the elimination of the point-ahead beam steerer group and made the selection of option A (See Section 4.1) possible.

The selection of an array tracking detector enabled the same detector to perform point-ahead, boresight alignment and Earth tracking functions. The point-ahead function of the OPTRANSPAC was designed to be an electrical rather than a mechanical (i.e. beam steerer) compensation. An area of the array detector, not used for Earth tracking, was used to determine the boresight of the transmit signal (See Figure 5-10). The artificial point-ahead boresight was commanded by the processor based on a known point-ahead angle and with respect to the transmit boresight. Alignment of the transmit and receive paths can also be achieved in this manner.

The requirements of the OPTRANSPAC on the Earth tracker (track, point-ahead, and alignment) made the choice of a Charge Injection Device (CID) as the Earth tracker, a good one. Random access (single pixel addressing) and nondestructive readout capability led to the choice of the CID over other array detectors such as Charge Coupled Devices (CCD). CID's, where readout does not involve destruction of the stored charge, have increased sensitivity over CCD's.

The Earth tracker design was based on developed CID technology. The CID consist of an array of photosensitive picture elements (pixels) which integrate incident signal charge, store it, and enable readout at the individual pixel site. The OPTRANSPAC Earth tracker was designed around a ST-256-CID developed by General Electric. The physical size of the array was 5.12mm x 5.12mm and encompasses 256 x 256 pixel. The 1 mrad by 1 mrad OPTRANSPAC field of view was

PREAMP NOISE CURRENT vs BANDWIDTH

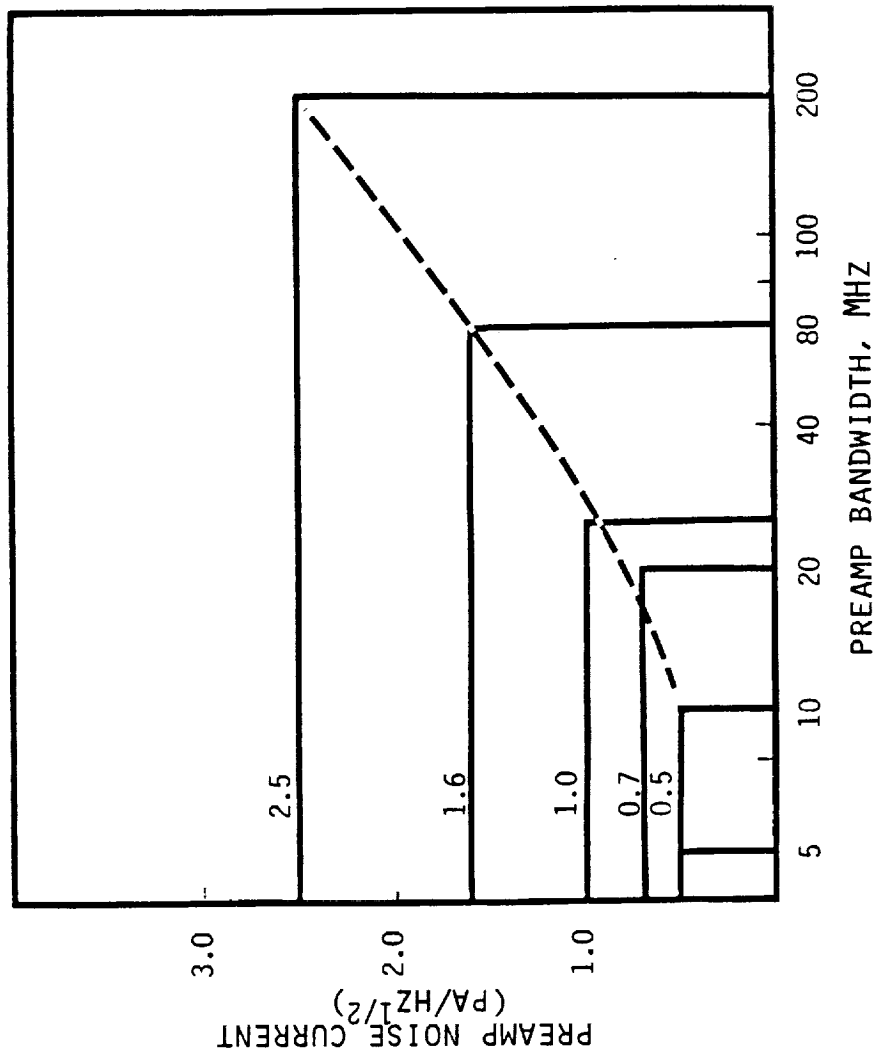

FIGURE 5–8

UPLINK MARGIN vs PREAMP NOISE CURRENT

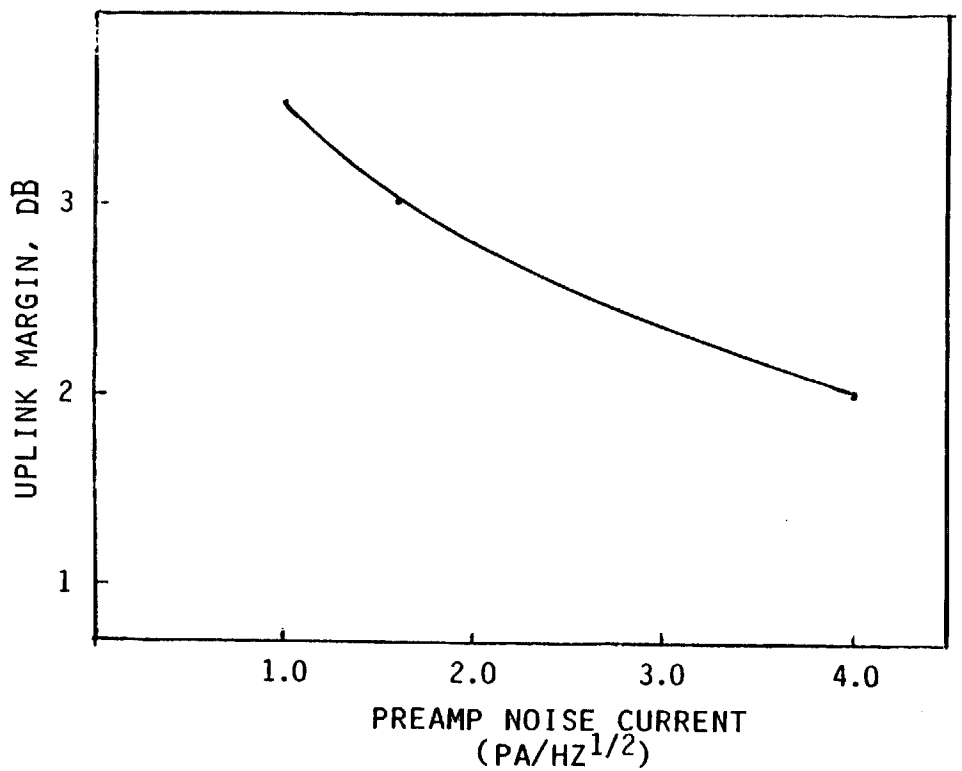

FIGURE 5-9

EARTH TRACKER/POINT AHEAD IMPLEMENTATION

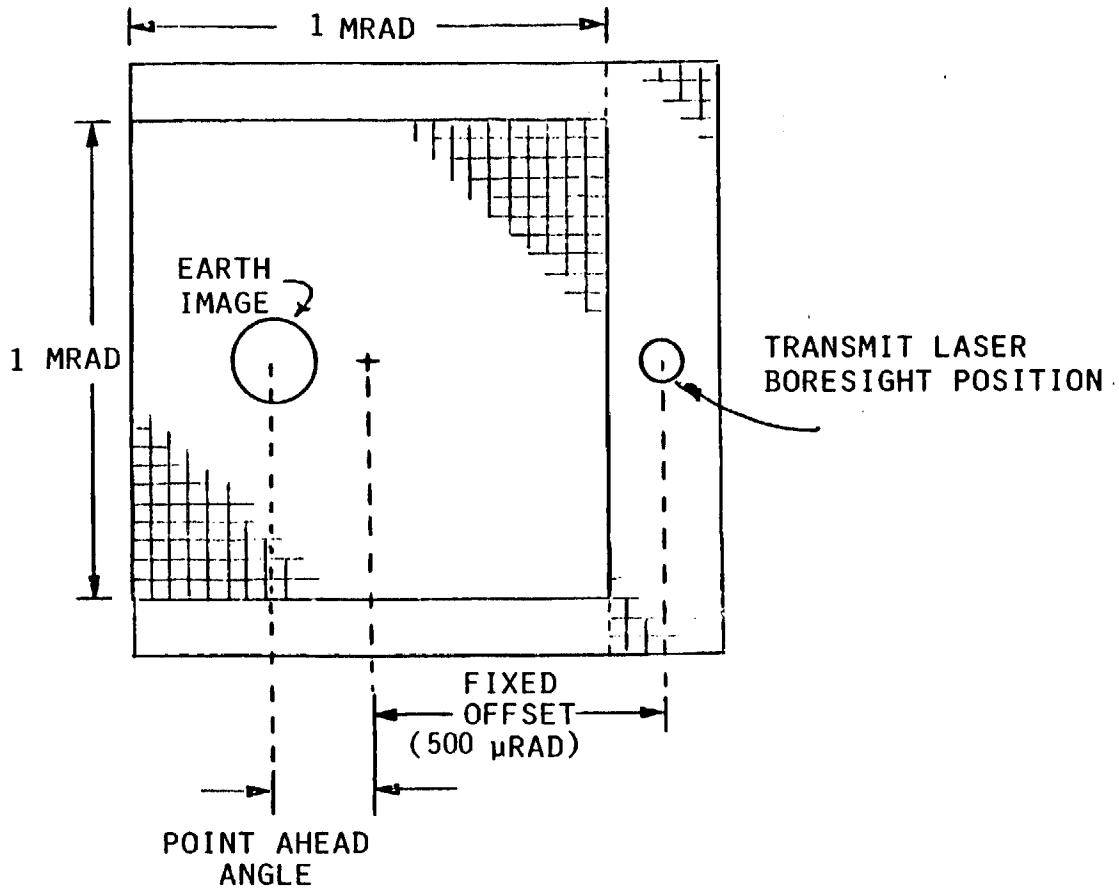

FIGURE 5-10

mapped into a 200 x 200 pixel area providing excellent background rejection due to small (5 microradian) pixel viewfields. A specification for the Earth tracker is given in Appendix B-5.

5.7 CODING SELECTION - Both the uplink and downlink were selected as candidates for channel coding. Coding of these links provides for a reduction in aperture size and laser power at a small cost in weight and complexity. Using a block code over the pulse position modulation frame provides the largest degree of error correction [Ref 3]. The selection of the Reed-Solomon block code for the OPTRANSPAC links was based primarily on the maturity of the technology, particularly the 8-bit Reed-Solomon encoders and decoders.

The spacecraft or command data is encoded into 8-bit Reed-Solomon channel symbols by a rate 7/8 Reed-Solomon encoder. These 8-bit channel symbols are further encoded into PPM symbols by appropriate pulse timing into one of 256 slots. At the receiver the PPM symbols are decoded in a "greatest-of" fashion selecting the slot with the greatest pulse amplitude out of the 256 possible slots. The PPM symbols are then converted back to channel symbols for the Reed-Solomon decoder, which in turn converts the channel symbols to source bits.

Figure 5-11 shows the relationship between the uncoded PPM bit error probability and the Reed-Solomon encoded bit error probability. It can be seen that to achieve a final bit error probability of 10^{-3}, the PPM channel must support a bit error probability of approximately 0.02 for a rate 7/8 Reed-Solomon code. Further coding gain is possible with higher order codes (i.e., rate 3/4, rate 1/2) but the increase in laser pulse rate required to accommodate the higher order codes reduces the available peak laser power per pulse. This effectively offsets a portion of the coding gain and from Figure 5-12 it is readily seen by the uplink example that the rate 7/8 code provides the largest available coding gain.

COMPARISON OF REED-SOLOMON CODING
TO UNCODED PPM

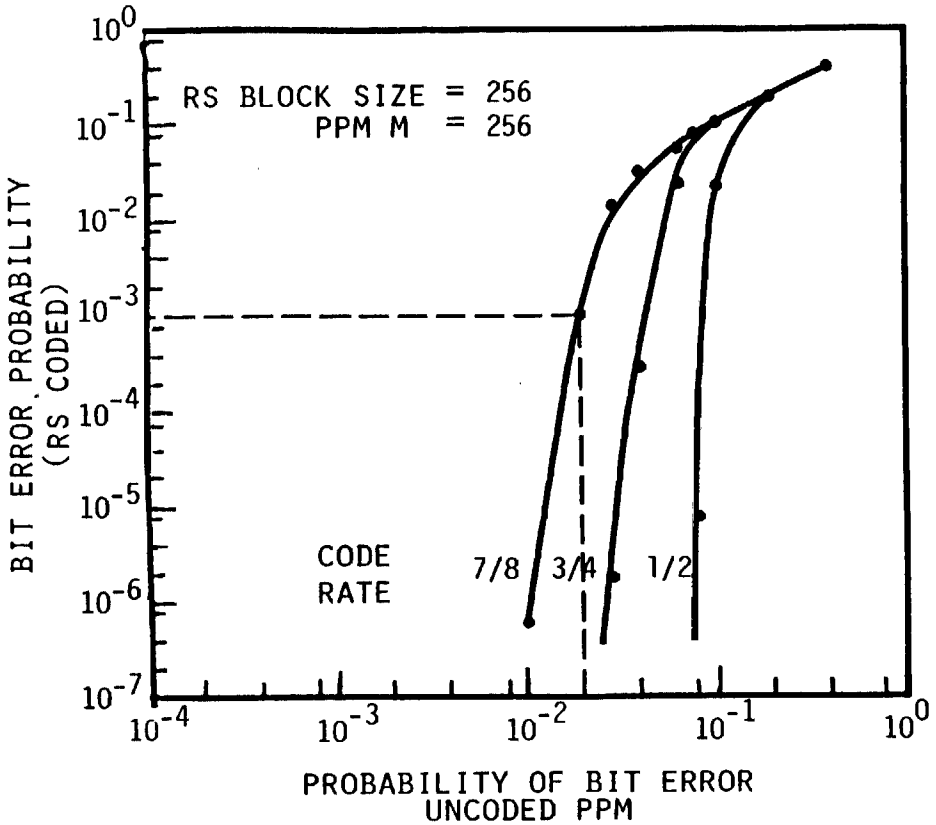

FIGURE 5-11

UPLINK MARGIN vs CODE RATE
11 INCH APERTURE
10^{-3} BIT ERROR RATE
MARGIN, DB
3
2
1
UNCODED
RATE 7/8
RATE 3/4
RATE 1/2

FIGURE 5–12

6.0 LINK ANALYSIS

The analysis that supports the validity of the OPTRANSPAC system operation is presented below. Because the two are interrelated, the system links from an acquisition and tracking standpoint as well as from a communication standpoint were analyzed.

6.1 ACQUISITION AND TRACKING - System concerns when considering the acquisition and tracking performance of the OPTRANSPAC include spacecraft dynamic characteristics, spacecraft uncertainty, tracking detector accuracy, boresight uncertainty and beam steerer noise to name a few. The acquisition and tracking system must compensate for some of these concerns and operate through others.

6.1.1 SPACECRAFT CHARACTERISTICS - The following spacecraft characteristics were assumed in order to estimate the spacecraft attitude dynamics for OPTRANSPAC inputs [Ref. 4]. A spacecraft whose mission is close scrutiny, deep space, has a mass of between 1000 and 3000 Kg. By choosing the smaller mass, a more conservative estimate of attitude motion was assumed. It was assumed a three axis stabilized attitude control system was needed to perform precision pointing and rapid retargeting tasks. The spacecraft was also assumed to employ an articulated science platform with a mass of about 80 Kg for tracking a target during close scrutiny. The respective control bandwidths of the spacecraft and the platform were assumed 1 and 0.1 Hertz. Control accuracy of the spacecraft was specified as 2 milliradians and the control stability of the platform was assumed to be 550 microradians. During target tracking the science platform slews at 1.2 milliradians per second and slews at a maximum rate of 35 milliradians/second during retargeting. Figure 6-1 outlines the spacecraft assumptions used.

6.1.2 ACQUISITION - The assumptions made during OPTRANSPAC acquisition of the Earth are outlined in Figure 6-2. The figure lists the driving assumptions for acquisition scanning and acquisition time. The spacecraft attitude control system, with a 2 milliradian accuracy, places the Earth inside the telescope field-of-view. A one milliradian square viewfield detector provides angle error updates at a 200/second rate. The false alarm rate was assumed to be once in two seconds and the computer switching time is 0.1 second. The beam steerer bandwidth required for acquisition was calculated to be 20Hz.

In order to cover the entire uncertainty area of the telescope viewfield, the detector array was assumed scanned in the pattern shown in Figure 6-3. This type of pattern, a raster scan, was chosen over a conical scan because of ease of implementation and no need for the most rapid average acquisition time possible. In order to assure no gaps are left in the scan coverage, an overlap of around 30 percent is usually allowed. For the telescope field-of-view and detector array size noted in Figure 6-2, a pattern of six swaths was determined necessary. This yielded an overlap factor of about 29 percent. Two alternatives existed for the sequence in which swaths were searched. In the first, the scan covered the inside two swaths first, as they were most likely to contain the target, and then proceeded outward to the next most likely swaths. A disadvantage of this general sequence in some laser communication systems was the separation between sequential swaths, which allowed more time for attitude drift between adjacent swaths. This was true of this application, where spacecraft attitude drift rates, on the order of 350 microradians per second, could

SPACECRAFT CHARACTERISTICS

SPACECRAFT

MASS:	1000 KG
ATTITUDE CONTROL SYSTEM:	THREE-AXIS STABILIZED
ATTITUDE CONTROL ACCURACY:	2 MRAD
ATTITUDE CONTROL BANDWIDTH:	1 Hz
ATTITUDE CONTROL STABILITY RATE:	350 μRAD/SEC

SCIENCE PLATFORM

MASS:	80 KG
MAX SLEW RATE:	35 MRAD/SEC
TRACKING SLEW RATE:	1.2 MRAD/SEC
CONTROL STABILITY:	550 μRAD
CONTROL BANDWIDTH:	0.1 Hz

FIGURE 6-1

ACQUISITION ASSUMPTIONS

- TELESCOPE FIXED TO SPACECRAFT
- SPACECRAFT ATTITUDE CONTROL OF $\pm$2 MRAD
- TELESCOPE FOV $\pm$2 MRAD
- DETECTOR ARRAY 1 MRAD X 1 MRAD
- DETECTOR ARRAY UPDATE PERIOD 0.005 SEC
- FALSE ALARM RATE 0.5/SEC
- BEAM STEERER BANDWIDTH 20 Hz
- COMPUTER MODE SWITCHING TIME 0.1 SEC

FIGURE 6-2

ACQUISITION SCAN PATTERN

- 6 SWATHS
- 29% OVERLAP
- SEQUENTIAL ADJACENT SWATHS

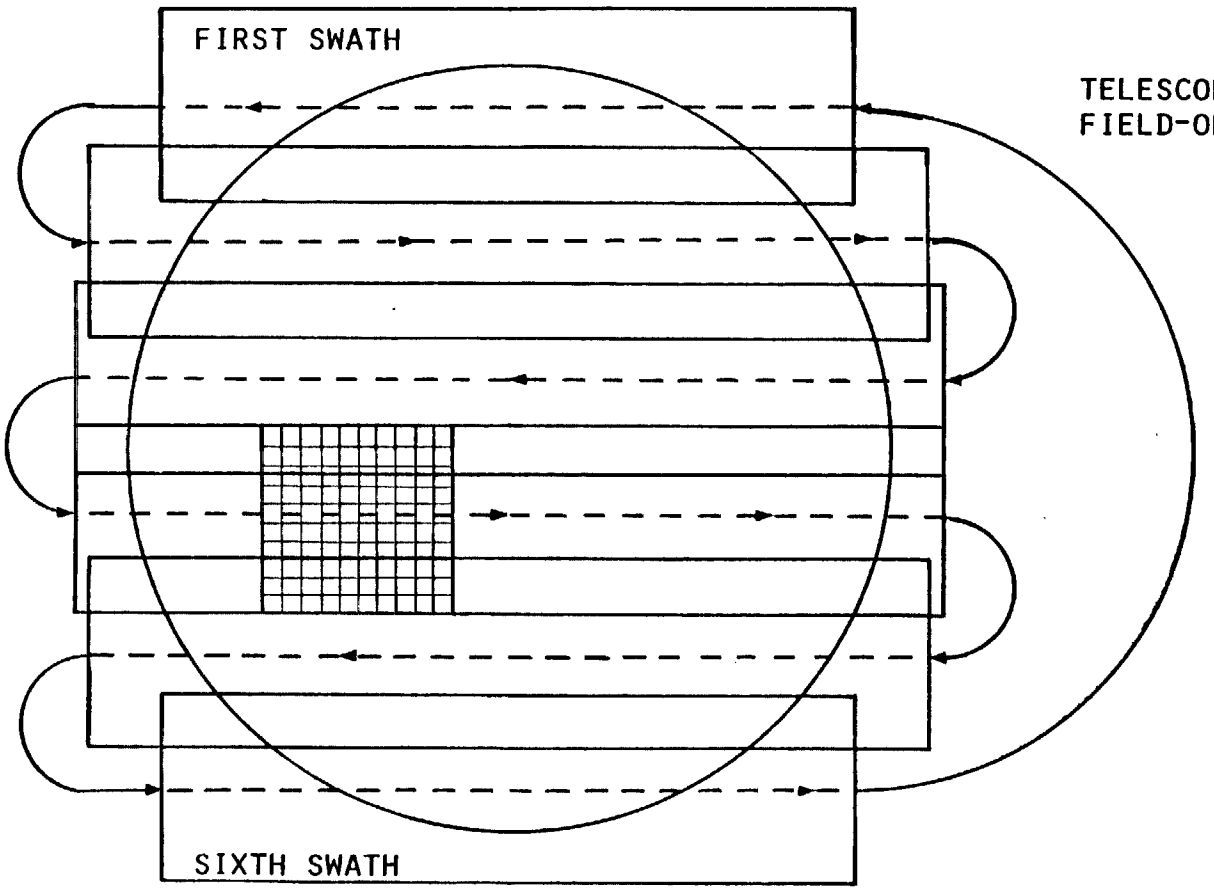

FIGURE 6-3

cause the target to move from one swath to the adjacent one before the detector array arrives at the original target position. In the other alternative for the search sequence of the swaths, the first swath was on one edge of the uncertainty region, and the next sequential swath was the adjacent one. This sequence did not search the highest probability areas first, so the average acquisition time was higher than the first alternative. However, since the adjacent swaths were searched sequentially, the attitude drift rate will not carry the target out of the swath before the detector array arrives at that position. Since acquisition time was not pressing in this application, this type of pattern and sequence was chosen. Given the above scan description, the acquisition time was calculated using the rationale outlined in Figure 6-4.

6.1.3 TRACKING - Tracking error contributors are separated into two categories, random and systematic. Random errors (or jitter terms) are assumed to be higher frequency and uncorrelated, so a root sum square gives the total expected error from these sources. Systematic errors (or bias terms) are assumed to be low frequency, and may be correlated, so the maximums may all occur simultaneously over a long period of time. The systematic errors must therefore be summed together. The total error budget for the tracking system is the sum of the 3 sigma random errors (RSS'ed together) and the systematic errors. Figure 6-5 indicates the tracking error contributions to the transmit beam pointing. While this represents a budget for each particular entry, the numbers were determined considering device limitations. The error magnitude determinations are evident from the comments, except for the last two. Spacecraft dynamics and spacecraft attitude are further explained below.

Three sources of spacecraft dynamic tracking error were considered (See Figure 6-6): Spacecraft maneuvers, with an attitude control bandwidth of 1 Hz; spacecraft vibration from control moment gyros or other machinery; and science platform slewing at maximum rate for retargeting. For a detector array update rate of 200/second, a tracking loop bandwidth of at least 20 Hz can be supported. Spacecraft maneuvers with a 1 Hz loop will therefore cause no significant errors. Vibration is expected to cause the science platform stability accuracy error quoted earlier. Since the science platform has a bandwidth of 0.1 Hz, and the OPTRANSPAC has a bandwidth of 20 Hz, the expected OPTRANSPAC error due to vibration was calculated to be less than 0.02 microradians. The largest contributor to tracking error is expected to be the science platform retarget slewing. The platform will jump to maximum rate as fast as possible to minimize retargeting time. This rate will be transmitted to the spacecraft by the ratio of the platform and spacecraft inertias, which are roughly proportional to the square of their masses. A step in attitude rate of that size, into a 20 Hz type II tracking loop with the beam steerers, causes a tracking error of 0.3 microradians. This value was inserted on the tracking budget chart.

Figure 6-7 depicts a three dimensional layout of the point-ahead angle necessary between the OPTRANSPAC and the target (Earth Relay Station). The tracking line is the line between and perpendicular to the reference plane of the OPTRANSPAC and the reference plane of the target. The point ahead angle is the angle away from this tracking line at which light has to be sent in order to compensate for relative velocities between the two platforms. This angle should lie within the plane defined by the tracking line and the velocity vector. The creation of this angle by the OPTRANSPAC may not be perfect,

ACQUISITION TIME

- DWELL TIME IS 10 x ARRAY UPDATE PERIOD = 0.05 SEC
- SWEEP RATE IS 1 MRAD ARRAY SIZE ÷ DWELL TIME = 1.15 °/SEC
- SWEEP DISTANCE FROM 6 SWATH SCAN PATTERN = 31.6 MRAD
- TURN AROUND TIME FOR 6 TURN AROUNDS WITH 20 Hz CONTROL = 192 M SEC
- FRAME TIME = SWEEP TIME + TURN AROUND TIME = 1.8 SEC
- FALSE ALARM ALLOWANCE OF 2 DECISIONS, 2 TURNS AND 1 DWELL = 0.3 SEC
- MAXIMUM ACQUISITION TIME = FRAME TIME + FALSE ALARM TIME = 2.1 SEC

FIGURE 6-4

OPTRANSPAC TRACKING BUDGET

ERROR CONTRIBUTOR	RANDOM ERROR μRAD (3σ)	SYSTEMATIC ERROR μRAD (MAX)	COMMENT
BEAM STEERERS	0.4		0.02% OF MAX RANGE
DETECTOR ACCURACY		0.1	1/50 OF PIXEL SIZE
DETECTOR NOISE	0.5		1/10 OF PIXEL SIZE
BORESIGHT ALIGNMENT		0.1	DETECTOR ACCURACY
SPACECRAFT DYNAMICS	0.3		20 HZ TRACK LOOP
SPACECRAFT ATTITUDE		0.1	POINT AHEAD DIRECTION
	0.7 (RSS)	0.3 μRAD	

TOTAL (RSS + Σ) 1.0 μRAD

FIGURE 6-5

SPACECRAFT DYNAMICS

- TRACKING ERROR SOURCES
  - SPACECRAFT MANEUVERS
  - SCIENCE PLATFORM SLEWING
  - SPACECRAFT VIBRATION

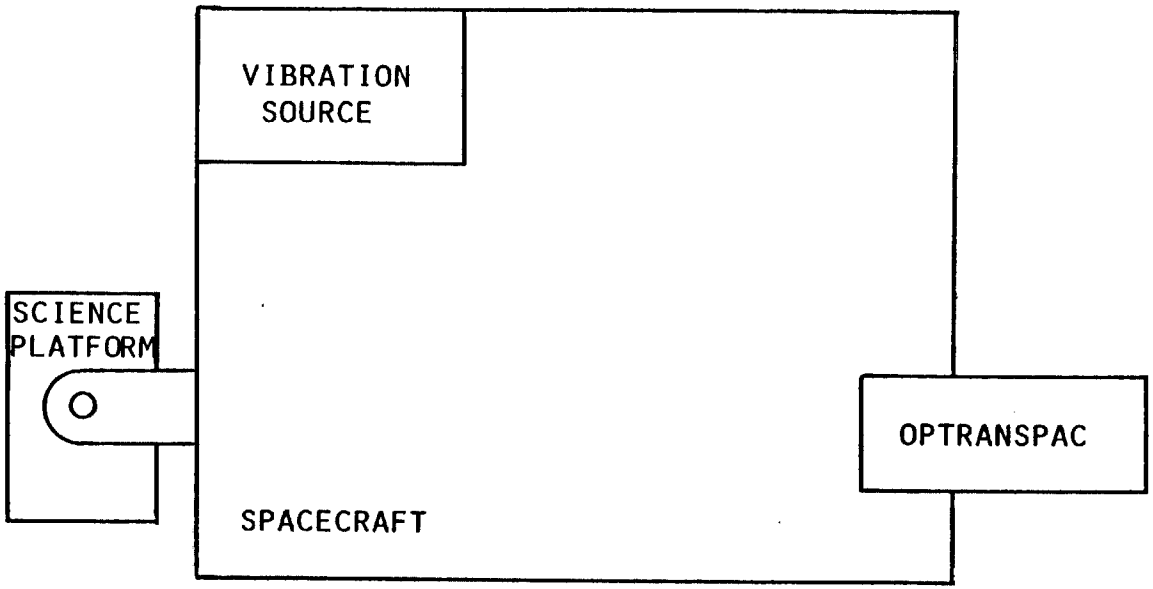

FIGURE 6-6

POINTING ERROR CAUSED BY SPACECRAFT ATTITUDE ERROR
IN CONJUNCTION WITH POINT AHEAD

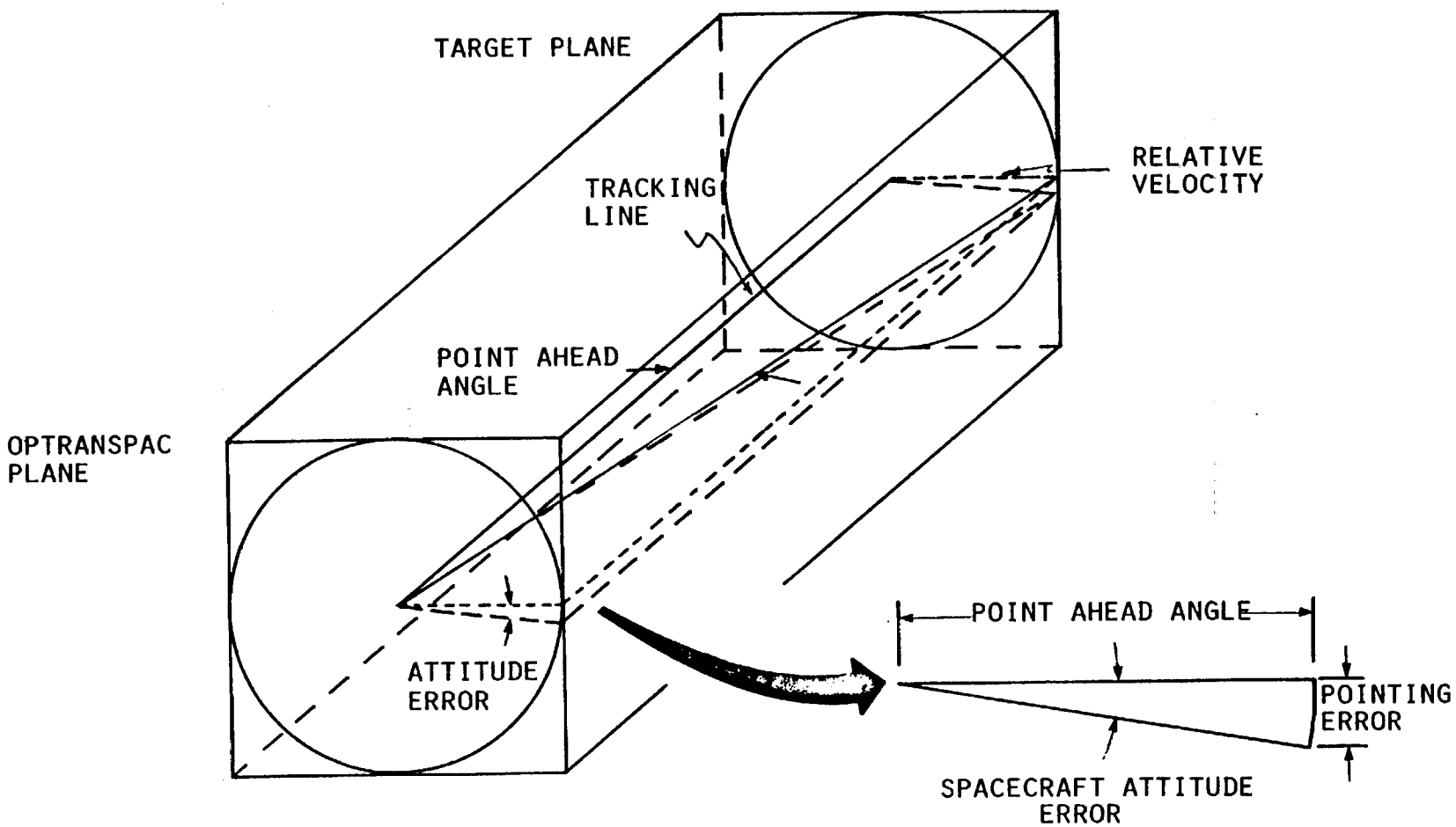

FIGURE 6-7

because the spacecraft may have an attitude error around the axis of the tracking line of up to 2 mrad. The exploded view in Figure 6-7 shows the effect of this attitude error projected by the point-ahead angle. The tracking error due to this effect is nearly 900 nanoradians. This error was too large to allow in the tracking budget.

The error can be reduced by compensating for the rotational error of the spacecraft around the tracking line with the point ahead, if the attitude of the spacecraft is known. Assuming that the attitude knowledge of the spacecraft is 0.1 times the control accuracy, the point-ahead induced pointing error can be reduced to less than 0.1 microradian. If the spacecraft attitude knowledge is worse than the above assumption, it would still be possible to reduce the tracking error contribution to about the same value by implementing a star tracking function around the tracking line with the detector array, and essentially determining the OPTRANSPAC's inertial attitude independently of the spacecraft.

6.1.4 EARTH TRACKING ANALYSIS - Figure 6-8 shows the relationship between Earth tracker angle error noise and aperture size at various ranges. The tracking budget amount is also indicated. The Earth tracker error becomes a function of the distance from the Earth, the optical resolution and the centroiding algorithm.

The range between the OPTRANSPAC and the Earth determines the amount of signal energy incident upon the array detector. The solar energy reflected from the Earth was assumed to be Lambertian distributed in intensity. The factor associated with the partial Earth phase was assumed to be 5%. That is, only 5% of the energy reflected by a full Earth is reflected by the partial Earth. The range also plays an important role in determining the spot size on the detector. The physical angular subtense of the Earth varies from 85 microradians at 1 AU to 8.5 microradians at 10 AU. The more Earth tracker pixels with 5 microradian fields of view required to receive the incident energy, the more noise incurred in the angle error measurements (i.e. the more signal required to maintain an acceptable signal to noise ratio).

The actual spot size on the detector array is a function of the optical resolution of the system. Figure 6-9 shows the relationship between the blur circle on the detector versus range for various receive path optical resolutions. Analysis determined a comfortable 30 microradian resolution would be sufficient for the receive tracking path part of the optical system.

The centroiding algorithm is the final measure of the angle error accuracy. The algorithm used must be able to accurately centroid the energy received even under Earth partial phase conditions. Knowledge of orbital position is imperative in the Earth tracker design. The actual centroiding algorithms used are beyond the scope of this report, rather the analysis was based on star tracker designs employing CID technology.

It is widely accepted [Ref. 5] that for a uniform circular spot, the slope at the origin is a function of the spot angular size and is given by

$$SF = 2.55 / \theta_{spot}$$

EARTH TRACKER ERROR vs APERTURE SIZE

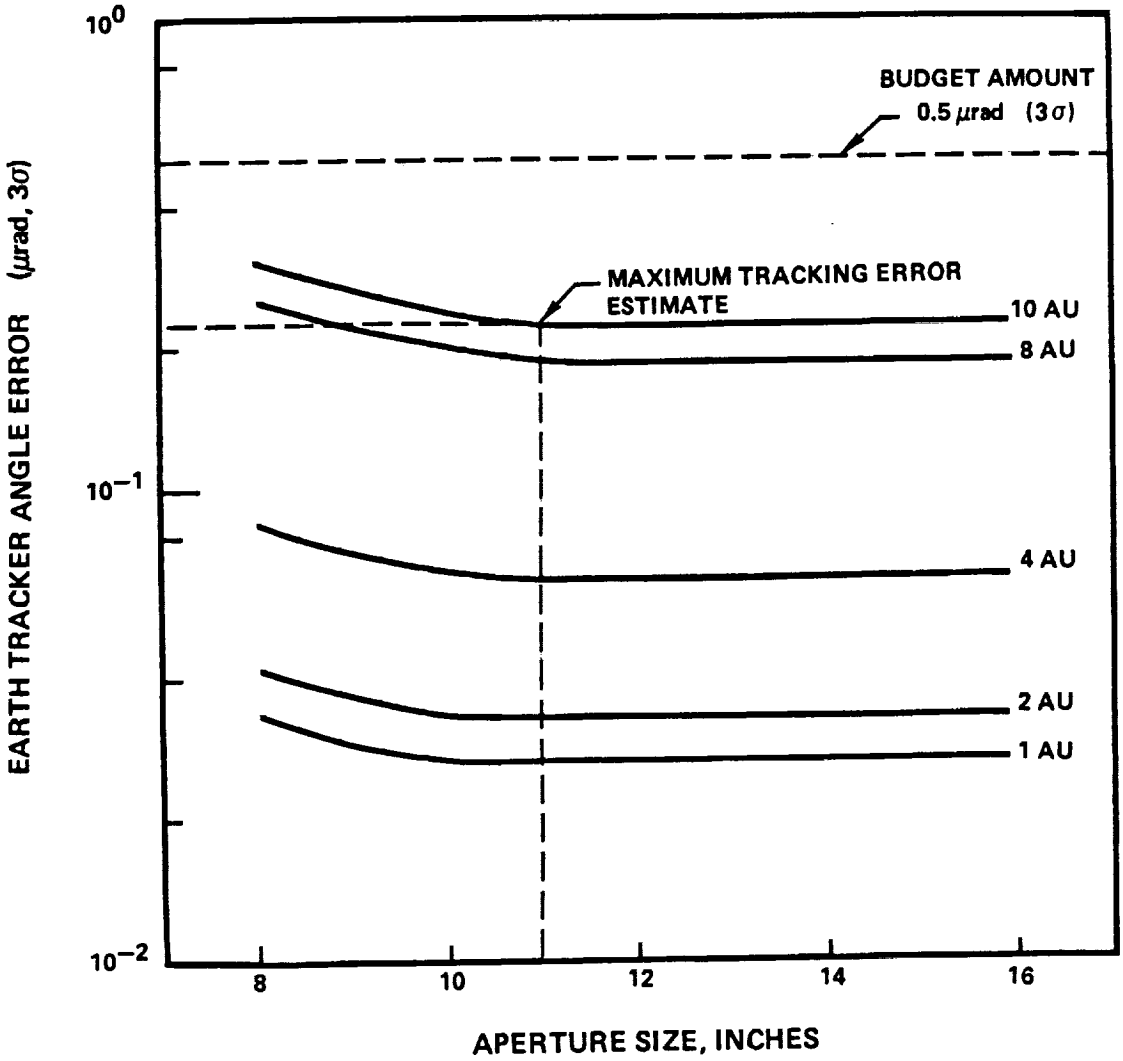

FIGURE 6–8

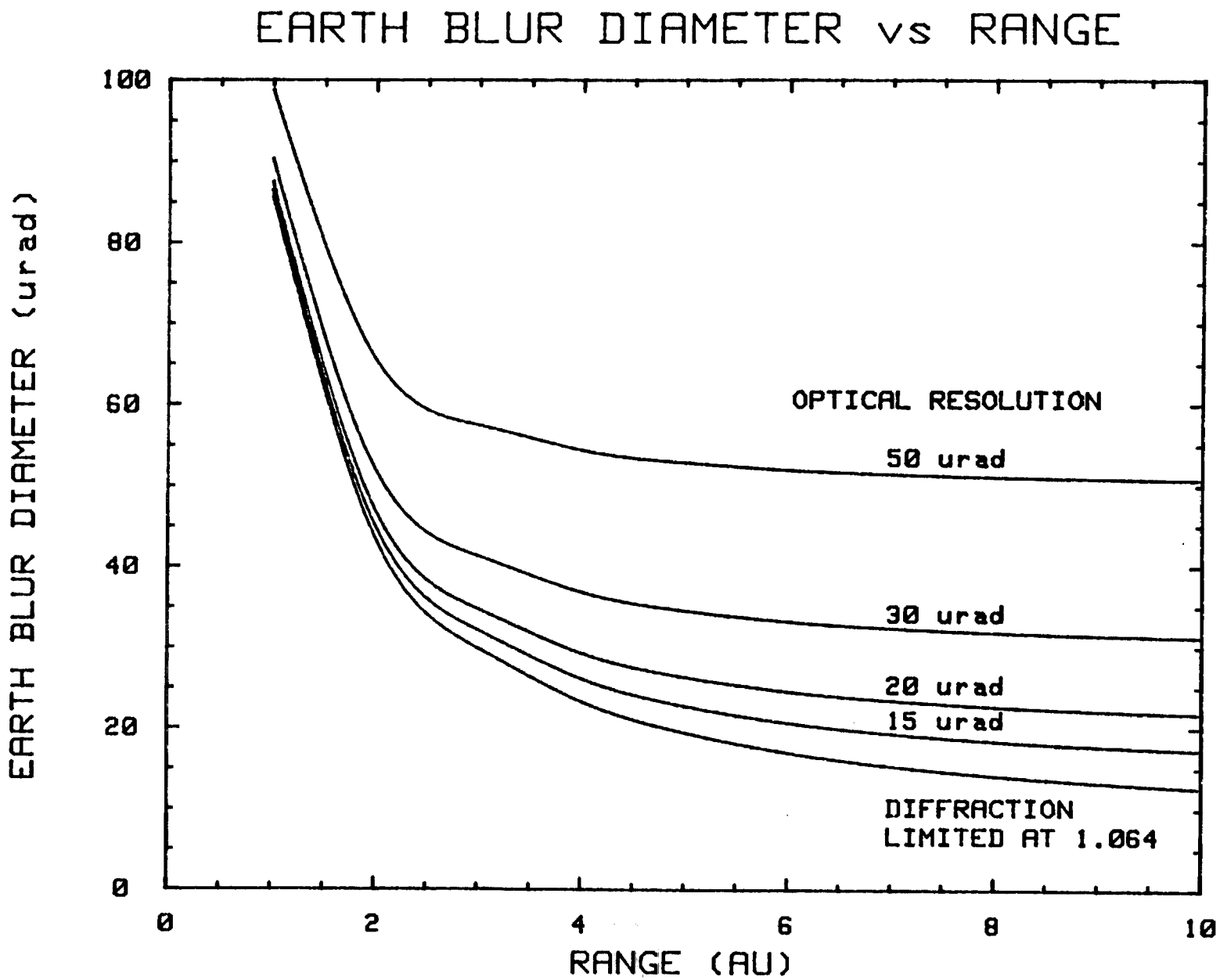
EARTH BLUR DIAMETER vs RANGE
EARTH BLUR DIAMETER (urad)
100
80
60
40
20
0
0
2
4
6
8
10
RANGE (AU)
OPTICAL RESOLUTION
50 urad
30 urad
20 urad
15 urad
DIFFRACTION
LIMITED AT 1.064

FIGURE 6-9

The angle error is then calculated using the following expression [Ref 4].

$$\theta_{RMS} = \frac{1}{SF * SNV} \sqrt{\frac{2F_c}{F_r}}$$

where

SF = Slope Factor

$SNV = SNR^{1/2}$

F_C = Tracking Loop Bandwidth

F_r = Output Sample Rate

$$SNR = \frac{\text{Total Signal Power}}{\text{Total Noise Power}}$$

The total noise power is composed of background power from solar scattering and the detector noise terms specified in Appendix B-5. The received signal is composed of a complex function involving non-destructive readouts and additional averaging times. These techniques are documented in [Ref. 6].

6.2 COMMUNICATION LINKS - With component values identified in Section 5.0 and background levels determined in Section 3.9, the final sizing of the OPTRANSPAC links involves definition and trades of laser powers and aperture sizes. The design rationale involving link margin analysis is outlined in Figure 6-10. The environment and pointing control as well as communication link parameters must be traded to obtain an overall acceptable link design with confidence. By the time the links are finalized, many iterations have occurred involving the control and communications aspects. Only the final links are given. The intermediate iterations are not shown, but their importance in optimizing the design should be noted.

6.2.1 TRANSMIT GAIN/POINTING LOSS RELATIONSHIP - The transmit gain intensity of a Gaussian fed Cassegrain telescope falls off in magnitude as a function of off-axis angle. Zero pointing error results in maximum on-axis gain. However, perfect pointing is unachievable with most real platforms and this results in a loss (from maximum on-axis gain) associated with the magnitude of the pointing error. This loss is referred to as pointing loss. Figure 6-11 illustrates the resulting transmit/gain pointing loss relationship for various diffraction limited transmit apertures and pointing errors. Note that large diffraction limited apertures cannot be supported by large pointing errors. Thus, minimum pointing errors become a design driver.

The tracking budget developed in Section 6.1.3 indicates a maximum tracking error of 1 microradian. From the curves in Figure 6-11, it is evident the maximum diffraction limited aperture size is approximately sixteen inches. The minimum aperture size will be set by one of two criteria; the transmit gain required on the downlink or the receiver gain required for the uplink. From a system point of view, the aperture size was determined by optimizing OPTRANSPAC weight and power. Figure 6-12 shows the OPTRANSPAC telescope weight versus

LINK DESIGN RATIONALE

FIGURE 6–10

C-2

TRANSMIT GAIN - POINTING ERROR RELATIONSHIP

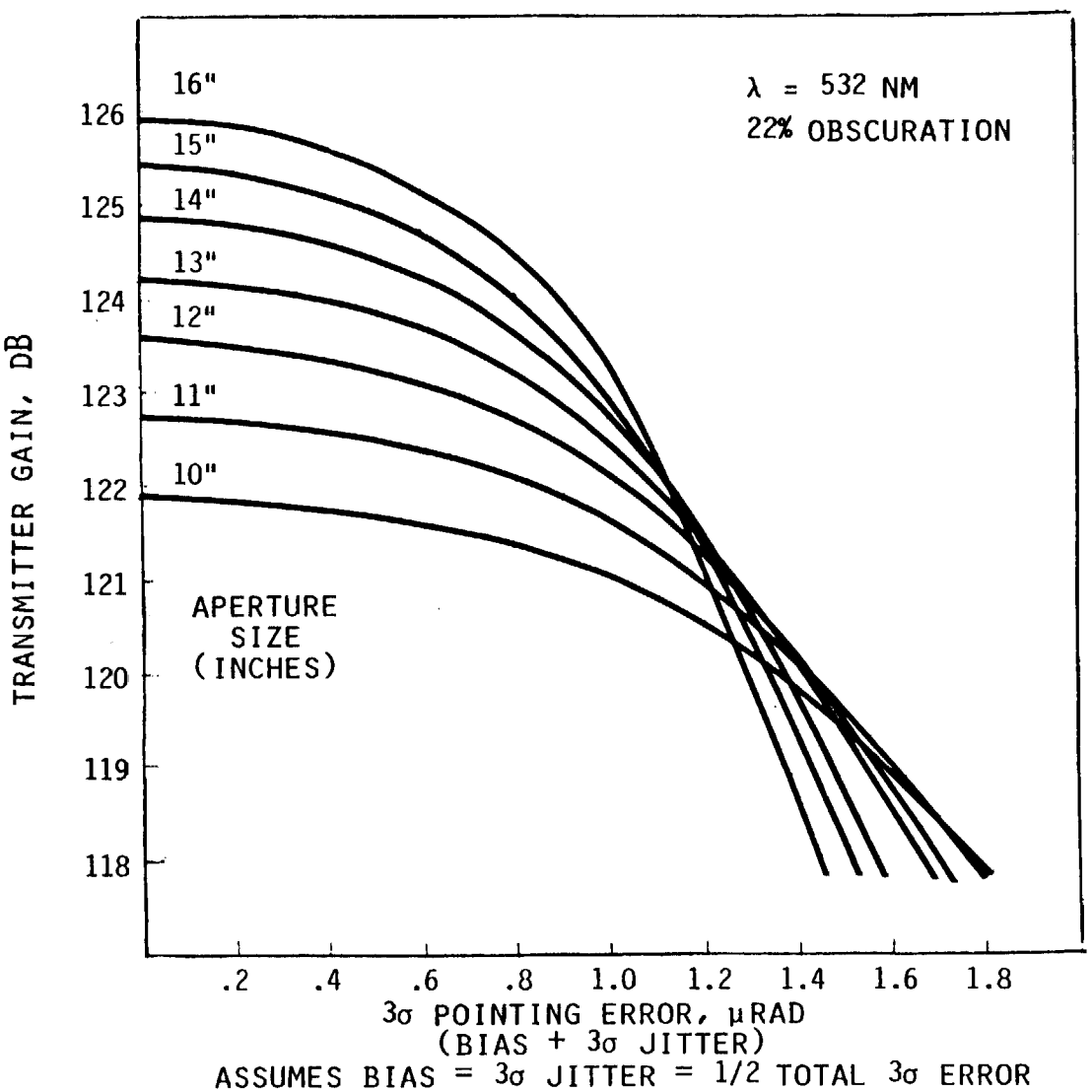

FIGURE 6-11

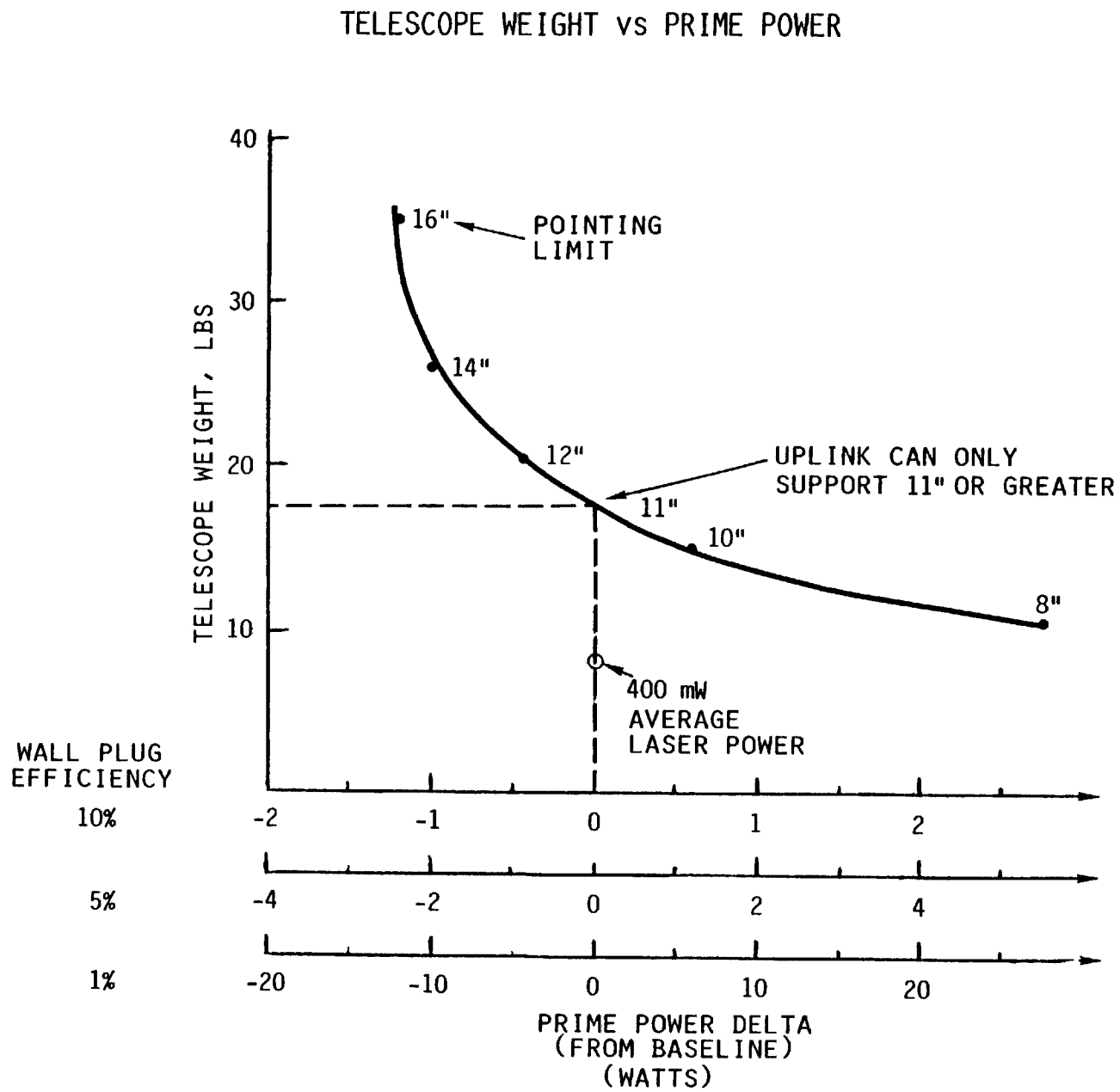
TELESCOPE WEIGHT vs PRIME POWER
TELESCOPE WEIGHT, LBS
40
30
20
10
16"
POINTING LIMIT
14"
12"
11"
10"
8"
UPLINK CAN ONLY SUPPORT 11" OR GREATER
400 mW AVERAGE LASER POWER
WALL PLUG EFFICIENCY
10%
5%
1%
-2
-1
0
1
2
-4
-2
0
2
4
-20
-10
0
10
20
PRIME POWER DELTA (FROM BASELINE) (WATTS)

FIGURE 6-12

prime power delta (from 400 mW average transmit power) needed to close the downlink with 3 dB of margin. The system design point is indicated. Weight and power indicate a baseline design of 115 pounds and 57 watts. The minimum system aperture size was limited to eleven inches by the uplink command beacon margin. As can be seen, an increase of 12 pounds (14" aperture) would yield a decrease in required prime power, but this amount is minimal when high efficiency lasers are used. The baseline design point appears on the bend in the curve and any increase or decrease in aperture size causes either a large weight increase for small power gain or large power need for small weight reduction. Weight was assumed most critical in meeting the overall OPTRANSPAC requirement, and thus, an eleven inch OPTRANSPAC aperture was chosen as baseline.

6.2.2 DOWNLINK MARGIN - The OPTRANSPAC downlink consists of a frequency doubled Nd:YAG laser modulated in a PPM format at one of three distinct rates (100 KBPS, 30 KBPS, and 10 KBPS). The transmit source radiates 400 milliwatts of 532 nanometer average power into a 3.4 microradian beam. The maximum range between the two platforms is 10 AU. The EORS detector is a photomultiplier with a 30 percent quantum efficiency at 532 nanometers. The receiver viewfield is one microradian and the worst case background is the off-axis scattering of solar energy into the telescope. The sensitivity of the receiver was calculated to be 0.9 nanowatts, peak (at 10^{-3} BER, RS coded). The link is given in Figure 6-13 with a design margin of 3dB.

The downlink margin versus aperture size relationship is given in Figure 6-14 for various ranges and data rates. The increase in margin at the lower data rates can be used to decrease the system bit error probability. Figure 6-15 indicates that bit error probabilities less than 10^{-7} can be achieved at the lower data rates with link margins in excess of 3dB.

Extrapolation of the downlink data rate to 300 KBPS requires modification of the transceiver design. If the same 8 bit per pulse PPM format is used, laser power or aperture size or both would need to be increased to accommodate this change. Increased prime power, added weight and possibly a new laser design may be required. If the PPM format is changed (more bits per pulse), a new Reed-Solomon encoder/decoder design and a new PPM electronics design would have to be required. Added weight and prime power may also be required. Overall, a modification to the present design by increasing the data rate will ripple through the entire system design.

6.2.3 UPLINK MARGIN - The uplink command beacon consists of a Nd:YAG Laser modulated in a PPM format at 1KBPS. The transmit source radiates 10 watts of average power into a 5 μradian beam. The maximum range between the two terminals is 10 AU. The OPTRANSPAC receive aperture is 11 inches in diameter and has a 22% obscuration. The viewfield is 1 milliradian and is driven by the Earth tracker and alignment requirements.

The beacon communication detector is an avalanche photodiode which, under the worst case background conditions (i.e., solar light scattered into the aperture) and associated preamplifier noise, provides a sensitivity of 2.6 nanowatts, peak (at 10^{-3} BER, RS coded). Figure 6-16 shows the OPTRANSPAC uplink sized for 3dB design margin. Figures 6-17 and 6-18 illustrate the effect of receive aperture size on uplink margin and the effect of link range on uplink margin. The OPTRANSPAC is limited in aperture size to 11 inches, minimum, by

DOWNLINK LINK MARGIN
(OPTRANSPAC TO EORS)

FILENAME: LSGLST1 DATE: 85/07/12

ND:YAG SATURN TO LEO LINK

LINK PARAMETERS			
1.	LASER TYPE	ND:YAG	
2.	WAVELENGTH, METERS	.5320E-06	
3.	LINK TYPE	COMMUNICATION	
4.	UNCODED PPM BIT ERROR PROBABILITY	.2000E-01	
5.	DATA RATE, BPS	.1000E+06	
6.	MODULATION FORMAT	PPM	
7.	NUMBER OF PIM SLOTS	256.	
		FACTOR	DB
TRANSMITTER PARAMETERS			
1.	PEAK POWER, WATTS	.2800E+04	34.47
	AVERAGE POWER, WATTS	.4000E+00	
	PULSEWIDTH, SECONDS	.1000E-07	
	PULSE RATE, PPS	.1429E+05	
2.	TRANSMISSION EFFICIENCY	.4520E+00	-3.45
	OPTICS EFFICIENCY	.5700E+00	
	RMS WAVEFRONT ERROR LOSS	.7930E+00	
	CIRCULARIZING LOSS	.1000E+01	
3.	POINTING LOSS	.8218E+00	-.85
	POINTING BIAS ERROR, RADIANS	.3000E-06	
	POINTING JITTER ERROR, RADIANS RMS	.2333E-06	
	POINTING ERROR PROBABILITY	.1000E-02	
4.	TRANSMITTER GAIN		
	(OPT FIXED APER/OBSCUR)	.1875E+13	122.73
	APERTURE DIAMETER, METERS	.2794E+00	
	OBSCURATION DIAMETER, METERS	.6147E-01	
	BEAM DIVERGENCE, RADIANS	.3360E-05	
	BEAM DIAMETER, METERS	.2621E+00	
CHANNEL PARAMETERS			
1.	FREE SPACE LOSS	.8008E-39	-390.96
	RANGE SEPARATION, METERS	.1496E+13	
2.	BACKGROUND RADIANCE, W/M**2/SR/A	.1220E-02	
3.	BACKGROUND IRRADIANCE, W/M**2/A	0.	
4.	ATMOSPHERIC LOSS	.1000E+01	0.00
RECEIVER PARAMETERS			
1.	RECEIVER ANTENNA GAIN	.3487E+16	155.42
	APERTURE DIAMETER, METERS	.1000E+02	
	OBSCURATION DIAMETER, METERS	0.	
2.	TRANSMISSION EFFICIENCY	.5000E+00	-3.01
	OPTICS EFFICIENCY	.5000E+00	
3.	OPTICAL FILTER TRANSMISSION	.6850E+00	-1.64
4.	OPTICAL FILTER BANDWIDTH, ANGSTROMS	.2500E+02	
5.	RECEIVER DIAMETRICAL FIELD OF VIEW RAD	.1000E-05	
6.	AC COUPLING LOSS	.1000E+01	0.00

DETECTOR PARAMETERS			
1.	DETECTOR TYPE	PMT	
2.	DETECTOR QUANTUM EFFICIENCY	.3000E+00	
3.	NOISE EQUIVALENT BANDWIDTH, HERTZ	.5000E+08	
	RECEIVER SLOTWIDTH, SECONDS	.1000E-06	
4.	PROCESSING LOSS	.6776E+00	
RECEIVED SIGNAL AND NOISE PARAMETERS			
1.	RECEIVED SIGNAL, WATTS PEAK	.1865E-08	-87.29
	RECEIVED PHOTOELECTRONS/PULSE	.1498E+02	
REQUIRED SIGNAL PARAMETERS			
1.	REQUIRED SIGNAL, WATTS PEAK	.9357E-09	-90.29
2.	REQUIRED SIGNAL TO NOISE RATIO	.7518E+01	
SYSTEM LINK MARGIN		.1993E+01	3.00

FIGURE 6-13

DOWNLINK MARGIN vs APERTURE SIZE

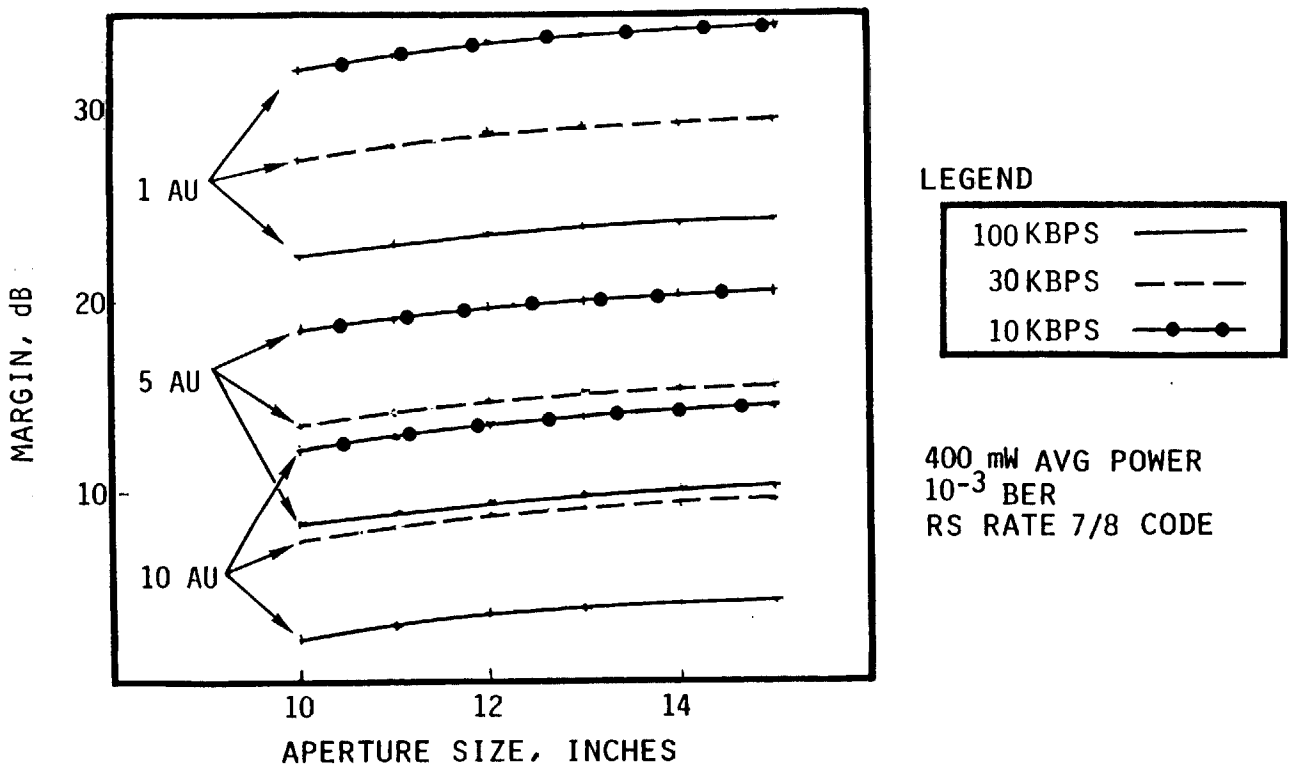

FIGURE 6-14

DOWNLINK BIT ERROR RATE
VERSUS SYSTEM MARGIN

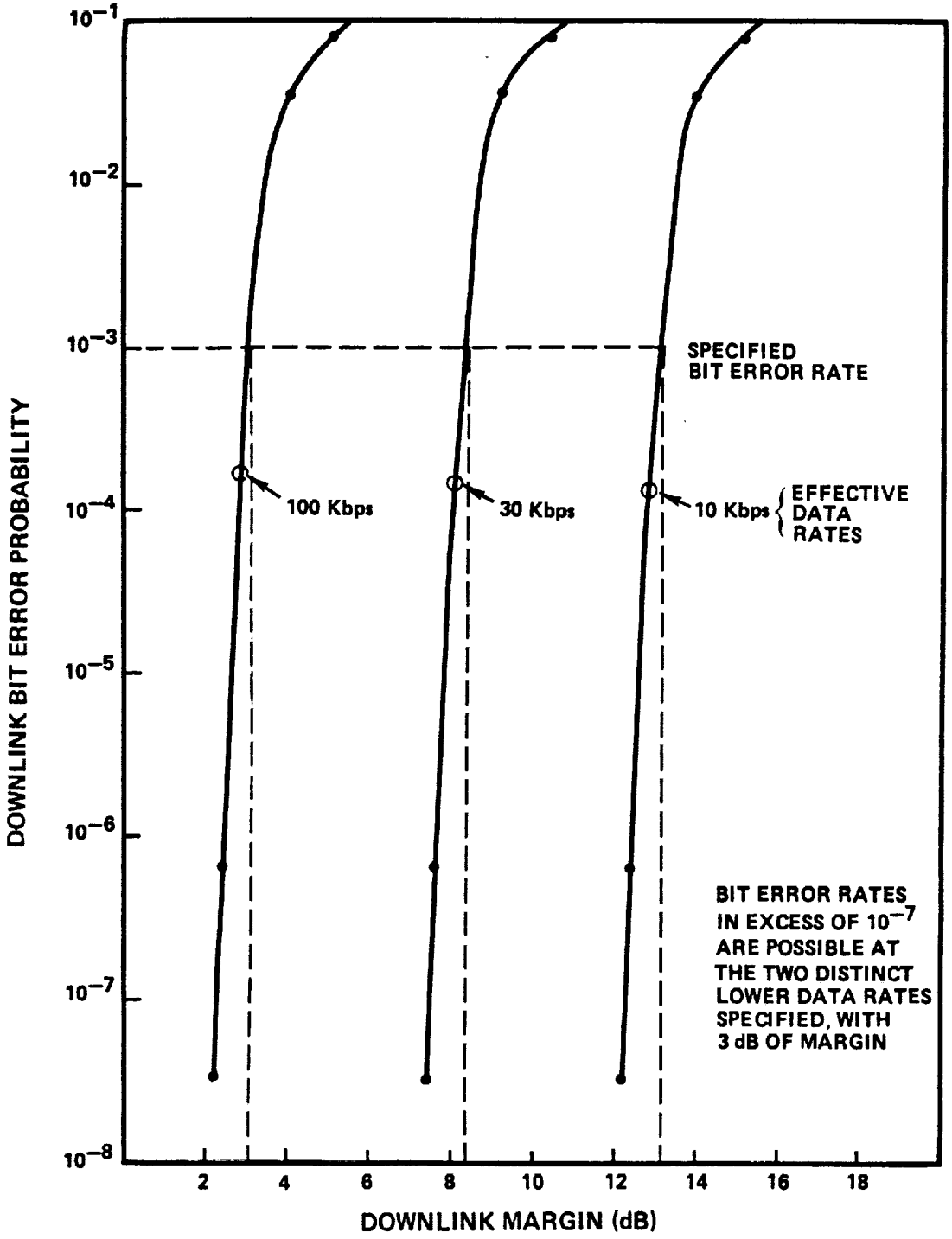

FIGURE 6–15

UPLINK LINK MARGIN
(EORS TO OPTRANSPAC)

FILENAME: LSGLST2 DATE: 85/07/12

EARTH ORBITING RELAY TO SATURN PROBE OPTRANSPAC

LINK PARAMETERS			
1.	LASER TYPE	ND:YAG	
2.	WAVELENGTH, METERS	.1064E-05	
3.	LINK TYPE	COMMUNICATION	
4.	UNCODED PPM BIT ERROR PROBABILITY	.2000E-01	
5.	DATA RATE, BPS	.1000E+04	
6.	MODULATION FORMAT	PPM	
7.	NUMBER OF PIM SLOTS	256.	
		FACTOR	DB
TRANSMITTER PARAMETERS			
1.	PEAK POWER, WATTS	.7000E+07	68.45
	AVERAGE POWER, WATTS	.1000E+02	
	PULSEWIDTH, SECONDS	.1000E-07	
	PULSE RATE, PPS	.1429E+03	
2.	TRANSMISSION EFFICIENCY	.7000E+00	-1.55
	OPTICS EFFICIENCY	.7000E+00	
	RMS WAVEFRONT ERROR LOSS	.1000E+01	
	CIRCULARIZING LOSS	.1000E+01	
3.	POINTING LOSS	.1000E+01	0.00
	POINTING BIAS ERROR, RADIANS	0.	
	POINTING JITTER ERROR, RADIANS RMS	0.	
	TOTAL POINTING ERROR BIAS+JITTER, RADIANS	0.	
4.	TRANSMITTER GAIN (HAND INPUT GTYPE=6)	.1280E+13	121.07
	APERTURE DIAMETER, METERS	.1000E+02	
	OBSCURATION DIAMETER, METERS	0.	
	BEAM DIVERGENCE, RADIANS	.5000E-05	
CHANNEL PARAMETERS			
1.	FREE SPACE LOSS	.3203E-38	-384.94
	RANGE SEPARATION, METERS	.1496E+13	
2.	BACKGROUND RADIANCE, W/M**2/SR/A	.2000E-03	
3.	BACKGROUND IRRADIANCE, W/M**2/A	.1100E-11	
4.	ATMOSPHERIC LOSS	.1000E+01	0.00
RECEIVER PARAMETERS			
1.	RECEIVER ANTENNA GAIN	.6476E+12	118.11
	APERTURE DIAMETER, METERS	.2794E+00	
	OBSCURATION DIAMETER, METERS	.6148E-01	
2.	TRANSMISSION EFFICIENCY	.5900E+00	12.29
	OPTICS EFFICIENCY	.5900E+00	
3.	OPTICAL FILTER TRANSMISSION	.6540E+00	-1.84
4.	OPTICAL FILTER BANDWIDTH, ANGSTROMS	.2500E+02	
5.	RECEIVER DIAMETRICAL FIELD OF VIEW,RAD	.1000E-02	
6.	AC COUPLING LOSS	.1000E+01	0.00

DETECTOR PARAMETERS			
1.	DETECTOR TYPE	APD	
	DETECTOR NOISE FACTOR	.3451E+01	
	AVALANCHE GAIN	.2100E+03	
	IONIZATION COEFFICIENT	.7000E-02	
2.	DETECTOR QUANTUM EFFICIENCY	.4000E+00	
3.	DETECTOR NOISE EQUIVALENT POWER, W/HZ^.5	.2100E-13	
4.	PREAMP NOISE CURRENT DENSITY, A/HZ^.5	.1400E-11	
	EFFEVTIVE RECEIVER TEMP., DEG K	.3000E+03	
	EFFECTIVE RECEIVER RESISTOR, OHMS	.8449E+04	
5.	NOISE EQUIVALENT BANDWIDTH, HERTZ	.5000E+08	
	RECEIVER SLOTWIDTH, SECONDS	.1000E-06	
6.	PROCESSING LOSS	.7244E+00	
RECEIVED SIGNAL AND NOISE PARAMETERS			
1.	RECEIVED SIGNAL, WATTS PEAK	.5021E-08	-82.99
	RECEIVED PHOTOELECTRONS/PULSE	.1076E+03	
2.	NOISE POWER SPECTRAL SENSITY, A^2/HZ	.1302E-27	
	IN (PE/PULSE)^2	.2537E+02	
	OPTICAL BACKGROUND POWER DENSITY, A^2/HZ	.3379E-28	
	IN (PE/PULSE)^2	.6583E+01	
	DETECTOR NOISE POWER DENSITY, A^2/HZ	.5195E-28	
	IN (PE/PULSE)^2	.1012E+02	
	PREAMP NOISE POWER DENSITY, A^2/HZ	.4446E-28	
	IN (PE/PULSE)^2	.8663E+01	
REQUIRED SIGNAL PARAMETERS			
1.	REQUIRED SIGNAL, WATTS PEAK	.2498E-08	-86.02
	REQUIRED SIGNAL, PE/PULSE	.5352E+02	
2.	REQUIRED SIGNAL TO NOISE RATIO	.1704E+01	
SYSTEM LINK MARGIN		.2010E+01	3.03

FIGURE 6-16

UPLINK MARGIN vs APERTURE SIZE

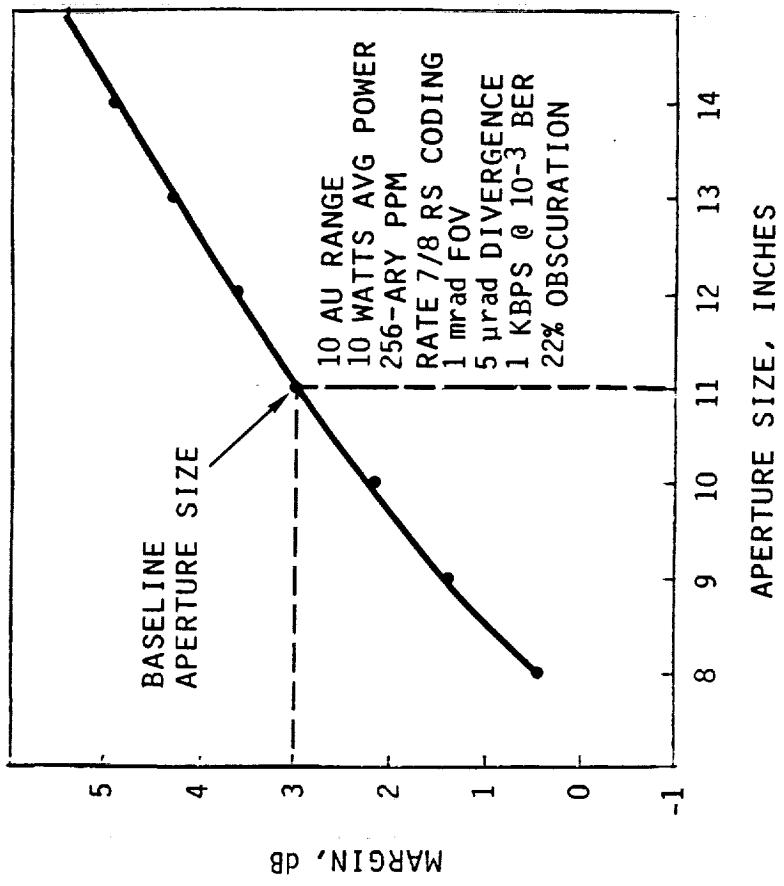

FIGURE 6–17

UPLINK MARGIN VS RANGE

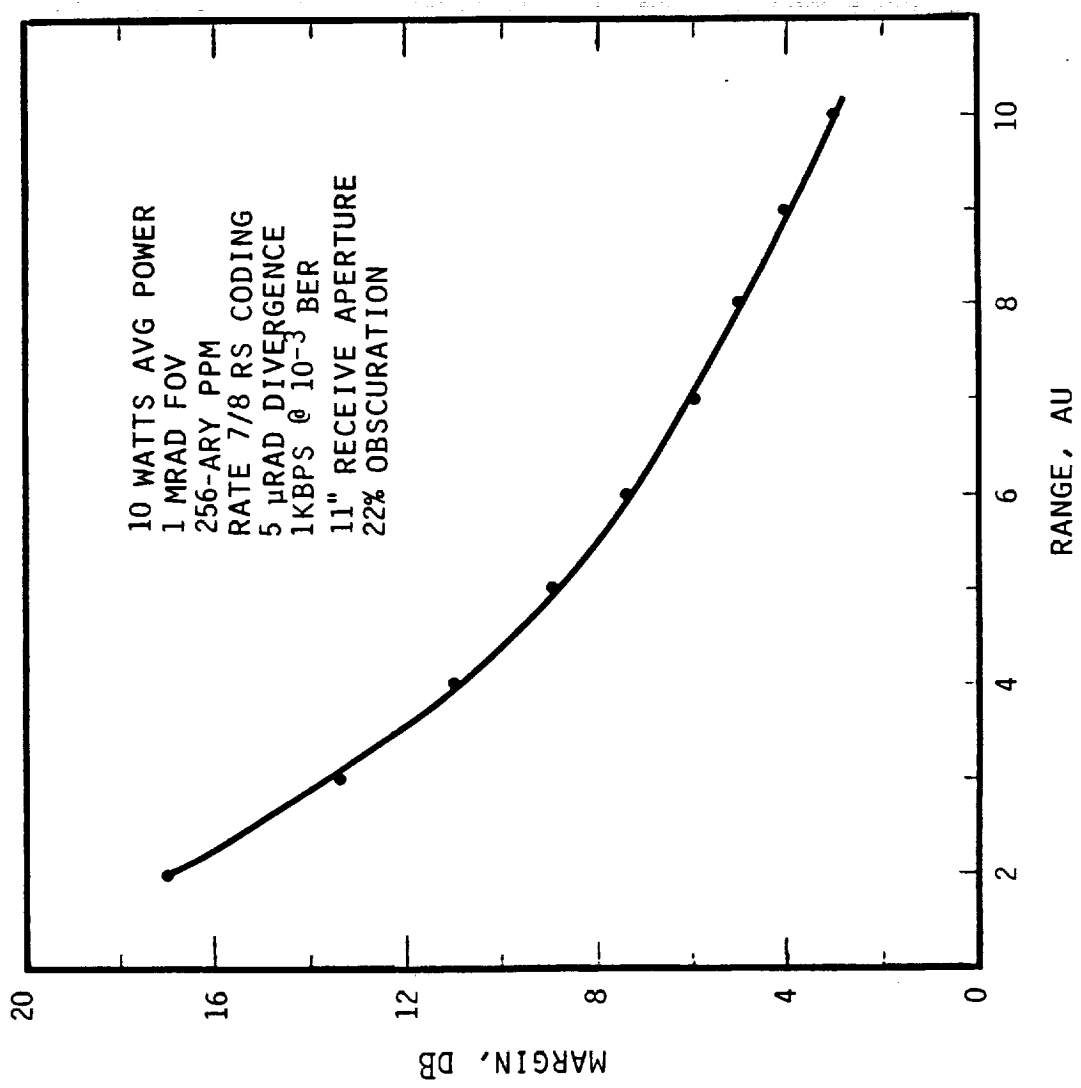

FIGURE 6–18

the command uplink. The maximum range offered to maintain the 3dB design margin is 10 AU. Command link operation out to approximately 14 AU may be possible with no design margin.

The specified command link bit error probability may require a decrease from 10^{-3} to 10^{-6} under certain command uplink conditions. Figure 6-19 shows the relationship between error probability and uplink margin for the OPTRANSPAC system. At all ranges less than 9.3 AU, this increase in bit error probability is offset by added margin. However, at ranges greater than 9.3 AU, the margin for a 10^{-6} command uplink is less than 3dB, becoming 2.4 dB at 10 AU. Thus, the maximum cost of maintaining a 10^{-6} command uplink is approximately 0.6dB at 1KBPS.

UPLINK BIT ERROR RATE
VERSUS SYSTEM MARGIN

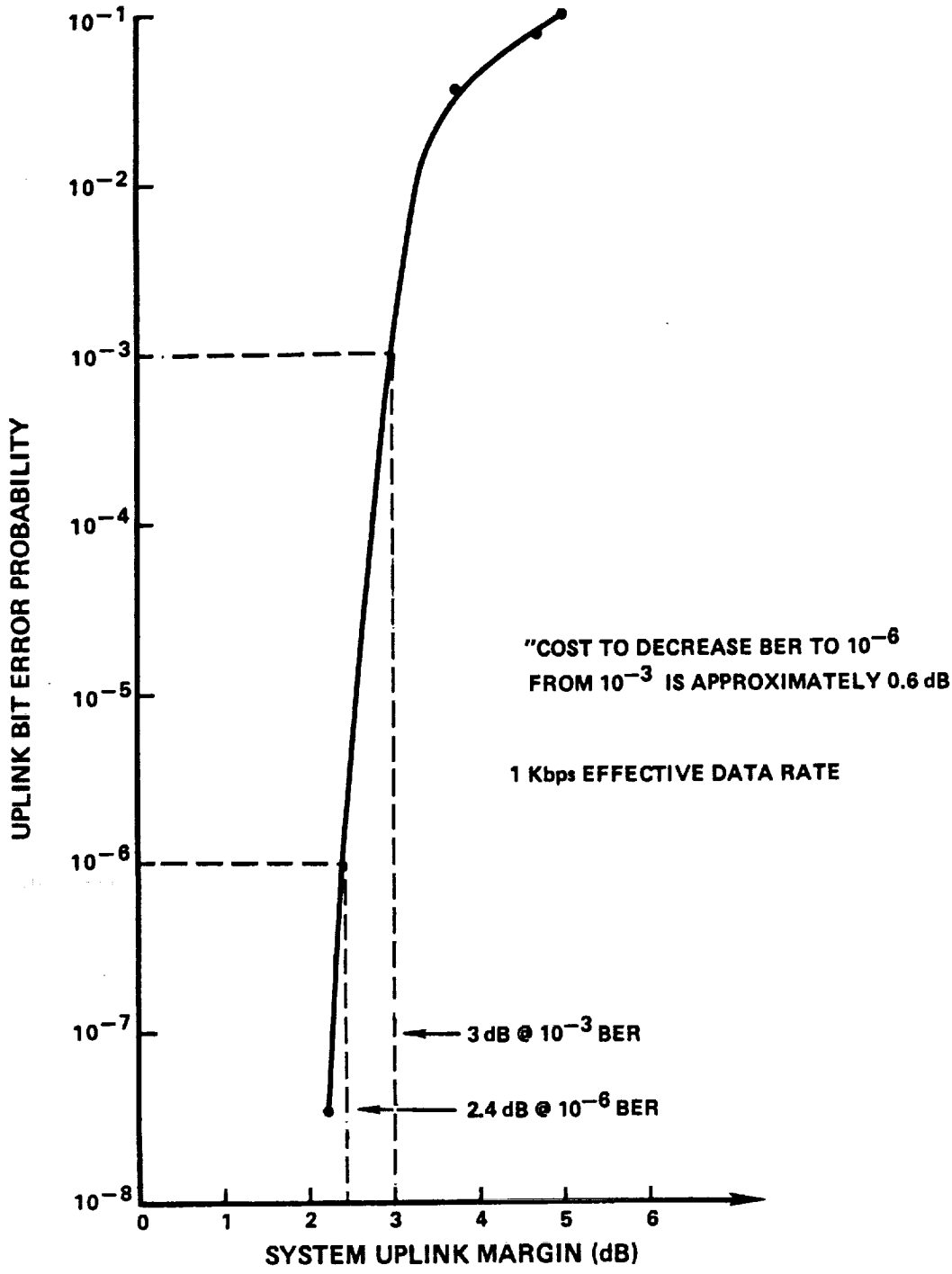

FIGURE 6–19

7.0 ELECTRONICS DESIGN

The electronics as configured consist of three assemblies which provide control, communication and power conditioning functions. A digital computer, input/output circuitry, and drive circuits within the Control Electronics Assembly provide the acquisition and tracking functions. The communication functions of coding/decoding and modulating/demodulating are provided by circuitry within the Communication Electronics Assembly. The Power Conditioner Unit converts the spacecraft power to the required secondary voltage levels, provides redundancy switching, mechanism and heater control, as well as command and telemetry interfaces.

7.1 CONTROL ELECTRONICS ASSEMBLY - The Control Electronics functional block diagram is depicted in Figure 7-1. Command signals to position the torque motor beam steerers (TMBS's) to direct the incoming and transmitted optical signals is the principle output of the Control Electronics digital processor. These commands are based on orbital ephemeris data, spacecraft position sensor data and Earth tracker angle error calculations. These outputs are provided at a 200 Hz rate to support the 20 Hz TMBS loop bandwidth and become the drivers for the operations rate of the control processor. Command signals for positioning the command focus mechanism are initiated by ground command. Mode control of the OPTRANSPAC operation is provided by the digital processor or via ground commands. Figure 7-2 describes in general terms the processor operations in each operating mode. Further description of the control electronics assembly including TMBS position commands and mode logic are given in Appendix C-1; a design note on the OPTRANSPAC electronics.

7.2 COMMUNICATION ELECTRONICS ASSEMBLY - The functional block diagram of the Communication Electronics Assembly is depicted in Figure 7-3. Both receive and transmit functions are required. The receive function consists of conditioning, decoding and formatting of the data pulses from the communication detector. The transmit function involves data formatting, encoding and generation of the required laser modulator drive signal. Further details of the Communication Electronics can be found in the design note in Appendix C-1.

7.2.1 RECEIVE FUNCTION - The output of the communication detector preamplifier consists of the electrical signal amplified and applied to a PPM decoder that operates on a "greatest-of" principle to select the slot containing the signal pulse. The output of the decoder is an NRZ data stream containing rate 7/8 Reed-Solomon encoded data at 1142.86 symbols per second. This data is applied to a Reed-Solomon decoder which produces a 1000 bit per second output. Finally, the 1000 bit per second data is formatted as spacecraft command data. The output of the formatter is applied to a command decoder located within the Power Conditioning Unit.

7.2.2 TRANSMIT FUNCTION - Transmit data consists of a fixed rate serial telemetry data stream from a telemetry formatter located in the Power Conditioner Unit or a serial data stream from the spacecraft sensor. Spacecraft sensor data rates can be 10,000 bits per second, 30,000 bits per second or 100,000 bits per second. This data is assumed to contain overhead including synchronization information. When spacecraft sensor data is available for transmission, the telemetry data is not transmitted. The output of the data selector is rate 7/8 Reed-Solomon encoded and output to a PPM encoder. The output data from the Reed-Solomon encoder is applied to a PPM encoder that produces output symbol

CONTROL ELECTRONICS
FUNCTIONAL BLOCK DIAGRAM

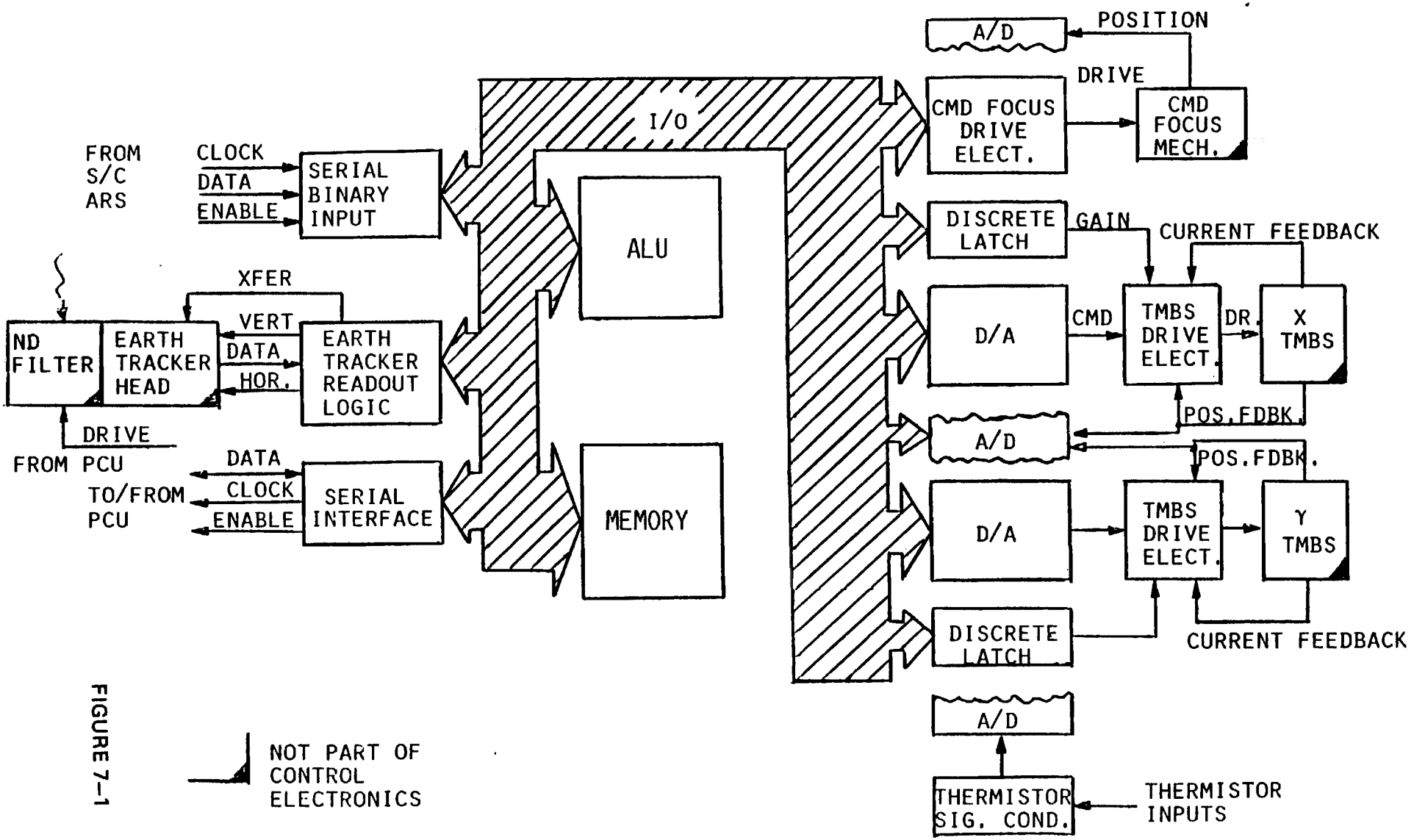

FIGURE 7-1

OPTRANSPAC MODE LOGIC

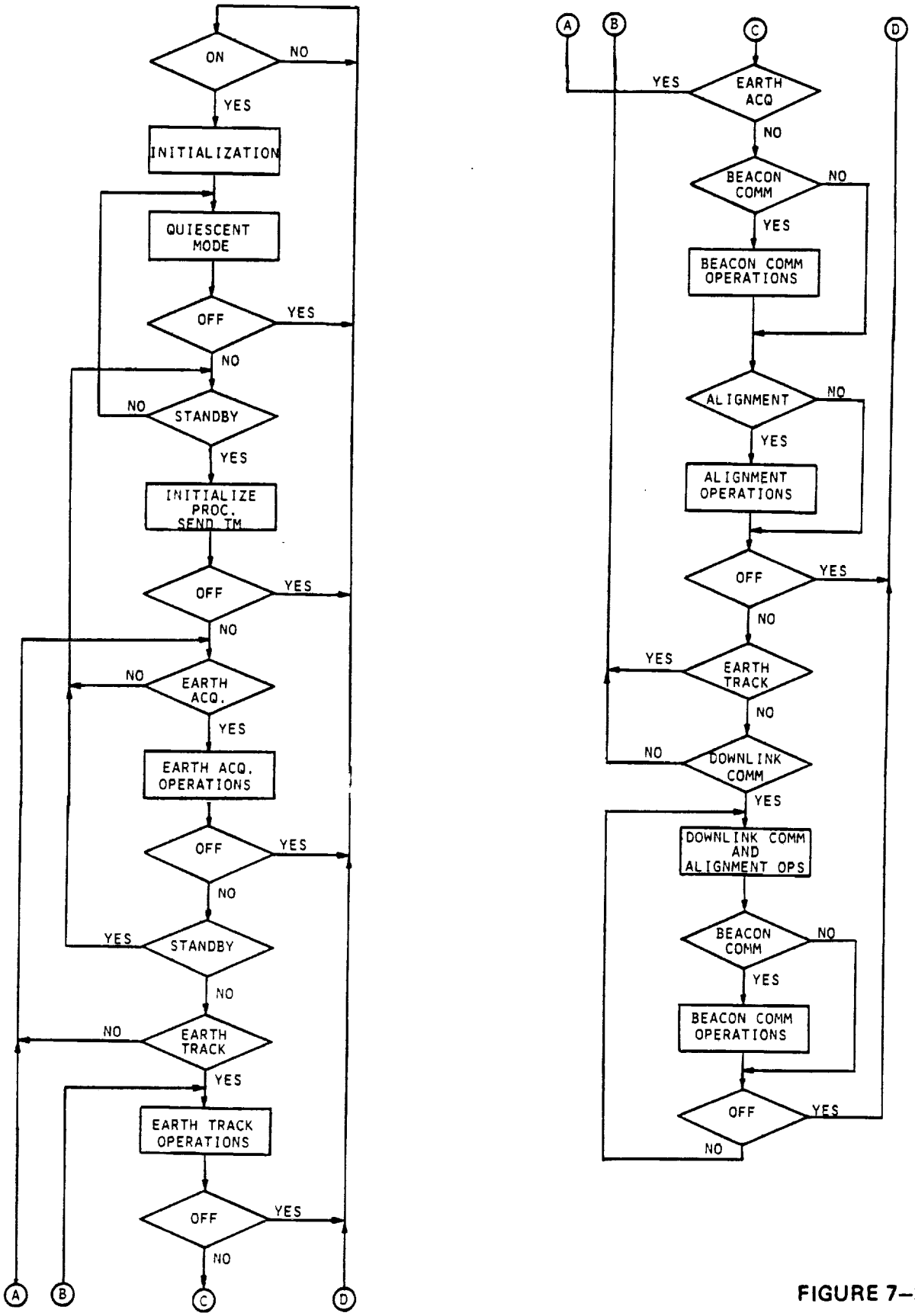

FIGURE 7–2

COMMUNICATION ELECTRONICS
FUNCTIONAL BLOCK DIAGRAM

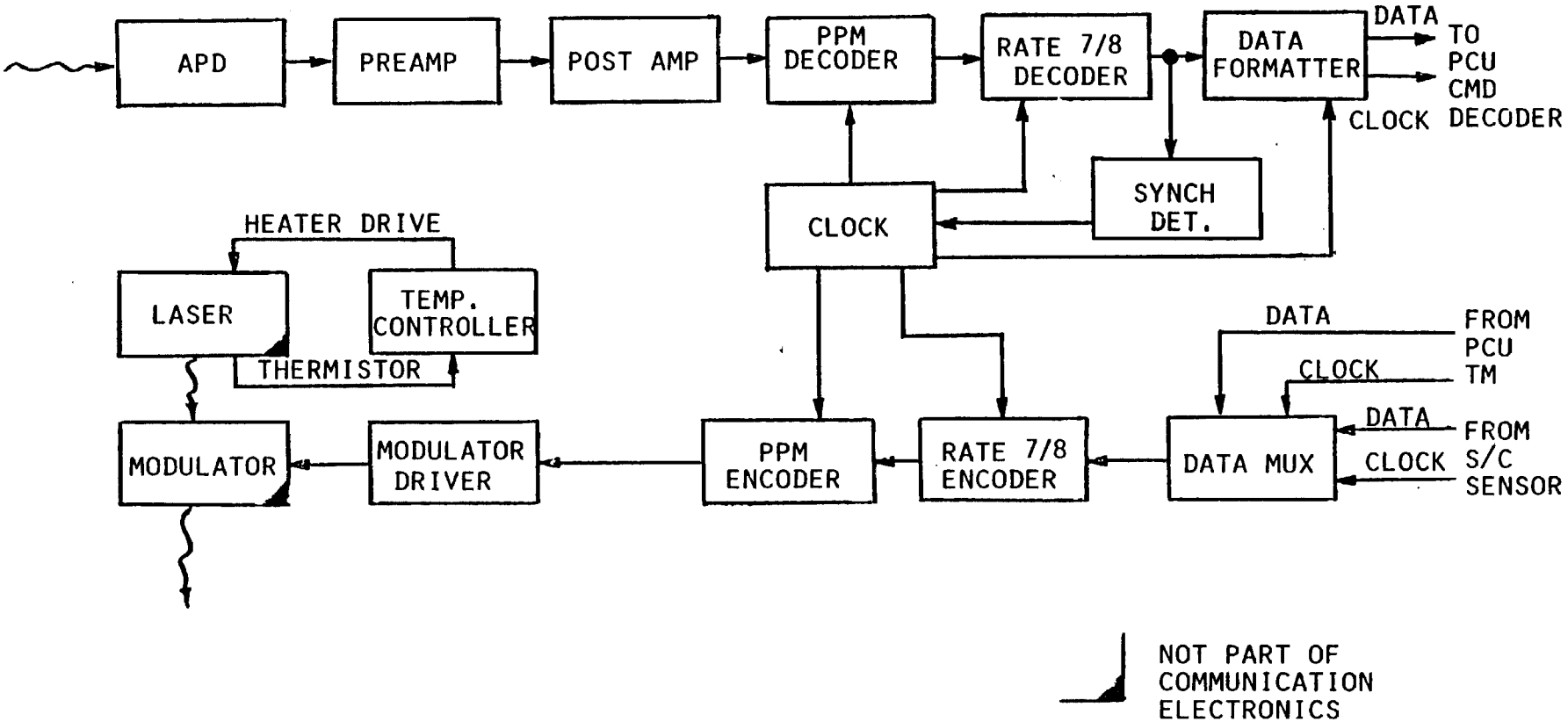

FIGURE 7-3

information at 1428.57, 4285.71 or 14285.71 symbols per second depending upon the sensor data rate. Symbols are encoded by outputting a pulse in one of 256 data slots following a fixed time interval that is referenced to the previous fixed time interval using an internal clock. The output of the PPM encoder is input to modulator drive circuitry. The circuitry converts the logic level input to signal levels required to operate the laser modulator located within the laser assembly.

7.2.3 DOPPLER CONSIDERATIONS - Variations in timing due to Doppler has been analyzed. Maximum velocities encountered are defined in Section 3.2. The temporal shift is dependent upon the instantaneous pulse rate. Because Pulse Position Modulation involves a variable interpulse period, a minimum and maximum temporal shift is associated with each specific data rate. For the specified slot widths at the receiver of 100 nanoseconds, the clock center frequency is 10 MHz. The Doppler shift associated with the specified data rates is calculated to be 2400 Hz. This equates to 240 parts per million which can be readily covered by a voltage controlled crystal oscillator driven by ephemeris data.

7.3 POWER CONDITIONING UNIT - Primary power from the spacecraft's electrical system is conditioned to provide secondary power for the OPTRANSPAC equipment. The power conditioning unit pictured functionally in Figure 7-4, provides the conversion and regulator circuitry required to produce the redundant secondary voltage outputs. Command and telemetry circuitry are also located within the power conditioning unit. Serial command data from the spacecraft's command decoder or the Communications Electronics Assembly is decoded. The output from this circuitry is provided to discrete drivers which control the OPTRANSPAC redundancy switching mechanisms, the active focus mechanism, or power control relays. Serial magnitude commands are relayed to the Control Electronics Assembly via bi-directional serial interface circuitry located within the PCU. This serial interface receives telemetry and heater control data from the Control Electronics Assembly. The telemetry from the Control Electronics Assembly as well as internal analog and discrete data is multiplexed to form a serial data output. This data is transmitted to the EORS via the Communication Electronics Assembly. Circuitry required to condition internal analog and discrete telemetry parameters is provided within the PCU. OPTRANSPAC heater drive circuitry is also located internal to this assembly. Further description of the Power Conditioning Unit is found in Appendix C-1.

7.4 REDUNDANCY IMPLEMENTATION - Figure 7-5 shows the OPTRANSPAC redundancy philosophy. All OPTRANSPAC electronics and mechanisms are redundant with the exception of the command focus mechanism. Cross-strapping for selected functional circuit blocks is provided to minimize the probability of system failure.

The elements of the control function and the cross-straps provided are described in Figure 7-6. All elements of the function are cross-strapped to other redundant elements with the exception of the beam steerers. Experience has proven that cross-strapping of the drivers and beam steerers does not provide significant enhancement of system reliability since the reliability of the drivers and beam steerers is high compared to other elements. In addition, this makes the design of the beam steerer drivers much simpler.

POWER CONDITIONER UNIT
FUNCTIONAL BLOCK DIAGRAM

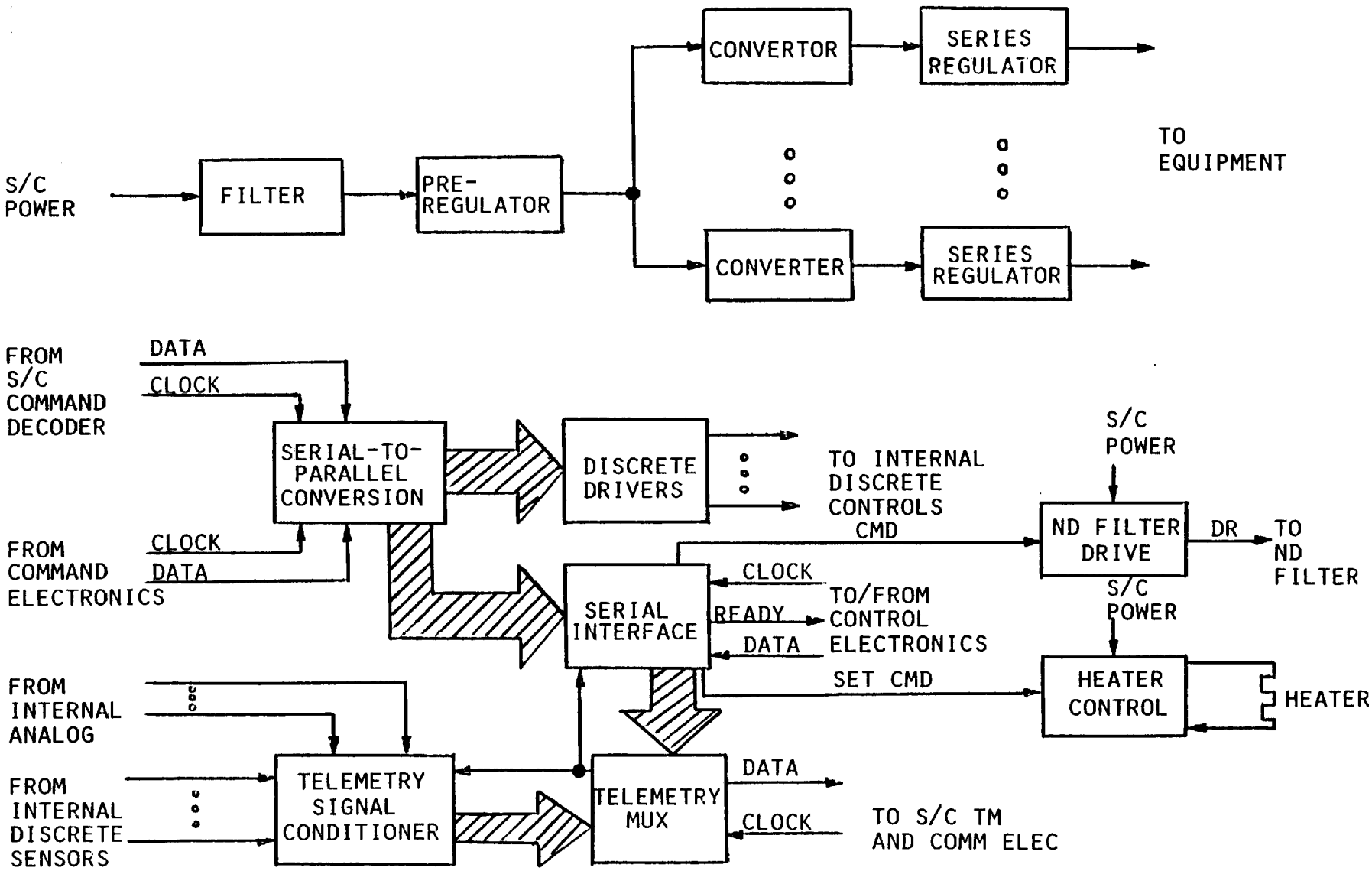

FIGURE 7-4

REDUNDANCY PHILOSOPHY

- HIGHEST PROBABILITY OF SUCCESS CONSISTENT WITH WEIGHT AND COMPLEXITY CONSTRAINTS
- ELIMINATE SINGLE POINT FAILURES
- CROSS-STRAP REDUNDANT ELEMENTS
- CROSS-STRAP AT SOURCE
- CROSS-STRAP SELECTION VIA POWER COMMAND
- COMMUNICATION ELECTRONICS IS BLOCK REDUNDANT WITH CROSS-STRAPPING AT OUTPUT TO PCU COMMAND DECODER AND THE INPUT FROM PCU T/M AND S/C SENSOR
- PCU CONVERTERS DEDICATED TO THE LOAD

FIGURE 7-5

CONTROL ELECTRONICS
REDUNDANCY IMPLEMENTATION

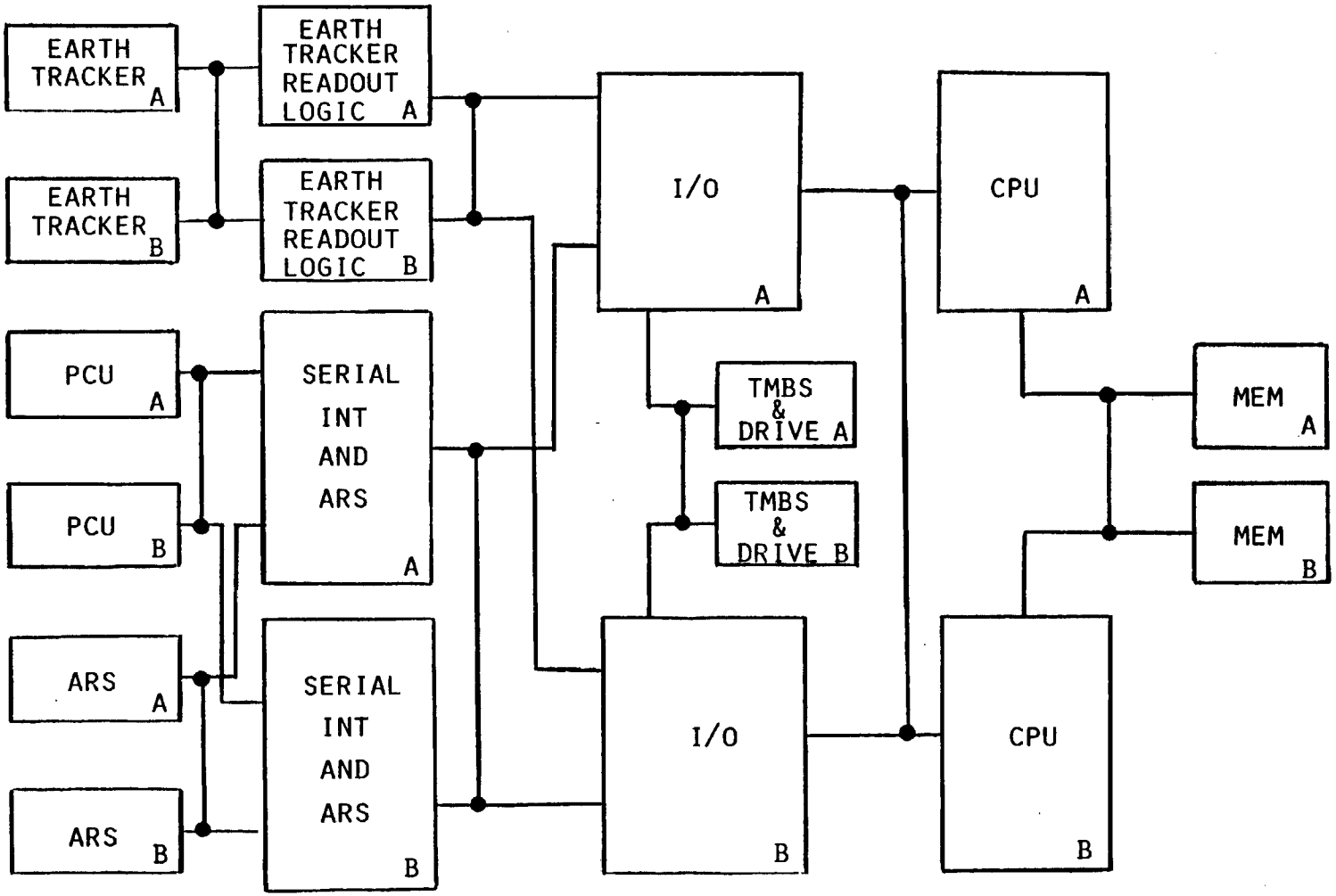

FIGURE 7-6

The elements of the communication function and the cross-strapping provided are detailed in Figure 7-7. Cross-straps are not provided between the communication avalanche photodiode and the preamplifier due to the low signal levels and noise sensitivity at this point. Similarly, design considerations are the principle reason for not cross-strapping the Communication Electronics to the laser assembly.

Figure 7-8 details the elements and cross-strapping of the power conditioning function. Implementation of these cross-straps is accomplished by use of relays controlled via EORS generated commands. Fuses are provided at the input to each converter to prevent load or converter failure propagation to the redundant converter.

7.5 ELECTRONICS PACKAGING - The OPTRANSPAC electronics are housed in packaged assemblies that are designed for minimal size, weight and power and provide thermal radiation through coverplates. A detailed breakout of the size, weight and power is given in the Electronics Design Note in Appendix C-1.

The Control Electronics design is based on 14 ceramic and 2 polyimide circuit boards. Digital circuits in leadless chip carrier packages will be mounted on the ceramic circuit boards. The polyimide boards will be populated with analog integrated circuits and discrete components. Dimensions of all circuit boards are approximately 4.6" by 3.8". Both prime and redundant circuitry will be implemented on the 16 circuit boards.

A total of 12 circuit boards are estimated for the redundant communication electronics. A pair of polyimide boards will be used for the analog integrated circuits and discrete components required. All other circuit boards will be populated with leadless chip carrier digital integrated circuit packages.

The circuitry required for the converters, regulators and relays will be implemented using a module concept. Each module will consist of two (prime and redundant) polyimide circuit boards housed in a frame. The dimensions of each module will be approximately 6" by 6" by 0.3". A total of 5 modules is required.

COMMUNICATION ELECTRONICS
REDUNDANCY IMPLEMENTATION

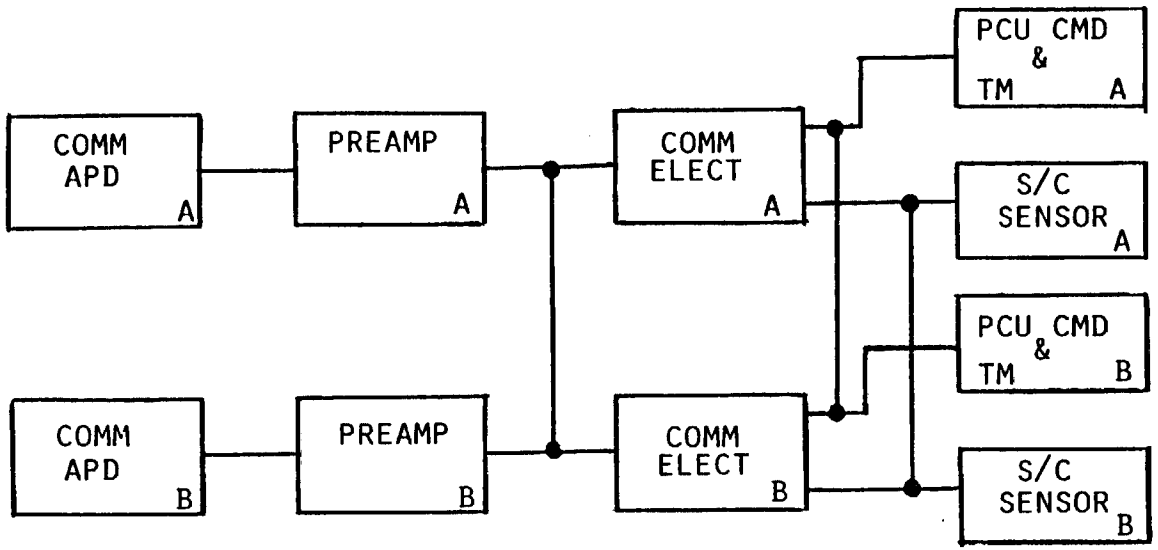

FIGURE 7-7

POWER CONDITIONER UNIT
REDUNDANCY IMPLEMENTATION

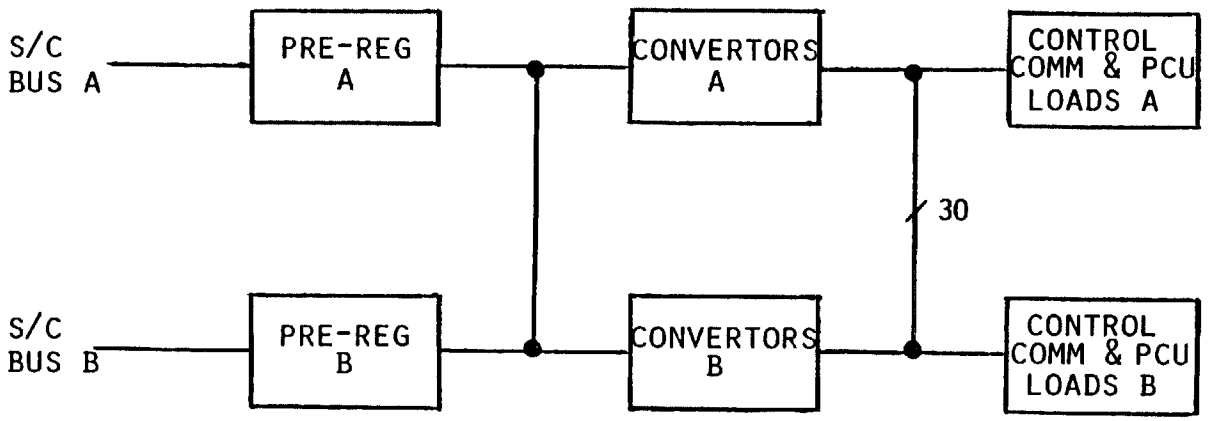

FIGURE 7-8

8.0 OPTICAL DESIGN

The optical system consists of two basic subassemblies: A telescope and an imaging optics assembly (IOA). The system performance requirements of each subassembly are outlined in Appendices B-2 and B-3. an optical system design was developed from the functional requirements through the thin lens stage. The details of the optical analysis can be found in the optical system design note - Appendix C-2. An optical isometric showing the lens layouts is given in Figure 8-1. An orthographic of the optical system is pictured in Figure 8-2.

In the design of the telescope and imaging optics for a spaceborne system, the size and number of optical elements used are kept to a minimum providing necessary functions within the required system performance levels. System optical transmission is usually maximized while system size, weight and procurement costs are minimized. Diffraction limited optical systems such as OPTRANSPAC require the use of multiple element lens components with moderately slow optical speeds to meet image quality requirements. Field of view and spectral range requirements further add to the design complexity. These requirements exact design constraints on optics transmission, optical system envelope and optical system weight.

8.1 TELESCOPE DESIGN - The telescope selected for the OPTRANSPAC system is a modified Cassegrain with refractive correcting elements in the converging beam after the secondary. The selection rationale is outlined in section 5.2. The telescope design is shown in Figure 8-3. Geometric ray tracing of this design both on-axis and at full field confirms that this design fulfills the image quality requirements over the ± 2.5 milliradian viewfield. Diffraction analysis indicates this telescope's wavefront quality is approximately $\lambda/30$ RMS at a wavelength of 532 nanometers. The telescope aperture diameter is eleven inches (297.4 mm) with a central obscuration of twenty-two percent. This section of the optical system is designed to be afocal and maps the 0.5 inch diameter axial bundle of the imaging optics paths to the eleven inch primary mirror diameter.

The Cassegrain telescope optics are designed to produce an f/10 output cone. This allows for a component package whose optical speed is still slow enough to ensure good image quality and readily manufacturable components. Further telescope analysis can be found in Appendix C-2.

8.2 IMAGING OPTICS DESIGN - For clarification the imaging optics paths are subdivided into four areas: the common path (prime and redundant), the transmit path, the receive communications path, and the receive tracking path.

In the common path and throughout the imaging optics it was desirable to use only a few basic lens groupings in a repetitive way to simplify the design and procurement of the optics. Such repetitive lens groupings must relay the telescope pupil through the imaging optics with minimal vignetting. This requires that sections of collimated space used for locating beam steerers or beamsplitters be rather short to minimize the need for large (> 50 mm diameter) optics. Further details and ray traces of the common path are given in Appendix C-2.

The optics in the transmit path are handling monochromatic (532 nanometer) light which is of small divergence and remains on-axis (all steering of the

OPTRANSPAC
OPTICAL ISOMETRIC VIEW

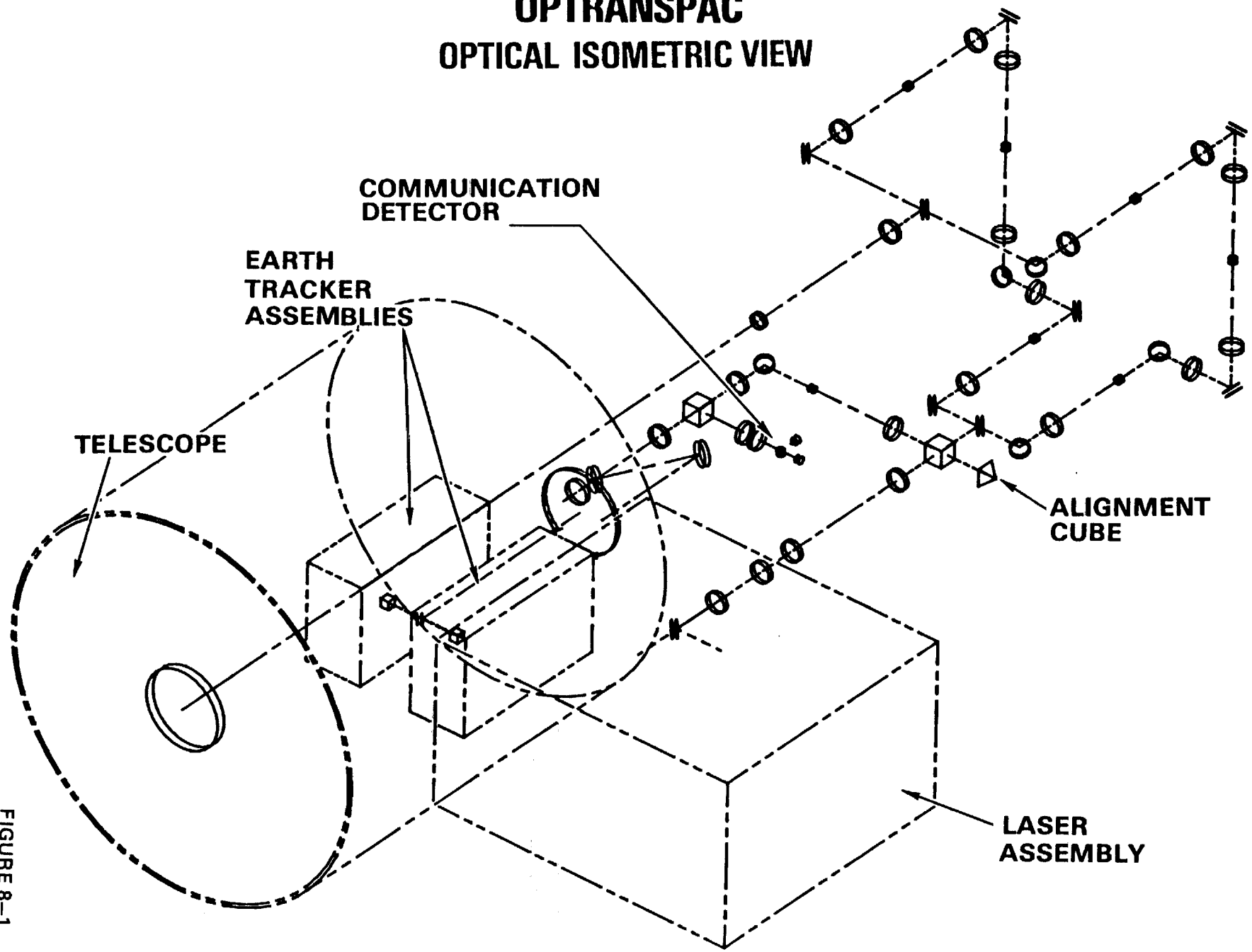

FIGURE 8–1

OPTRANSPAC
ORTHOGRAPHIC
TOP VIEW

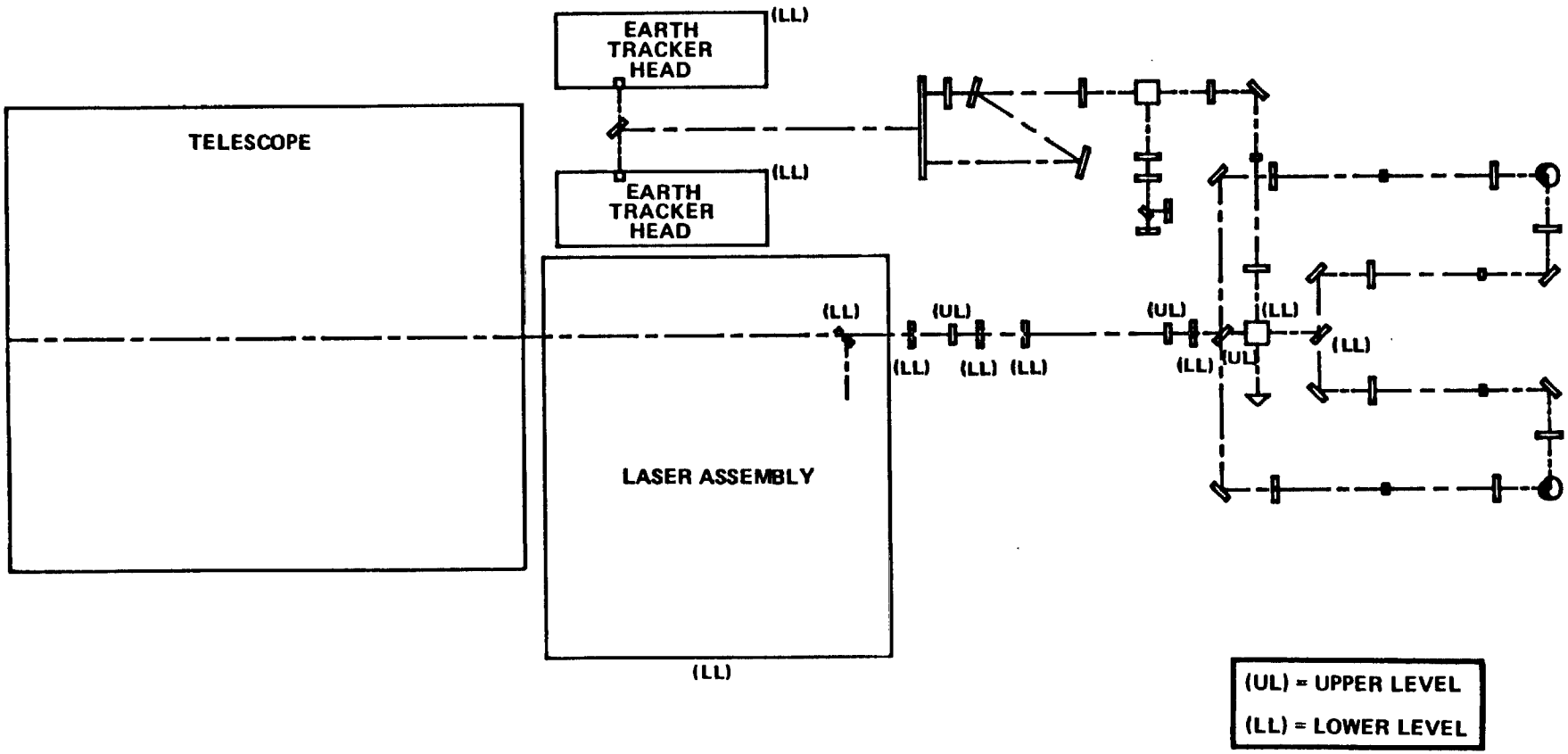

FIGURE 8–2 A

OPTRANSPAC
ORTHOGRAPHIC
SIDE VIEW

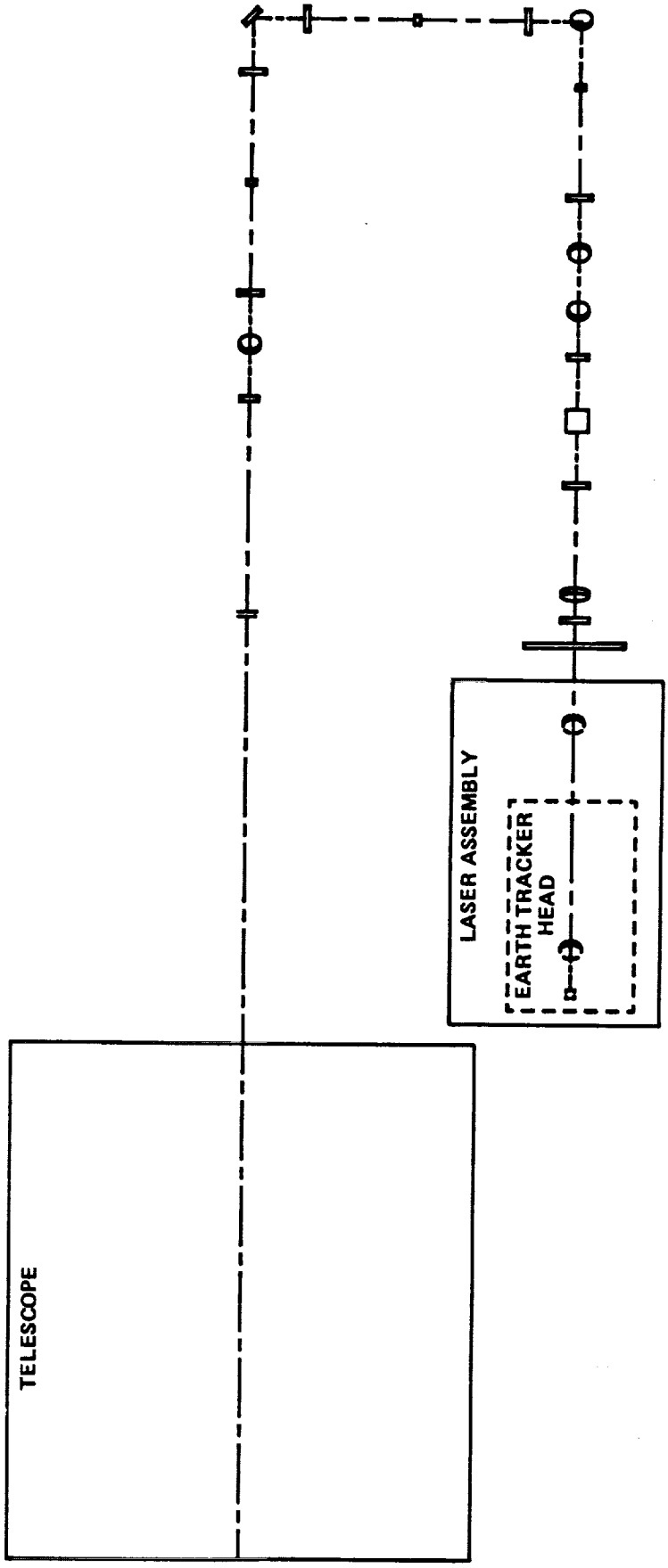

FIGURE 8–2 B

CASSEGRAIN WITH REFRACTIVE CORRECTING ELEMENTS

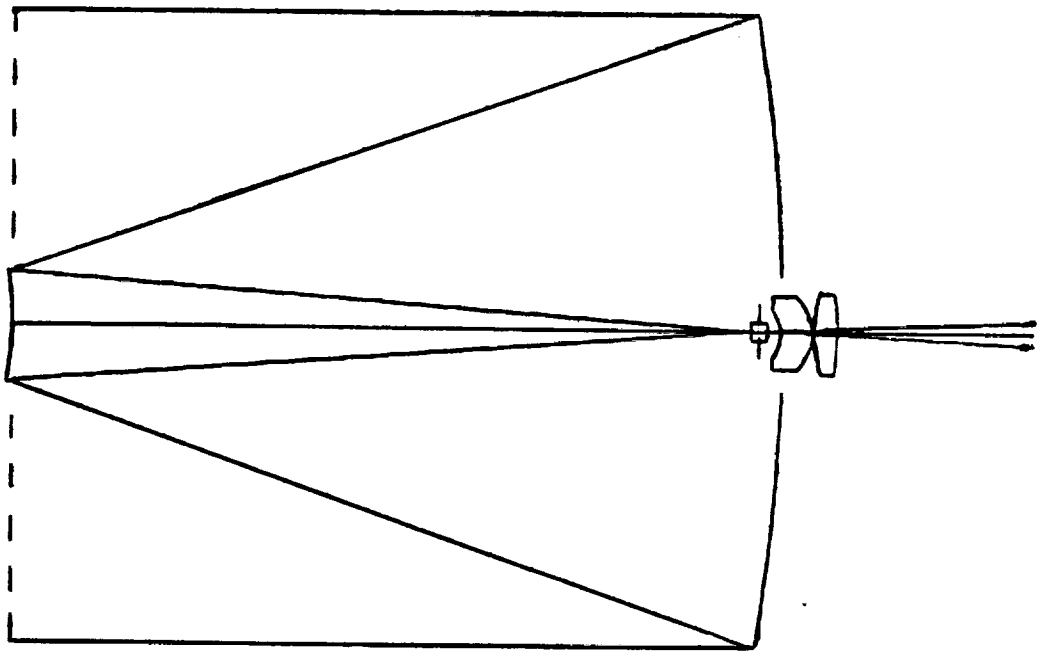

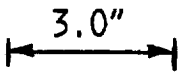

FIGURE 8–3

transmit beam is accomplished in the common optics path). The prime and redundant lasers are selected by a "pop mirror" mechanism. The output laser light passes through an afocal relay. One of the components of this relay can be shifted axially to introduce specific amounts of focus error to partially compensate for wavefront errors introduced by component shifts. These component alignment shifts can arise from the forces during launch, from stress relief of structural parts over time, or from long term temperature changes during the course of the mission. (In a diffraction limited system even such minor motions can have a serious effect on performance). Upon exiting the focus mechanism, the beam enters an afocal beam expander to increase the beam in diameter to 12.7 mm for entry into the common optics path. Specific details of the transmit optics path are found in Appendix C-2.

The receive communication path consists of all elements from the receive/transmit dichroic beamsplitter through to the communications detectors. The received 1064 nanometer light from the EORS is received by the telescope and relayed through the common path optics. The received energy is reflected at the receive/transmit beamsplitter and relayed to the communications/tracking dichroic beamsplitter where the 1064 nm energy is reflected and filtered by a 25 Angstrom bandpass filter and focussed onto a communication detector (avalanche photodiode). The avalanche photodiodes are operated in a slightly defocussed position to keep the spot size large enough that the variation in detector responsivity over its surface has a negligible effect on communication link margin. Further design of the communication optics path details are given in Appendix C-2.

To accommodate the tracking and point-ahead functions on the same array detector an offset is introduced between the broadband reflected sunlight from the Earth and the 532 nanometer transmit spot retroreflected from the transmit beam. A dichroic beamsplitter separates the broadband and 532 nm light into two separate channels. A wedge prism deviates the 532 nm light prior to entering the tracking detector lens. The broadband light enters the tracking detector lens undeviated yielding the angular offset required. The tracking detector lens axis is decentered with respect to the input receiver axis to accommodate the two spatially separated Earth track and point-ahead track channels. Details of the receive track channel are given in Appendix C-2.

8.3 OPTICAL TRANSMISSION - A summary of overall optics path transmission is given in Figure 8-4. The transmission estimates for beginning of life and end of life are listed. The individual component performance estimates given are readily manufacturable specification values and are based on the measured performance of optical components built and used in Lasercom systems over the past eight years. The component substrates and coating materials are restricted to materials with demonstrated radiation resistance. Transmissions are based on optical surface counts for each path. Specific transmission values for lenses, mirrors, filters and dichroics are multiplied to yield the values in Figure 8-4. Monochromatic performance numbers for the transmit and receive communication paths are based on measured values from previous systems. The coatings are optimized for the monochromatic paths.

The antireflection coating performance will be substantially poorer over the broadband visible and near infrared band of the reflected sunlight. The same will be true over the blue-green end of the spectrum for the high reflectance coatings on telescope primary and secondary minors. The overall transmission

OPTRANSPAC TRANSMISSION BUDGET

CONTRIBUTOR	532 NM TRANSMIT	1064 NM RECEIVE	BROADBAND VISIBLE RECEIVE	532 NM OFFSET TRACK
• TELESCOPE TOTAL	0.93	9.93	0.82	-
• IMAGING OPTICS BREAKDOWN				
A. COMMON PATH	0.81	0.79	0.46	-
B. TRANSMIT PATH	0.97	-	-	0.97
C. COMMUNICATION RECEIVE	-	0.62	-	-
D. TRACKING RECEIVE	-	-	0.59	-
E. OFFSET TRACKING RECEIVE	-	-	-	0.0031
• IMAGING OPTICS TOTAL	0.79	0.49	0.27	0.0030
• TOTAL BOL TRANSMISSION (TELESCOPE & IMAGING OPTICS)	0.73	0.46	0.22	0.0030
• ESTIMATED TOTAL EOL TRANSMISSION (TELESCOPE & IMAGING OPTICS)	0.66	0.41	0.20	0.0029

FIGURE 8-4

for the tracking receive path will be substantially less because of this. Detailed transmission estimates on an element basis is given in Appendix C-2.

8.4 WAVEFRONT ERROR AND IMAGE QUALITY - In order to meet the image quality requirements at 10 AU, a near diffraction limited wavefront needs to be radiated from the transmitter. Both the telescope and imaging optics are required to maintain $\lambda/20$ RMS wavefront quality at 532 nanometers. This equates to a total system performance of $\lambda/14$ RMS. Analysis indicates surface quality of $\lambda/104$ RMS ($\lambda/20$ - $\lambda/30$ peak to valley) per element is required. This is within the state of the art for today's optical fabrication technology but is considerable more labor intensive than for the more commonly encountered $\lambda/4$ or $\lambda/8$ peak to valley surfaces. Other sources of wavefront error including glass inhomogeneity, thermal gradients, mounting stresses, misalignments and residual uncorrected design aberrations are not included in the above design. Further discussion of transmit wavefront error is given in Appendix C-2.

The image requirements are less stringent for the receive path than for the transmit path. Receive image quality is driven by the tracking requirements. Figure 8-5 illustrates the variation in the size of the Earth image on the tracking detector as a function of range. Diffraction limited image quality is not necessary to meet the required tracking uncertainty. An optics resolution in the 15-25 microradian range is acceptable.

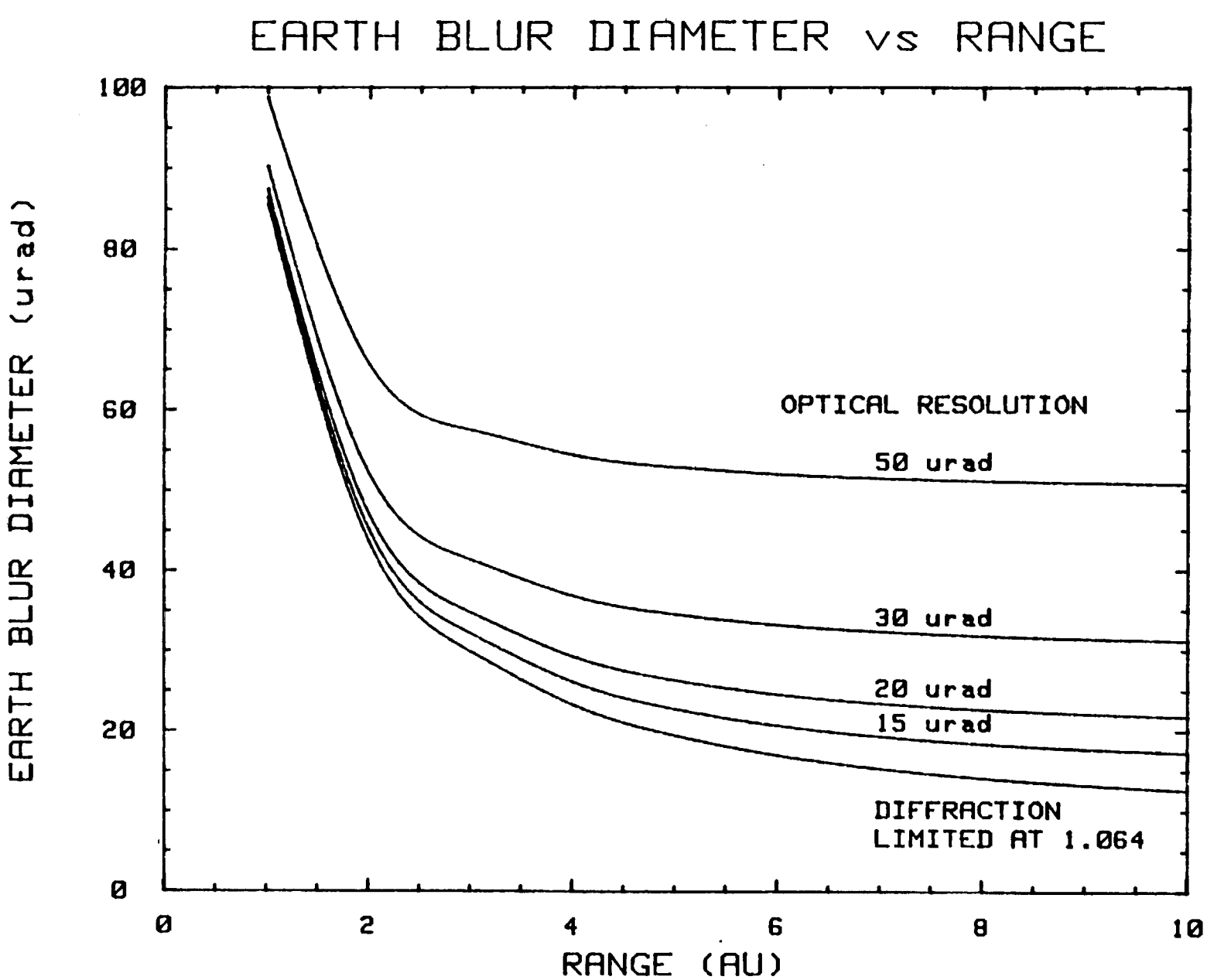
EARTH BLUR DIAMETER vs RANGE
EARTH BLUR DIAMETER (urad)
100
80
60
40
20
0
0
2
4
6
8
10
RANGE (AU)
OPTICAL RESOLUTION
50 urad
30 urad
20 urad
15 urad
DIFFRACTION
LIMITED AT 1.064

FIGURE 8-5

9.0 MECHANICAL DESIGN

The OPTRANSPAC terminal design is the result of various trades which culminated in the final baseline mechanical design. Maximum use of existing space qualified optical communication components and packaging techniques were employed in the final design. Weight and power guidelines were imposed to obtain the optimum configuration. The envelope size was not considered a large design driver because a specific host platform was not known.

The OPTRANSPAC terminal is pictured isometrically in Figure 9-1. An orthographic view is given in Figure 9-2. A single baseplate concept was employed which provides interface mounting surfaces between the host platform, the optical assembly and the electronics. The plate is thermally isolated from the spacecraft to maintain and adiabatic interface. Three lap pads are provided to allow a strain free attachment to the spacecraft. The plate is composed of two Beryllium facesheets with an aluminum honeycomb core. The strength to weight ratio is optimized with this baseplate concept and the Beryllium facesheets provide a good optical bench. For the telescope mount, a truss structure has been designed to provide a strain free, three point mount to the baseplate. The cover has been designed for minimum weight and size and does not obstruct the laser's view of space for a radiator to reject heat.

The optical elements are all supported by the single baseplate. The optics path includes two flip mirrors which provide a totally redundant optics path. An optical isometric is pictured in Figure 9-3. The baseplate supports optical elements from both faces, and openings in the baseplate are provided to relay the optical signals from the top side to the bottom side of the optical baseplate.

The electronics have been divided into three boxes; the Power Conditioning Unit, the Control Electronics Assembly, and the Communications Electronics Assembly. The Power Conditioning Unit was located at the bottom of the baseplate with the laser assembly so it can reject heat into space. Figures 9-4 and 9-5 depict isometric and orthographic views of the PCU. The PCU has been designed using the module concept where appropriate. These modules are attached to a thermally conducting top housing plate with the components mounted in such a manner as to place the hottest closest to the plate.

The Communication Electronics Assembly (see Figures 9-6 and 9-7) and the Control Electronics Assembly (see Figures 9-8 and 9-9) are structured using the doubled sided card concept. This allows tight packaging into reduced volumes. The boxes provide slide mounts with end connectors for each of the electronics cards. The heat is dissipated through the top face plate surface away from the optical baseplate.

OPTRANSPAC
ISOMETRIC VIEW

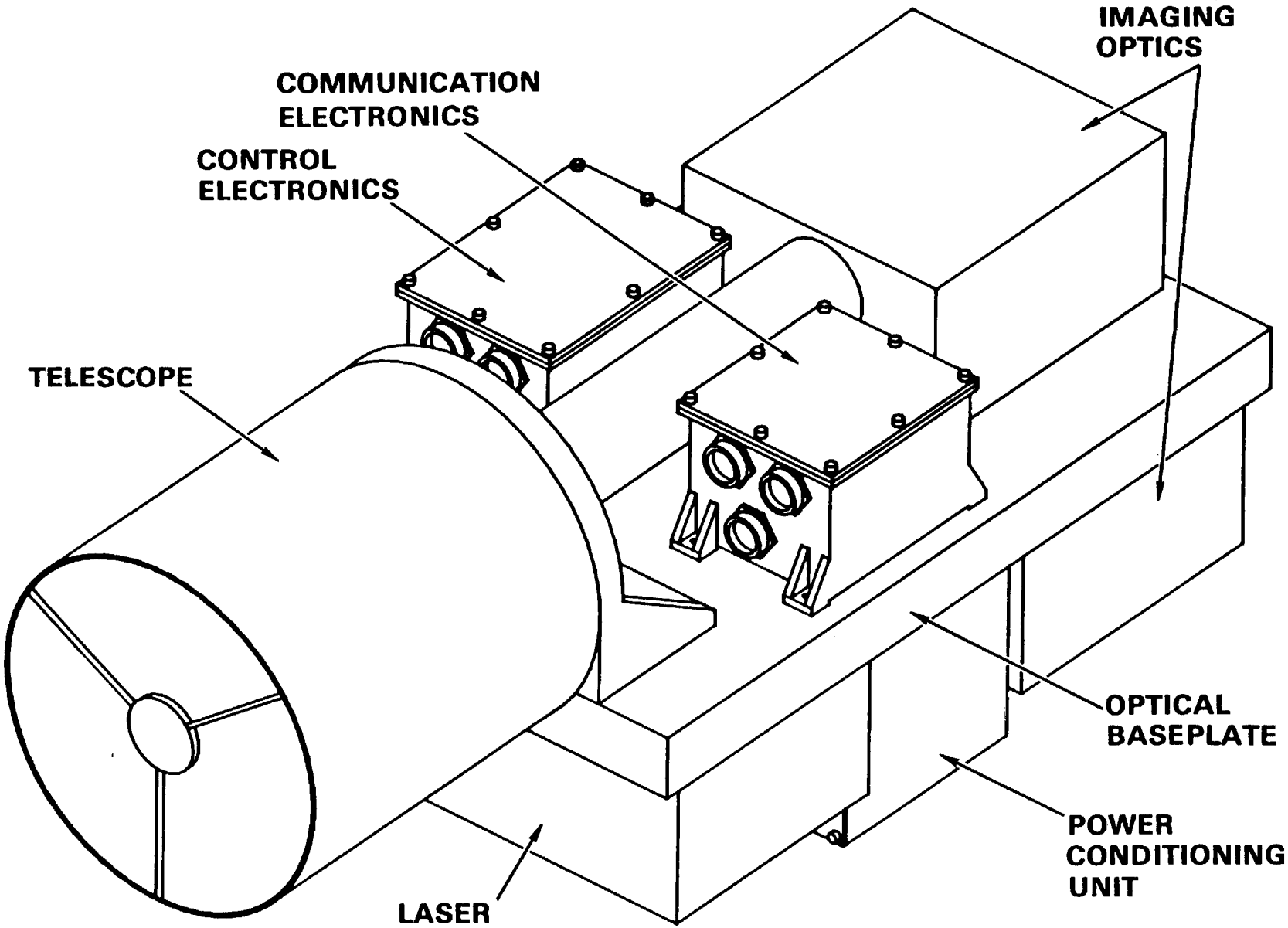

FIGURE 9–1

OPTRANSPAC
ORTHOGRAPHIC
TOP VIEW

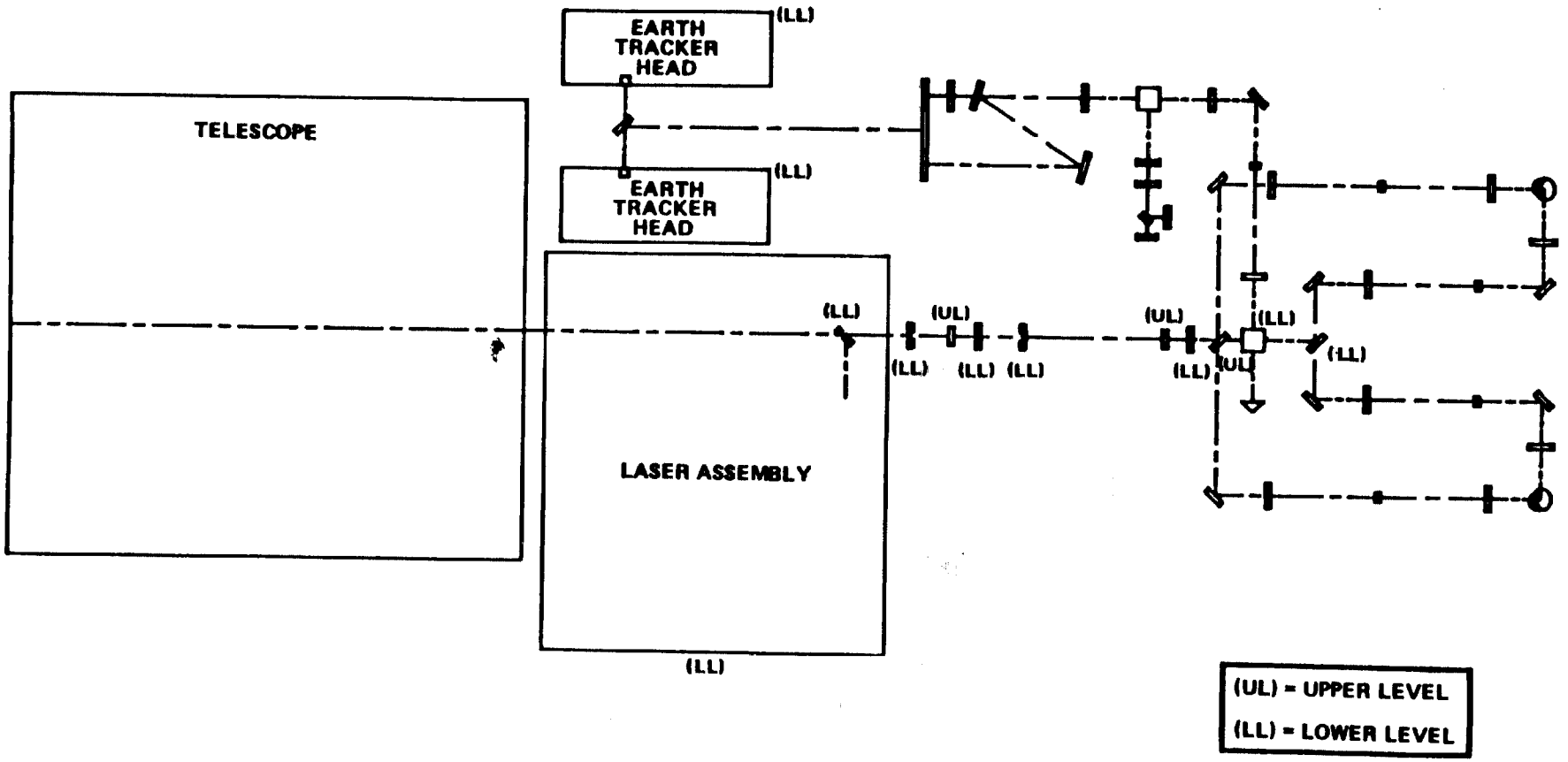

FIGURE 9–2A

OPTRANSPAC
ORTHOGRAPHIC
SIDE VIEW

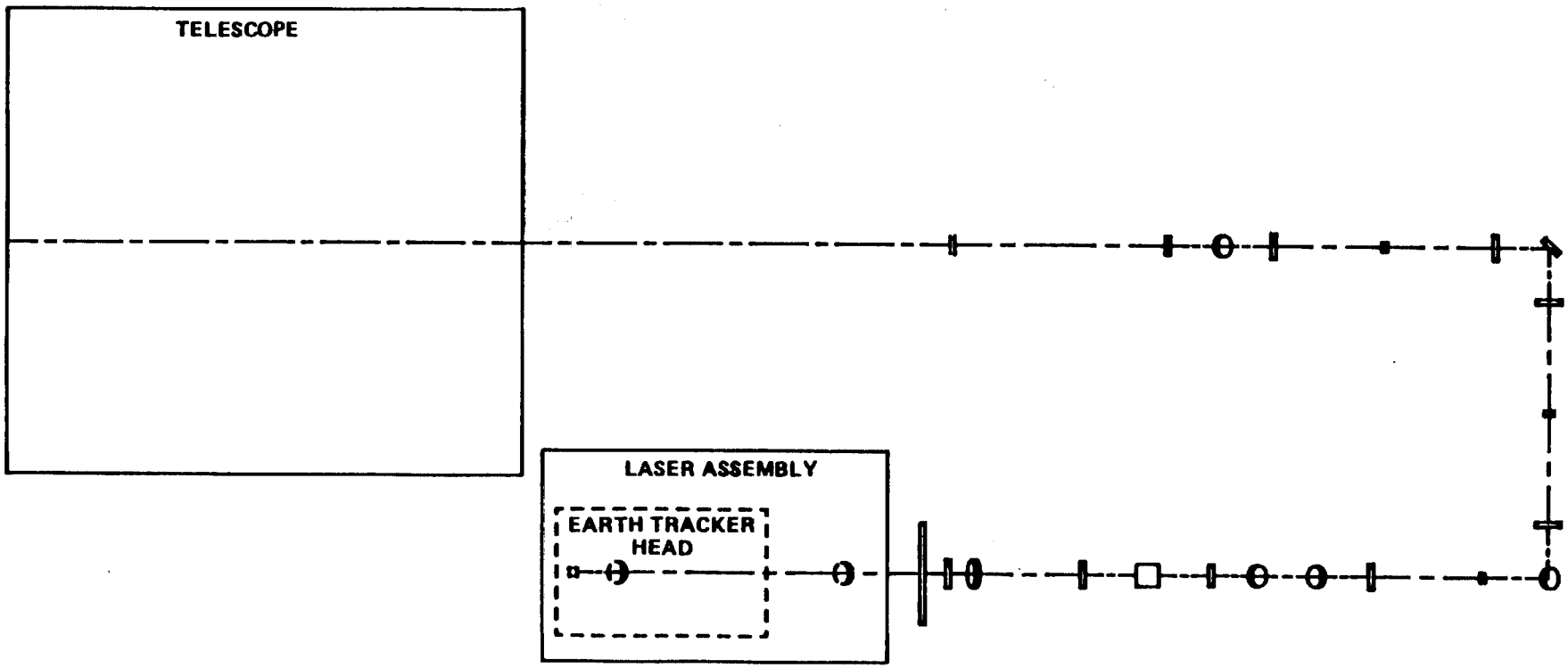

FIGURE 9–2 B

OPTRANSPAC
OPTICAL ISOMETRIC VIEW

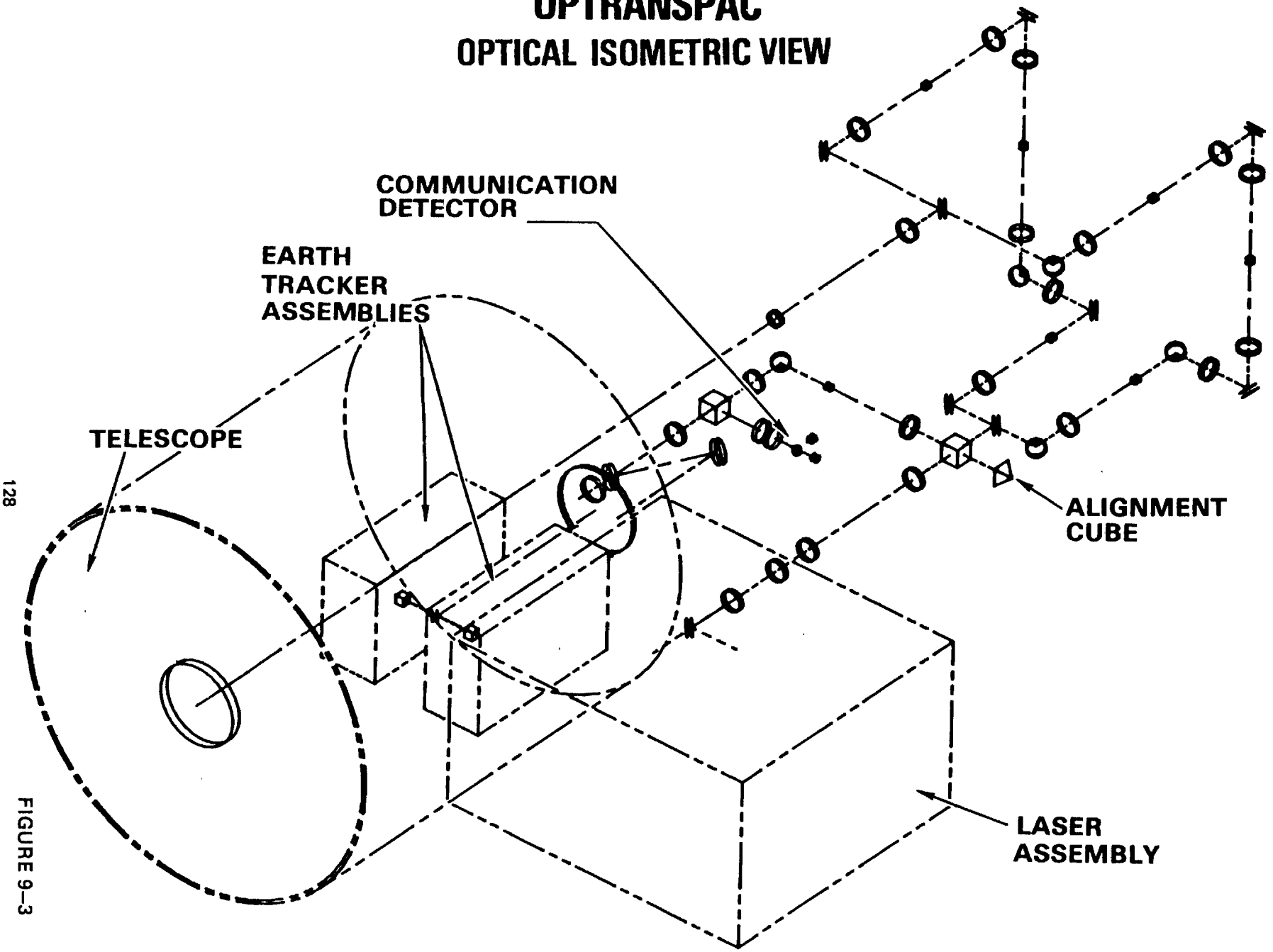

FIGURE 9–3

POWER CONDITIONING UNIT ISOMETRIC

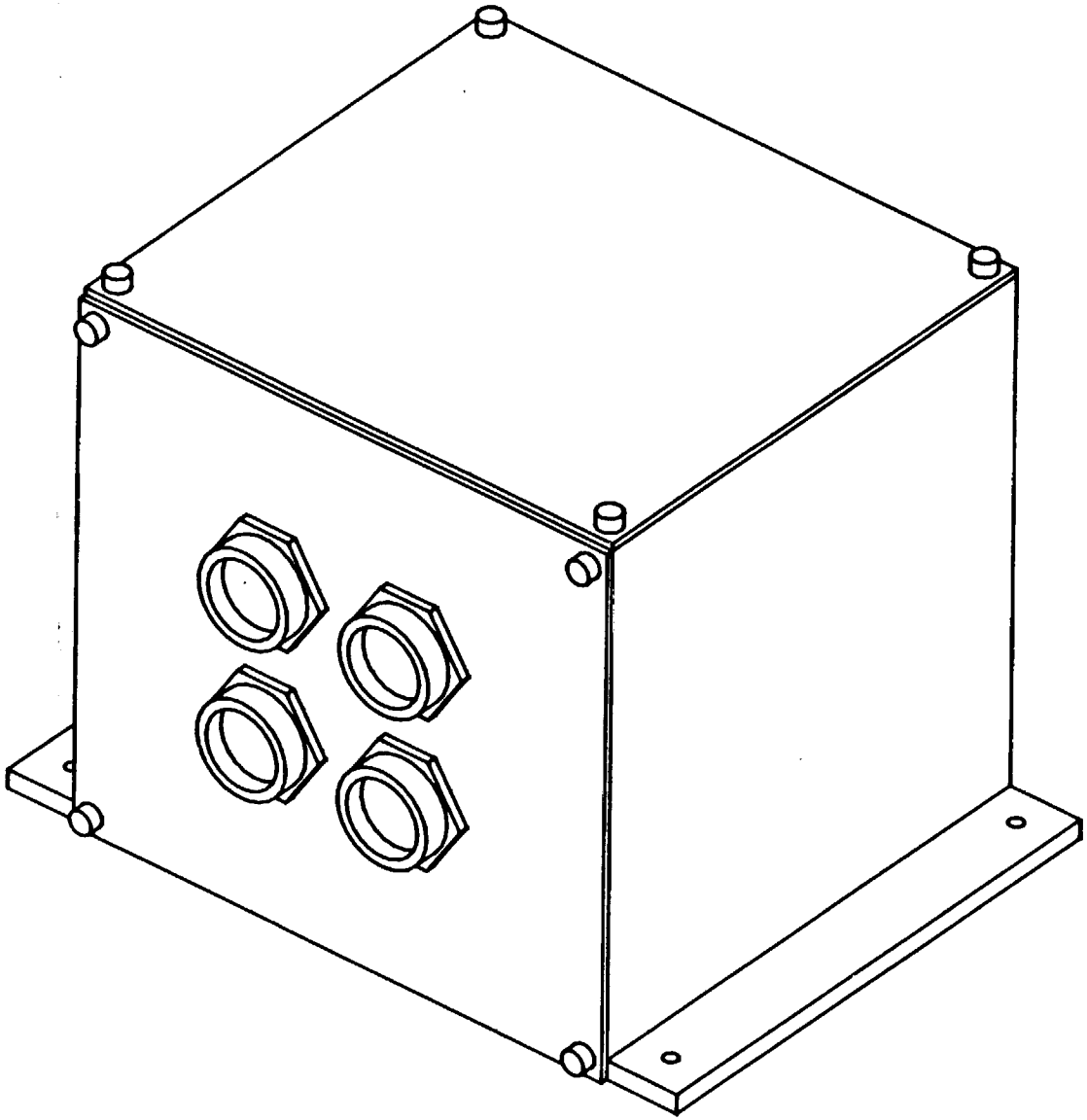

FIGURE 9–4

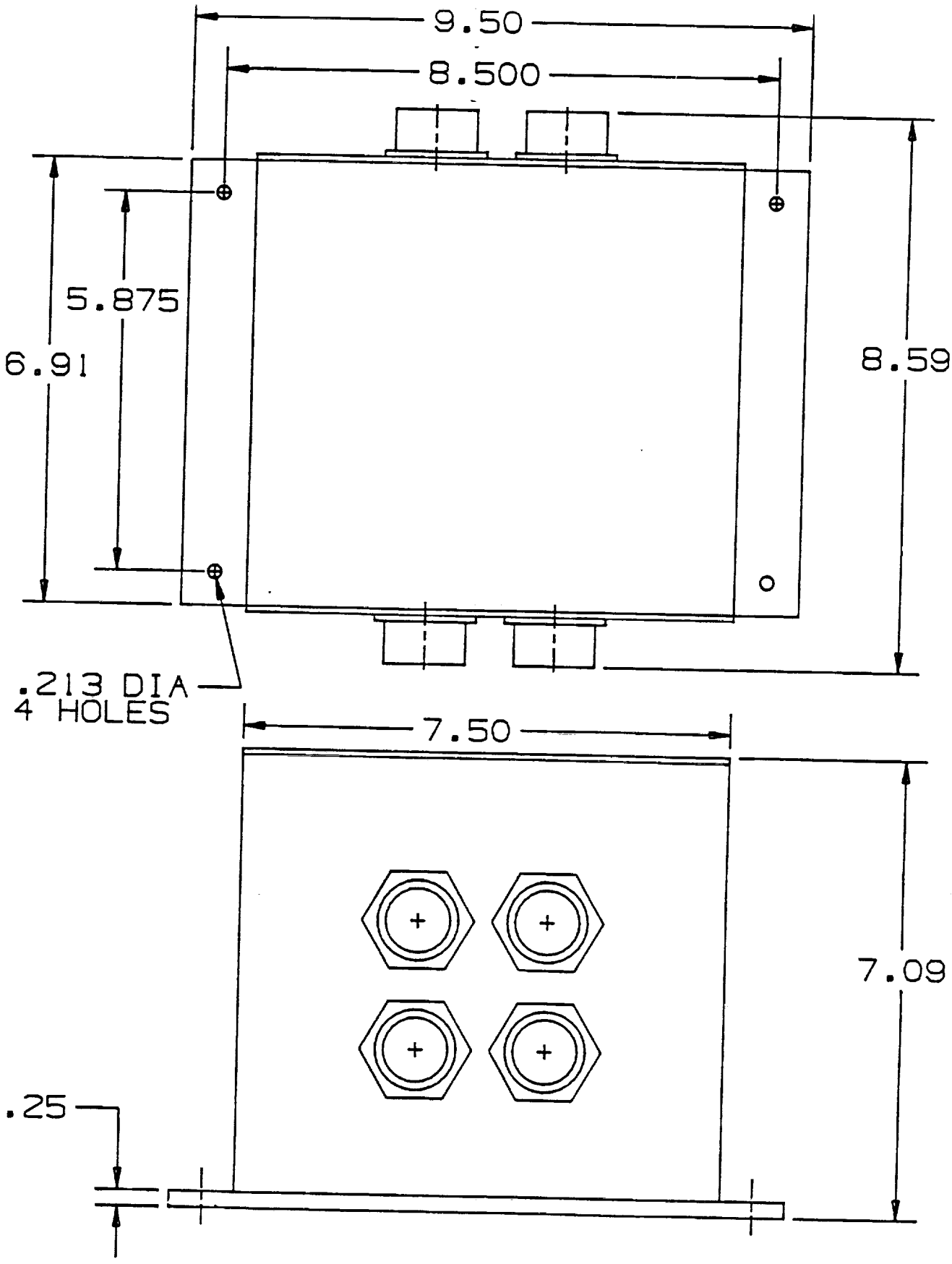

POWER CONDITIONING UNIT

FIGURE 9–5

COMMUNICATION ELECTRONICS ISOMETRIC

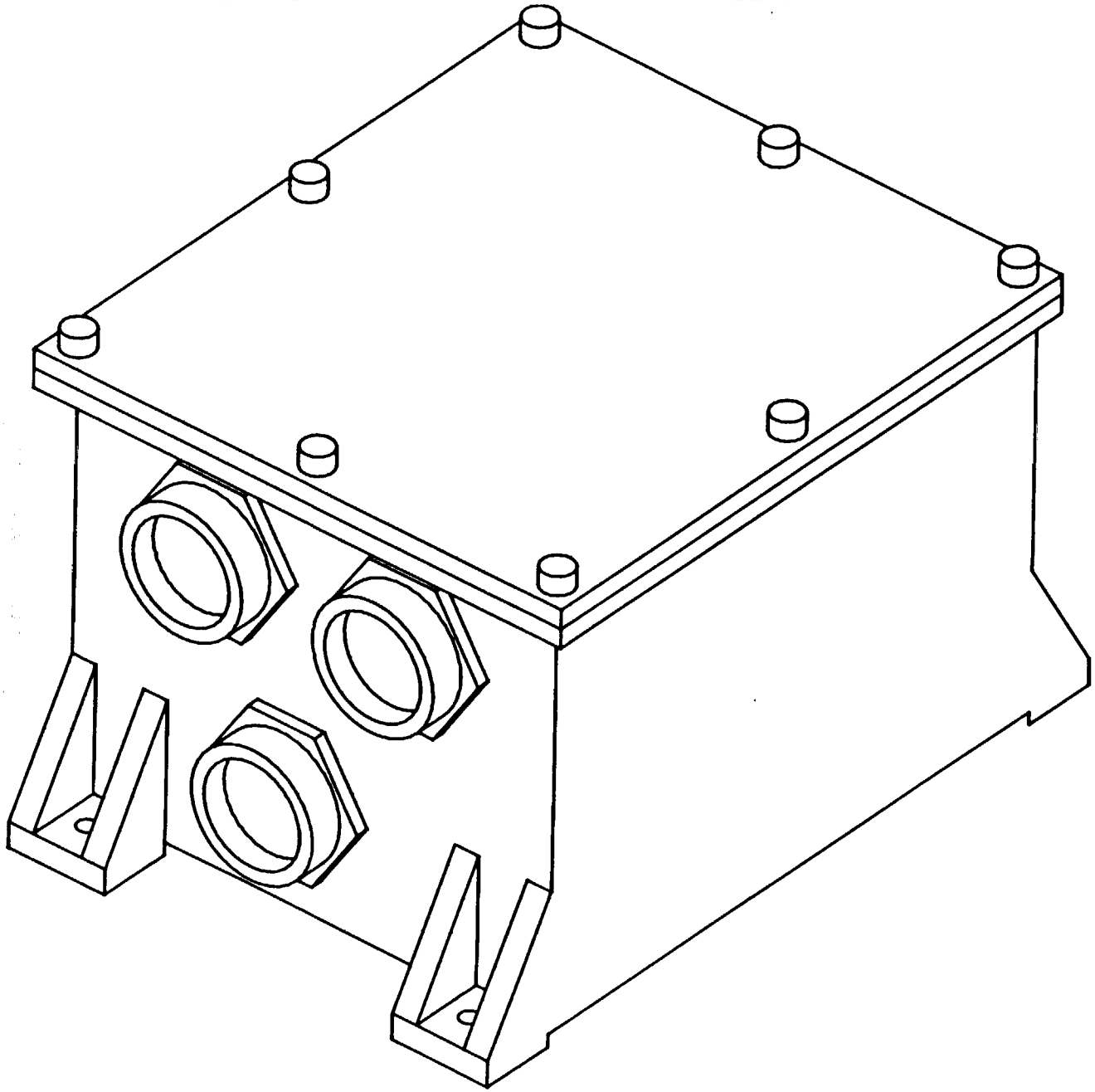

FIGURE 9–6

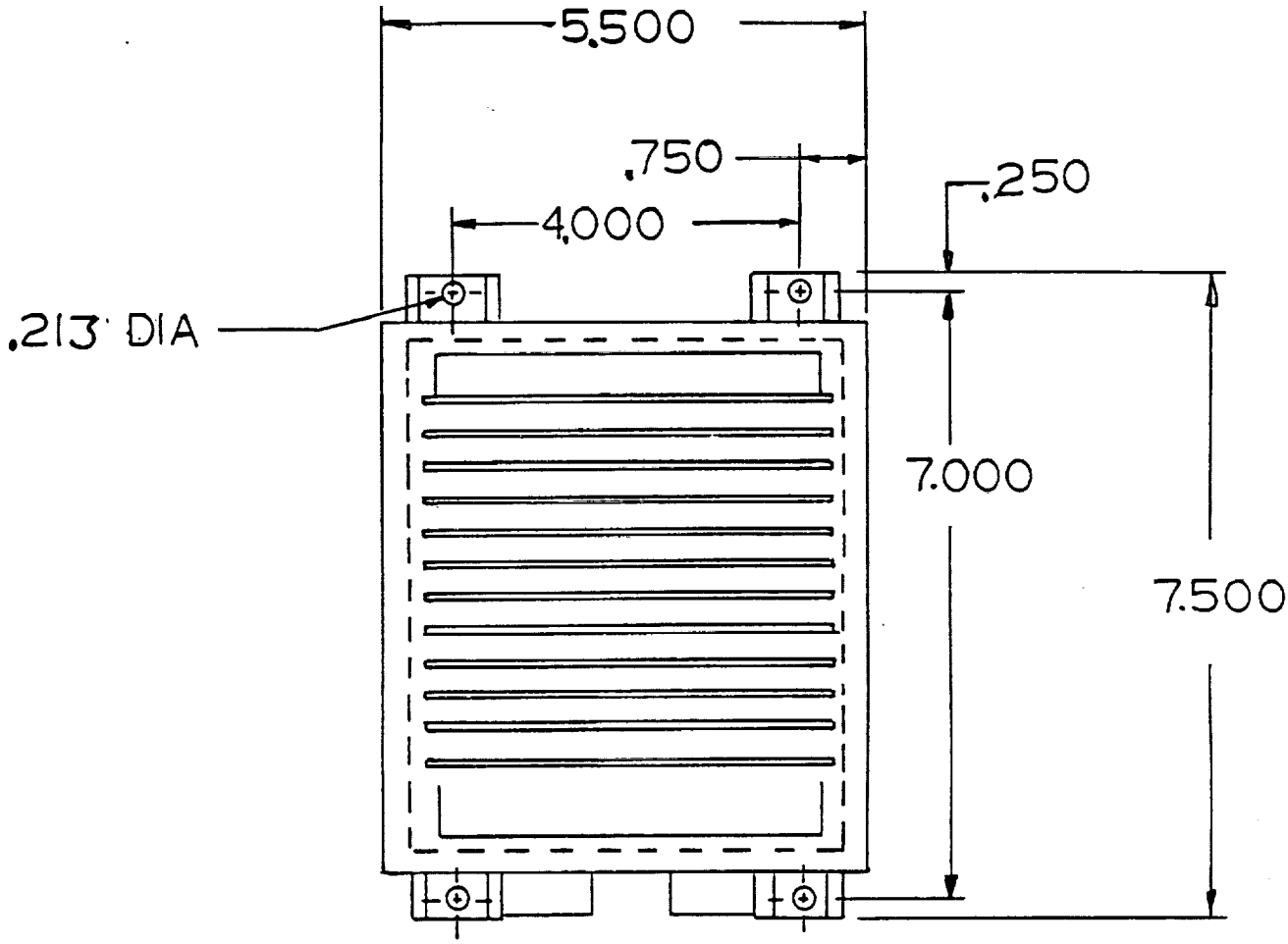

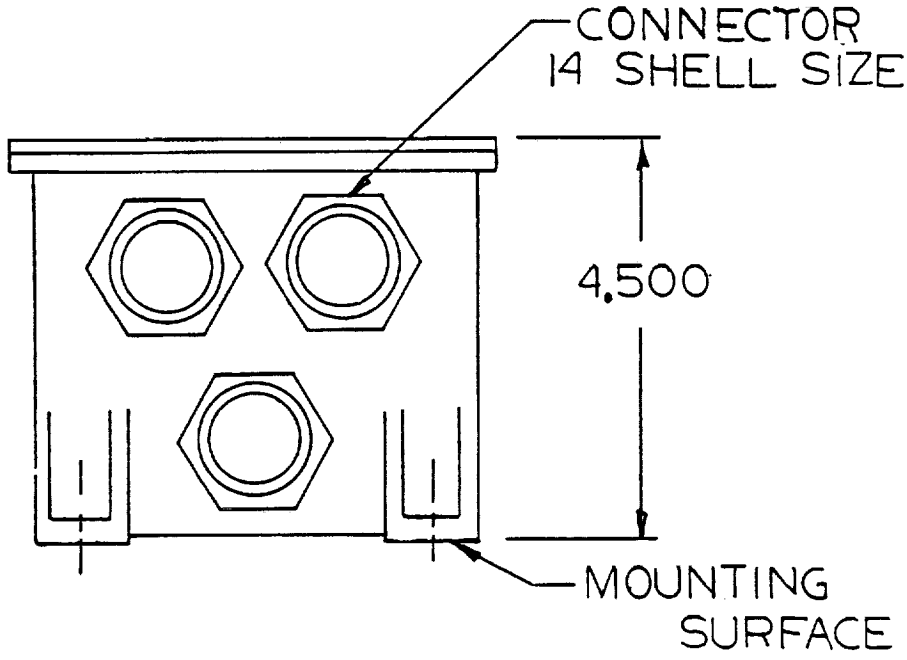

COMMUNICATIONS ELECTRONICS

FIGURE 9–7

CONTROL ELECTRONICS
ISOMETRIC
MCDONNELL DOUGLAS ASTRONAUTICS COMPANY-ST. LOUIS DIVISION

FIGURE 9–8

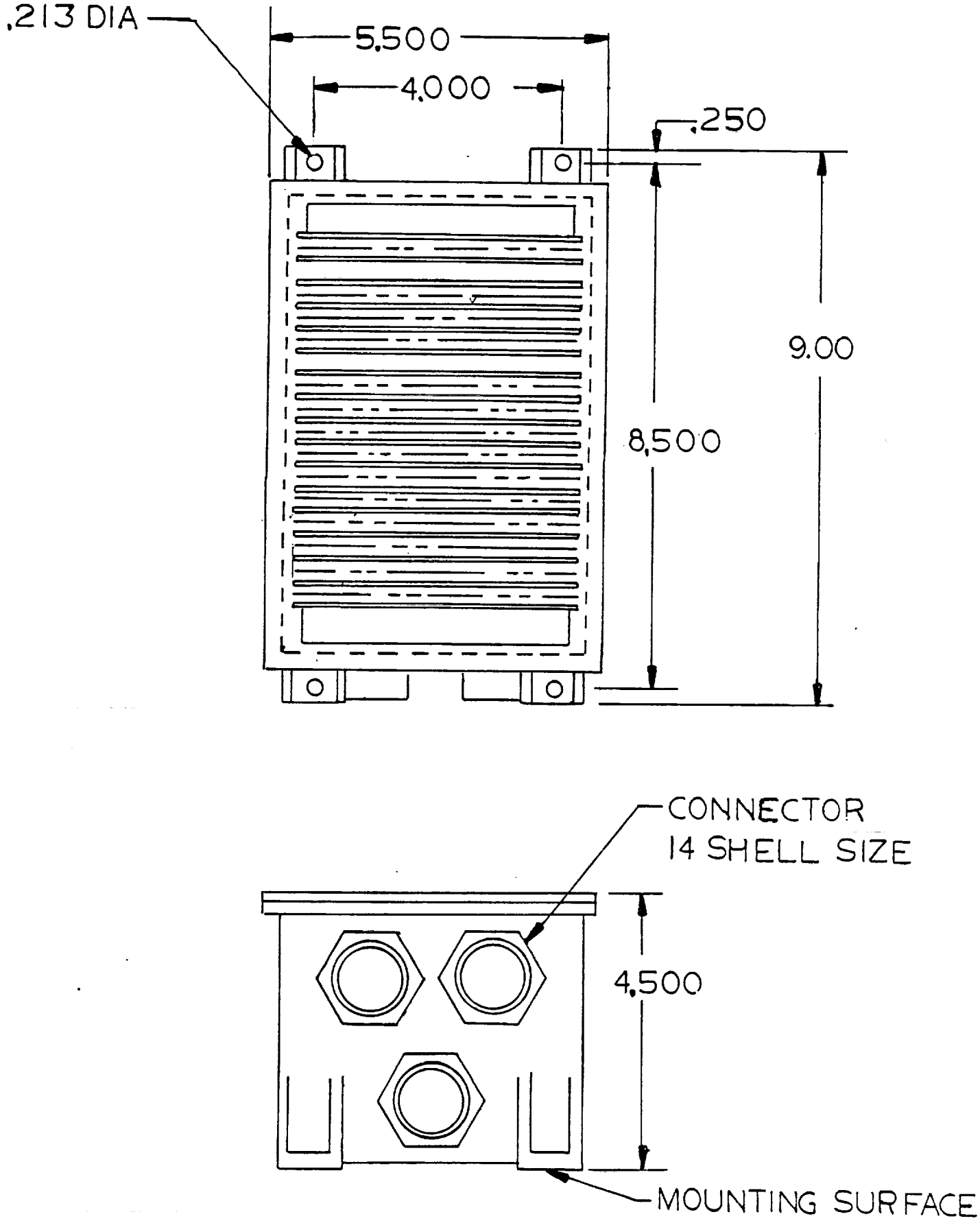
.213 DIA
5.500
4.000
.250
9.00
8.500
CONNECTOR
14 SHELL SIZE
4.500
MOUNTING SURFACE
CONTROL ELECTRONICS

FIGURE 9–9

10.0 WEIGHT AND POWER

The OPTRANSPAC final weight and power summary is presented in Figure 10-1. These results of 115.0 pounds and 57.0 Watts are broken down by the major components defined by the functional block diagram. The weight allocations were optimized within the constraints of the functional requirements, materials, environments and cost. Whenever possible these allocations were also modified to reflect 1988 technology to further ensure the achievement of a minimum weight design.

The power allocations for the OPTRANSPAC system were established by reviewing each piece of equipment to determine it's power requirements. This data was compared to similar hardware program equipment, and/or data taken from breadboard circuits, in order to provide substantiation. This analysis also allowed for a 3 percent line loss and conversion efficiencies of 68 percent. An additional 10 percent was allocated for heater power. The electrical power design provides the user with both flexibility and growth.

The OPTRANSPAC component weight summary is presented in Figures 10-2 and 10-3. All of the weights presented are nominal weights. Nominal weight is the most probable weight and it is composed of a base weight plus contingency. Contingency is defined as that weight which must be added to a base weight to obtain a nominal weight. Contingency includes such things as an allowance for gage tolerances in sheet metal or machined parts, weight from correlation factors, or an assigned weight based on the type of subsystem and its current development state. In general the base weights for this study were derived using one of the following methods: analytical models, empirical equations, detailed component analysis, or weights of similar existing components with allowances for modifications.

All of these methods of weight analysis have been employed in the electrooptics assembly. The basic telescope weight was derived from an analytical model. Even though this approach gives proper trends for the critical system parameters, the model fails to account for the entire system weight. Therefore, by using the model on existing hardware, a plot of estimated versus actual weights was obtained. The correlating factor which resulted from this plot accounts for the added contingency. The structural weights in the imaging optics and laser assemblies were derived by using a schematic. A weight was determined for each component on the schematic. These component weights were based on similar on-going laser communication hardware program components and on vendor supplied data. The weight of all the other components of these assemblies such as wire and fasteners were based on empirical equations. The detector and Earth tracker assemblies were primarily based on vendor supplied data.

In the electronics area the weight is primarily driven by the design and size of the circuit boards. The control electronics design features 14 ceramic boards populated with leadless chip carrier packages containing the digital circuits, and 2 polyimide boards populated with analog circuits and discrete components. The communication electronics is a similar design with 10 ceramic and 2 polyimide boards. The size of each of these boards is approximately 4.6 inches by 3.8 inches. The weight of these boards was derived from actual weights of similar existing boards. This resulting pounds per square inch was applied to the area of the OPTRANSPAC boards. All other weights in these

WEIGHT AND POWER SUMMARY

ITEM	WEIGHT (LBS.)	POWER (WATTS)
• ELECTRO-OPTICS ASSEMBLY	(57.0)	(11.0)
TELESCOPE (11 IN)	18.0	-
IMAGING OPTICS ASSEMBLY	13.5	2.0
LASER ASSEMBLY	20.0	4.0
DETECTOR ASSEMBLY	1.0	.4
EARTH TRACKER	4.5	4.6
• ELECTRONICS	(41.0)	(39.3)
COMMUNICATIONS ELECTRONICS	9.0	7.7
CONTROL ELECTRONICS	12.5	14.5
POWER CONDITIONER UNIT	19.5	17.1
• STRUCTURE/WIRE/MISC	(17.0)	(6.7)
TOTAL	115.0	57.0

FIGURE 10-1

ELECTRO-OPTIC ASSEMBLY WEIGHT SUMMARY

COMPONENT		WEIGHT (LBS.)
• ELECTRO-OPTICS ASSEMBLY		
TELESCOPE ASSEMBLY		18.0
IMAGING OPTICS ASSEMBLY		13.5
OPTICS BASEPLATE	4.43	
DUST COVERS	2.30	
LIGHT TUBE	.29	
OPTICS COMPONENTS	5.48	
WIRE/CONNECTORS/FASTENERS	1.00	
LASER ASSEMBLY		20.0
STRUCTURE	12.60	
OPTICAL BENCH ASSEMBLY	5.00	
DIODE ARRAY ASSEMBLY	2.40	
DETECTOR ASSEMBLY		1.0
EARTH TRACKER		4.5
HEAD ASSEMBLY	3.00	
ELECTRONICS	1.50	

FIGURE 10-2

ELECTRONIC AND STRUCTURE WEIGHT SUMMARY

COMPONENT		WEIGHT (LBS.)
• ELECTRONICS		
COMMUNICATIONS ELECTRONICS		9.0
CIRCUIT BOARDS	5.22	
MOTHER BOARD	.45	
WIRE/CONNECTORS	1.35	
STRUCTURE	1.98	
CONTROL ELECTRONICS		12.5
CIRCUIT BOARDS	7.30	
MOTHER BOARD	.68	
WIRE/CONNECTORS	1.82	
STRUCTURE	2.70	
POWER CONDITIONER ASSEMBLY		19.5
MODULES	12.00	
WIRE/CONNECTORS	1.30	
STRUCTURE	6.20	
• STRUCTURE/WIRE/MISC		17.0
WIRE/CONNECTORS	10.50	
SUPPORT STRUCTURE	2.60	
MISC STRUCTURE	3.90	

FIGURE 10-3

assemblies were derived from modifications to existing hardware. The Power Conditioner unit weight was based on vendor supplied data. The circuitry required for the converter, regulators, etc. is in module form. Each module consists of two polyimide circuit boards housed in a frame. Five modules are required for the OPTRANSPAC design.

In the structures area, the weight of the support structure was based on the material gages necessary to provide strength and structural stiffness, while the miscellaneous structural weight was based on empirical equations. The wire and connector weight was obtained from existing wire bundles modified to meet the requirements of the OPTRANSPAC design.

11.0 GROWTH AND UNCERTAINTY

Areas in the OPTRANSPAC design that may require further examination beyond the scope of this study are identified. At the level of system maturity and analysis performed under this study, detailed thermal design, structural dynamic design, electronics design, optical design and host interface design have not been performed. Detail design considerations associated with each of these may slightly perturb the OPTRANSPAC design in terms of size, weight or power. Figure 11-1 outlines the OPTRANSPAC design considerations where a variation from the baseline in size, weight or power may occur.

Due to the harsh Saturnian radiation environments identified in Section 3.8, additional shielding may be required beyond the nominal shielding provided by the baseline design. The Earth tracker and the command uplink detector may require localized shielding to reduce radiation induced false detections. Radiators and/or heaters may be required to maintain the OPTRANSPAC components within the specified operating and non-operating temperature limits. Structural analysis using launch loads and acoustic environments may indicate the need for strengthening and prudent material selection. Further detailed optical analysis (ray tracing, telescope baffling design, and element definition) will determine the exact number of elements required.

Because of the detail design that already exists and because of the few design considerations still unknown, a growth and uncertainty factor of only 10-15% for both weight and power is recommended. The margin for weight and power growth then becomes 11.5 to 17.25 pounds and 5.7 to 8.55 watts above the 115 pounds and 57 watts determined for the baseline design.

OPTRANSPAC DESIGN CONSIDERATIONS

- RADIATION SHIELDING REQUIREMENTS
  - LOCALIZED SHIELDING AROUND DETECTORS AND CRITICAL COMPONENTS
- THERMAL SYSTEM DESIGN
  - RADIATORS AND/OR HEATERS
- STRUCTURAL ANALYSIS
  - DESIGN TO LAUNCH LOADS AND ACOUSTIC ENVIRONMENT
  - MAY REQUIRE STRENGTHENING AND STIFFENING
- OPTICAL DESIGN
  - RAY TRACING, COMPONENT SELECTION
  - DETERMINES ACTUAL NUMBER OF ELEMENTS IN COLLIMATOR GROUPS

FIGURE 11-1

12.0 FOLLOW-ON HARDWARE DESIGN

To achieve the 1988 technology base required for the OPTRANSPAC design, funding of key component technologies is required. Although some of these technologies are advancing through other funding centers, design criteria specific to the OPTRANSPAC may not be advanced to the desired state-of-the-art level by 1988 if development is not pursued with the OPTRANSPAC terminal in mind. The specific technologies that require special attention are: 1) The downlink laser; 2) the Earth tracker; and 3) the offset dichroic optical boresight alignment device in the Earth tracker optics.

The OPTRANSPAC technology advancements required in the area of the downlink laser include the development of a high efficiency (> 10% optical output power to pump source input power) frequency doubled (532 NM) Nd:YAG laser and the development of a compatible cavity dumped modulator capable of operation at pulse repetition rates from 1 KBPS to 25 KBPS. These technologies are vital to the OPTRANSPAC system design.

The advancements required in the area of the array tracker involve Earth track capability along with continuous tracking of the transmit laser to provide alignment and electrical point-ahead capability. Centroid algorithms that provide the required accuracies and resolutions at the desired output rates must be determined and made compatible with the array tracker design. The capability of Earth track is imperative to the OPTRANSPAC design and the development of electrical point-ahead will provide a reduced weight optical design by eliminating additional redundant point-ahead beam steering mirrors.

The final technology area needing development involves the novel offset alignment device that allows a common boresight to be tracked at two positions on the array tracker. Fabrication and testing of this design will allow for verification of the design and will define the optical tolerances required for such a design.

Beyond tracking and developing pertinent hardware designs for the OPTRANSPAC, breadboard design of the terminal to demonstrate system concepts appears as the next logical step. Because a host platform is still unknown, the breadboard design will demonstrate the operational feasibility and allow for design modifications where appropriate.

The final hardware follow-on involves the design and fabrication of an OPTRANSPAC terminal for a specific JPL spacecraft employed in outer planet exploration.

13.0 CONCLUSION

The net effect of this study has been to prove the feasibility of operating a laser communication link from a deep space probe to an Earth Orbiting Relay Receiver. A system level terminal design of an optical transceiver package has been performed. System analysis supported by communication link analysis indicates an OPTRANSPAC system design that is capable of communication from Saturn at data rates up to 100 KBPS (10^{-3} BER). Reception of command data at 1 KBPS is also possible. First order optical, electrical and mechanical analysis and design has been performed. A system mechanical envelope based on the optical system layout and electrical component packaging has been developed. System weight and power estimates of 115 pounds of 57 watts have been established.

All system level requirements, outlined in Section 2.1, with the exception of the weight and power estimates, were met. Although not within the specified limits required, the weight and power estimates establish the best fit terminal design based on data from existing laser communication components and system designs.

THIS PAGE LEFT INTENTIONALLY BLANK

APPENDIX A

OPTICAL TRANSCEIVER PACKAGE (OPTRANSPAC)

DYNAMIC ENVIRONMENTS
SPECIFICATION
28 JUNE 1985

1.0 SCOPE

1.1 Definition

This document defines the dynamic environments that the Optical Transceiver Package (OPTRANSPAC) is expected to encounter during its mission.

1.2 OPTRANSPAC Definition

OPTRANSPAC is an optical communications terminal to be mounted to a deep space vehicle whose mission is outer planet exploration. The transceiver will communicate with an Earth-orbiting relay station (EORS) from distances of Saturn and beyond, at downlink data rates up to 100 Kbps, and an uplink rate of 1 Kbps. The transceiver package must be reliable enough to ensure full operation over the 10 to 20 year life of such a mission.

2.0 PURPOSE

This document shall be used as a reference to develop adequate design specifications to ensure proper OPTRANSPAC operation in the presence of the dynamic environments specified herein.

3.0 OPTRANSPAC DYNAMIC ENVIRONMENTS

3.1 Orbit Analysis

3.1.1 Earth to Saturn Transfer Orbit - A generic Hohmann (minimum energy) transfer orbit for a deep space probe from Earth to Saturn is shown in Figure 3.1-1. The semi-major axis of this eliptical orbit is 5.67 astronomical units (AU) and the eccentricity is 0.826. Transit time is 1827 days. The true anomaly at launch is 6.9 degrees and at Saturn encounter is 172 degrees. This orbit was used to calculate the relative velocities between the Earth and the OPTRANSPAC spacecraft for Doppler and point ahead calculations.

3.1.2 Earth to Spacecraft Range - Figure 3.1-2 is a plot of range versus time between the Earth and the OPTRANSPAC spacecraft for the transfer orbit. The 2 AU oscillations are due to Earth orbital motion.

3.1.3 Earth and Spacecraft Velocities - Figure 3.1-3 shows the velocities of the Earth and spacecraft in the directions of the axes of the transfer orbit. The spacecraft has an original velocity of about 10 km/sec more than the Earth's in the minor axis direction and the same as Earth's in the major axis direction. The relative velocities between the Earth and spacecraft in axes parallel and perpendicular to the instantaneous line-of-sight are plotted versus time in Figure 3.1-4.

3.1.4 Point Ahead Angle and Doppler Shift

3.1.4.1 Point Ahead and Doppler Contributors - The Doppler shift of light transmitted between the OPTRANSPAC and the Earth relay satellite and the point ahead angle necessary for correct illumination are determined by the relative velocity between the two platforms. The four contributors to this velocity when the spacecraft is

encountering Saturn are the Earth's and Saturn's orbital rates about the sun, the relay satellite's orbital rate around the Earth, and the spacecraft's flyby or orbital rate around Saturn. The maximum velocity contribution of each is given in Figure 3.1-5. Up to the time of Saturn encounter, only the Earth, the relay satellite, and the spacecraft transfer orbit motion apply.

3.1.4.2 Point Ahead Angle - Figure 3.1-6 shows part of the necessary point ahead angle for the OPTRANSPAC during the Hohmann transfer between Earth and Saturn due to the relative velocities in Figure 3.1-4. The other part of the necessary point ahead angle is that needed to compensate for the relay satellite motion. The maximum angle contribution from the Earth relay station is limited by the extremes of where it can be in its orbit about the Earth. That contribution of up to 51 microradians, which is reduced by the inverse of range after a range of 1.8 au, creates a total point ahead angle of 322 microradians maximum for the Hohmann transfer.

During the spacecraft's encounter with Saturn, Saturn's velocity also contributes to point ahead. Since all four contributors may have their total velocity perpendicular to the line-of-sight, the maximum velocity of each contribute to point ahead. The maximum contribution to point ahead of each velocity is given below.

Point Ahead Maximum Contributions (μrad)

Earth	199
Relay Satellite	51, range 1.8 AU
	92.7/R, range 1.8 AU
Saturn	64
Spacecraft Flyby	167
	440, range = 9.5 AU

Since the contribution of Saturn's velocity is only in one direction, the maximum point ahead in the other axis direction is only 312 microradians.

3.1.4.3 Doppler Shift - The Doppler shift expected during the Hohmann transfer without the relay satellite contribution is plotted versus flight time in Figure 3.1-7. Adding in the maximum contribution of the relay satellite gives a maximum expected Doppler shift of 1.67 angstroms during the transfer from Earth to Saturn.

During the Saturn encounter, Saturn's velocity contributes through the sine of the minimum angle of it with respect to the line-of-sight, defined by the minimum distance from Earth to Saturn and the maximum cross-range of the Earth's position. The Earth and spacecraft flyby contributing velocities are the same as the point ahead case. The maximum Doppler contributions are shown below.

Doppler Maximum Contributions (Å)(λ = 1.064 μ m)

Earth	1.06	
Relay Satellite	.27	
Saturn	.08	sin (arc tan (2/8.5))factor
Spacecraft Flyby	.89	
	2.30	

3.2 Solid Particles - Meteoroids

3.2.1 Nominal Environment Meteoroids - The OPTRANSPAC should expect to encounter the meteoroid fluences and particle characteristics tabulated in Figure 3.2-1. for a deep space mission which includes crossing Saturn's E-ring. Column two of the figure provides the total number of impacts on each square meter of exposed spacecraft surface for meteoroids having mass greater than the value specified in column one. The meteoroids are omnidirectional having no preferred direction.

3.3 Magnetic Field

The OPTRANSPAC will be subjected to the magnetic fields defined below.

Earth (non-operating)	5×10^4 nT @ surface
Interplanetary	25 nT
Saturn	8×10^3 nT @ 2 R_S
Shuttle (non-operating)	32 mT

3.4 Gravitational Field

The OPTRANSPAC will encounter the following gravitational field differential accelerations.

Earth (non-operating)	3.0×10^{-6} m/sec/m @ surface
Sun	7.9×10^{-14} m/sec/m @ 1 AU
Saturn	4.3×10^{-8} m/sec/m @ 2 R_S

3.5 Thermal Radiation

Exposed portions of the OPTRANSPAC should expect to encounter the thermal radiation levels specified below.

Earth Reflected	57.3 $mWcm^{-2}$ @ R_E
Solar	163.0 $mWcm^{-2}$ @ 1 AU
Saturn Reflected	1.1 $mWcm^{-2}$ @ R_S

3.6 Electrical Field

The maximum expected Saturn induced electric field is 116 v/m @ 2 R_S.

3.7 Launch Vibrations

The expected Space Shuttle vibration environment is shown in Figure 3.7-1. The OPTRANSPAC shall be designed to operate after exposure to this environment.

3.8 Launch Acoustic

The OPTRANSPAC shall be designed to operate after exposure to the expected Space Shuttle acoustic environment shown in Figure 3.8-1.

3.9 Pyrotechnic Shock

Figure 3.9-1 shows the maximum shock spectrum during spacecraft/launch vehicle separation. This spectrum shall be attenuated by intervening spacecraft structure.

3.10 Radiation Environments

3.10.1 Total Dose - The mission environments contributing to total dose include the interplanetary electrons, protons, and solar flare particles plus the Saturn electron and proton Van Allen belts. The proton and electron dose environments are shown as a function of shielding in Figures 3.10-1 and 3.10-2. The total dose environment is shown in Figure 3.10-3.

3.10.2 Displacement Damage - The major contributing environments to displacement damage in semiconductor electronics are the protons trapped in Saturn's Van Allen belt and the interplanetary cosmic ray protons. Minor contributions are made by the nuclear power source and the mission electron environments. The proton, electron, and total displacement damage environments are shown as a function of shielding in Figures 3.10-4, 3.10-5, and 3.10-6, respectively.

3.10.3 Galactic Particles - The OPTRANSPAC can expect to see a galactic particle environment on the same order as shown below.

Atomic Number	Particles/cm^2-sec
1 (proton)	4.0
2 (alpha particle)	0.5
8 (oxygen)	3.0×10^{-2}
14 (silicon)	7.0×10^{-3}
26 (iron)	3.0×10^{-4}

3.11 Optical Background

3.11.1 Earth Background at OPTRANSPAC - The expected worst case Earth background at OPTRANSPAC is shown in Figure 3.11-1. These data were developed assuming "full Earth" illumination.

3.11.2 Solar Background at OPTRANSPAC - The effective background radiance at the OPTRANSPAC due to the off-axis solar scattering is plotted versus range in Figure 3.11-2.

3.11.3 Saturn Background at EORS - The background flux at the Earth Orbiting Relay Satellite (EORS) platform due to Saturn is given in Figure 3.11-3. These data are from recorded Earth orbit measurements of Saturn's irradiance. The radiance function is used directly with the field-of-view, aperture size, optical filter bandwidth, and optics transmission to obtain the optical background power on the EORS detector.

3.11.4 Solar Background at EORS - The solar background radiance at the EORS due to off-axis scattering is shown in Figure 3.11-4.

EARTH TO SATURN TRANSFER ORBIT

- HOHMANN TRANSFER
- SEMI-MAJOR AXIS 5.67 AU
- ECCENTRICITY 0.826

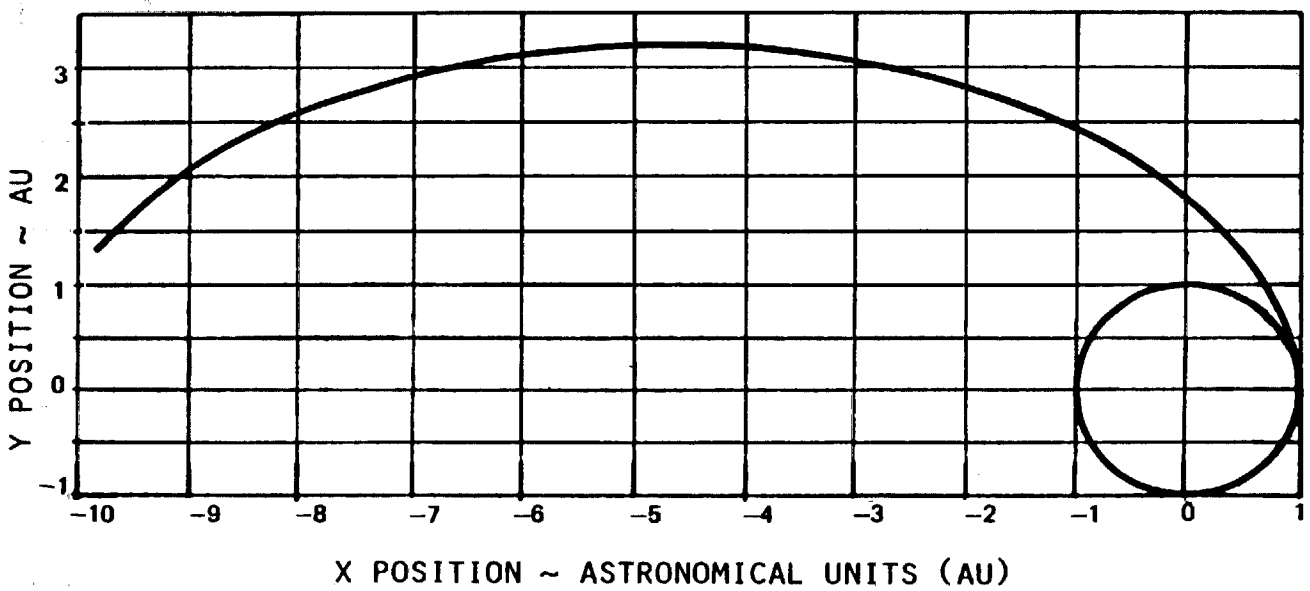

FIGURE 3.1-1

EARTH TO SPACECRAFT RANGE

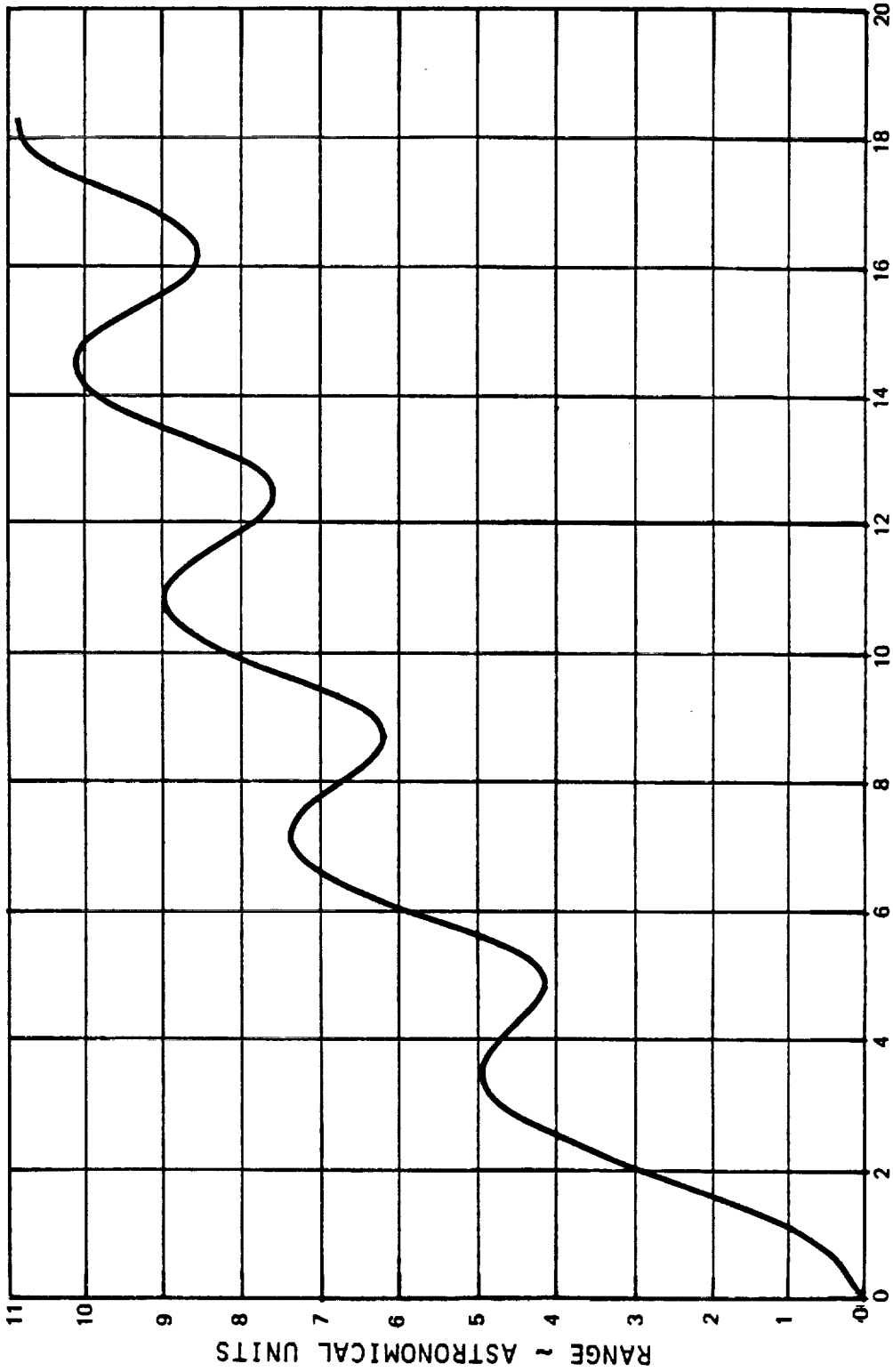

FIGURE 3.1-2

EARTH AND SPACECRAFT VELOCITIES

- HOHMANN TRANSFER TO SATURN

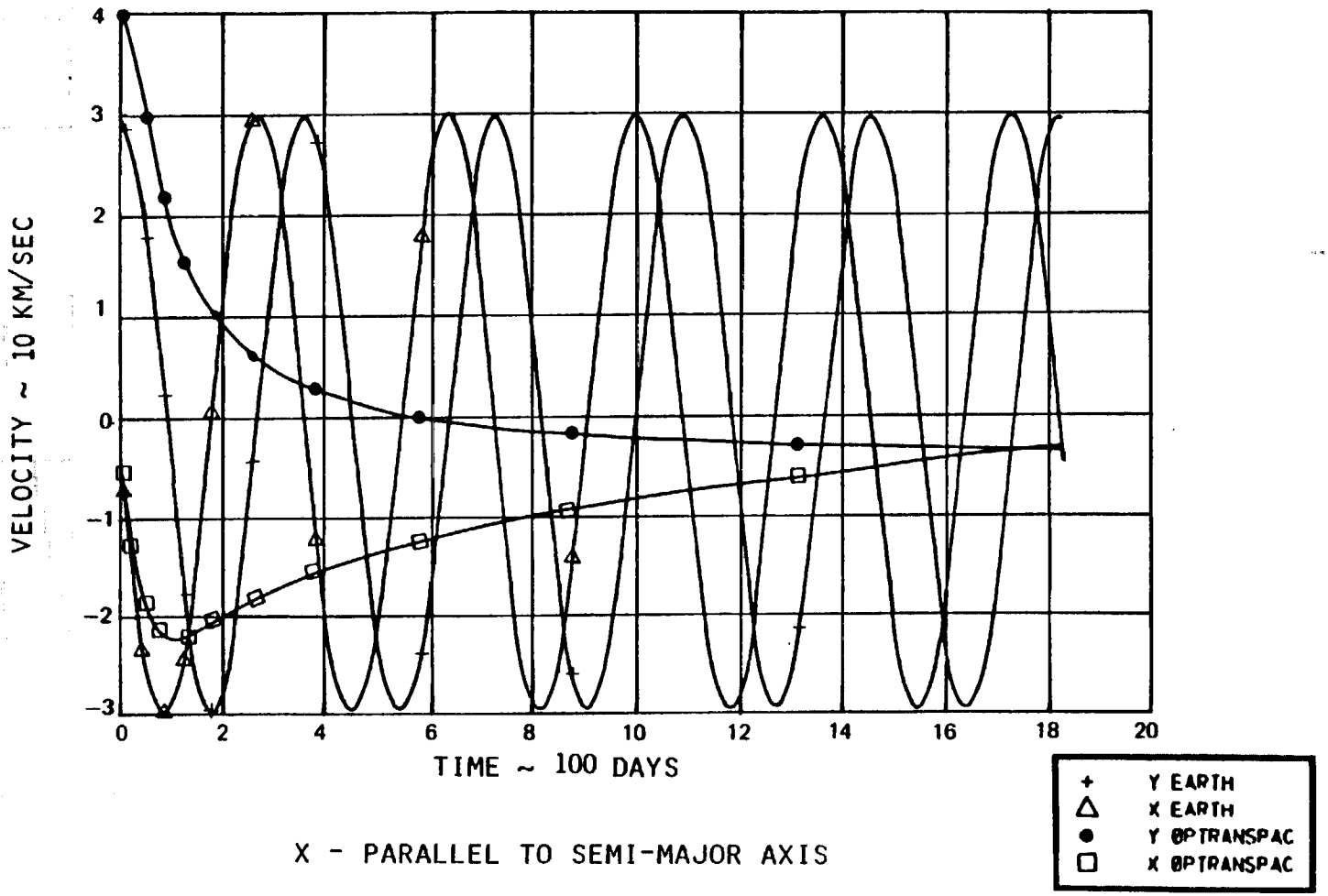

X - PARALLEL TO SEMI-MAJOR AXIS

Y - PARALLEL TO SEMI-MINOR AXIS

FIGURE 3.1-3

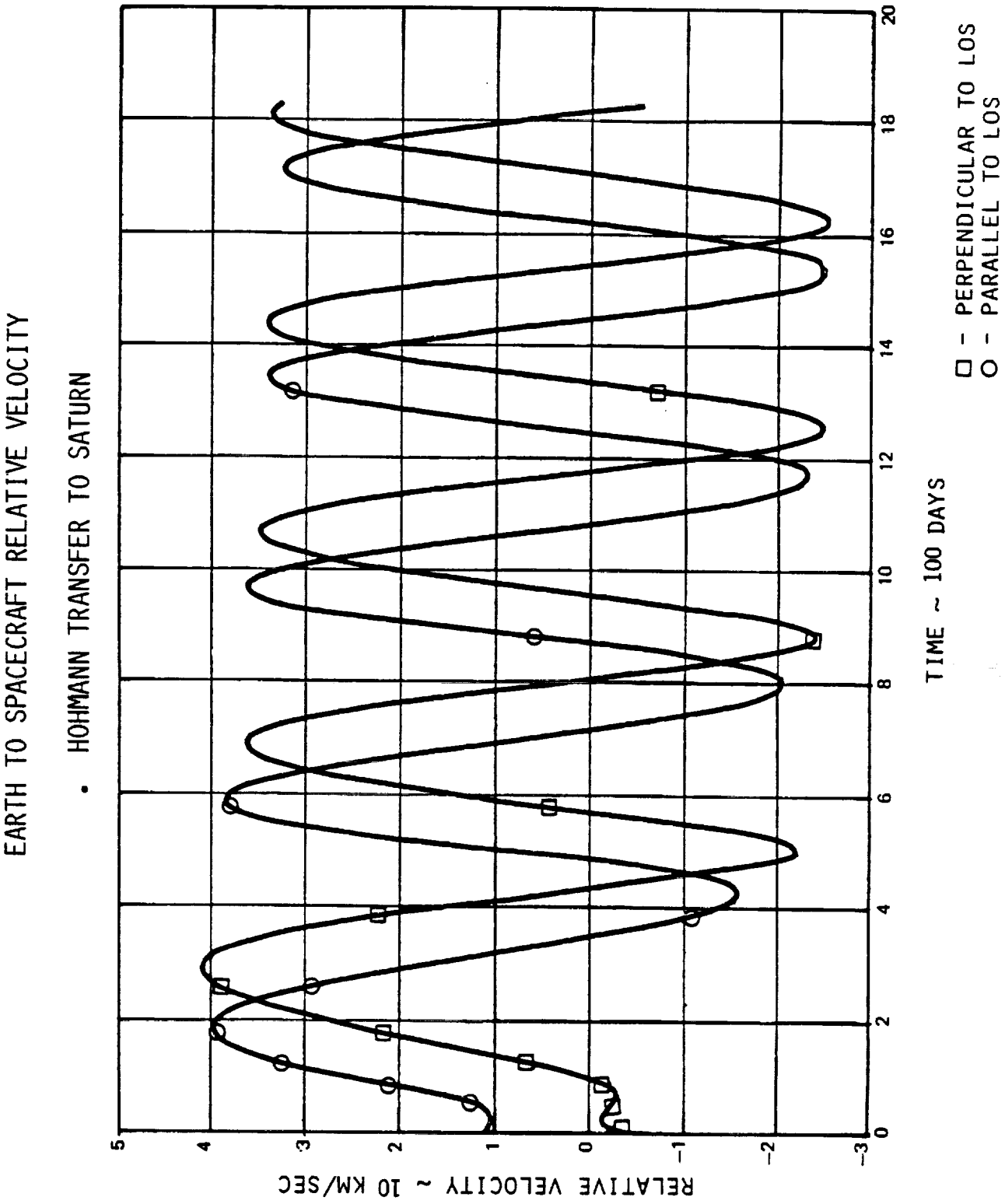
EARTH TO SPACECRAFT RELATIVE VELOCITY
• HOHMANN TRANSFER TO SATURN
RELATIVE VELOCITY ~ 10 KM/SEC
5
4
3
2
1
0
-1
-2
-3
0
2
4
6
8
10
12
14
16
18
20
TIME ~ 100 DAYS
□ - PERPENDICULAR TO LOS
○ - PARALLEL TO LOS

FIGURE 3.1-4

POINT AHEAD AND DOPPLER CONTRIBUTORS

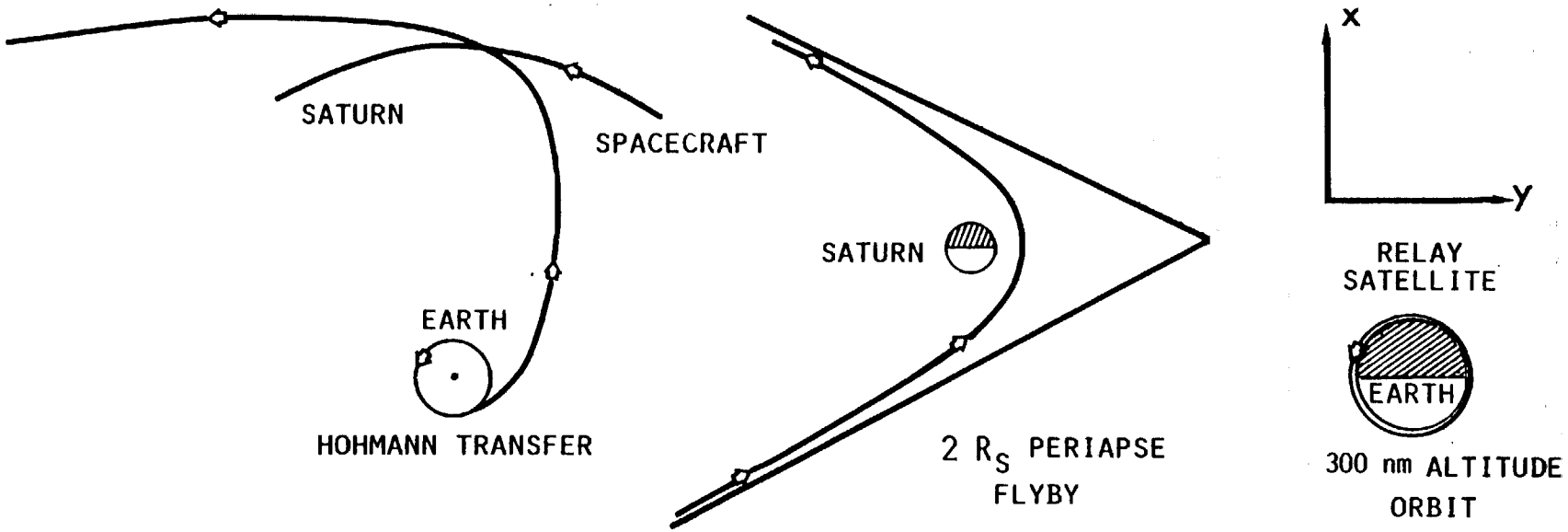

MAXIMUM VELOCITIES

	DIRECTION	
	X (KM/SEC)	Y (KM/SEC)
EARTH	±29.8	±29.8
RELAY	± 7.6	± 7.6
SATURN	SMALL	- 9.6
FLYBY	±25.1	±25.1

FIGURE 3.1-5

DOPPLER SHIFT

- HOHMANN TRANSFER TO SATURN
- NO RELAY SATELLITE EFFECTS
- $\lambda = 1.064\ \mu M$

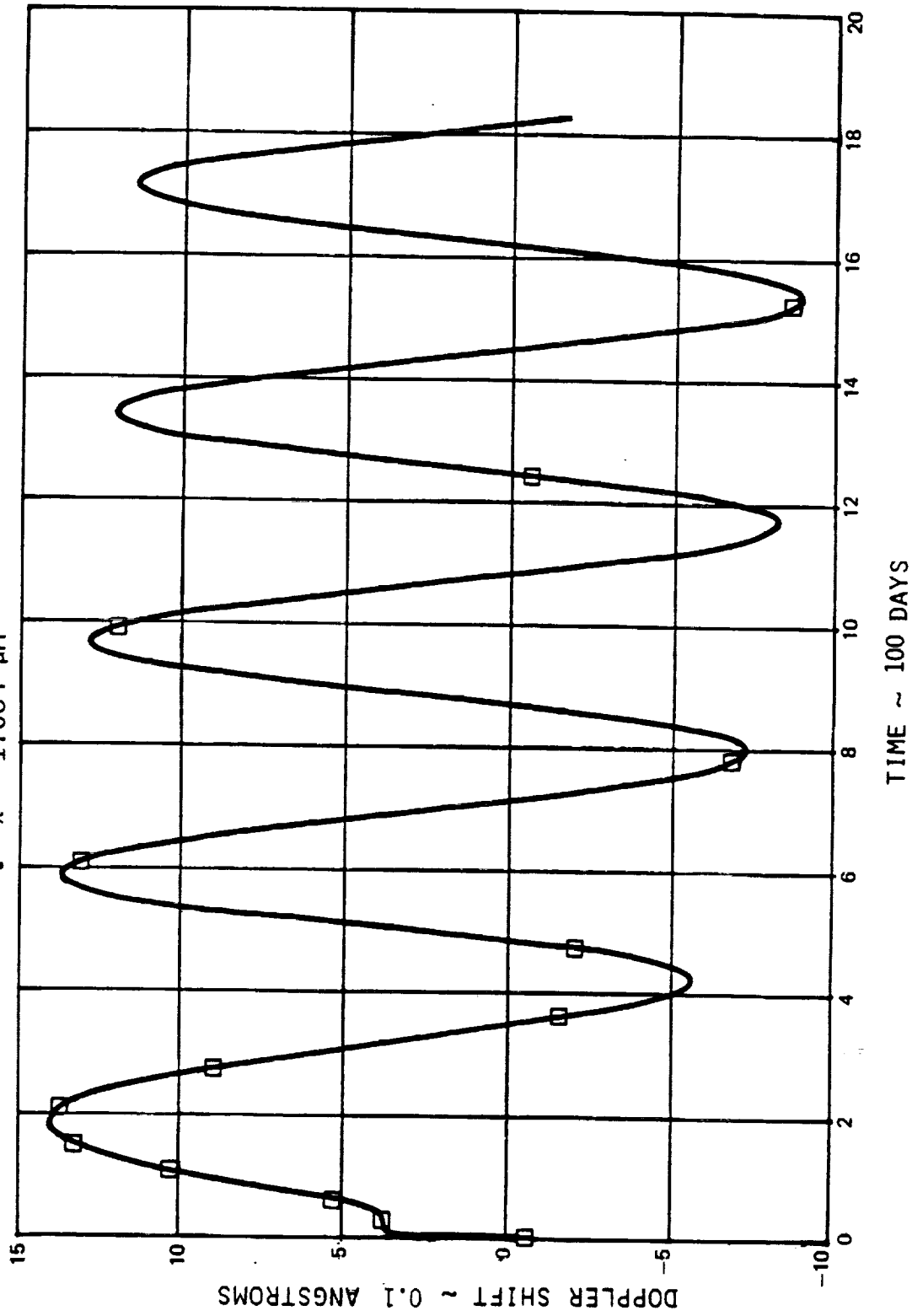

FIGURE 3.1-6

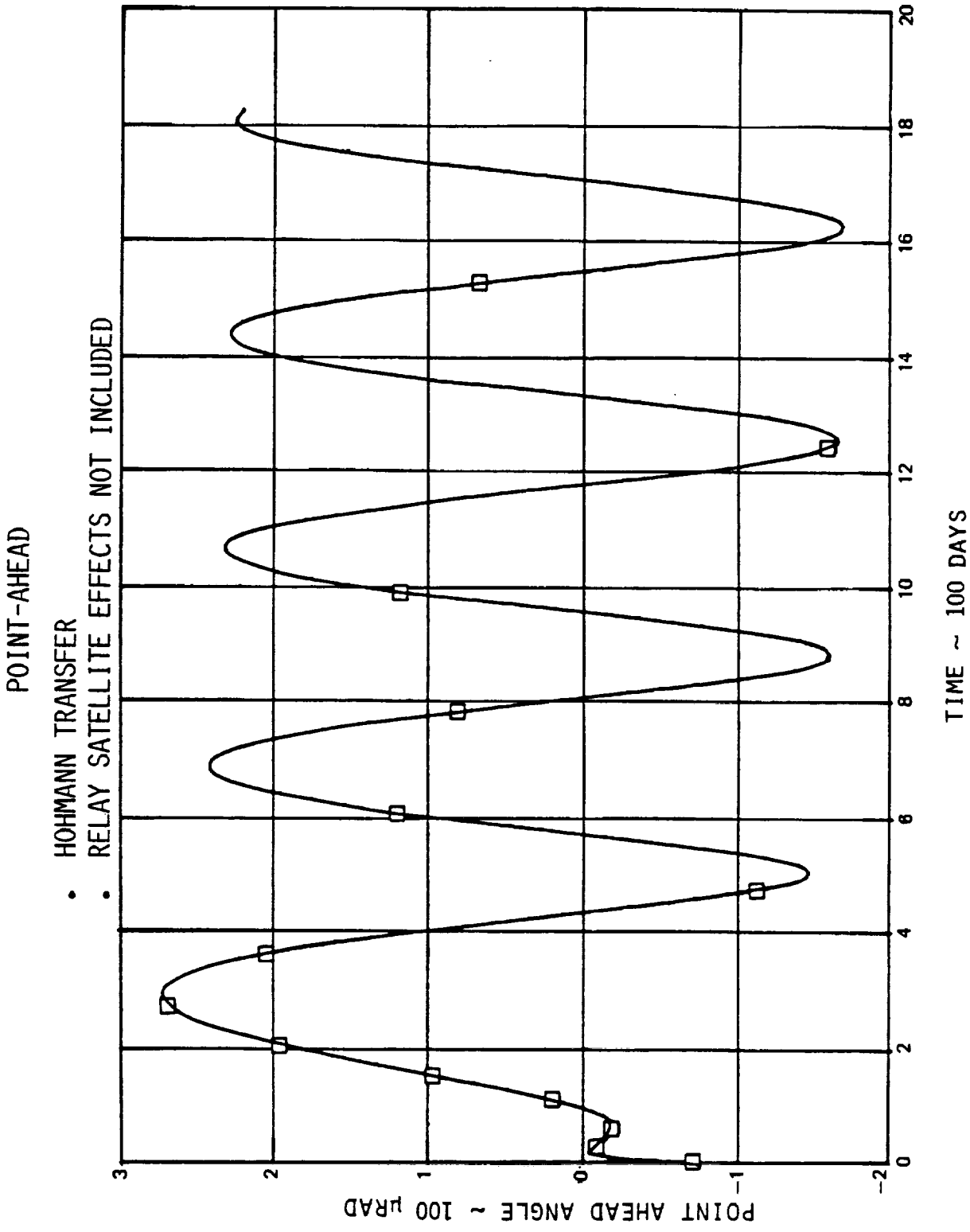
POINT-AHEAD
• HOHMANN TRANSFER
• RELAY SATELLITE EFFECTS NOT INCLUDED
POINT AHEAD ANGLE ~ 100 μRAD
TIME ~ 100 DAYS
3
2
1
0
-1
-2
0
2
4
6
8
10
12
14
16
18
20

FIGURE 3.1-7

EXPECTED METEROID ENVIRONMENT

INTEGRAL FLUENCE DURING TRANSIT

PARTICLE MASS (G)	FLUENCE (PARTICLES/M^2)
10^{-12}	2.2×10^{5}
10^{-10}	1.8×10^{3}
10^{-8}	2.3×10^{2}
10^{-6}	9.2
10^{-5}	5.7×10^{-1}
10^{-4}	3.5×10^{-2}
10^{-3}	2.1×10^{-3}
10^{-2}	1.2×10^{-4}
10^{-1}	7.7×10^{-5}
10^{0}	4.8×10^{-7}

MEAN RELATIVE SPEED

15 KM/SEC

PARTICLE MASS DENSITY

0.5 G/CM^3

FIGURE 3.2-1

SPACE SHUTTLE VIBRATION ENVIRONMENT

- LAUNCH

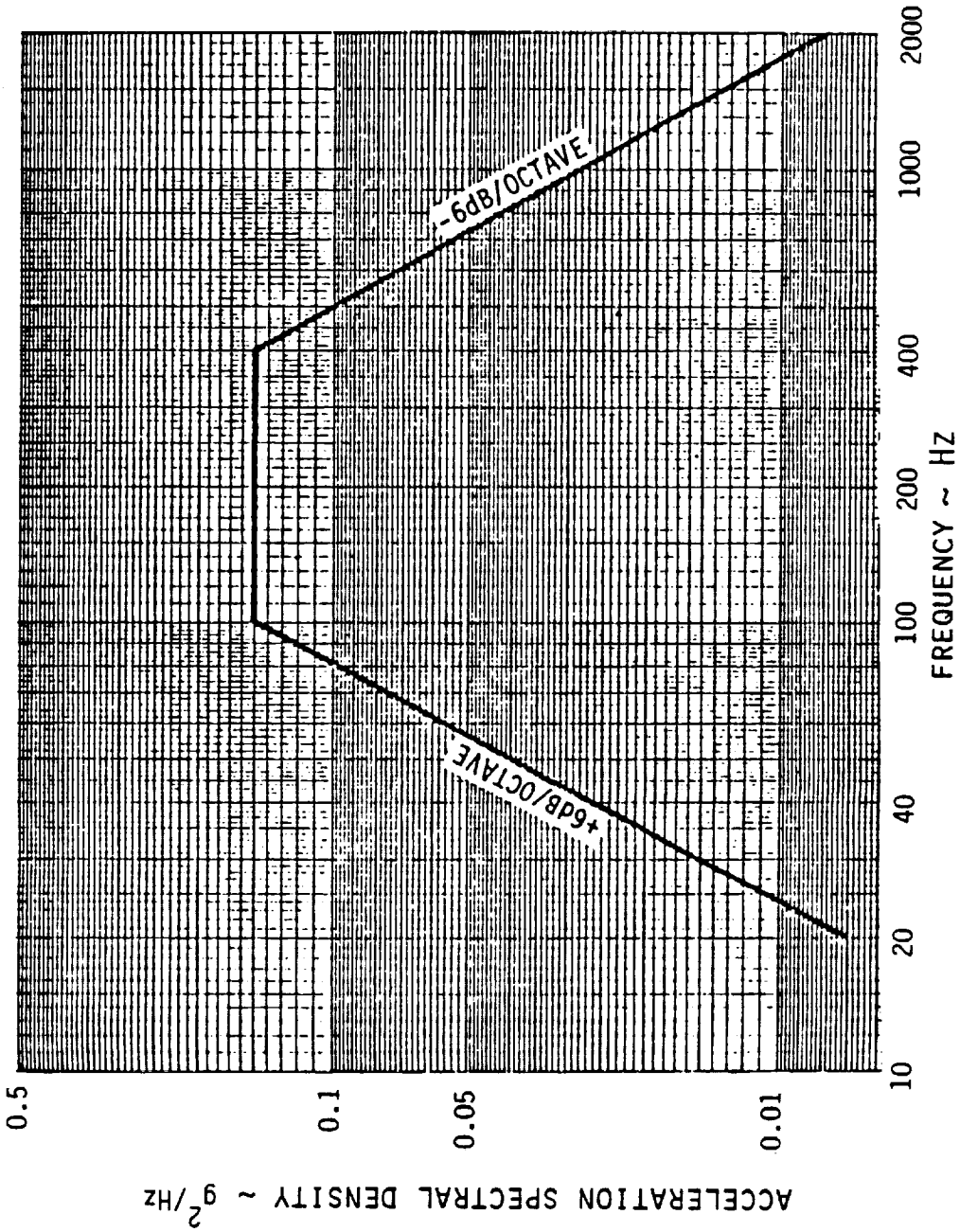

FIGURE 3.7-1

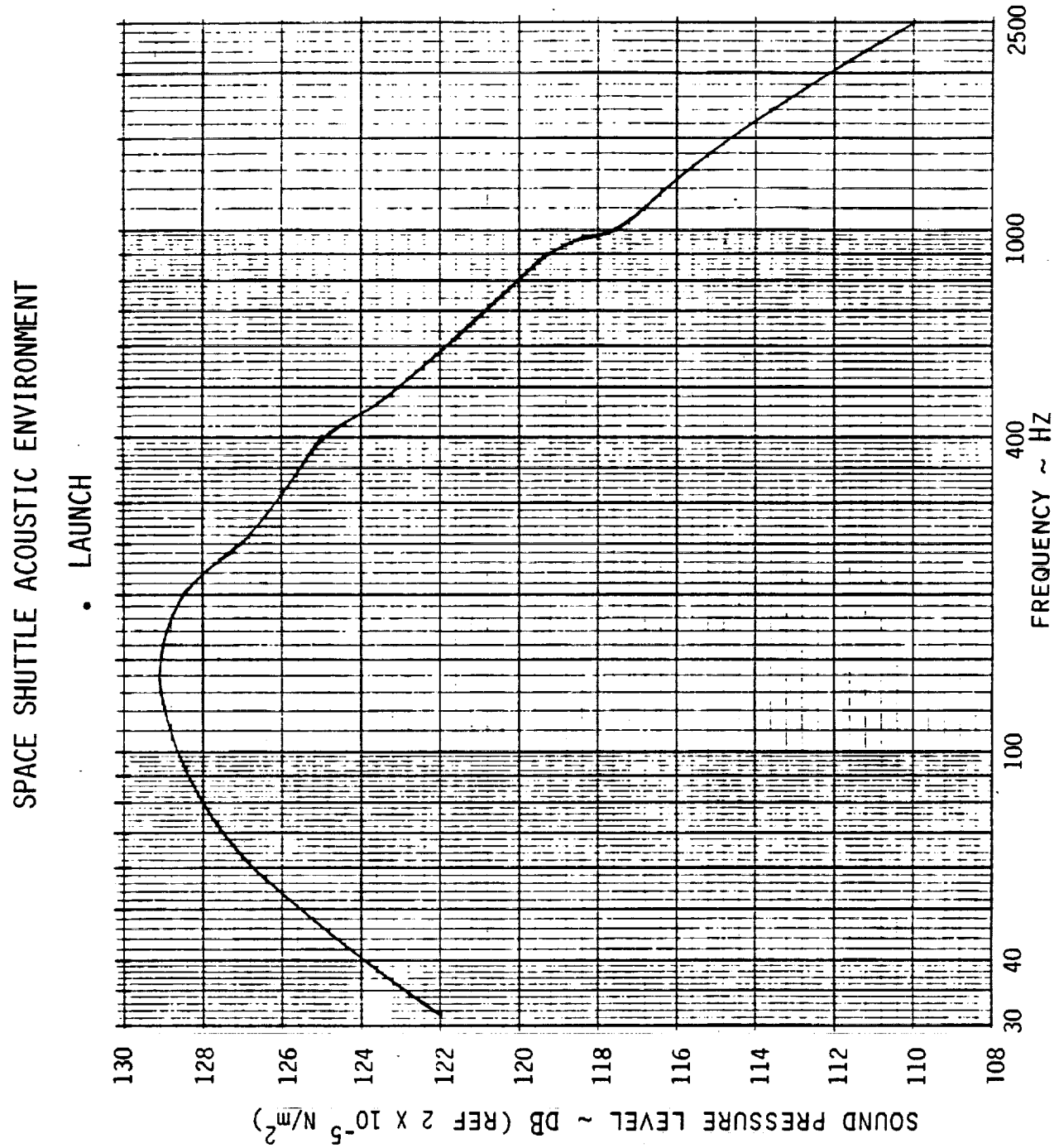
SPACE SHUTTLE ACOUSTIC ENVIRONMENT
• LAUNCH
SOUND PRESSURE LEVEL ~ DB (REF 2 X 10⁻⁵ N/m²)
130
128
126
124
122
120
118
116
114
112
110
108
30
40
100
400
1000
2500
FREQUENCY ~ HZ

FIGURE 3.8-1

PYROTECHNIC SHOCK

- SPACECRAFT/LAUNCH VEHICLE SEPARATION

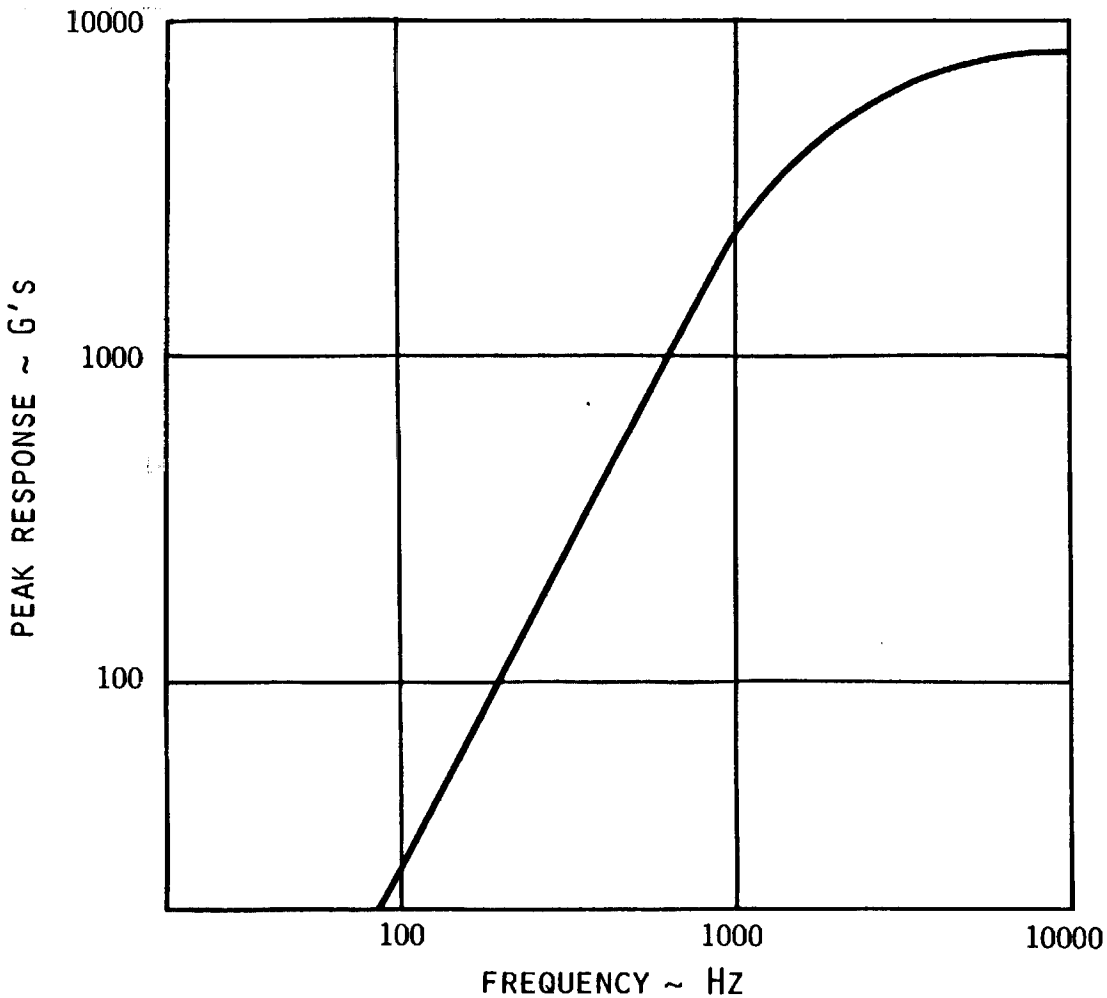

FIGURE 3.9-1

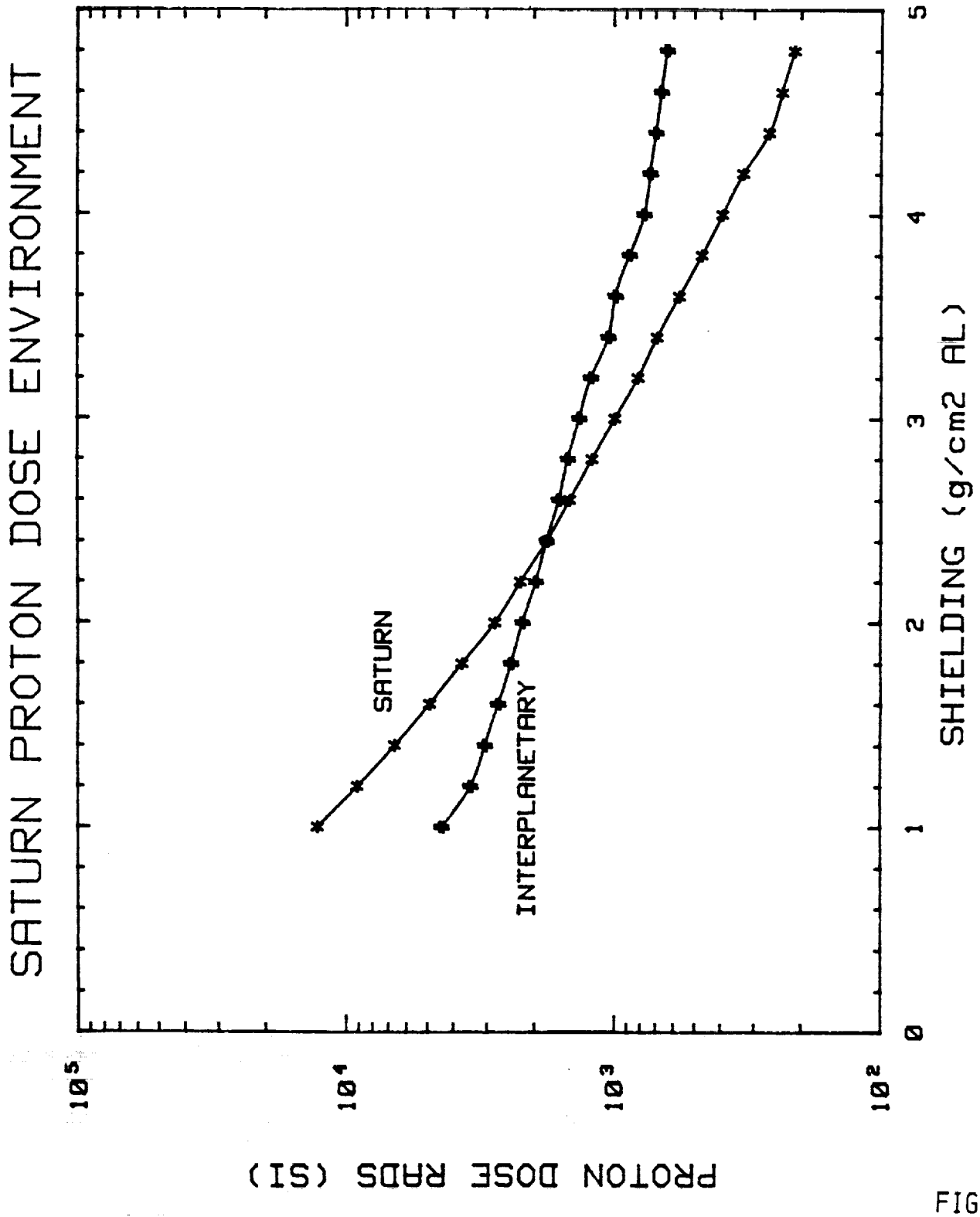
SATURN PROTON DOSE ENVIRONMENT
SATURN
INTERPLANETARY
PROTON DOSE RADS (SI)
SHIELDING (g/cm2 AL)
10⁵
10⁴
10³
10²
0
1
2
3
4
5

FIGURE 3.10-1

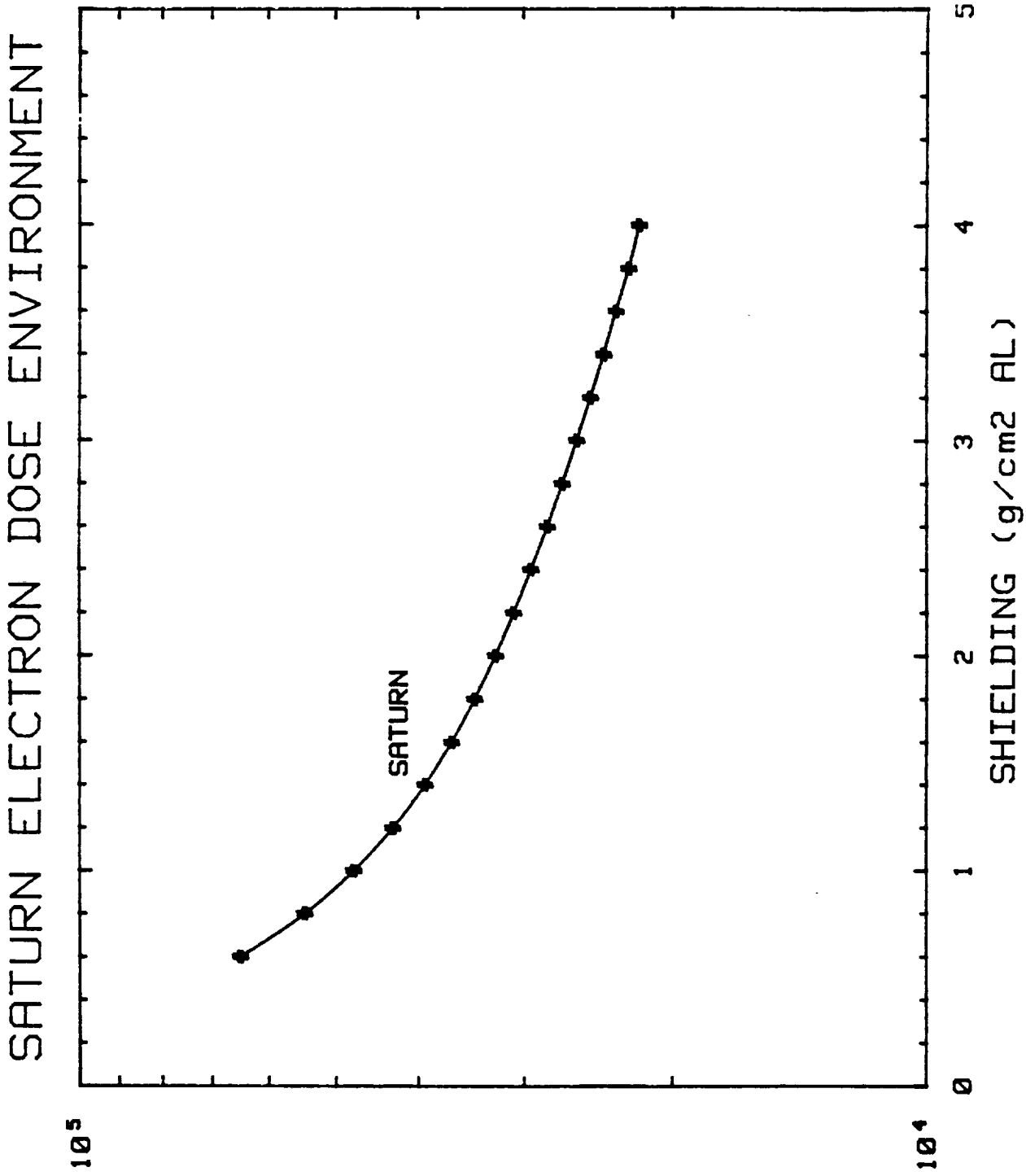
SATURN ELECTRON DOSE ENVIRONMENT
SATURN
ELECTRON DOSE RADS (SI)
SHIELDING (g/cm2 AL)
10⁵
10⁴
0
1
2
3
4
5

FIGURE 3.10-2

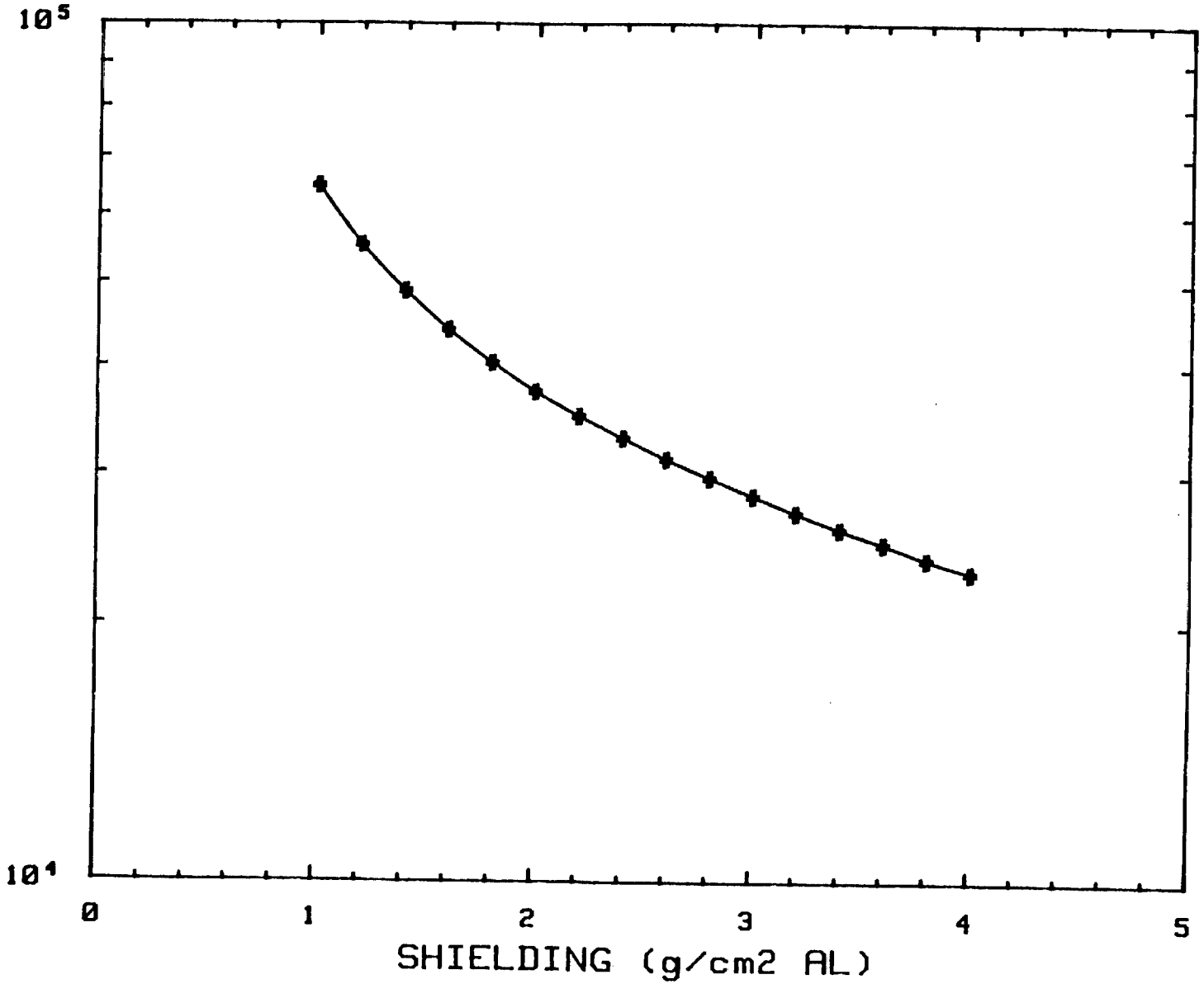
SATURN TOTAL DOSE ENVIRONMENT
10⁵
10⁴
TOTAL DOSE RADS (SI)
0
1
2
3
4
5
SHIELDING (g/cm2 AL)

FIGURE 3.10-3

SATURN PROTON DISPLACEMENT DAMAGE ENVIRONMENT

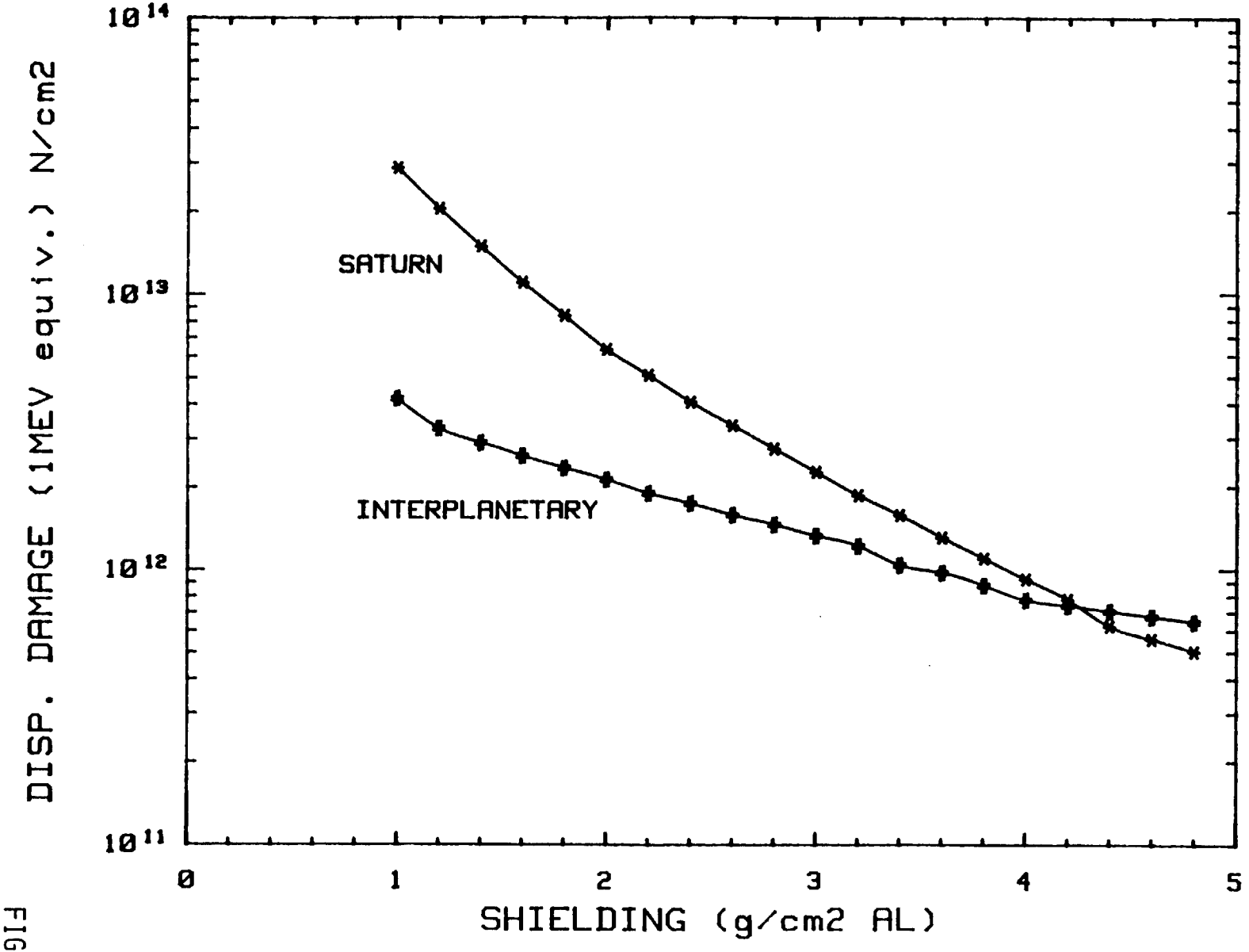

FIGURE 3.10-4

SATURN ELECTRON DISPLACEMENT DAMAGE ENVIRONMENT

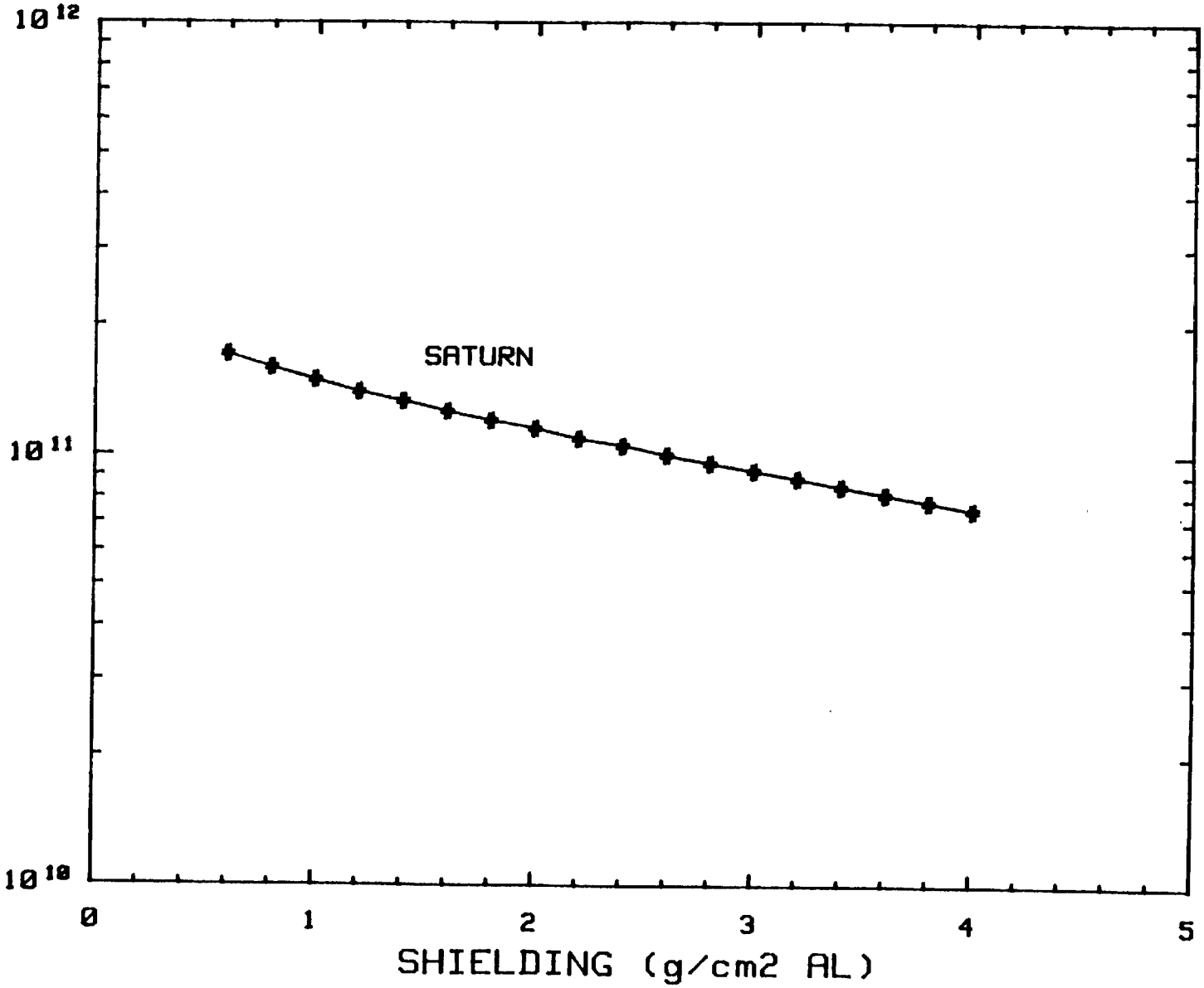

FIGURE 3.10-5

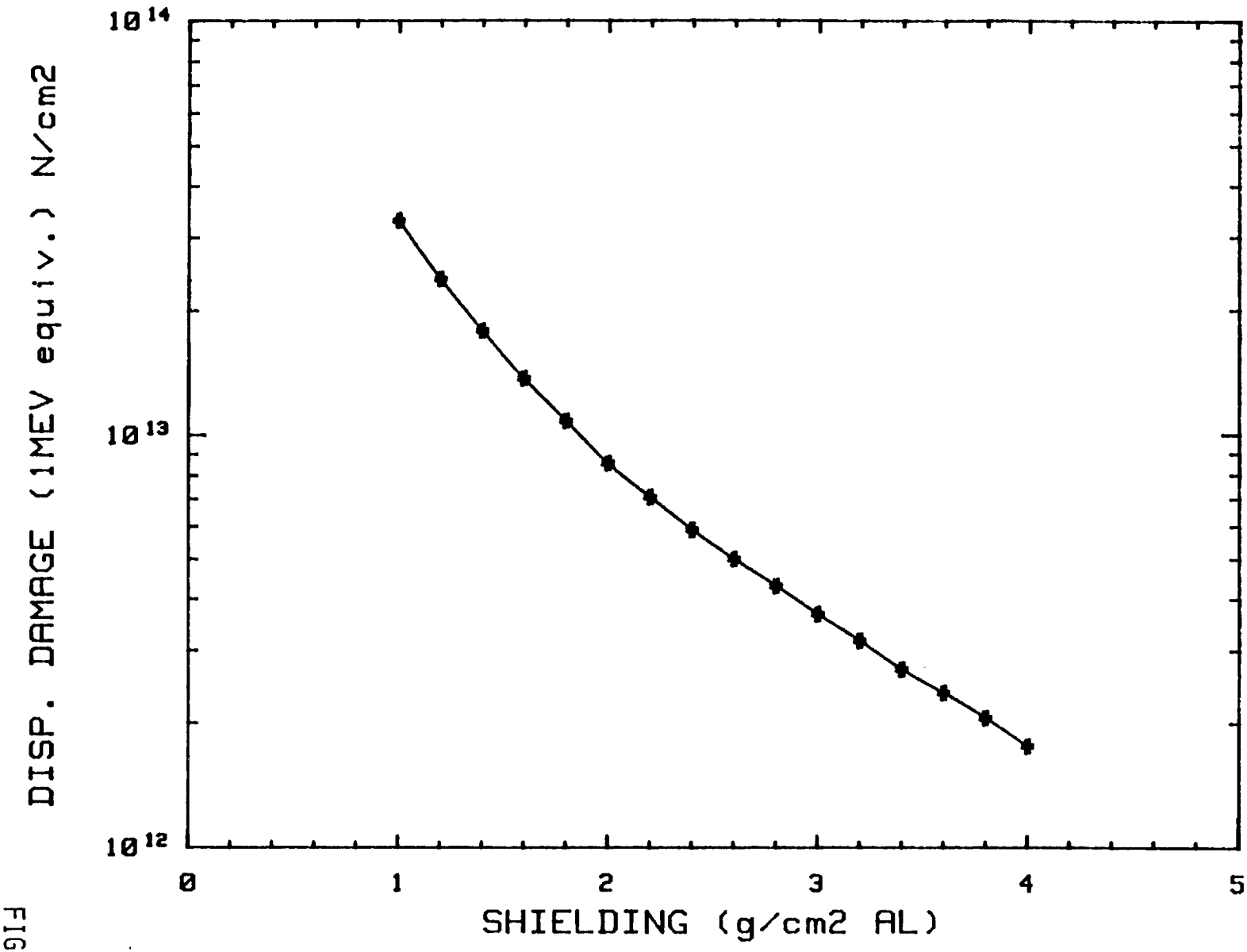
SATURN TOTAL DISPLACEMENT DAMAGE ENVIRONMENT
DISP. DAMAGE (1MEV equiv.) N/cm2
10 14
10 13
10 12
0
1
2
3
4
5
SHIELDING (g/cm2 AL)

FIGURE 3.10-6

EARTH BACKGROUND AT OPTRANSPAC

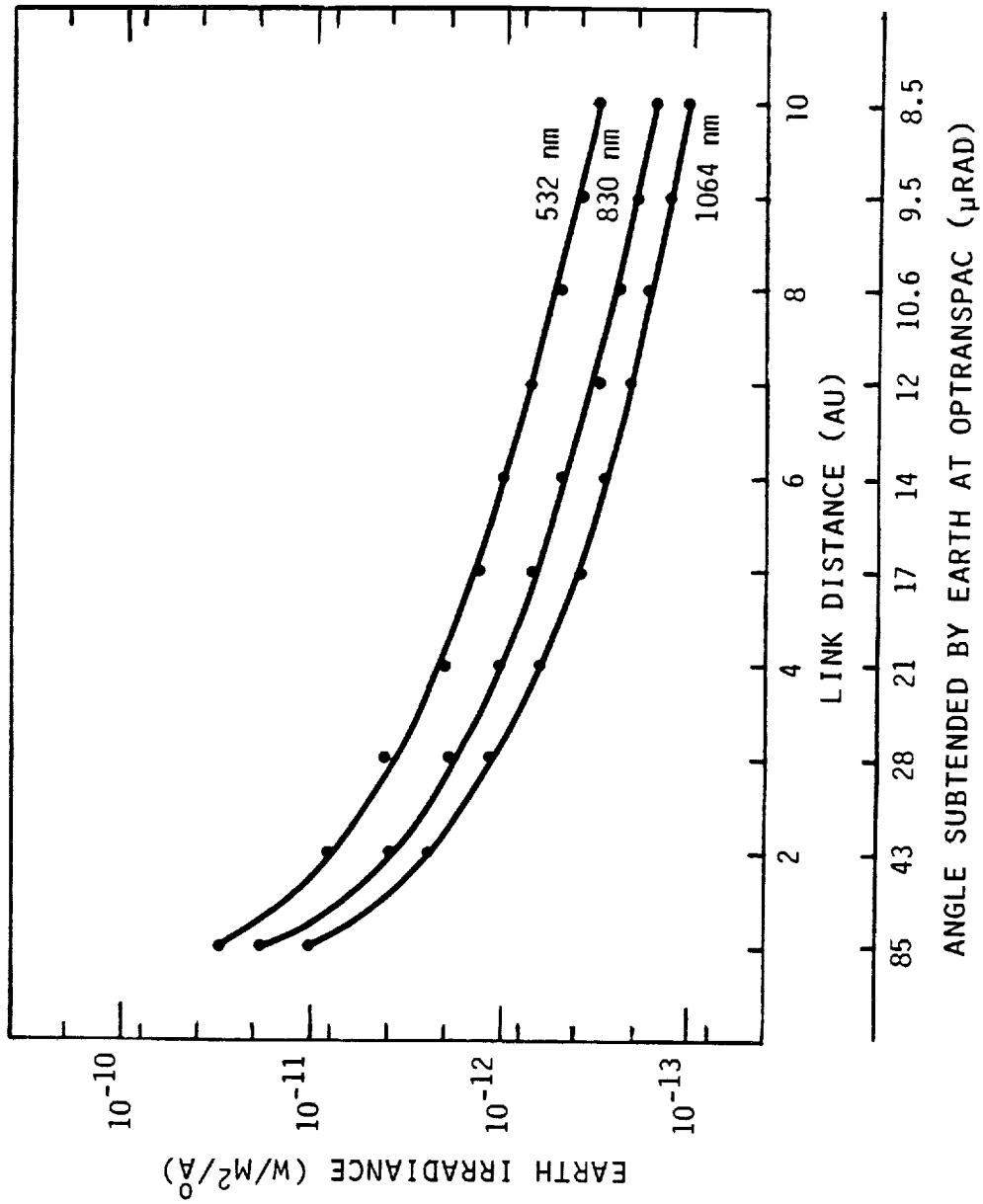

FIGURE 3.11-1

SOLAR BACKGROUND RADIANCE AT OPTRANSPAC
DUE TO OFF-AXIS SCATTERING

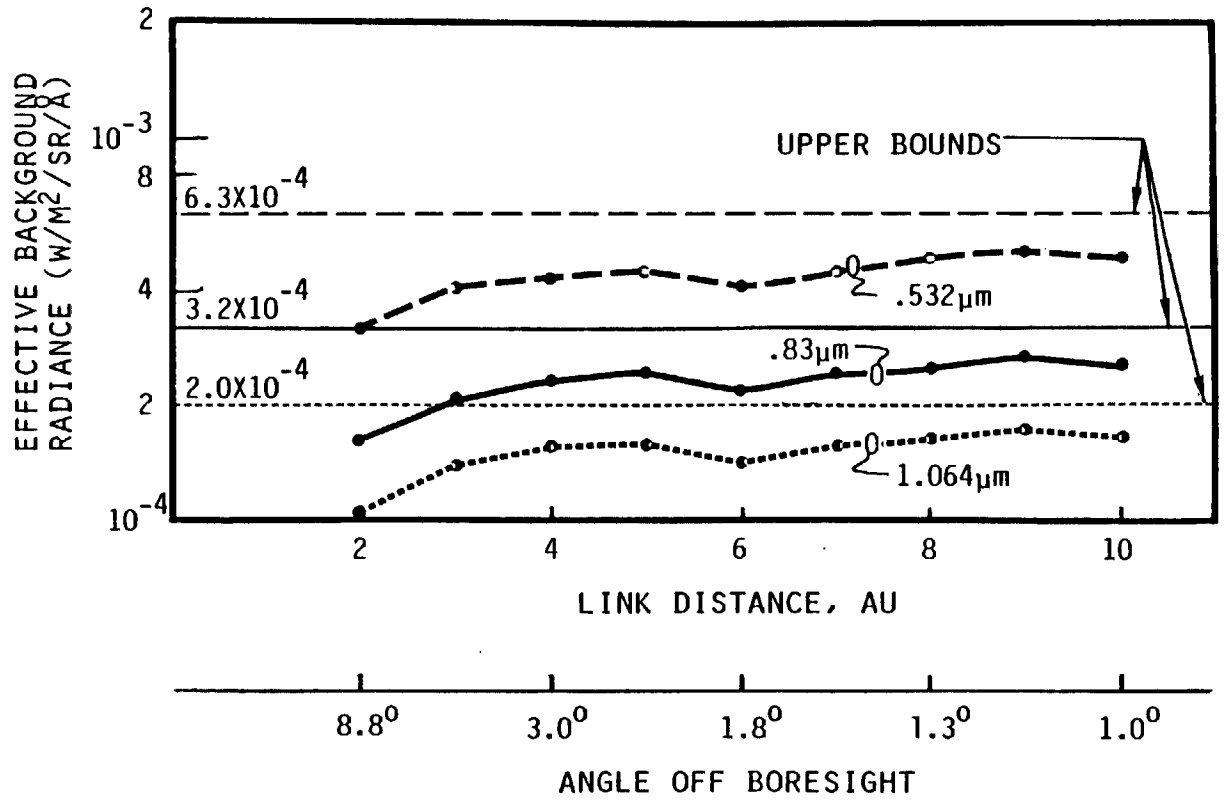

FIGURE 3.11-2

SATURN BACKGROUND AT EORS

λ NM	IRRADIANCE $W/M^2/\overset{o}{A}$	RADIANCE* $W/M^2/SR/\overset{o}{A}$
532	$8X10^{-12}$	$1.14X10^{-3}$
830	$3.2X10^{-12}$	$4.55X10^{-4}$
1064	$2X10^{-12}$	$2.85X10^{-4}$

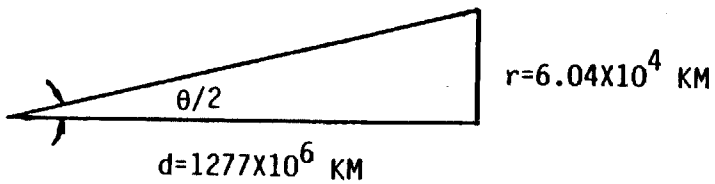

$\theta = 2.\text{ARC TAN } (\frac{r}{d})$

$\theta = 94.6\ \mu\text{RAD}$

* VALID FOR FIELD-OF-VIEWS LESS THAN θ

FIGURE 3.11-3

SOLAR BACKGROUND RADIANCE
AT EORS
(DUE TO OFF-AXIS SCATTERING)

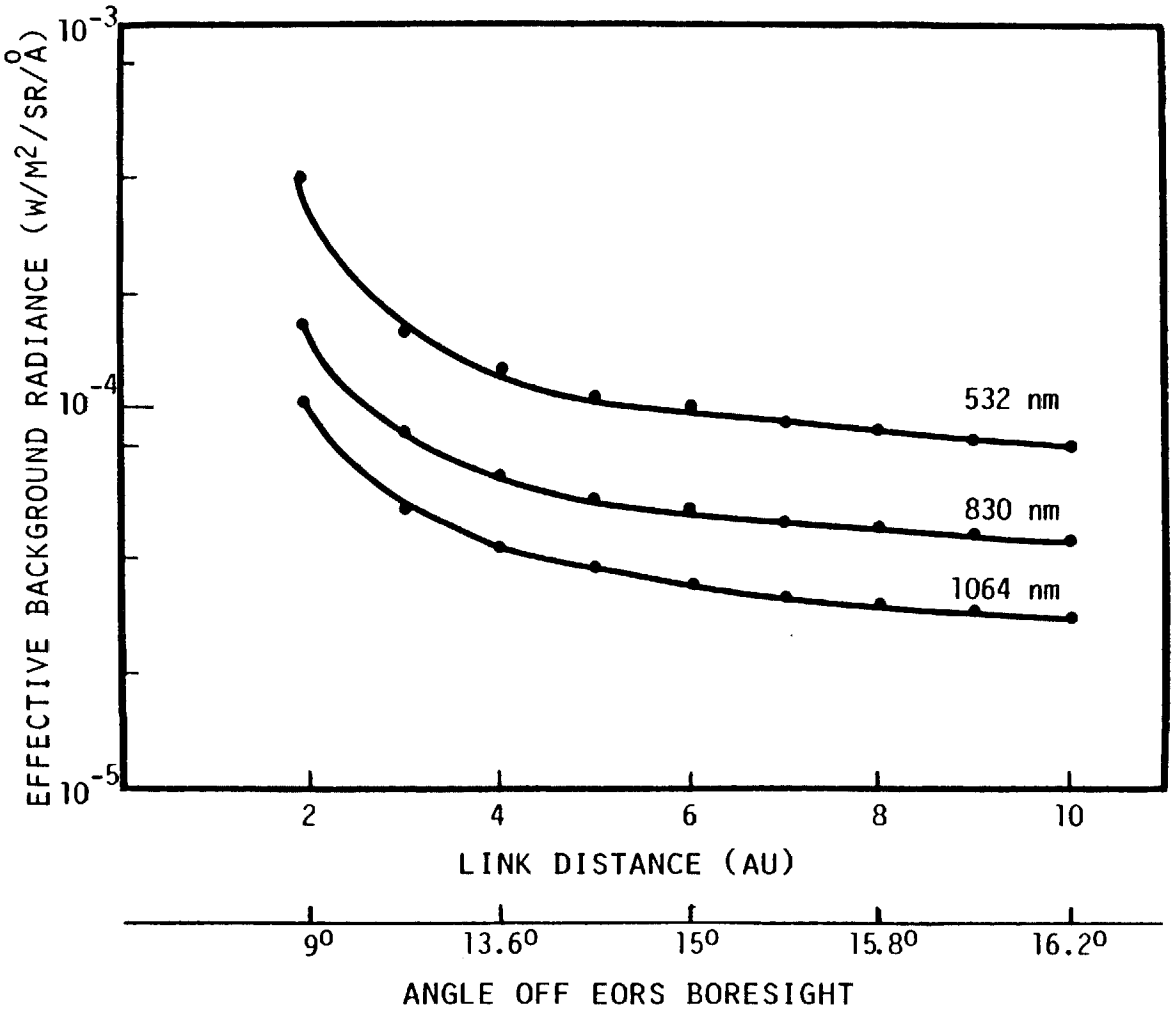

FIGURE 3.11-4

THIS PAGE LEFT INTENTIONALLY BLANK

APPENDIX B-1

DOWNLINK LASER SPECIFICATION

Type	Frequency Doubled Nd:YAG	
Configuration	Diode Pumped Slab	
Output Wavelength	532 Nanometers ± 5 Angstroms	
Interpulse Period	70 ± 25.6 μsec	(1)
	233.3 ± 25.6 μsec	(2)
	700.0 ± 25.6 μsec	(3)
Nominal Repetition Rates	14285.71 PPS	(1)
	4285.71 PPS	(2)
	1428.57 PPS	(3)
Pulsewidth	10 nsec FWHM	
Energy Per Pulse(4)	28 μ Joules	(1)
	93 μ Joules	(2)
	280 μ Joules	(3)
Efficiency (Regulated Pump Power To Optical Output)	>10%	
Weight	≤ 20 LBS	
Power	≤ 4 Watts	
Envelope	8.2" x 9.5" x 5.0"	

(1) 100 KBPS Data Rate
(2) 30 KBPS Data Rate
(3) 10 KBPS Data Rate
(4) Based On Nominal Repetition Rates

THIS PAGE LEFT INTENTIONALLY BLANK

APPENDIX B-2

TELESCOPE
SPECIFICATION

Type	Fixed Mounted
Clear Aperture	11 inches (279.4 mm)
Obscuration	61.47 mm
Wavelength	
Receive	400-1100 Nanometers
Transmit	532 Nanometers
Quality	Diffraction Limited Transmit at 532 Nanometers
Wavefront Error	$< \lambda/20$ RMS at 532 Nanometers
Viewfield	$\pm$ 2.5 Milliradians
Collimated Beam Size	$\leq$ 0.5 inches
Transmission	$\geq$ 95% (excluding wavefront loss)
Magnification	$\leq$ 24:1
Weight	$\leq$ 18 pounds

THIS PAGE LEFT INTENTIONALLY BLANK

APPENDIX B-3

OPTICAL SYSTEM
SPECIFICATION

Type	Common Path With Dichroic Combined Transmit - Receive
Transmission	> 65% Transmit at 532 NM > 65% Receive Com at 1064 NM > 20% Earth Track > 40% Alignment at 532 NM
Wavefront Error	< λ/20 RMS Transmit
Filter Bandwidth	25 Angstroms Centered About 1064 NM
Filter Transmission	> 70% at 1064 NM
Collimated Beam Size	$\leq$ 0.5 inches
Commandable Focus	Yes
Alignment Path	Yes
Weight	$\leq$ 13.5 Pounds

THIS PAGE LEFT INTENTIONALLY BLANK

APPENDIX B-4

DETECTOR/PREAMPLIFIER SPECIFICATION

Detector	
Type	Silicon Avalanche Photodiode
Configuration	low -k, dimpled
Quantum Efficiency	$\geq$ 40% at 1064 nm
Ionization Coefficient	$\leq$ .007
Avalanche Gain	210
Noise Equivalent Power	$\leq 2.1 \times 10^{-14}$ W/Hz$^{1/2}$ Based on RCA 30954E
Bandwidth	$\geq$ 50 MHz
Preamplifier	
Type	Transimpedance
Bandwidth	$\geq$ 50 MHz
Noise Equivalent Current	$\leq 1.4 \times 10^{-12}$ A/Hz$^{1/2}$

THIS PAGE LEFT INTENTIONALLY BLANK

APPENDIX B-5

EARTH TRACKER DETECTOR SPECIFICATION

Type	Charge Injection Device (CID)
Sensitive Area	5.12mm x 5.12mm
Pixel Size	20 microns
Earth Track Active Area	4.0mm x 4.0mm
Alignment Active Area	4.0mm x 1.12mm
Earth Track Viewfield	1.0 mrad x 1.0 mrad
Earth Track Pixel FOV	5 μrad x 5μrad
Pixel Saturation	$\geq 1.5 \times 10^6$ e^-
Dark Current	$\leq 6.2 \times 10^4$ e^-/sec-pixel @ 23°C
Dark Current Variations	$\leq$ .022 (RMS) for adjacent pixels
Readout Noise Constant	≤ 3.16 $e^-/Hz^{1/2}$
Response Variation	$\leq$ .006 (RMS) For adjacent pixels
Quantum Efficiency	>40% for 0.4 μm $\leq \lambda \leq$ 1.0 μm

THIS PAGE LEFT INTENTIONALLY BLANK

APPENDIX C-1

OPTRANSPAC

DESIGN NOTE

TITLE:	NUMBER 1
ELECTRONICS SYSTEM DESIGN	REVISION
	DATE 22 July 1985
	TOTAL SHEETS

SUMMARY:

The baseline OPTRANSPAC Electronics are described. The electronics as configured consist of three assemblies which provide the control, communication, and power conditioning functions. The functional requirements of each assembly are presented. A redundancy implementation based on attaining the highest achievable probability of mission success is presented. The physical characteristics of the electronic assemblies are presented.

PREPARED BY: H. J. Mingo
H. J. MINGO
SECTION CHIEF ELECTRONICS

CHECKED BY: S. G. Lambert
S. G. LAMBERT
OPTRANSPAC ENGINEERING MANAGER

APPROVED BY: J. A. Pautler
J. A. PAUTLER
OPTRANSPAC PROGRAM MANAGER

DISTRIBUTION:

J. P. Carter, S. G. Lambert, H. J. Mingo, J. A. Pautler

OPTRANSPAC ELECTRONICS

1.0 INTRODUCTION

The OPTRANSPAC Electronics assemblies (reference shaded blocks of Figure 1) provide the acquisition and tracking control function as well as the communication function. A digital computer, input/output circuitry, and drive circuits within the Control Electronics Assembly provide the acquisition and tracking function. The communications function is provided by circuitry within the Communication Electronics Assembly. The Power Conditioning Unit converts the spacecraft power to the required secondary voltage levels, provides redundancy switching, mechanism, and heater control as well as command and telemetry interfaces.

2.0 FUNCTIONAL REQUIREMENTS

2.1 CONTROL ELECTRONICS (Reference Figure 2)

Command signals to position the torque motor beam steerers (TMBSs) to direct the incoming and transmitted optical signals is the principal output of the Control Electronics Digital Processor. These outputs must be provided at a 200 Hz rate to support the 20 Hz TMBS loop bandwidth and are the drivers for the processor operation rate. Command signals for positioning the command focus mechanism are initiated by ground command. Mode control of the OPTRANSPAC operation is provided by the digital processor or via ground commands. Figure 3 describes (in general terms) the processor operations in each operating mode.

2.1.1 TMBS Command Operations - Command signals for TMBS position are computed using the formula described in Figure 4.

2.1.2 Command Focus - Positioning of the command focus mechanism is accomplished via ground command. The ground command is processed to generate a discrete output which causes the focus mechanism to move until its position sensor signal fed back to the processor is equal to the commanded position.

2.1.3 Mode Logic - The operational modes of the OPTRANSPAC are depicted in Figure 5 and the mode logic is described in Figure 6.

2.2 COMMUNICATIONS ELECTRONICS (Reference Figure 7)

Both receive and transmit communication functions are required. The receive function consists of conditioning, decoding, and formatting of the data pulses from the communication detector. The transmit function is data formatting, encoding, and generation of the required laser modulator drive signal.

2.2.1 Receive Function - The output from the Communication Detector's preamplifier consists of an electrical signal with the following characteristics:

Rate: 142.86 pulses/sec
Coding: PPM data with 8 bits/pulse
Pulse Width: 10 nS
Amplitude: 0.100 to 1.0 volts-peak

OPTRANSPAC SYSTEM CONFIGURATION

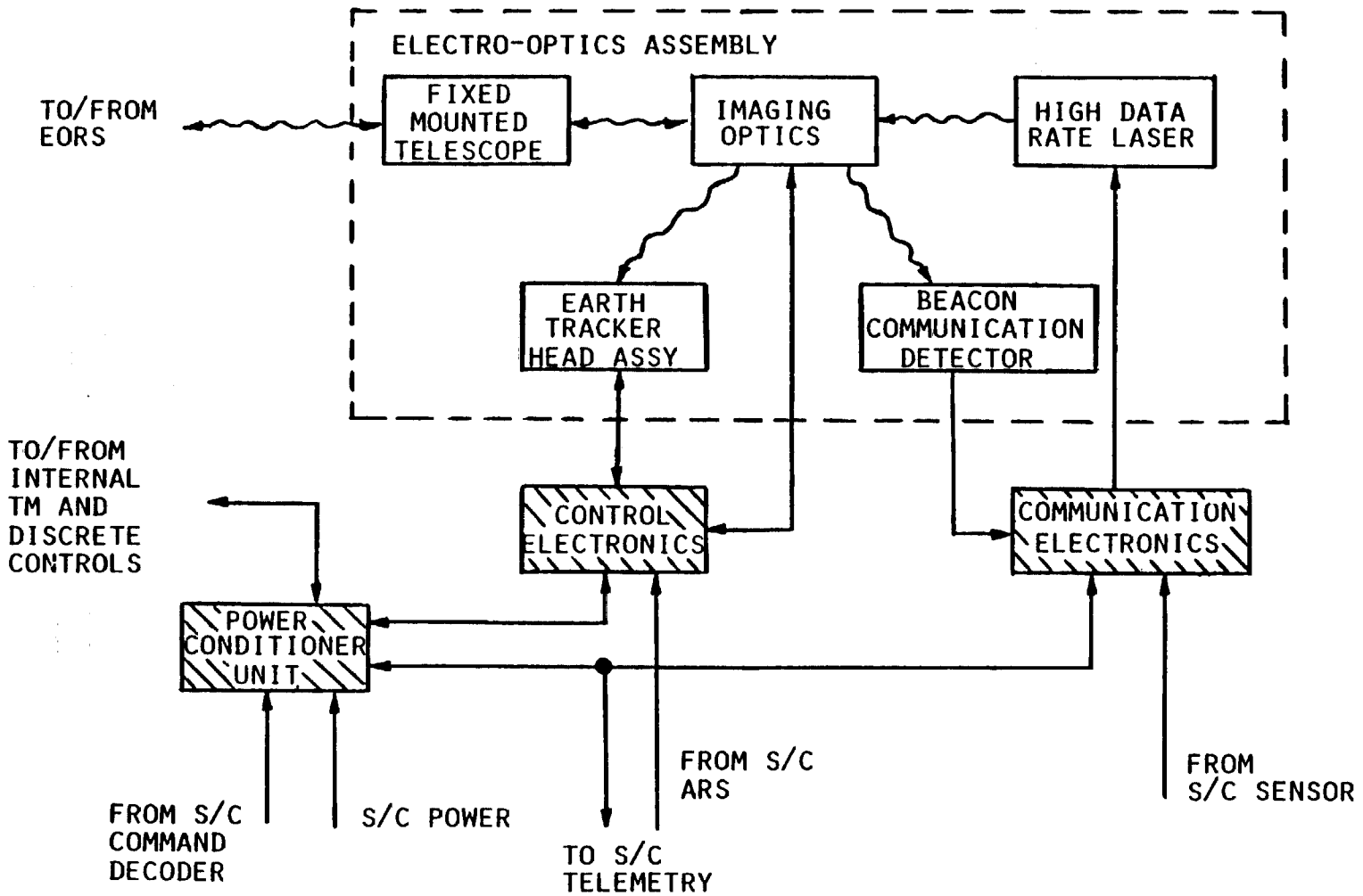

FIGURE 1

CONTROL ELECTRONICS
FUNCTIONAL BLOCK DIAGRAM

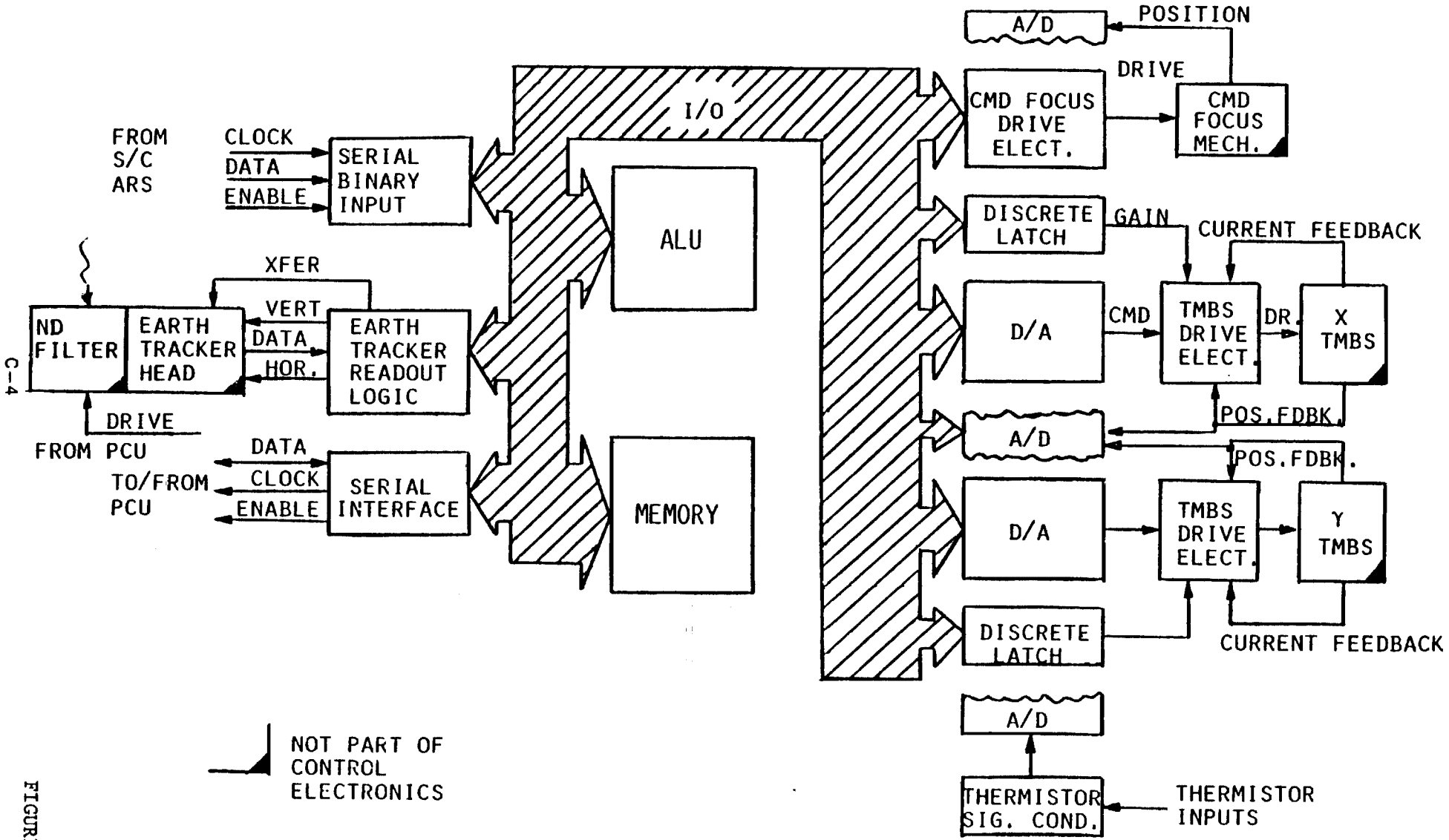

FIGURE 2

OPTRANSPAC OPERATIONS LOGIC
EARTH TRACK

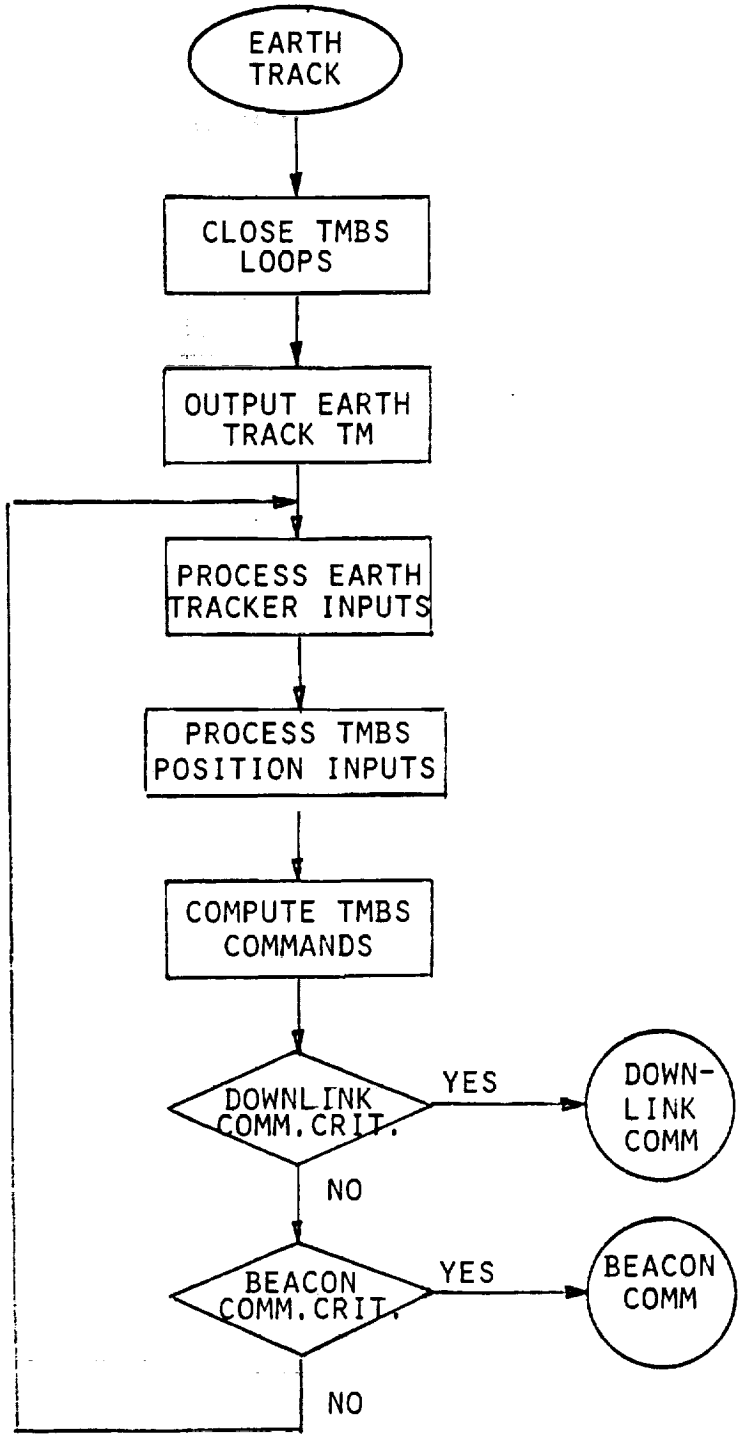

FIGURE 3
SHEET 1 OF 6

OPTRANSPAC OPERATIONS LOGIC
BEACON COMMUNICATION

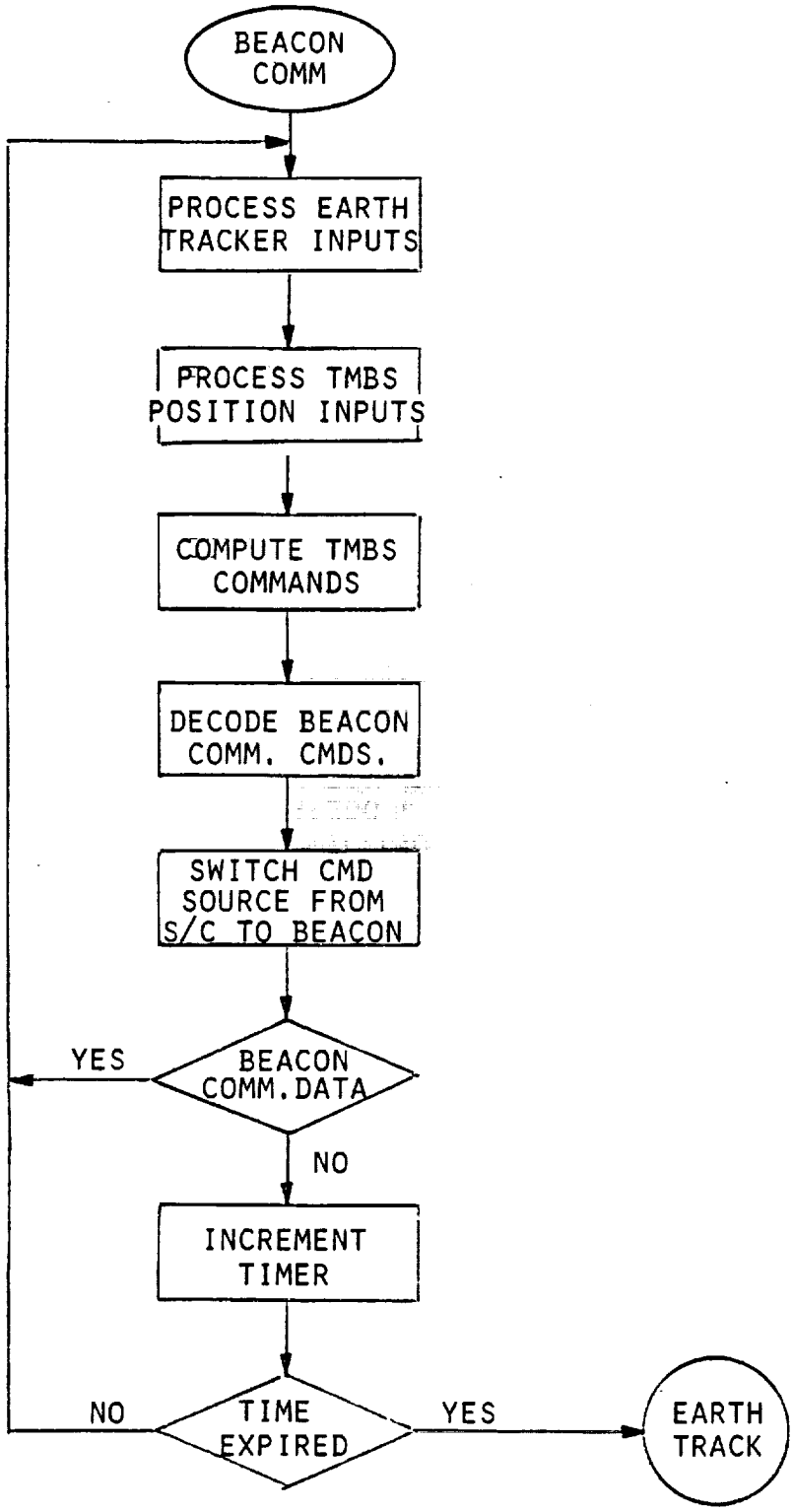

FIGURE 3
SHEET 2 OF 6

OPTRANSPAC OPERATIONS LOGIC
DOWNLINK COMMUNICATION

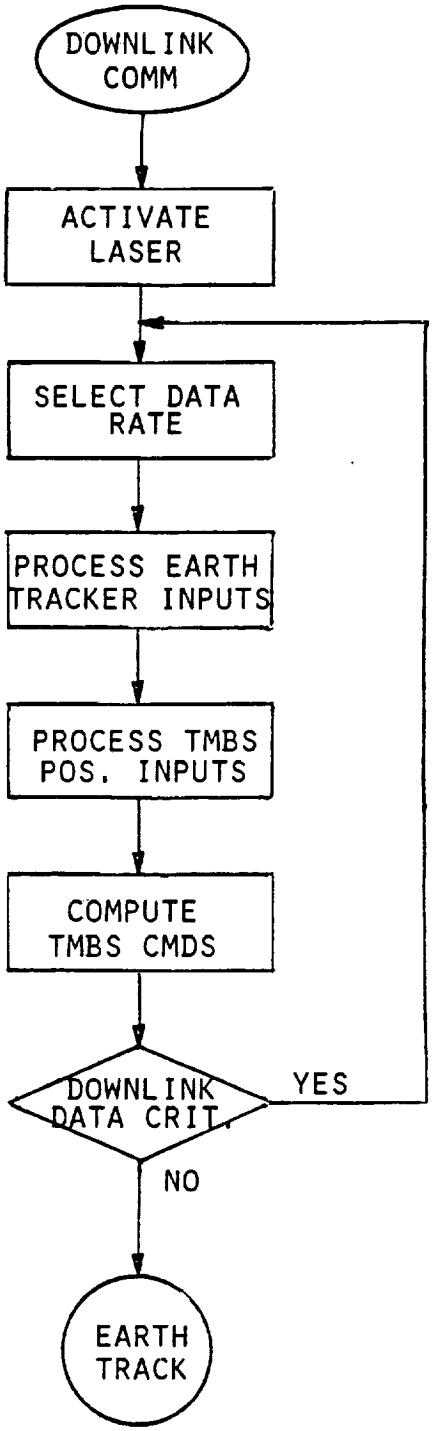

FIGURE 3
SHEET 3 OF 6

OPTRANSPAC OPERATIONS LOGIC
ALIGNMENT

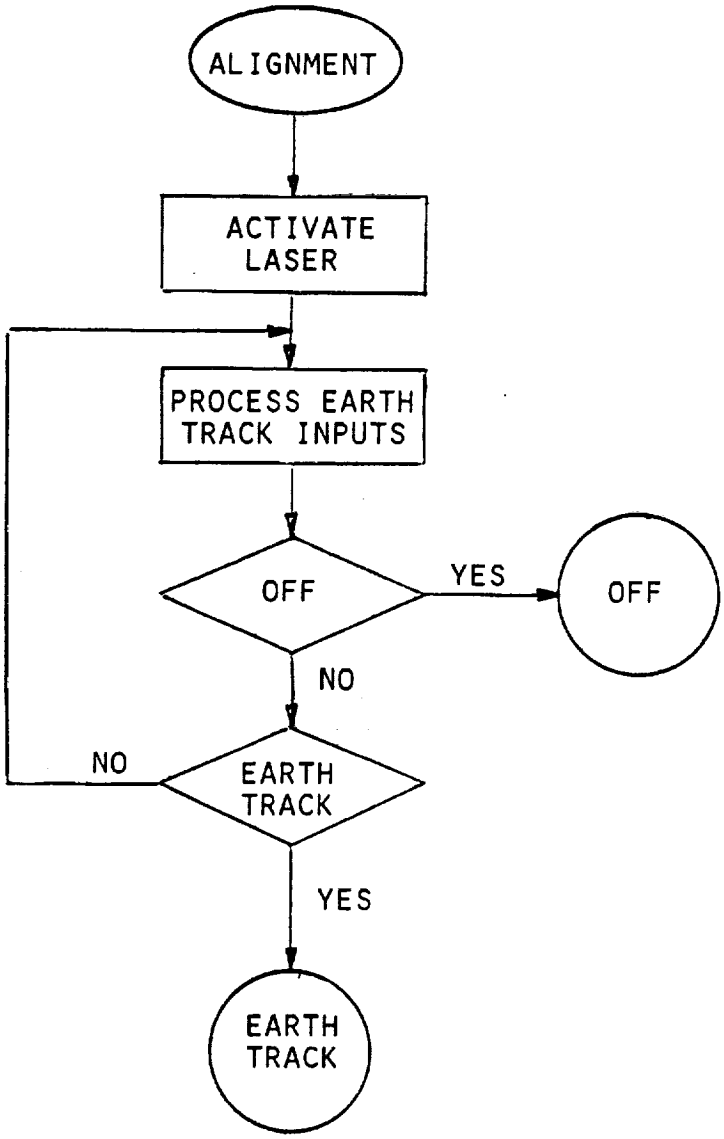

FIGURE 3
SHEET 4 OF 6

OPTRANSPAC OPERATIONS LOGIC
STANDBY

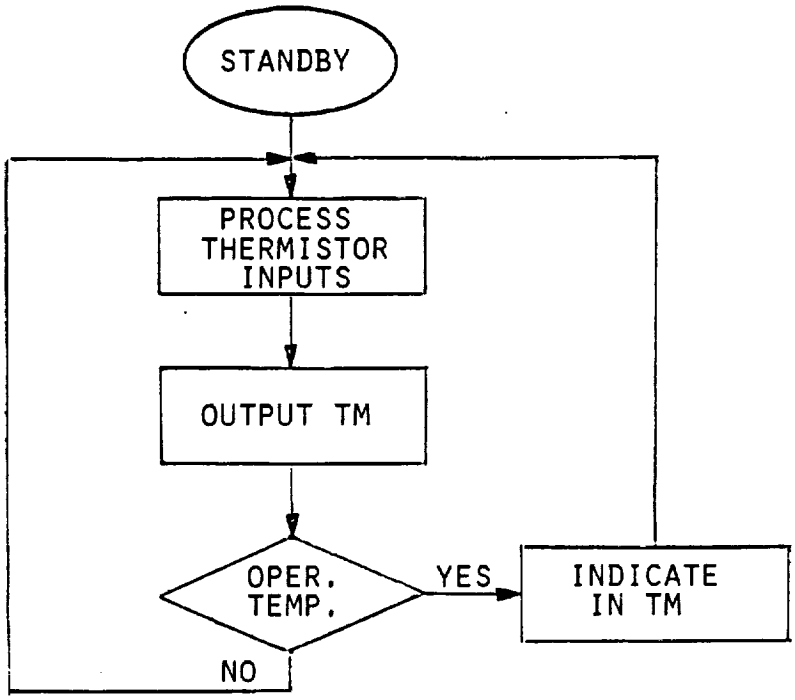

FIGURE 3
SHEET 5 OF 6

OPTRANSPAC OPERATIONS LOGIC
EARTH ACQUISITION

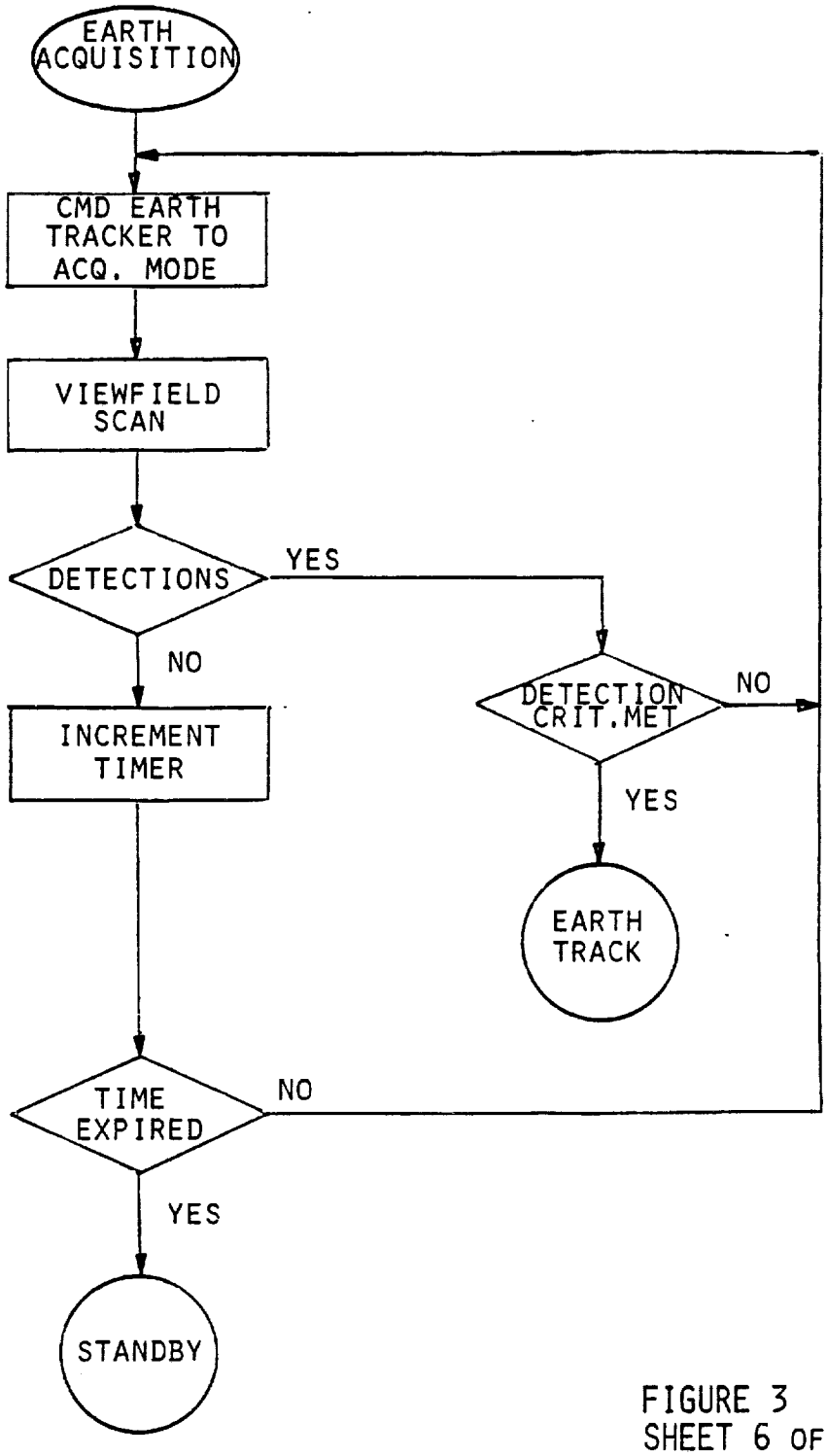

FIGURE 3
SHEET 6 OF 6

OPTRANSPAC TMBS COMMANDS

EARTH VISIBLE

$$\text{TMBS COMMAND} = \left[\text{DETECTOR AXES TO TMBS AXES CONVERSION}\right]\left[\left[\text{EARTH POSITION IN DETECTOR AXES}\right] + \left[\text{INERTIAL AXES TO DETECTOR AXES CONVERSION}\right]\left[\text{EARTH AXES TO INTERNAL AXES CONVERSION}\right]\left[\text{PREDICTED EORS POSITION WRT EARTH POSITION}\right] + \left[\text{RESIDUAL POINT AHEAD}\right] - \left[\text{BORESIGHT POSITION IN DETECTOR AXES}\right]\right]$$

EARTH NOT VISIBLE

$$\text{TMBS COMMAND} = \left[\text{DETECTOR AXES TO TMBS AXES CONVERSION}\right]\left[\left[\text{INERTIAL AXES TO DETECTOR AXES CONVERSION}\right]\left[\text{PREDICTED EORS POSITION WRT EARTH POSITION}\right] + \left[\text{PREDICTED EARTH POSITION IN INERTIAL AXES}\right] + \left[\text{RESIDUAL POINT AHEAD}\right] - \left[\text{BORESIGHT POSITION IN DETECTOR AXES}\right]\right]$$

FIGURE 4

MODE DESCRIPTION

MODE	ACTIVITY	ENTER	EXIT	EXIT METHOD
OFF	ALL OPTRANSPAC POWER OFF EXCEPT FOR REQUIRED HEATERS		QUIESCENT	GROUND CMD.
QUIESCENT	WARM-UP MODE FOR OPTRANSPAC EQUIPMENT. POWER ON - ACTIVE CIRCUITRY INOPERATIVE	OFF	STANDBY & OFF	GROUND CMD. AFTER EXAMINING TELEMETRY
STANDBY	PROCESSOR PROGRAM INITIALIZED AND OPERATING	QUIESCENT EARTH ACQ.	EARTH ACQ. OFF	GROUND CMD. GROUND CMD.
EARTH ACQ.	PROCESSING EARTH TRACKER INPUTS, GENERATING TMBS COMMANDS	STANDBY EARTH TRK.	EARTH TRK. STANDBY OFF	AUTOMATIC AUTOMATIC GROUND CMD.
EARTH TRK.	PROCESSING EARTH TRACKER INPUTS, GENERATING TMBS COMMANDS BASED ON EARTH TRACKER CENTROID ALGORITHMS	EARTH ACQ. BEACON COMM. ALIGN. DWN. COMM.	EARTH ACQ. BEACON COMM. ALIGN. DWN. COMM. OFF	AUTOMATIC AUTOMATIC GROUND CMD. AUTOMATIC GROUND CMD.
BEACON COMM.	PROCESSING EARTH TRACKER INPUTS, GENERATING TMBS CMDS. BASED ON EARTH TRK. CENTROID CMDS., RECEIVING CMDS. VIA BEACON	EARTH TRK.	EARTH TRK. OFF	AUTOMATIC GROUND CMD.
DOWNLINK COMM.	PROCESSING EARTH TRACKER INPUTS, GENERATING TMBS CMDS. BASED ON EARTH TRK. CENTROID ALGORITHMS, GENERATING ACTIVE FOCUS CMDS. BASED ON GRD. CMDS. RECEIVED VIA BEACON, OUTPUTTING DOWNLINK DATA TO LASER.	EARTH TRK.	EARTH TRK. OFF	AUTOMATIC GROUND CMD.
ALIGNMENT	PROCESSING ALIGNMENT CMDS. BASED ON SIGNALS RECEIVED ON DETECTOR FROM LASER WHILE PERFORMING EARTH TRK. OPERATIONS.	EARTH TRK.	EARTH TRK. OFF	GROUND CMD. GROUND CMD.

C-3

FIGURE 5

OPTRANSPAC MODE LOGIC

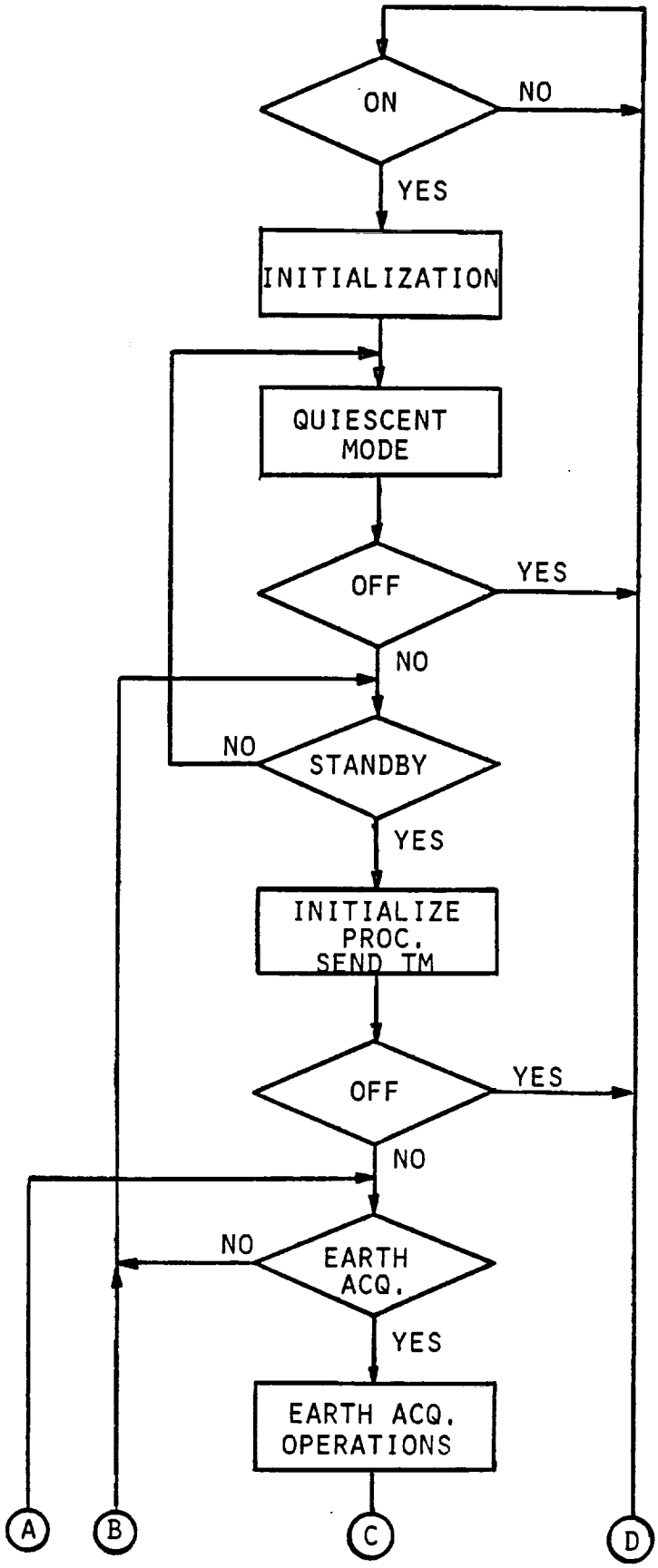

FIGURE 6
SHEET 1 OF 3

OPTRANSPAC MODE LOGIC
(CONTINUED)

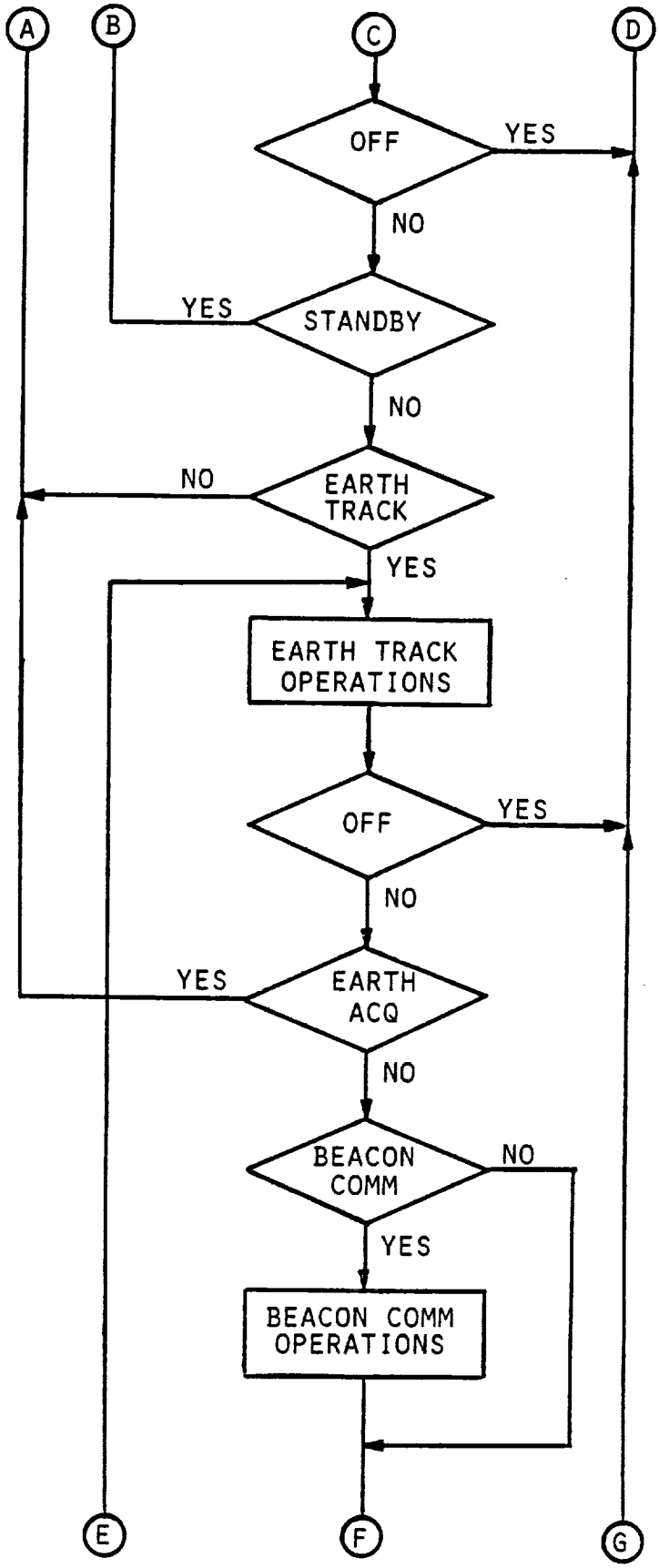

FIGURE 6
SHEET 2 OF 3

OPTRANSPAC MODE LOGIC
(CONTINUED)

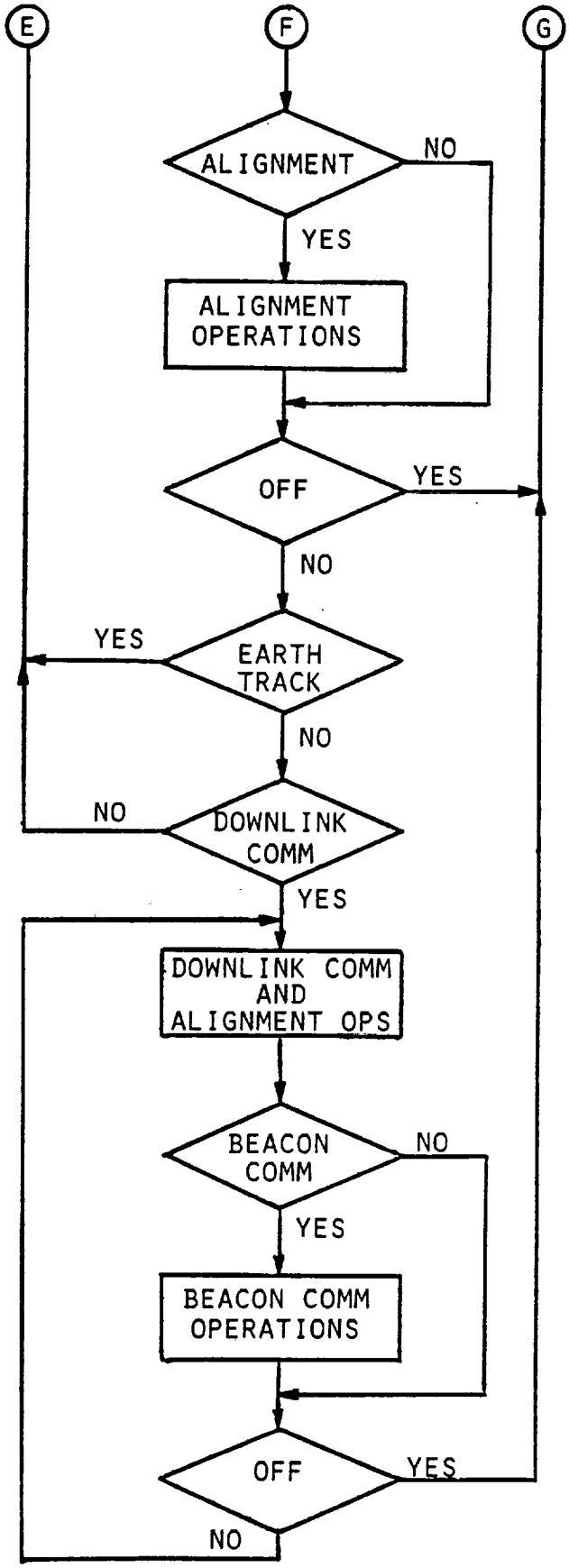

FIGURE 6
SHEET 3 OF 3

COMMUNICATION ELECTRONICS
FUNCTIONAL BLOCK DIAGRAM

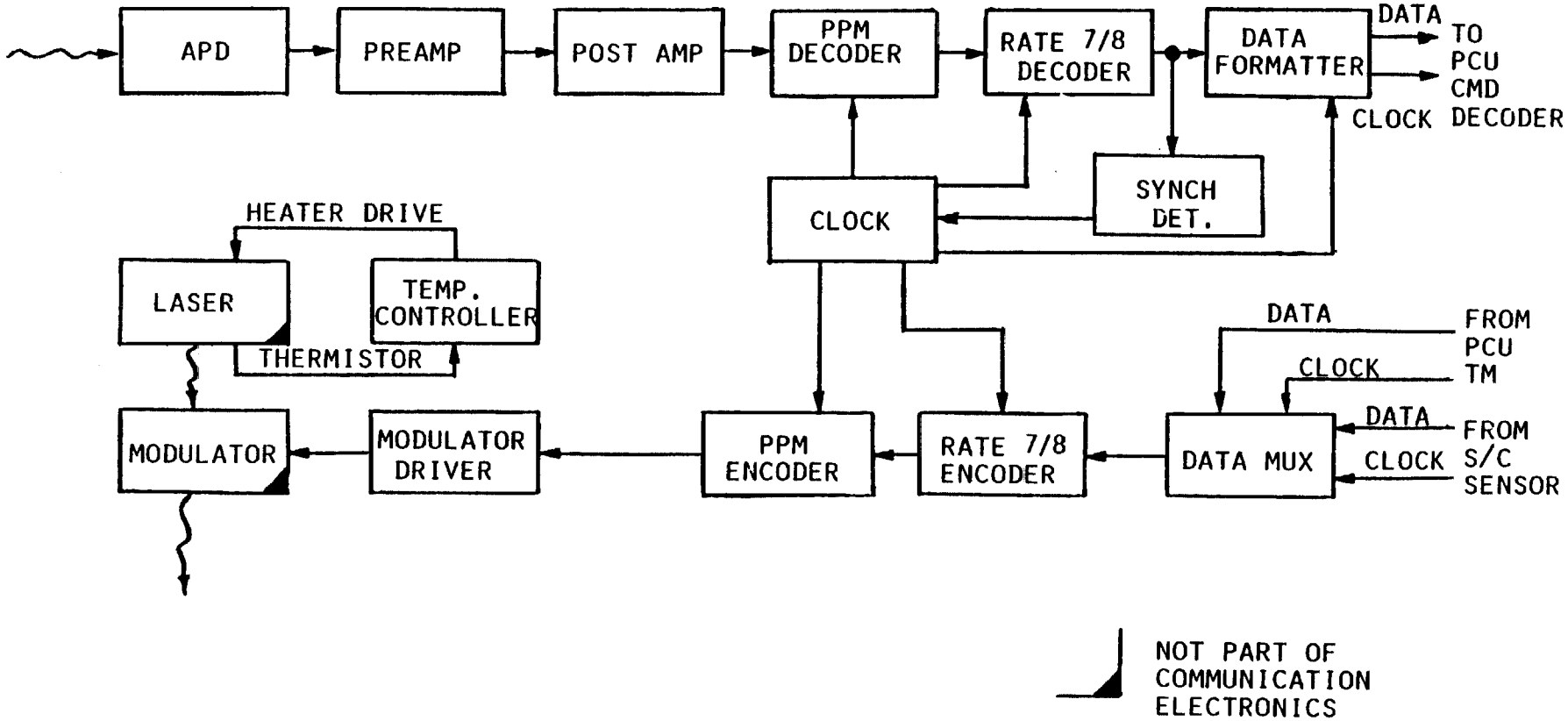

FIGURE 7

This signal is amplified and applied to a PPM decoder that operates on a "greatest of" principle to select the slot containing the signal pulse. The output of the decoder is a NRZ data stream containing rate 7/8 Reed-Solomon encoded data at 1142.86 bits/sec. This data is applied to a Reed-Solomon decoder which produces a 1000 bit/sec output. Finally, the 1000 bit/sec data is formatted to be identical to the command data received via the radio frequency command link. The output of the formatter is applied to a command decoder located within the Power Conditioner Unit.

2.2.2 Transmit Function - Transmit data consists of a fixed rate serial telemetry data stream from a telemetry formatter located in the Power Conditioner Unit or a serial data stream from the Spacecraft sensor. Spacecraft sensor data rates can be 10,000 bits/sec, 30,000 bits/sec or 100,000 bits/sec. Figure 8 illustrates the transmit data frame. Overhead is limited to less than 3%. When spacecraft sensor data is available for transmission, the telemetry data is not transmitted. The output of the data selector (either telemetry or sensor data) is rate 7/8 Reed-Solomon encoded and output to a PPM encoder. The Reed-Solomon encoder adds a coding bit to each input word resulting in the following output rates:

Input Rate	Output Rate
10,000 bits/sec	11,428.57 bits/sec
30,000 bits/sec	34,285.71 bits/sec
100,000 bits/sec	114,285.71 bits/sec

The output data from the Reed-Solomon encoder is applied to a PPM encoder that produces output symbol information at 1428.57, 4285.71, or 14,285.71 symbols/sec depending upon the sensor data rate. Symbols are encoded by outputting a pulse in one of 256 data slots following a fixed time interval that is referenced to the previous fixed time interval using an internal clock. The following are the timing requirements for the PPM encoder:

Slot Width: 100 nsec
Fixed Interval: $1/f_s$, where f_s is the transmitted symbol rate

The output from the PPM encoder is input to modulator driver circuitry. The circuitry converts the logic level input to signal levels required to operate the laser modulator located within the Laser Assembly.

2.3 POWER CONDITIONING (Reference Figure 9)

Primary power from the spacecraft's electrical system is conditioned to provide the required secondary power for the OPTRANSPAC equipment. The Power Conditioning Unit provides the conversion and regulator circuitry required to produce the following secondary outputs:

REPRESENTATIVE DATA FRAME
100 KBPS DOWNLINK

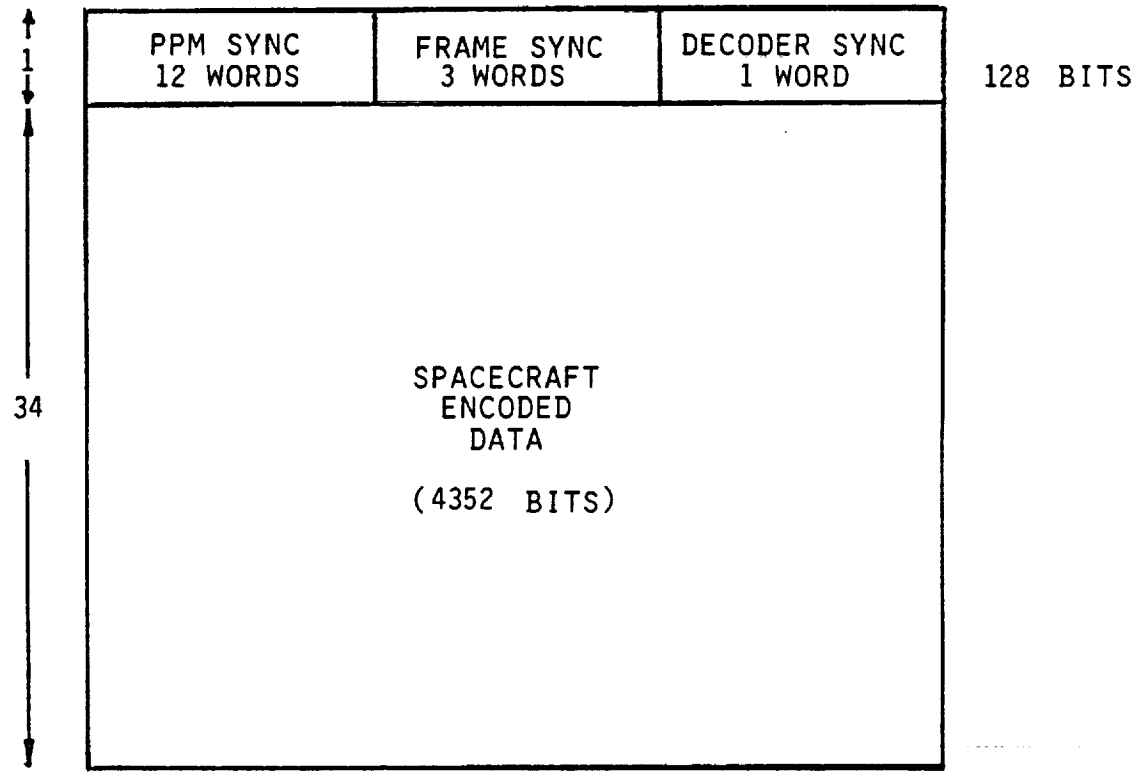

FRAME RATE 26.26/SEC
OVERHEAD PERCENTAGE ~ 2.9%

FIGURE 8

POWER CONDITIONER UNIT
FUNCTIONAL BLOCK DIAGRAM

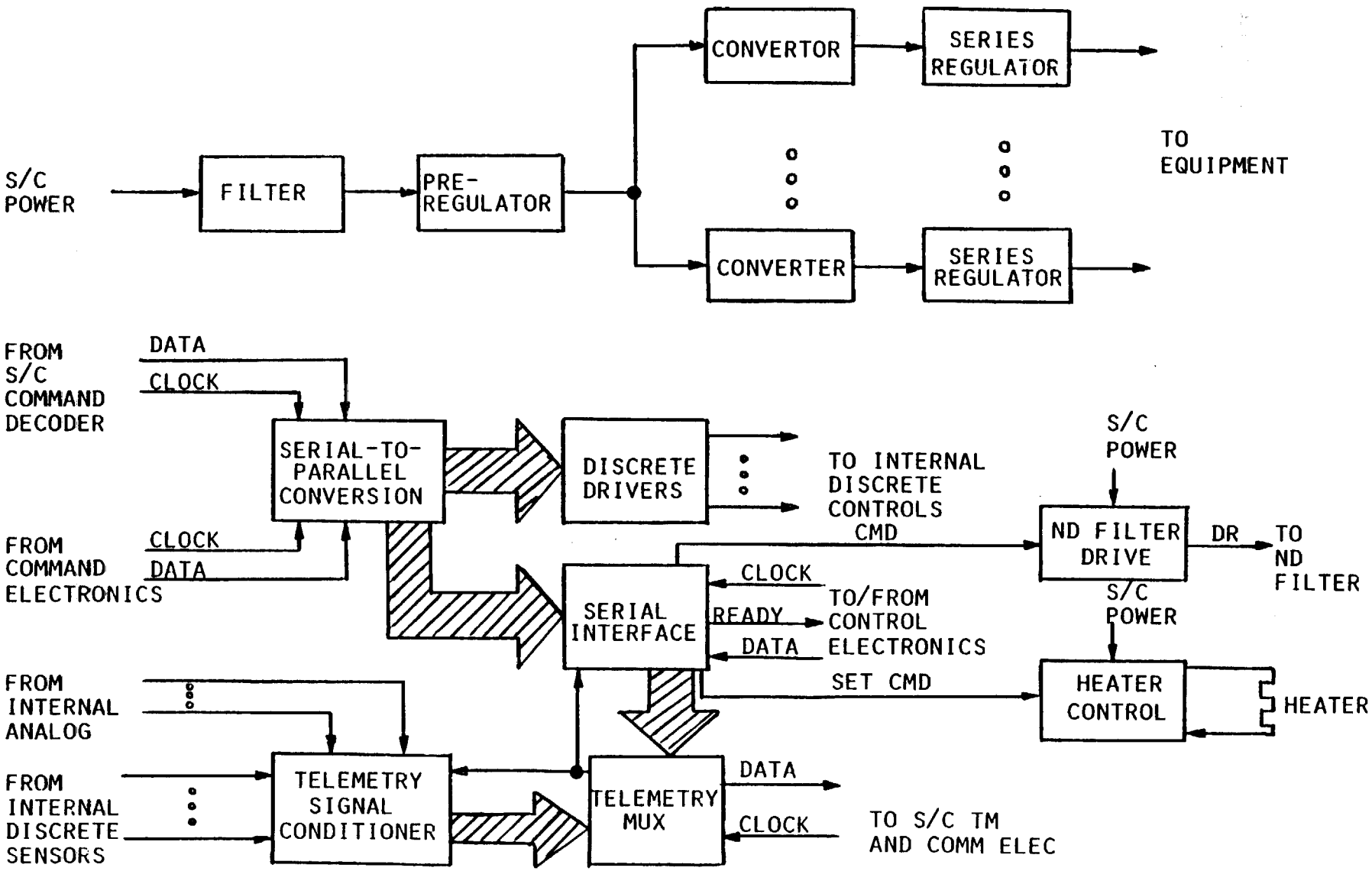

FIGURE 9

Level	Current	User
+ 5 Vdc	1.2 A	Earth Tracker
+ 5 Vdc	0.3 A	Control Electronics
+ 5 Vdc	0.2 A	Control Electronics
+ 5 Vdc	1.3 A	Control Electronics
+ 5 Vdc	0.6 A	Control Electronics
+ 5 Vdc	1.0 A	Comm. Electronics
+ 5 Vdc	0.5 A	Power Conditioning
+/- 15 Vdc	0.1 A	Earth Tracker
+/- 15 Vdc	0.013 A	Control Electronics
+/- 15 Vdc	0.11 A	Control Electronics & TMBS's
+/- 15 Vdc	0.05 A	Comm. Electronics
+/- 15 Vdc	0.01 A	Comm. Detector
+/- 15 Vdc	0.02 A	Power Conditioning
+ 28 Vdc	0.01 A	Power Conditioning
+ 28 Vdc	0.04 A	Comm. Electronics
+ 400 Vdc	250 μA	Comm. Detector

Figure 10 describes the converter implementation. Command and telemetry conversion circuitry is also located within the Power Conditioning Unit. Serial command data from the spacecraft's command decoder or the Communication Electronics is decoded. The output from this circuitry is provided to discrete drivers which control OPTRANSPAC redundancy switching mechanisms, the active focus, or power control relays. Serial magnitude commands are relayed to the Control Electronics via bi-directional serial interface circuitry located within the Power Conditioning Unit. This serial interface receives telemetry and heater control data from the Control Electronics. The telemetry from the Control Electronics as well as internal analog and discrete data is multiplexed to form a serial data output. This data is transmitted to the Earth station via the Communication Electronics or on the spacecraft radio frequency links. Circuitry required to condition internal analog and discrete telemetry parameters is provided within the Power Conditioning Unit. OPTRANSPAC heater drive circuitry is also located internal to this unit.

POWER CONVERTERS

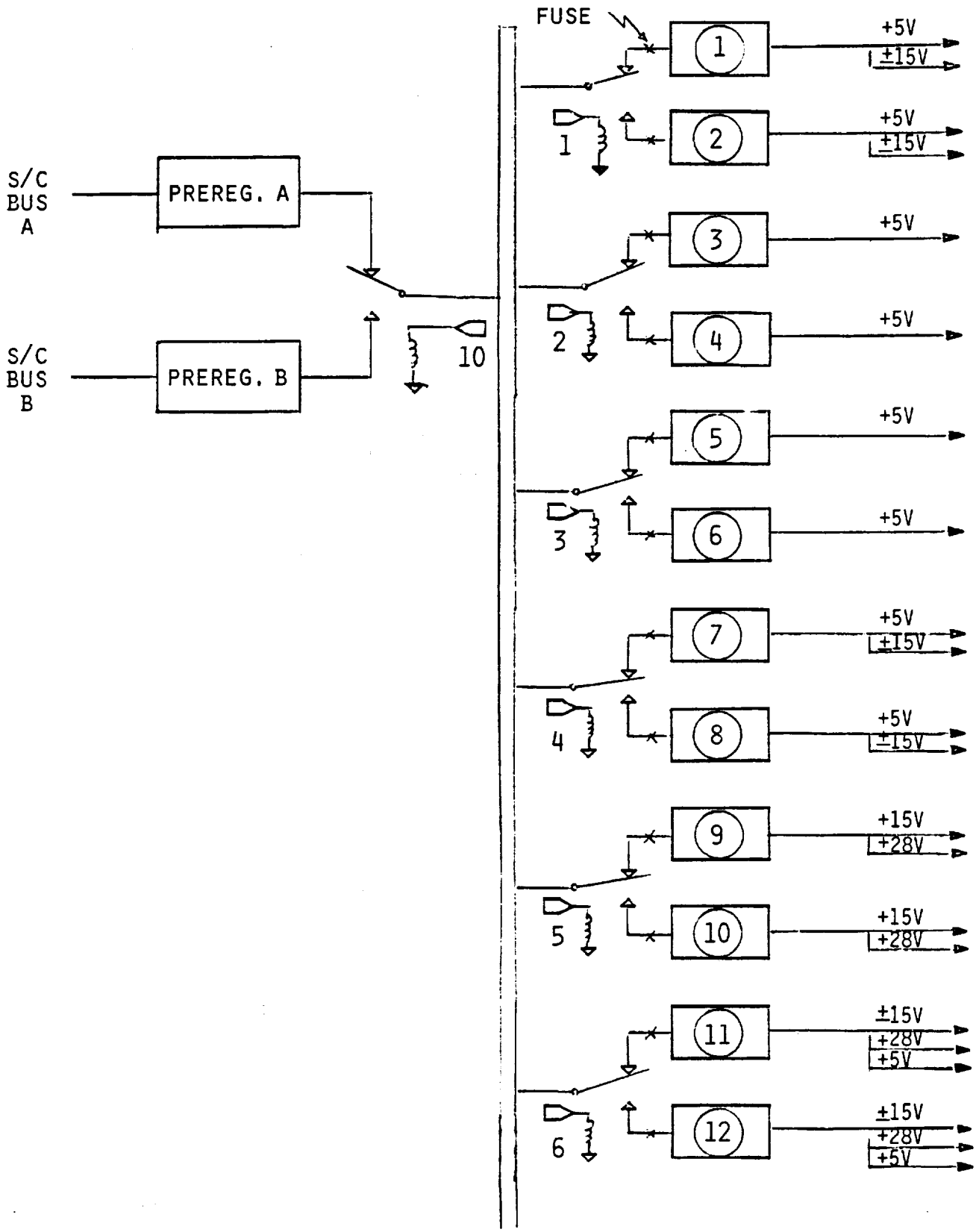

(CONTINUED ON NEXT PAGE)

FIGURE 10
PAGE 1 OF 3

POWER CONVERTERS
(CONTINUED)

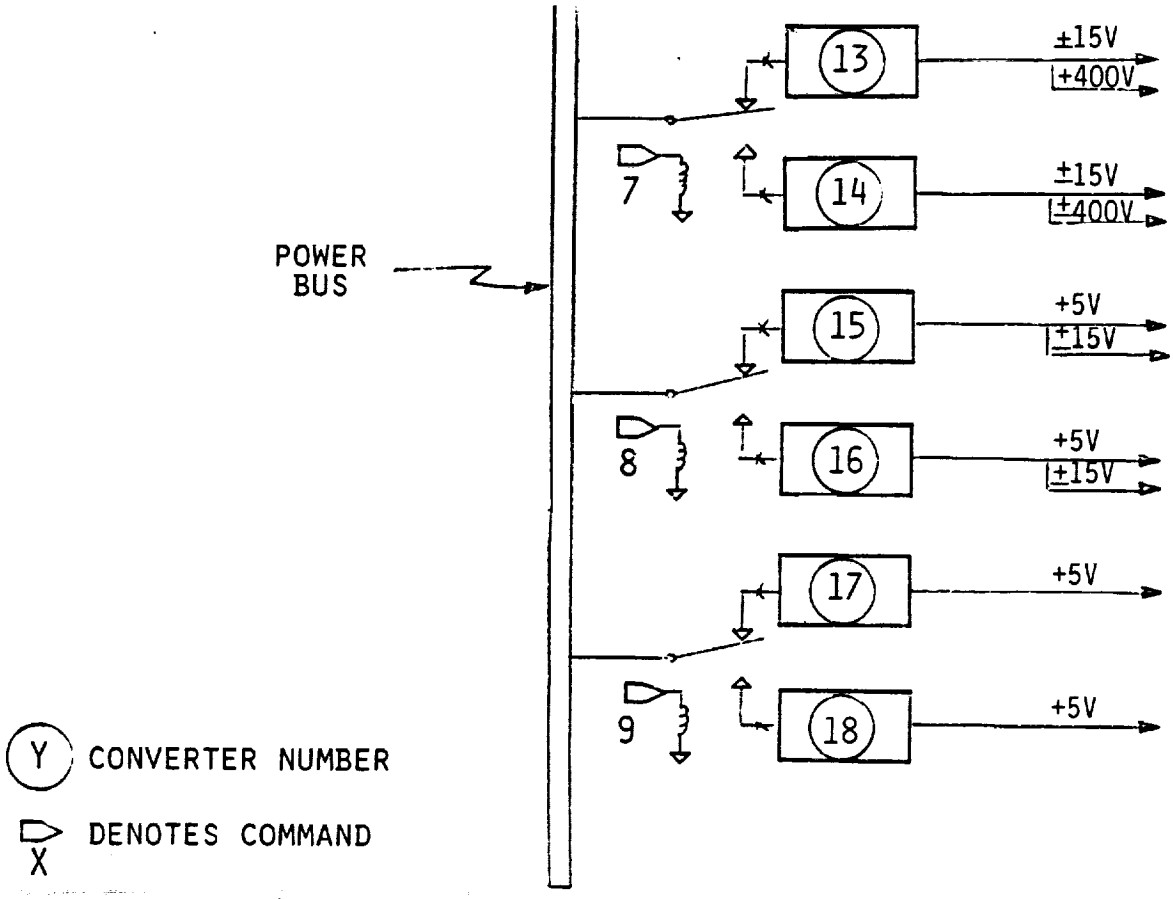

FIGURE 10
PAGE 2 OF 3

Figure 7 Continued

Power Converter Designations

1	A	Earth Tracker
2	B	
3	A	Earth Tracker Readout Elect.
4	B	
5	A	Serial Interface and ARS
6	B	
7	A	CPU
8	B	
9	A	TMBS and Drivers
10	B	
11	A	Comm. Electronics
12	B	
13	A	APD
14	B	
15	A	PCU Internal
16	B	
17	A	Memory
18	B	

FIGURE 10
PAGE 3 OF 3

3.0 REDUNDANCY

3.1 CHARACTERISTICS

Redundancy implementation shall be provided to eliminate single-point failures and provide the highest possible probability of success consistent with practical weight and complexity constraints. The following "ground rules" regarding cross-strapping of redundant elements have been established.

A. All cross-straps at source.
B. All cross-strap selection via power command in the PCU and digital serial magnitude commands for addressing the selected memory block or I/O port.
C. The Communication Electronics is block redundant with cross-strapping at the output to PCU Command Decoder and inputs (provided by source) from PCU TM and S/C Sensor.
D. The Power Conditioner Unit converters are dedicated to the load. There is no power converter output cross-strapping.

3.2 REDUNDANCY IMPLEMENTATION

All OPTRANSPAC electronics and mechanisms are redundant with the exception of the Command Focus Mechanism. Cross-strapping for selected functional circuit blocks is provided to minimize the probability of system failure.

3.2.1 Control Function - The elements of the function and the cross-straps provided are described in Figure 11. All elements of the function are cross-strapped to other redundant elements with the exception of the TMBS's. Cross-strapping of the drivers and TMBS's does not provide significant enhancement of system reliability since the reliability of the drivers and TMBS's is high (based on previous designs) compared to other elements. In addition, a simpler design for the TMBS drivers is possible.

3.2.2 Communications Function - The elements of the communication function and the cross-strapping provided are detailed in Figure 12. Cross-straps are not provided between the Communications Avalanche Photodiode and the preamplifier due to the low signal levels and noise sensitivity at this point. Similarly, design considerations are the principle reason for not cross-strapping the Communication Electronic - Laser interface.

3.2.3 Power Conditioning Function - Figure 13 details the elements and cross-strapping of the power conditioning function. Implementation of these cross-straps is accomplished by use of relays controlled via Earth station generated commands. Fuses (reference Figure 10) are provided at the input to each converter to prevent load or converter failure propagation to the redundant converter.

CONTROL ELECTRONICS
REDUNDANCY IMPLEMENTATION

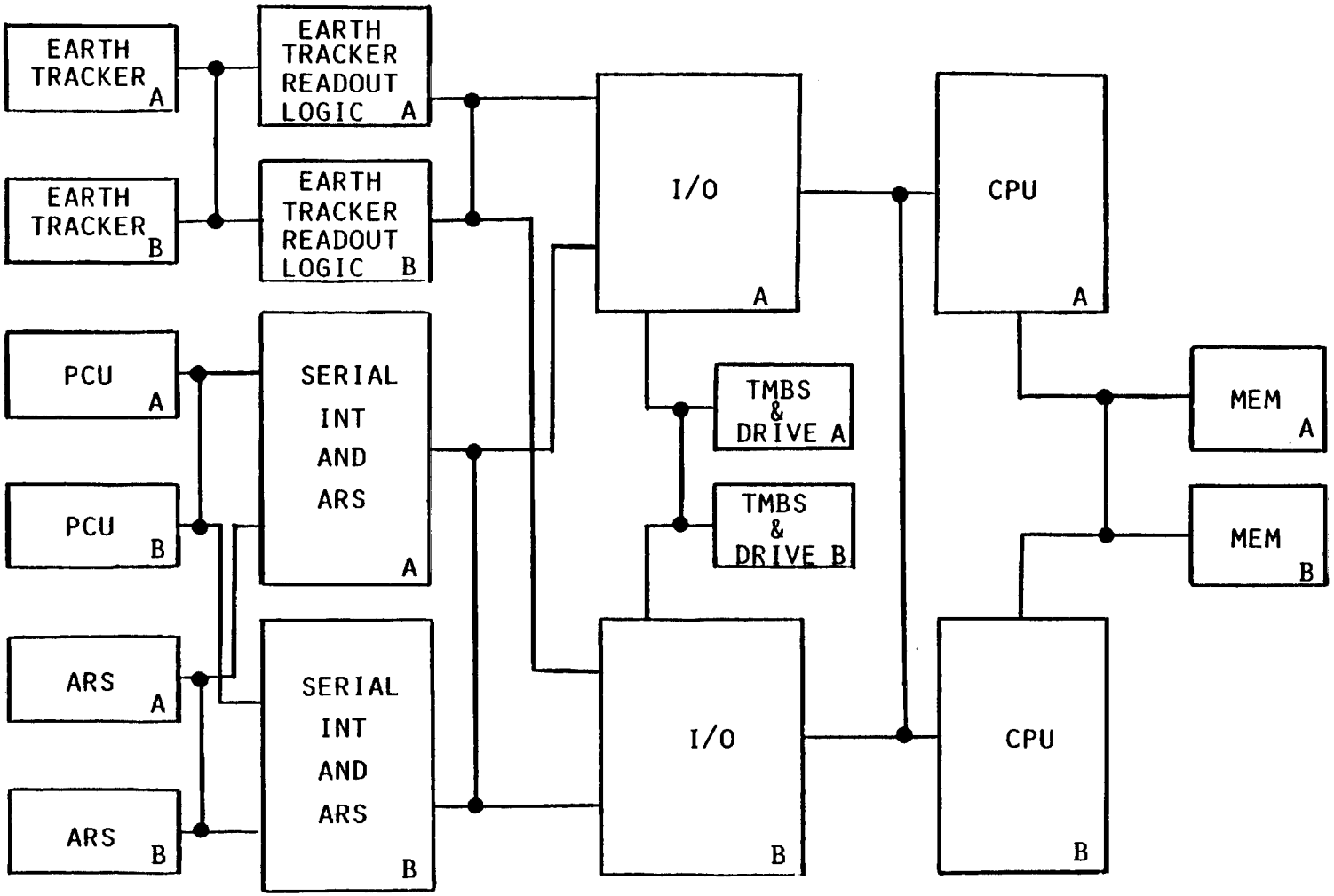

FIGURE 11

COMMUNICATION ELECTRONICS
REDUNDANCY IMPLEMENTATION

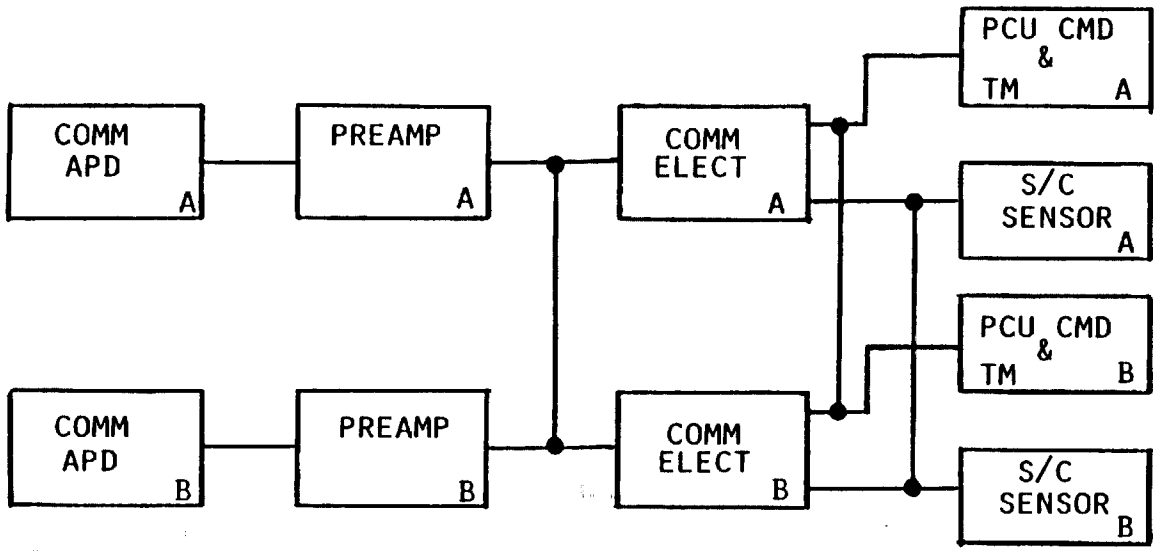

FIGURE 12

POWER CONDITIONER UNIT
REDUNDANCY IMPLEMENTATION

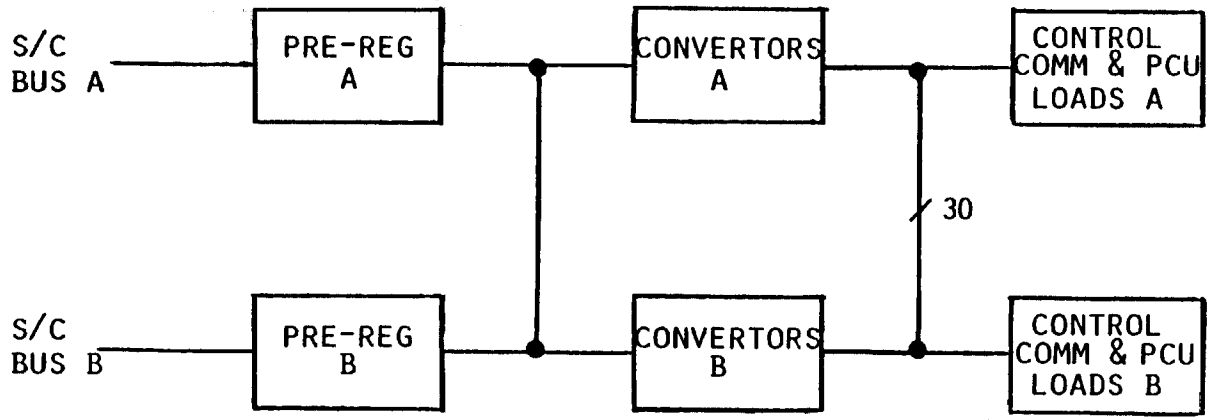

FIGURE 13

4.0 DESIGN IMPLEMENTATION

The OPTRANSPAC Electronics are housed in package assemblies having the following characteristics (estimated):

Assembly	Power Disc.	Weight	Length	Width	Height
Control Electronics	14.5 W	12.5 lb	9.0"	6.0"	6.0"
Communication Electronics	7.7 W	9.0 lb	7.0"	6.0"	6.0"
Power Conditioning Unit	17.1 W	19.5 lb	6.0"	8.0"	7.5"
Earth Tracker	4.6 W	4.5 lb	---	---	---
Comm. Detector	0.4 W	1.0 lb	---	---	---
TMBS's	1.4 W	(Included in Imaging Optics)			
Laser	4.0 W	(Included as Laser)			
Wire and Misc.	6.7 W				

4.1 CONTROL ELECTRONICS

The Control Electronics design is based on 14 ceramic and 2 polyimide circuit boards. Digital circuits in leadless chip carrier packages will be mounted on the ceramic circuit boards. The polyimide boards will be populated with analog integrated circuits and discrete components. Dimensions of all circuit boards is approximately 4.6" x 3.8". Both prime and redundant circuitry will be implemented on the 16 circuit boards.

4.2 COMMUNICATION ELECTRONICS

A total of 12 circuit boards are estimated for the redundant Communication Electronics. A pair of polyimide boards will be used for the analog integrated circuits and discrete components required. All other circuit boards will be populated with leadless chip carrier digital integrated circuit packages.

4.3 POWER CONDITIONING UNIT

The circuitry required for the converter, regulators, relays, and etc. will be implemented using a module concept. Each module will consist of two (prime and redundant) polyimide circuit boards housed in a frame. The dimensions of each module will be approximately 6" x 6" x 0.3". A total of 5 modules are required.

OPTRANSPAC ELECTRONICS

Control Electronics Circuit Boards

Qty*	Function	Power Required
2	CPU and Clock	2.0 W
2	Analog I/O	4.4 W
2	Memory	3.0 W
2	Serial Interface & ARS Logic	1.0 W
2	Discrete I/O	0.5 W
2	TMBS and Command Focus Drive	2.1 W
4	Earth Tracker Readout Logic	1.5 W
16		14.5 W

Communication Electronics Circuit Boards

Qty*	Function	Power Required
2	Post Amp. & PPM Decode	1.0 W
2	Rate 7/8 Decode & Sunc. Det.	1.0 W
2	Data Mux., Data Format., & Clock	1.0 W
2	Modulator Drivers	2.0 W
2	Temperature Controller	1.5 W
12		7.7 W

*Prime and redundant, only 1 board powered.

OPTRANSPAC ELECTRONICS

Power Conditioning Unit Power

Converter	Output Current in Amps +28 Vdc	+/-15 Vdc	+5 Vdc	Bias	Total Power
Earth Tracker		0.1	0.32		4.6 W
Earth Tracker Readout			0.3		1.5 W
Serial Int. & ARS			0.2		1.0 W
CPU and Clock			0.4		2.0 W
I/O (analog & discrete)		0.013	0.9		4.9 W
Memory			0.6		3.0 W
TMBS, TMBS and CMD. Focus Dr.	0.01	0.11			4.1 W
Comm. Elect.	0.04	0.05	1.0		7.7 W
APD		0.01		250 µA	0.4 W
Misc/Wire					6.7 W
Laser					4.0 W
TOTAL					39.9 W
Converter Losses (based on 70% eff.)					17.1 W

APPENDIX C-2

OPTRANSPAC

DESIGN NOTE

TITLE:	NUMBER 2
OPTICAL SYSTEM DESIGN	REVISION A
	DATE 19 AUGUST 1985
	TOTAL SHEETS

SUMMARY:

The optical system performance requirements of the OPTRANSPAC system are summarized. An optical system design is developed from functional requirements through the thin lens design stage. Component performance requirements and packaging/envelope requirements are discussed.

PREPARED BY: T. C. Willis

T. C. WILLIS
OPTICAL SYSTEM ENGINEER

CHECKED BY: S. G. Lambert

S. G. LAMBERT
OPTRANSPAC ENGINEERING MANAGER

APPROVED BY: J. A. Pautler

J. A. PAUTLER
OPTRANSPAC PROGRAM MANAGER

DISTRIBUTION:

J. P. Carter, E. C. Clarke, L. M. Gnojewski, S. G. Lambert, H. J. Mingo, J. A. Pautler, M. Ross, J. D. Zino

1.0 OPTICAL SYSTEM REQUIREMENTS

The basic configuration of the OPTRANSPAC optical system is defined in Figure 1. OPTRANSPAC optical system performance requirements are summarized in Table 1. The receiver aperture size and path transmissions are governed by the range losses out at the maximum range of 10 AU. The fields of view are selected for background rejection and to support the chosen acquisition sequence. The angular steering range is governed by the limitations on the pointing ability of the spacecraft attitude control system. The wavelength range is set by the need to track the Earth in broadband visible light (reflected sunlight) and the need to monitor the frequency doubled Nd:YAG laser transmitter.

The optical system consists of two basic subassemblies: a telescope and an imaging optics assembly (or IOA). The optical system performance of Table 1 can be flowed down to the individual subassemblies. This is illustrated in Table 2.

2.0 TELESCOPE SELECTION

The performance requirements of the telescope flow down from the system level requirements for OPTRANSPAC. These telescope requirements are defined in Table 2.

To meet these requirements a mirror based (reflective) telescope is the system of choice. An 11" aperture refractor would require several lens elements to meet image quality requirements and would be heavy as a result. A refractive telescope would also be prone to thermal gradients, which would adversely affect the transmitted wavefront by the temperature induced change of the glass refractive indices.

The wide variety of reflective telescope design forms is illustrated in Figure 2. The image quality requirements over the field of view limit the choice of telescopes. The Newtonian form is unacceptable over this field due to the coma inherent in the base paraboloid mirror. The Gregorian form is too long

and bulky. The Maksoutoff arrangement tends to be either too long (with a thin corrector plate) or too heavy. The corrector plate thickness must increase as the telescope length is reduced to maintain the required state of correction. The Cassegrain design form, in one of its many variants, offers the best approach to meeting the diffraction limited performance requirement over the field of view with a compact, light weight, stable package.

The Classical Cassegrain consists of a paraboloid primary mirror with a hyperboloid secondary mirror. This arrangement can cover a larger field of view than the single paraboloid mirror with substantially better imaging performance. It will however not be able to cover the full 5 mrad field with the required near diffraction limited performance.

There are several variants of the Classical Cassegrain which offer improved image quality over the field at the cost of an increase in design complexity. One of these variants is the Ritchey Chretien. This configuration consists of aspheric primary and secondary mirrors whose zonal curvatures are slightly weakened with respect to the paraboloid/hyperboloid mirrors of the Classical Cassegrain to reduce coma over the field. Another variant is the Schmidt-Cassegrain which dispenses with the aspheric primary mirror and incorporates a full aperture aspherized refractive plate to correct the resulting spherical aberration. This plate must cover the full aperture and is prone to thermal gradients perturbing wavefront quality. Another variant on the Classical Cassegrain (and on the Ritchey Chretien) is to incorporate small refractive correcting elements in the converging beam after the secondary. This allows additional aberration correction. It is this final variant that offers the best approach to meeting the rigorous image quality requirement of $\lambda/20$ RMS over the relatively large 5 mrad field of view.

In the OPTRANSPAC telescope design the primary mirror is an f/1.75 hyperboloid (only slightly changed from a paraboloid). A hyperboloid secondary mirror, operating at a magnification of 5.7, produces a final f/# of ≈f/10 for the telescope. The refractive correctors are of zero net power and affect the

final f/# very little. A field lens of ≈600 mm focal length relays the system aperture stop (at the primary mirror) into the rest of the optical system. A thick lens design of this telescope was not completed during the study. However, a very similar telescope designed on a different program was available for study. This telescope design, incorporating small refractive correcting elements, is shown in Figure 3. A detailed design prescription is listed in Table 3. Geometric raytracing of this design both on axis and at full field (Figure 4) confirms that this design fulfills the OPTRANSPAC image quality requirements over the field of view. Diffraction analysis indicates this telescope's design wavefront quality is ≈ $\lambda/30$ RMS at a wavelength of λ = 532 nm.

3.0 OPTICAL SCHEMATIC

Following the definition of the optical system performance requirements and selection of a telescope type, the optical paths need to be defined. The optical schematic (Figure 5) shows the general arrangement of the Cassegrain telescope and the imaging optics that interfaces the telescope with the system's transmitter laser source and various detectors. Table 4 lists the components in the optical schematic.

Figure 6 breaks down the schematic into the individual optical paths. The telescope section serves as the common antenna for both transmit and receive channels. The prime and redundant common optical path are also shared by the transmit and receive channels. These paths incorporate the fine beam steering function. The chosen beam steering mechanism is a torque motor beam steerer (TMBS). Selection between the prime and redundant common path is accomplished by means of rotary mirror mechanisms. The final component in the common optical path is the transmit/receive beamsplitter. This is a dichroic beamsplitter set to transmit 532 nm light while reflecting the 1064 nm uplink light and broadband visible light (earth tracking).

The transmit path consists of prime and redundant lasers with a "pop mirror" select mechanism, a focal beam expanding optics, and a commandable focus.

The receive path is subdivided into a communication and a tracking section. The communication section consists of prime and redundant avalanche photodiodes selected by the "pop mirror" mechanism, 25 Å band pass filters centered on the 1064 nm uplink for background rejection, and a dichroic beamsplitter to reflect 1064 nm light and pass the shorter wavelengths used in tracking. The tracking section is somewhat more complex. The broadband solar energy reflected off the Earth is used for tracking. Prime and redundant charge transfer detectors (CTD) selected via "pop mirrors" are used to track the Earth and hence the low Earth orbit terminal. The point ahead function is accomplished via offset tracking. A small amount of the transmit 532 nm light is continuously leaked by the transmit/receive beamsplitter into the receive/tracking path. A 532 nm bandpass filter reflects the broadband light and admits the 532 nm light to a deviating prism which steers this transmit light to an offset point on the CTD.

4.0 FIRST ORDER LAYOUT OF OPTICAL PATHS

In design of the telescope and imaging optics for a spaceborne system one must keep the size and number of elements used to the minimum necessary to perform all system functions within the required system performance levels. This maximizes system optical transmission while minimizing system size, weight, and procurement cost. In diffraction limited optical systems such as this, one is forced to multiple elements less components with moderately slow optical speed to meet image quality requirements. Field of view and spectral range requirements further complicate the lens components. This exacts a penalty on optics transmission, optical system envelope and optical system weight.

4.1 FIRST ORDER LAYOUT OF TELESCOPE - The elements and their first orders properties for the telescope section are given in Table 5. A thin lens ray trace through this section both on axis and at full field is shown in Figure 7. This section is designed to be afocal. It maps the 0.5" (12.7 mm) diameter axial bundle of the imaging optics paths (i.e. common path) to the 11" (279.4 mm) diameter of the primary mirror. The system aperture stop and

entrance pupil are at the primary mirror. This pupil is relayed by the telescope field lens to a convenient location within 30.5 mm of the first collimator lens in the common path of the imaging optics.

The Cassegrain telescope optics are designed to produce an f/10 output cone. This allows for a compact package whose optical speed is still slow enough to ensure both good image quality and readily manufacturable components. The f/1.75 concave hyperboloid primary and f/2.0 convex hyperboloid secondary mirror are well within the state of the art for aspheric fabrication.

4.2 FIRST ORDER LAYOUT OF COMMON PATH (PRIME/REDUNDANT) OPTICS - In the common path throughout the imaging optics it is desirable to use a few basic lens grouping in a repetitive way to simplify the design and procurement of the optics. Such repetitive lens groupings must relay the telescope pupil through the imaging optics with minimal vignetting. This requires that the sections of collimated space used for locating TMBS mirrors or beamsplitters be rather short to minimize the need for large (> 50 mm diameter) optics. This is because the local field of view covered by the imaging optics components is 88 mrad ($\pm$ 2.5°), a factor of 18 times the telescope field. A typical grouping of collimator - field lens - collimator ("CFC Group") is shown in Figure 8. The two collimators symmetrically flanking the field lens work at f/5. This f/# was selected as the best compromise between the two extremes of fast f/#, compact, many element lens components and slow f/#, space wasting, few element lens components.

The elements and first order properties for the prime and redundant common path optics are given in Table 6. A thin lens ray trace on axis and at full field through the common path are given in Figure 9.

4.3 FIRST ORDER LAYOUT OF TRANSMIT PATH - The optics in the transmit path are considerably simplified by the fact that they are handling monochromatic (532 nm) light which is of small divergence and remains on axis (all steering of the transmit beam is accomplished in the common optics path). The prime and redundant lasers are selected by a "pop mirror" mechanism. The laser light passes through an afocal relay. One of the components of this relay can be shifted axially to introduce specific amounts of focus error to partially

compensate for wavefront errors introduced by component shifts. These component alignment shifts can arise from the forces during launch, from stress relief of structural parts over time, or from long term temperature changes during the course of the mission. In a diffraction limited system even such minor variations can have a serious effect on performance. After leaving the focus mechanism relay the beam enters an afocal expander to increase the beam to 12.7 mm diameter for entry into the common optics path.

Table 7 lists the transmit path optics properties. Figure 10 shows a ray trace of the emerging transmit beam.

4.4 FIRST ORDER LAYOUT OF RECEIVE COMMUNICATION PATH - The 1064 nm uplink from the terminal in low Earth orbit is collected by the telescope, and relayed through the common path optics, reflected by the dichroic transmit/receive beam splitter, relayed by a CFC lens group, reflected by the dichroic communication/tracking beamsplitter, and filtered by a 25 Å bandpass filter. The prime or redundant detector are selected by a "pop mirror" mechanism. The elements and first order properties for the receive path from the transmit/receive beamsplitter through the communication detectors are given in Table 8. On and off axis ray traces are shown in Figure 11. Note that the avalanche photodiodes are operated in a slightly defocussed position to keep the spot size large enough that the variation in detector responsivity over its surface has a negligible impact on communication link margin.

4.5 FIRST ORDER LAYOUT OF RECEIVE TRACKING PATH - To accommodate the tracking and point ahead functions on the same detector, an offset is introduced between the broadband reflected sunlight from earth and the 532 nm transmit spot retroreflected from the transmit beam. A dichroic beamsplitter separates the broadband and 532 nm light into two separate channels. A wedge prism deviates the 532 nm light prior to entering the tracking detector lens. The broadband light enters the tracking detector lens undeviated yielding the angular offset required. Note that the tracking detector lens axis is decentered with respect to the input receiver axis to accommodate the two spatially separated Earth track and point-ahead offset track channels. The elements and first order properties of the receive path from the communication/tracking

beamsplitter through the tracking detector are shown in Table 9. On and off axis ray traces for the broadband visible light are shown in Figure 12. On and off axis ray traces for the 532 nm light are shown in Figure 13.

5.0 MECHANICAL LAYOUT, PACKAGING, AND ENVELOPE

Using the component distances and sizes given in Secton 4.0 the optical paths can be layed out to determine the envelope of the resulting package. Figure 14 illustrates an isometric view of this layout. Figure 15 shows the same layout in orthographic projection. The optics are divided into two planar sections above and below a mounting baseplate. To this same baseplate the 11" telescope is attached in a cantilevered configuration. When baseplate, optics covers and electronics boxes are included a more complete picture of the system envelope emerges (Figure 16). The entire system fits within a 2'x2'x4' envelope yet offers uncrowded, ready access to the optical paths for alignment, adjustment and performance characterization.

6.0 TRANSMISSION BUDGETING

A summary of overall path transmission is given in Table 10. A detailed breakdown on the contributers to transmission in each path is included in this Section. These numbers are for beginning of life. The individual component performance estimates contained herein are readily manufacturable specification values and are based on the measured performance of optical components built and used in Lasercom systems over the past eight years. The component substrates and coating materials are restricted to materials with demonstrated radiation resistance. Radiation resistance test indicate element transmittance degradation is typically small ($\approx$ 0.2% per element at $\approx 10^5$ Rad (Si)). Equivalent end of life transmissions based on this are also shown in Table 10.

6.1 TELESCOPE PATH

6.1.1 TRANSMIT (532 nm) USAGE

Telescope Collimator (4 Element) - - $T_1 = (0.998)^8$

Field Lens/Refractive Corrector Lens Set (3 Element) - - $T_2 = (0.998)^6$

Secondary Mirror/Primary - - $T_3 = (0.98)^2$

Telescope Transmission At 532 nm = $T_1 T_2 T_3 = 0.93$

6.1.2 RECEIVE (1064 nm) USAGE

Telescope Transmission at 1064 nm ≈ Telescope Transmission at 532 nm

= 0.93

6.1.3 RECEIVE (BROADBAND 400 nm - 100 nm) USAGE

Unlike the monochromatic performance numbers in Section 6.1.1 and 6.1.2, the antireflection coating performance will be substantially poorer over the broadband visible and near infrared band of reflected sunlight. The same will be true over the blue-green end of the spectrum for the high reflectance coatings on telescope primary and secondary mirrors. This is due to the inherent limitations in multilayer interference coatings which can only function at their maximum performance over spectral bandwidths much less than the required 700 nm.

Telescope Collimator (4 Element) - - $T_1 = (0.99)^8$

Field Lens/Refractive Corrector Lens Set (3 Element) - - $T_2 = (0.99)^6$

Secondary Mirror/Primary Mirror - - $T_3 = (0.97)^2$

Telescope Transmission (400-1100 nm) = $T_1 T_2 T_3 = 0.82$

6.2 COMMON (PRIME/REDUNDANT) PATH

6.2.1 TRANSMIT (532 nm) USAGE

Transmission of Basic Collimator Field Lens - Collimator Group on "CFC" Group (Consisting of 9 Elements) = $(0.998)^{18}$ = 0.965 = T_{cfc}

Reflectance of Fold Mirror Or TMBS Mirror = (0.98) = Rm

Transmittance of Dichroic At 532 nm = (0.98) = T_d

The Common Path (Prime or Redundant) consists of three CFC groups, two prime/redundant select mechanism mirrors, two TMBS mirrors, and two passive fold mirrors. The resulting transmission is given by

$$T \text{ of Common Path at 532 nm} = (T_{cfc})^3 (Rm)^4 T_d$$

$$= 0.81$$

6.22 RECEIVE (1064 nm) USAGE

Common Path performance at 1064 nm is similar to that at 532 nm except for the dichroic transmit/receive performance.

R_D = Dichroic Reflectance at 1064 nm = 0.95

So, we have

$$T \text{ of Common Path at 1064 nm} = (T_{cfc})^3 (RM)^4 R_D$$

$$= (0.965)^3 (0.98)^4 (0.95)$$

$$= 0.79$$

6.2.3 RECEIVE (BROADBAND VISIBLE) USAGE

Broadband Transmission of Basic CFC Group (9 Elements) = $(0.99)^{18}$
= 0.83 = T_{CFC}

Broadband Reflectance of Fold Mirror or TMBS = (0.97) = Rm

Broadband Reflectance of Dichroic = (0.90) = R_D

The resulting Common Path broadband transmission is given by

$$T \text{ Common Path Broadband} = (0.83)^3 (0.97)^4 (0.90)$$
$$= 0.46$$

6.3 TRANSMIT PATH

6.3.1 TRANSMIT (532 nm ONLY) USAGE

Transmission of Focus Compensator Group (4 Elements) = $(0.998)^8$ = 0.984
= T_{FC}

Transmission of Beam Expander (4 Elements) = $(0.998)^8$ = 0.984 = T_{BE}

Transmission of Transmit Path at 532 nm = T_{FC} T_{BE} = 0.97

6.4 RECEIVE COMMUNICATION PATH

6.4.1 RECEIVE COMMUNICATION (1064 nm ONLY) USAGE

Transmission of CFC Group at 1064 nm = (0.965) = T_{CFC}

Reflectance of Passive Fold Mirror = (0.98) = R_M

Reflectance of Communication/Track Dichroic = (0.95) = R_D

Bandpass Filter Tranmsmittance = (0.70) = T_{BPF}

Detector Lens Transmittance (3 Element) = $(0.998)^6$ = (0.988) = T_{DL}

Transmission of Receive Communicaton Path at 1064 nm
= $T_{CFC}\ R_M\ R_D\ T_{BPF}\ T_{DL}$ = (0.62)

6.5 RECEIVE TRACKING PATH

6.5.1 BROADBAND VISIBLE USAGE

CFC Group Transmission = $(0.99)^{18}$ = 0.83 = T_{CFC}

Passive Fold Mirror Reflectance = (0.97) = RM

Dichroic Transmittance = (0.90) = T_D

Variable Attenuator Base Transmittance = $(0.99)^2$ = (0.98) = T_{VA}

532 nm Bandpass Filter Reflectance = (0.90) = R_{BPF}

Tracking Lens Transmittance (3 Element) = $(0.99)^6$ = (0.94) = T_{TL}

Total Transmission In Broadband Visible Light For Tracking
= $(T_{CFC}\ (R_M)^2\ (T_D)\ (T_{VA})\ (R_{BPF})\ (T_{TL})$
= 0.59

6.5.2. TRANSMIT (532 nm) USAGE FOR OFFSET TRACKING

Reference Transmit Path Trasmittance At 532 nm
= (0.97) = T_{TP}

"Transmittance" of Xmit/Receive Dichroic (Leakage to Corner Cube and Retransmission into Tracking Path) = (0.005) (0.98) - 0.00490 = T_{DPA}

Transmittance of CFC Group at 532 nm = (0.965) = T_{CFC}
Reflectance of Fold Mirror = (0.98) = RM

Transmittance of Tracking/Comm Dichroic Beamsplitter = 0.98 = T_D

Variable Attenuator Transmittance = $(0.998)^2$ = T_{VA}

Band Filter Transmittace = (0.70) = T_{BPF}

Wedge Transmittance = $(0.998)^2$ = (0.996) = T_W

Tracking Lens Transmittance (3 Element) = $(0.998)^6$ = (0.988) = T_{TL}

Total Transmission For 532 nm Offset Tracking

$$= (T_{TP})\ (T_{DPA})\ T_{CFC})\ (R_M)(\ T_D)\ (T_{VA})\ (T_{BPF})\ (T_W)\ (T_{TL})$$
$$= 0.0030$$

7.0 IMAGE QUALITY AND WAVEFRONT BUDGETING

The most critical requirement on image quality for the OPTRTANSPAC system is that for the transmit path. In order to meet link margin requirements at the 10 AU maximum range a near diffraction limited wavefront needs to be radiated from the transmitter. Both telescope and imaging optics are each individually required to maintain the transmiter wavefront to $\leq \lambda/20$ RMS (λ = 532 nm). The total system performance resulting from combined telescope and imaging optics will then be $\approx\lambda/14.1$ RMS.

For the telescope to maintain $\lambda/20$ RMS what is required of the individual optical surfaces within the telescope? Recall that the total RMS wavefront error of a system is given by the root sum square of the individual contributors:

$$W_T = \sqrt{\sum_{i=1}^{N} W_i^2}$$

For each individual refracting surface the RMS wavefront error contributor is given by:

$$Wi,\ Refracting = (N_2 - N_1)\ E_{RMS}$$

where $N_2 - N_1$ = index difference across refracting surface
≃ 0.5 for "air" spaced elements

and E_{RMS} = RMS surface error specified for surface (in waves)

For each individual reflecting surface the RMS wavefront error contributor is given by:

$$W_i, \text{ Reflecting} = \frac{2\ E_{rms}}{\cos\ \theta}$$

where E_{RMS} = RMS surface error specified for surface (in waves)
θ = incidence angle on mirror

It can be seen from these two expressions that the contributions to wavefront error from mirrors are far larger than for lens elements specified to the same amount of figure error. Strain free mounting of the optics is an important requirement on the mechanical packaging of the system, particularly with regard to mirrors.

In the telescope part of the system there are two mirrors (primary and secondary) at near normal incidence, six refractive elements located away from the telescope focal plane (the 4 element telescope collimator and the two element refractive corrector) and one lens in or very near the focal plane (telescope field lens). The impact of the field lens on transmit wavefront error can be ignored due to the very small section of the clear aperture actually used. This section has figure errors far smaller than the value specified over the entire clear aperture. In the root sum square process producing the total RMS wavefront error of the system this very small contributor is swamped by the

much larger contributors from the collimator lenses and mirrors. In the imaging optics paths that carry the transmit beam to the telescrope there are four mirrors at 45° incidance, and 33 lens elements (not including 3 single element field lenses).

If we designate E = alloted RMS surface error then we have

$$W_{rms,Total} = E\sqrt{M_o \cdot 2 + M_{45} \cdot 2\sqrt{2} + L}$$

where Mo = # of mirrors at near normal incidence
= 2 for telescope and imaging optics together
M_{45} = # of mirrors at 45° incidence
= 4 for telescope and imaging optics together
L = # of lens elements
= 39 for telescope and imaging optics together

Yielding W_{RMS}, total = (7.37) E.

To meet a requirement of W_{RMS}, total $\simeq \lambda/14.1$ suggests that surfaces would need to be specified to above $\lambda/100$ RMS (i.e. $\simeq\lambda/20$ Peak-to-Valley). This requirement is within the state of the art for today's optical fabrication technology. Performance like this has been successfully demonstrated on the Laser Crosslink program. The fabrication and testing of surfaces to this quality level is considerably more labor intensive (and therefore costly) than for the more commonly encountered $\lambda/4$ or $\lambda/8$ peak-to-valley surfaces.

The above analysis does not address the other potential sources of wavefront error. These other sources include glass inhomogeneity, thermal gradients over optical components, mounting stresses, misalignments and residual uncorrected design aberrations.

Glass inhomogeneity effects are controlled by using only optical glasses available in the better homogeneity grades. Fused silica and the radiation resistant (i.e, cerium doped glasses) are available in these better homogeneity grades for the small ($\leq$ 60 mm) lenses used in the OPTRANSPAC optical system. In fact most of the lenses are < 25 mm in diameter. Homogeneity for the large telescope mirrors is inconsequential since the light never transmits through them. This is one benefit of the reflective telescope over a refractive design.

Assessment of the effects of thermal gradients on the optics is not possible without a representative thermal model of the system. Typically, imaging optics subsystems can be kept at a fairly constant temperature. this is accomplished passively by the thermally conductive (typically aluminum) box enclosure. This tends to evenly distribute the heat throughout the sub-system. If necessary one can also emplace an active heater and insulation over the imaging optics baseplate to aid the process (at the cost of the power needed to run and control the heater). Imaging optics wavefront performance can be degraded by the heat generated internally by mechanisms or electronics boxes. This can be kept under control by ensuring an adequate heat flow out of these source locations coupled with insulation of critical components from the heat loading. The OPTRANSPAC imaging optics are inherently insensitive to thermally or structurally induced misalignments of the transmit and receive paths due to the basic optical design which allows continuous pointing readjustment based on offset tracking information.

Typically, telescope optics are more often affected by thermal gradients than are imaging optics. The large aperture optics in telescopes can have far larger temperature differences over their clear apertures than one would find over a typical 25 mm diameter imaging optics lens cell. This can perturb the figure of the mirror surface and degrade the transmitted wavefront. Passive thermal control is not always effective since the telescope faces directly out into space (there must be a hole in any thermal shrouding to allow the transmitted and received beams to pass). The telescope primary to secondary mirror alignment is generally critical to the maintenance of a good transmit wavefront. Only slight (say 3 μm) motions can severely degrade the image quality of a near diffraction limited system. This can happen from very small

thermal gradients even when the telescope structure is made from low expansion materials such as Invar. If passive thermal control means are inadequate to maintain the required image quality active heating may be required. The decision can only be made on the basis of a thermal model whose results are fed back into the optics model to determine optical performance in the baseline environment and configuration.

Mounting stresses can be mimimized by good mechanical design practices. Stresses coupled into the optical component will distort surface quality and induce index changes in the glass. Both effects degrade the system image quality. Stress free mounting techniques include component retention with elastomeric agents, maintenance of sufficient clearance between cells and elements over thermal excursions, seating of components on either 3 point or lapped multipoint pads, and the application of compressive rather than tensile loads when loading of glass element is required.

Component misalignment effects can only be calculated when the structural and thermal modeling can provide reasonable estimates of component motions over environment. These motions can be inserted back into the optics model for an assessment of the impact on transmit wavefront quality. Component misalignments can arise from differential expansion with temperature excursions or from thermal gradients across the optical system structure. Misalignments can also result from component shifts as a result of launch loads, spacecraft internal vibrations, or mechanism vibrations coupled into the optical system structure. Some misalignments can be built into a system while in the alignment process due to a lack of sufficient adjustment range or resolution of motion on the optics mounts. The optics mount designs are based on a tradeoff of the conflicting requirements of adjustability and stability under launch loading. During the alignment process the test equipment used to monitor alignment must have sufficient resolution to measure in or out of spec alignment conditions. For instance the OPTRANSPAC optics that carries the near diffraction limited transmit beam will have to be aligned using an interferometer.

While exact budgeting of the wavefront error associated with misalignment must await a better definition of the mechanical structure and thermal environment

one can still make some conclusions based on alignment sensitivities. It is anticipated that OPTRANSPAC, like most diffraction limited optical communication systems, will be sensitive to misalignments in the telescope. The telescope misalignment sensitivities are shown in Table 11. It can be seen that this telescope is fairly sensitive to despacing of the primary and secondary mirrors. To maintain the specified wavefront quality the despace should remain well below ≈3μm. Should the despace exceed this value the active focus will need to be utilized to compensate for this added focus error. The other misalignments cause smaller effects and the solution is the same.

Residual uncorrected wavefront errors can be left in the optical system by the design process itself. This will leave a residual wavefront error in the optical system regardless of the fabrication process errors or lack thereof. The way to control this is to continue to increase the complexity of the optical system and keep optimizing until either all wavefront requirements are within spec, the number of elements start to increase weight and decrease transmission to unacceptable levels, or the time or money spent exceed the levels the contract will suppport. The amount of residual design aberrations and their impact on wavefront error will have to await the performance of a thick lens design and optimization of the OPTRANSPAC optical system.

The image quality requirements in the OPTRANSPAC receive paths are far less stringent than those for the transmit path. Receive image quality is driven by the tracking requirements. Figure 17 illustrates the variation in the size of the Earth image on the tracking detector as a function of range during the mission. This image size vs range curve is plotted parametrically as a function of receive path image quality. Diffraction limited performance is not necessary to meet the required tracking uncertainity. An optics resolution in the 15 - 25 μrad range is acceptable. This allows optics in the receive only portion of the imaging optics to have much less stringent surface quality requirements, say $\lambda/8$ or $\lambda/10$ peak-valley figure error (with λ = 500 or 600 nm, i.e. still measured in the visible).

8.0 FUTURE WORK

This design note represents the results of work completed under the current contract toward design of the OPTRANSPAC optical system. To carry on the development of this system under future contracts the following tasks will need to be accomplished next:

(a) Thick Lens Design and Optimization - The current thin lens design defined herein will need to be converted to a thick lens prescription using the optimization features of ACCOS V, Code V or an equivalent optical design code. This is necessary to determine the number of optical elements needed, determine nominal optical performance, determine required manufacturing tolerances, determine alignment requirements, and define the system in sufficient detail for detailed mechanical design to proceed.

(b) Thermal-Structure-Optical Analysis - Thermal and structural analysis of the optical and mechanical design will need to be conducted to determine the expected range of component motions and anticipated thermal gradients. These results will be folded back into the optical model to calculate optical performance of the perturbed optical system. The wavefront budgets and alignment budgets can then be fully computed.

(c) Breadboard Offset Tracking Configuration - To reduce risk and gain useful engineering data it would be worthwhile to procure optics and CTD camera and breadboard the offset tracking configuraton. This will validate performance of the optics and provide a useful test bed for evaluation of electronics, computer interfaces, and tracking software.

(d) Baffle Design and Stray Light Analysis - The Cassegrain telescope baffle system is not yet designed. It needs to be designed and its performance estimated using a stray light code such as APART or GUERAP (or, at least Mini-APART) to ensure in specification solar rejection.

FIGURE 1
OPTRANSPAC OPTICAL CONFIGURATION
OPTION A

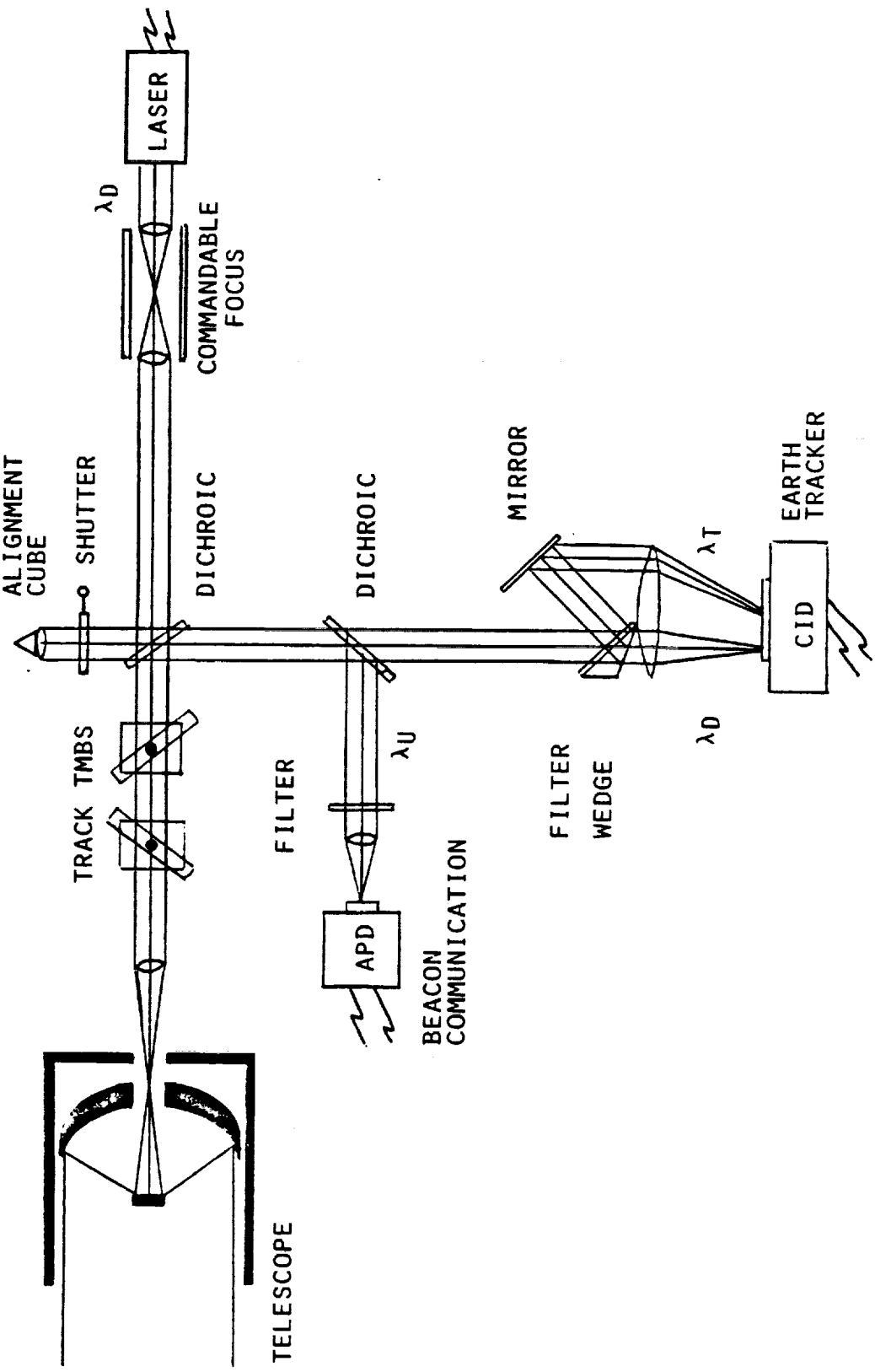

TELESCOPE CONFIGURATIONS

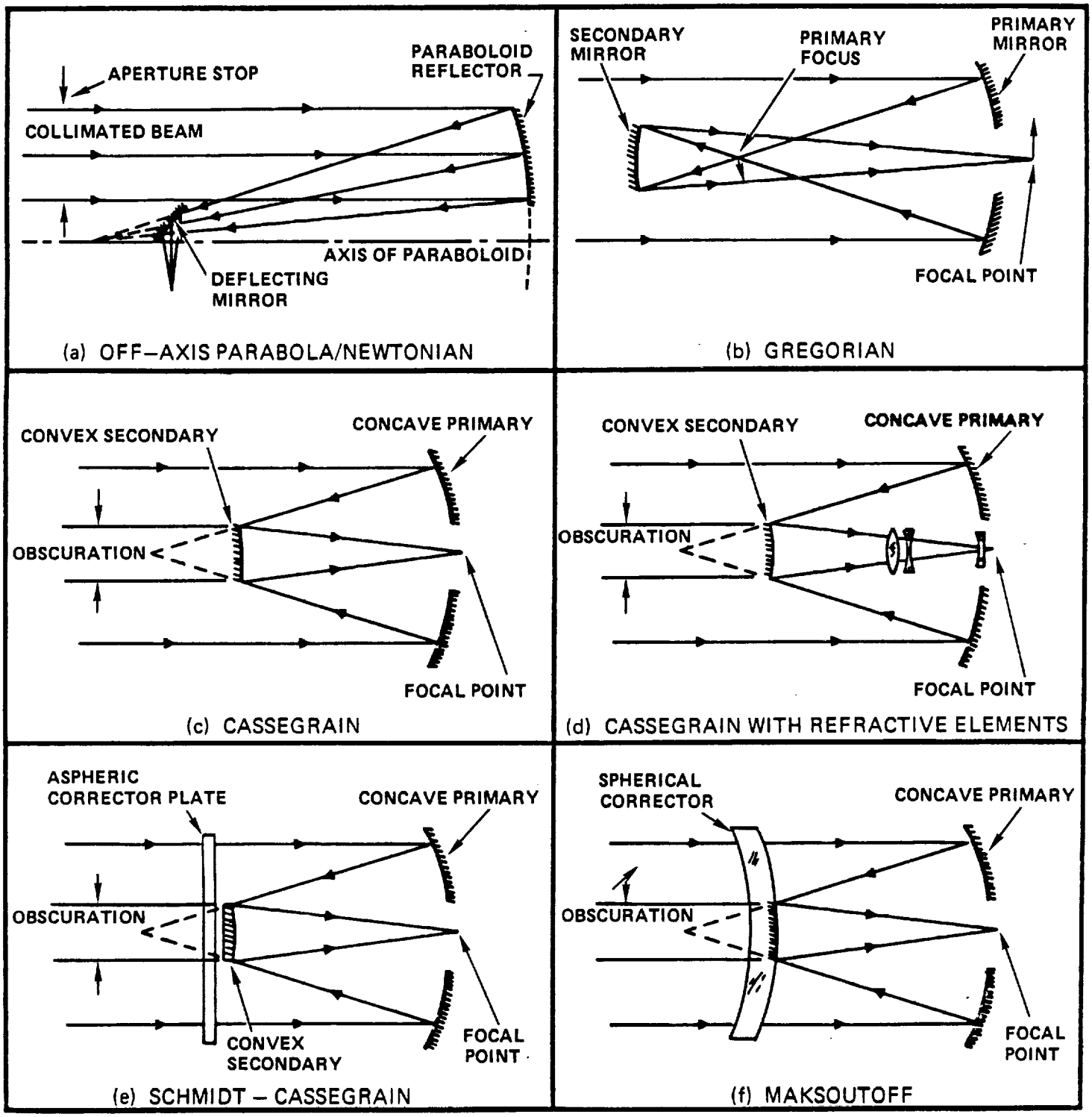

FIGURE 2

FIGURE 3
CASSEGRAIN WITH REFRACTIVE CORRECTING ELEMENTS

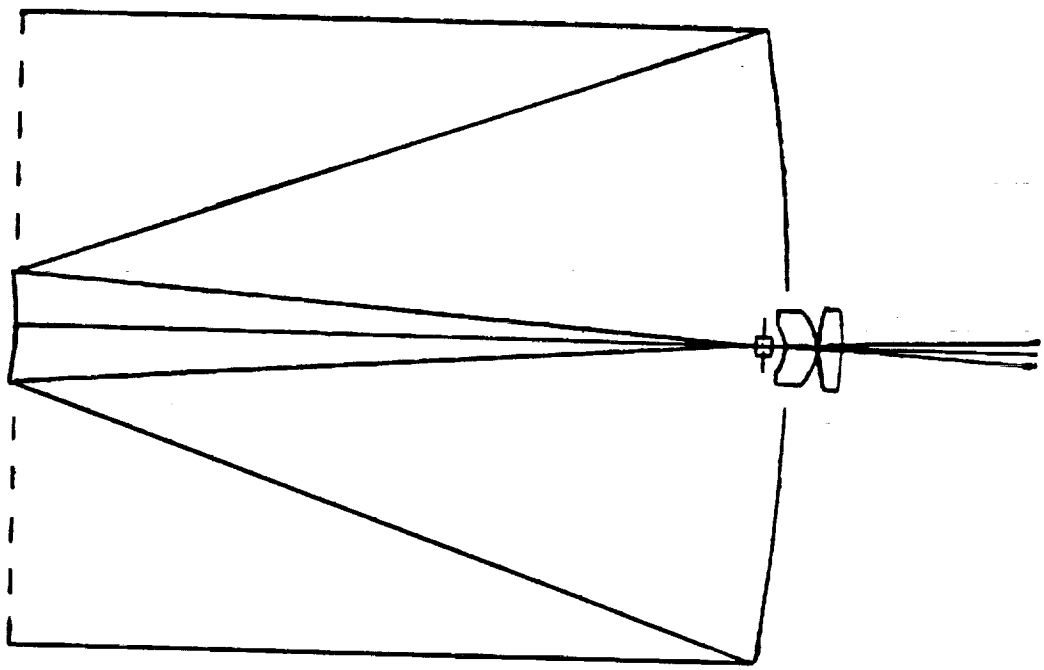

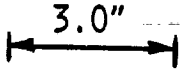

FIGURE 4 CASSEGRAIN WITH REFRACTIVE ELEMENTS
OPTICAL PERFORMANCE

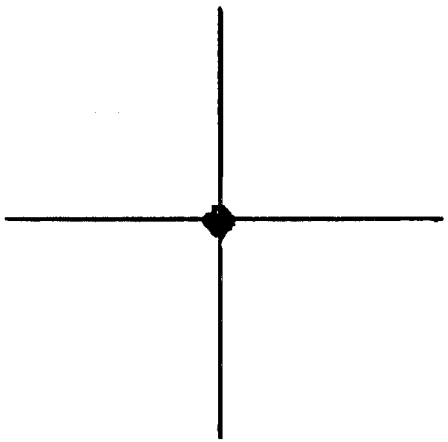

ON AXIS

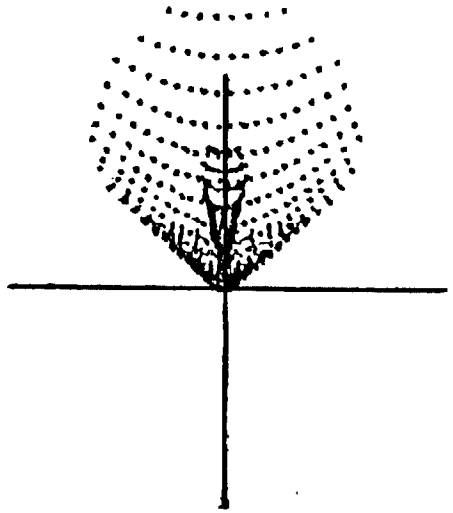

FULL FIELD

0.00020"

(AIRY DISK DIAMETER = 0.00053")

FIGURE 5

OPTRANSPAC OPTICAL SCHEMATIC

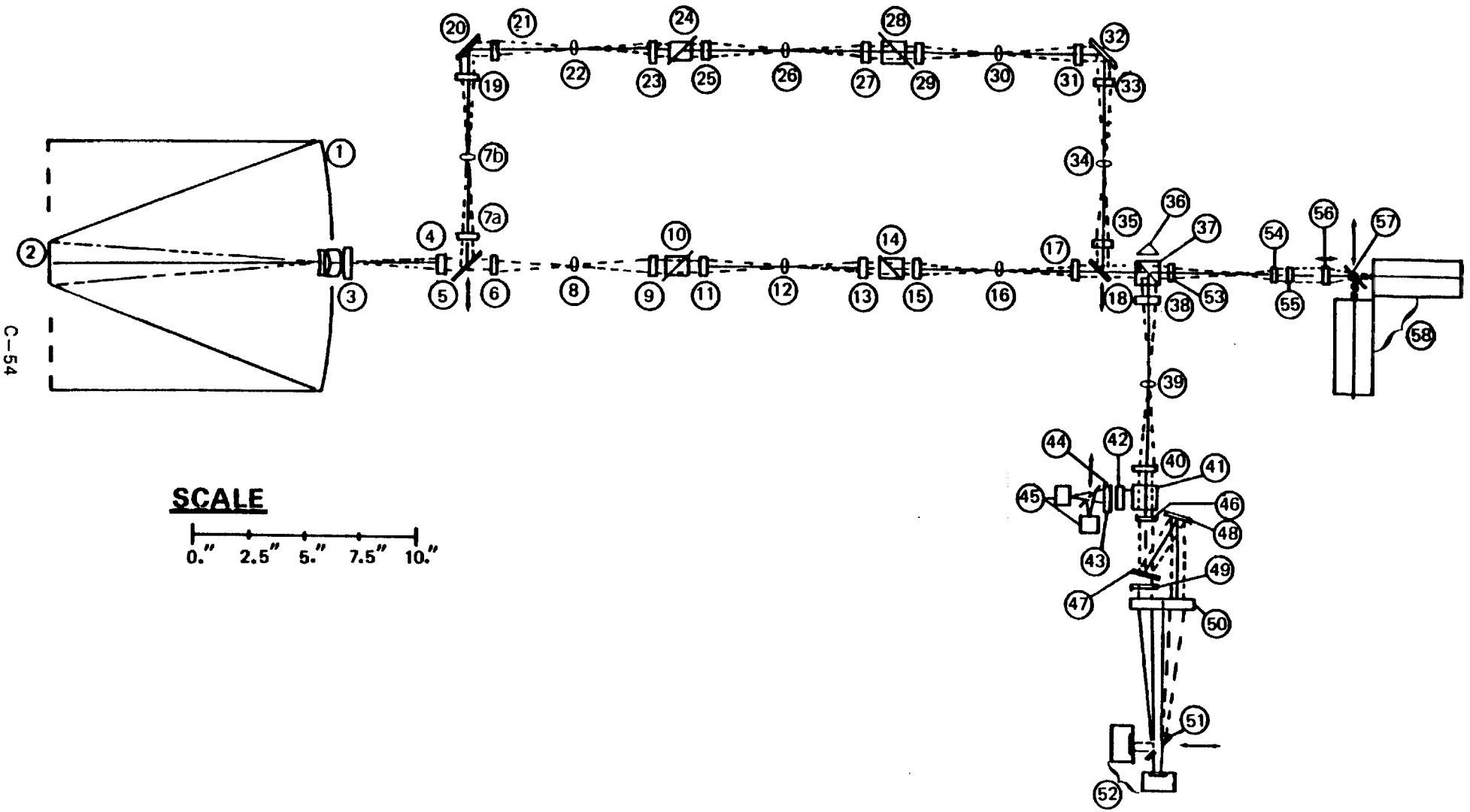

FIGURE 6 OPTRANSPAC OPTICAL SCHEMATIC - PATH BREAKDOWN

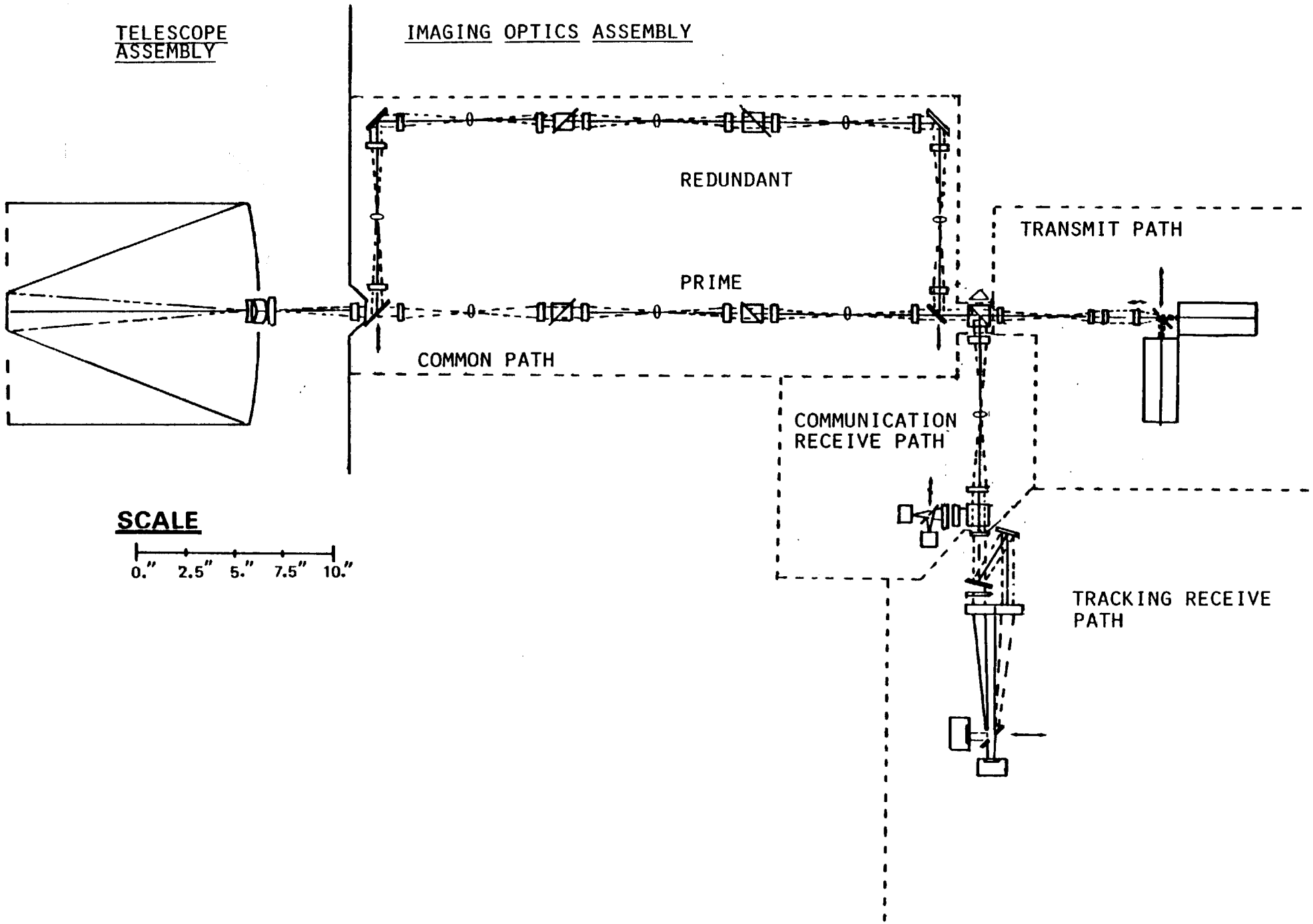

FIGURE 7 TELESCOPE THIN LENS LAYOUT

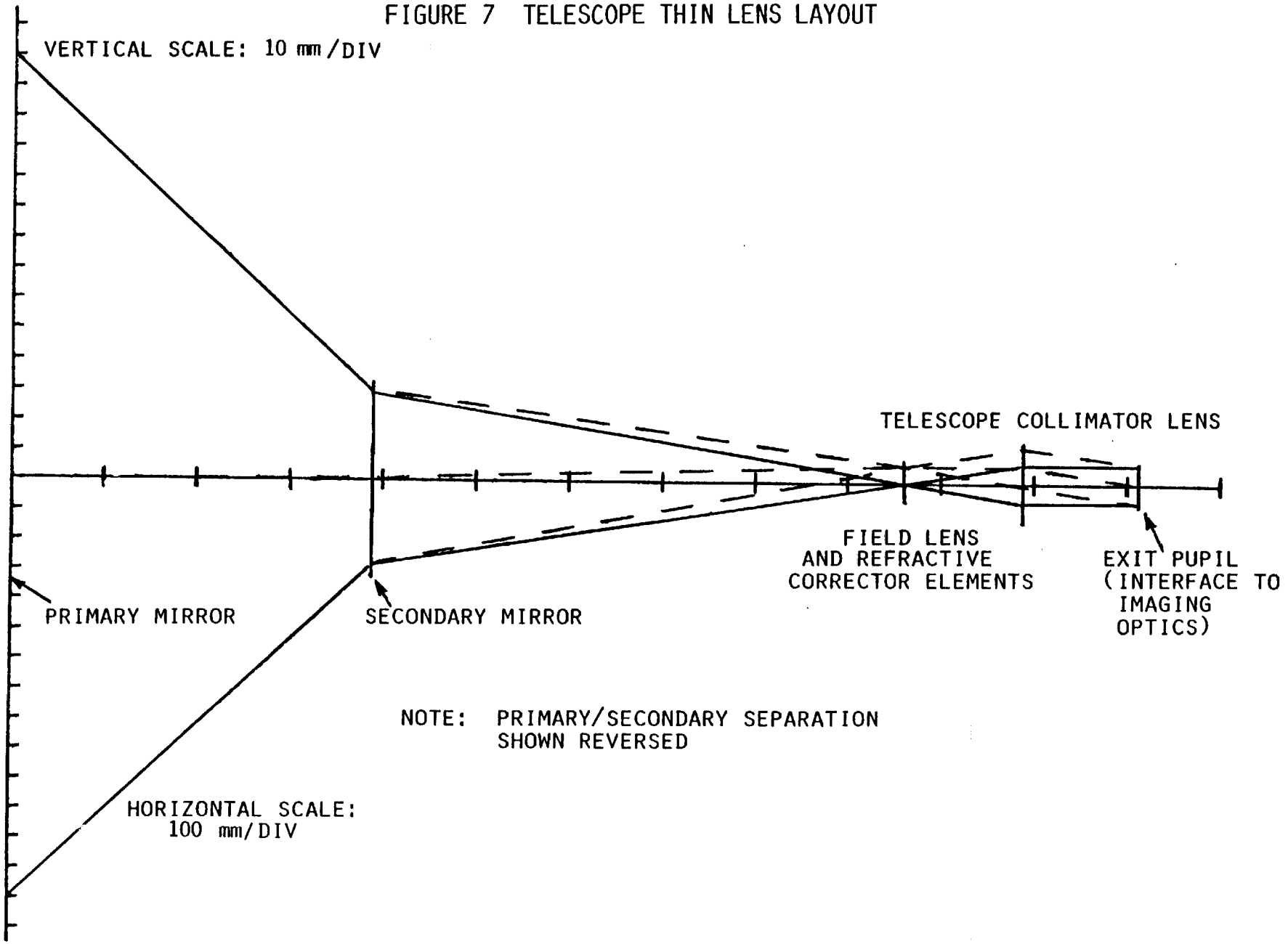

FIGURE 8 TYPICAL COLLIMATOR-FIELD LENS-COLLIMATOR (CFC) GROUP

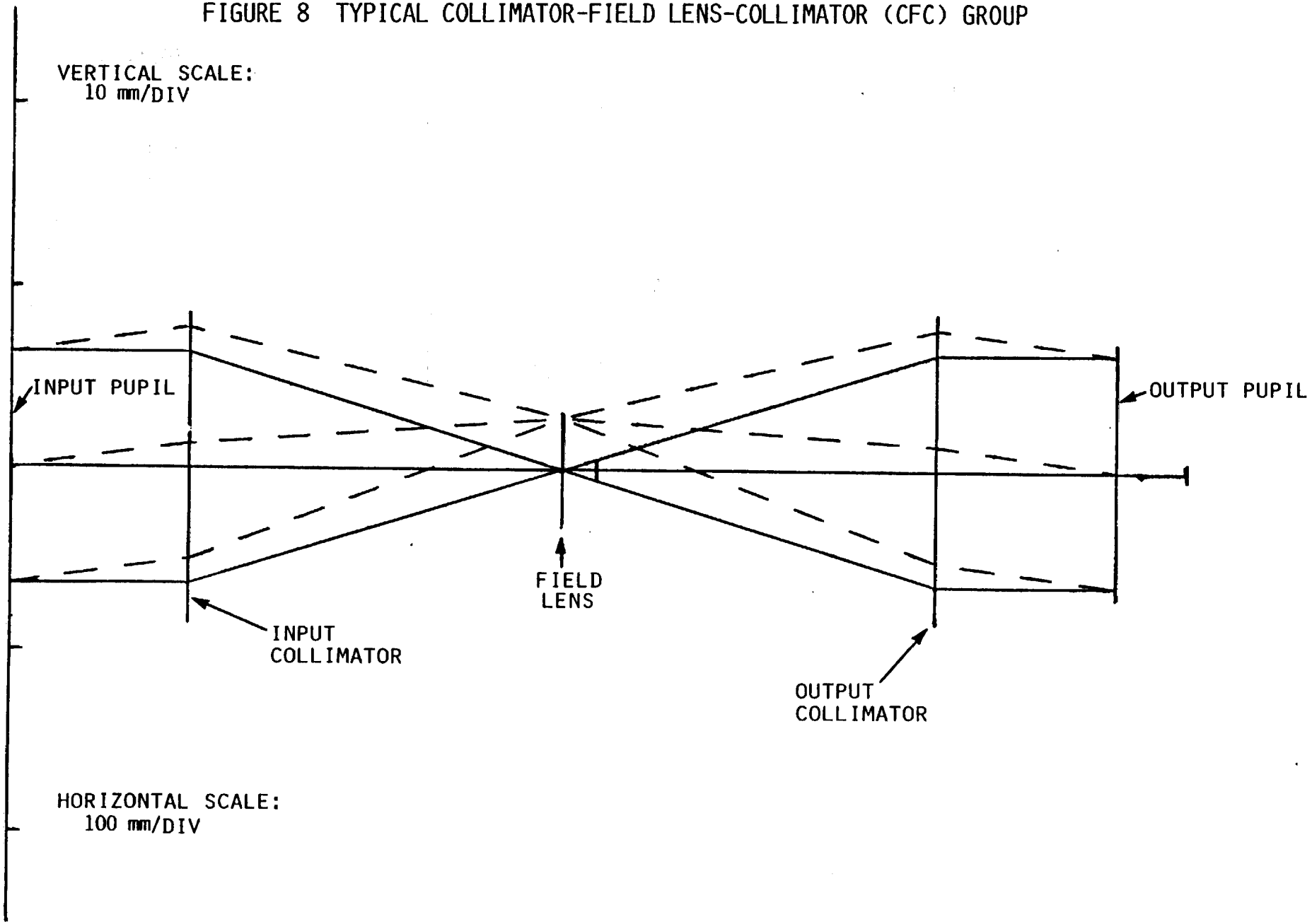

FIGURE 9 COMMON PATH THIN LENS LAYOUT

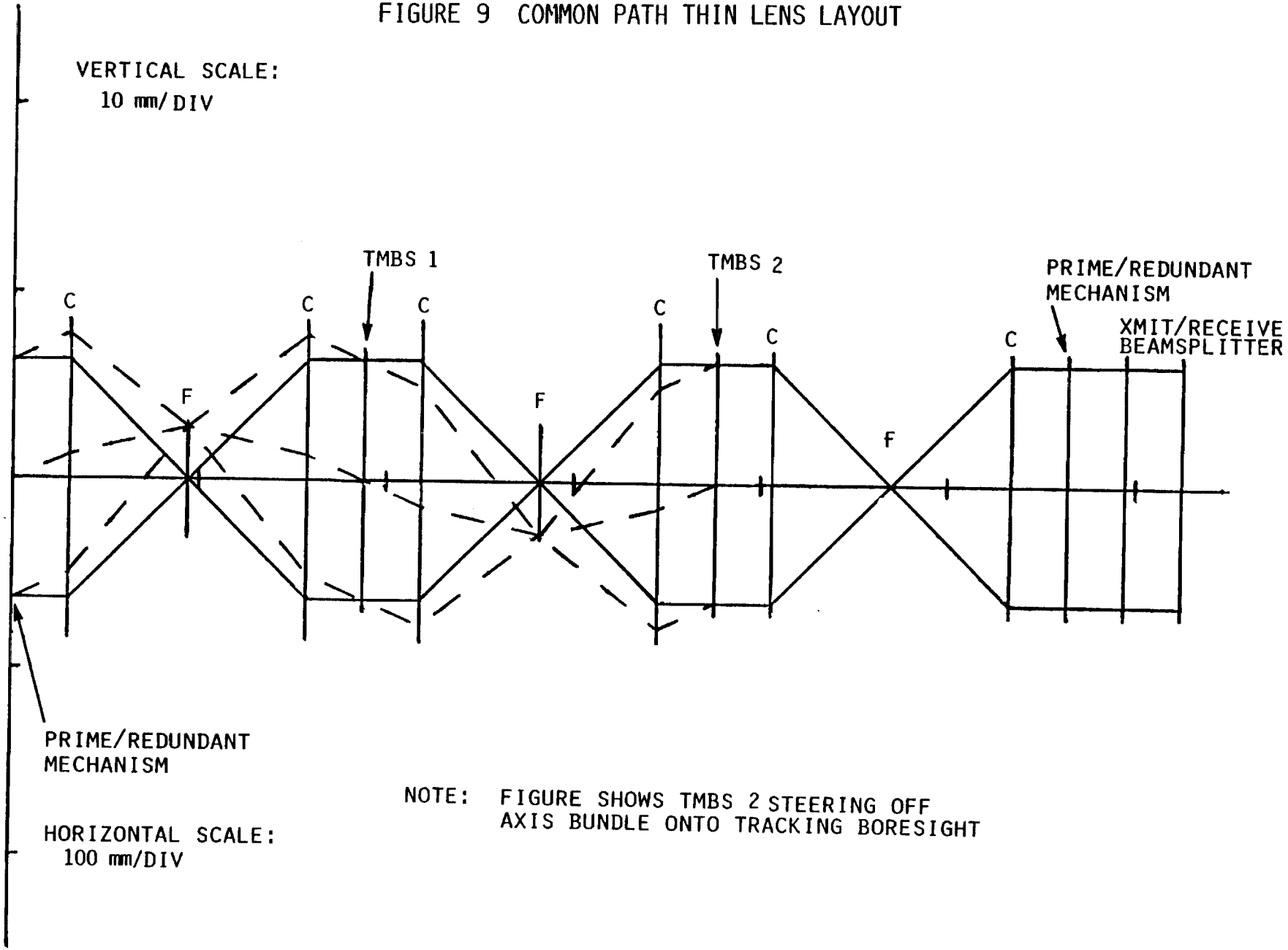

NOTE: FIGURE SHOWS TMBS 2 STEERING OFF AXIS BUNDLE ONTO TRACKING BORESIGHT

FIGURE 10 TRANSMIT PATH THIN LENS LAYOUT

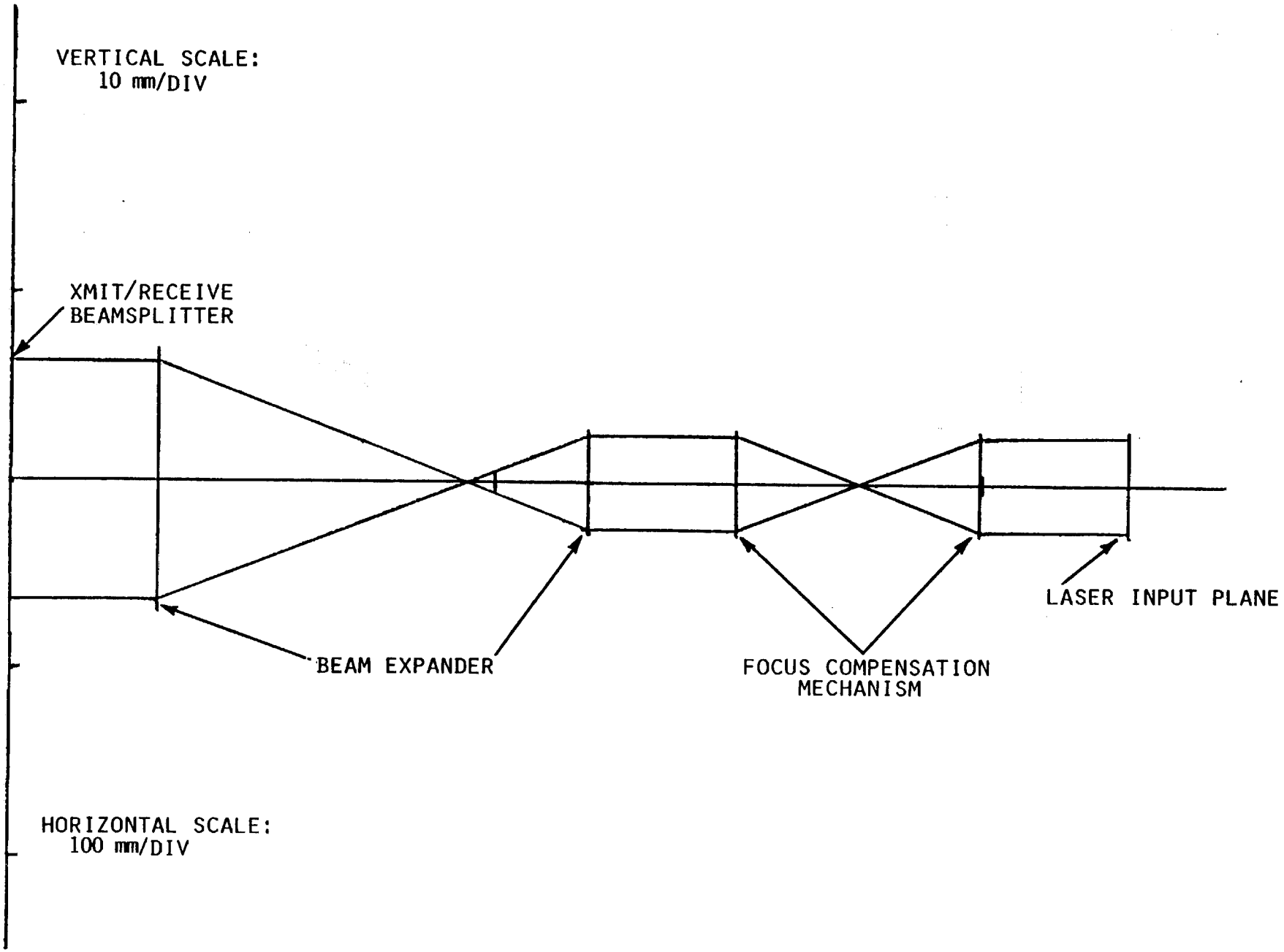

FIGURE 11 COMMUNICATION PATH THIN LENS LAYOUT

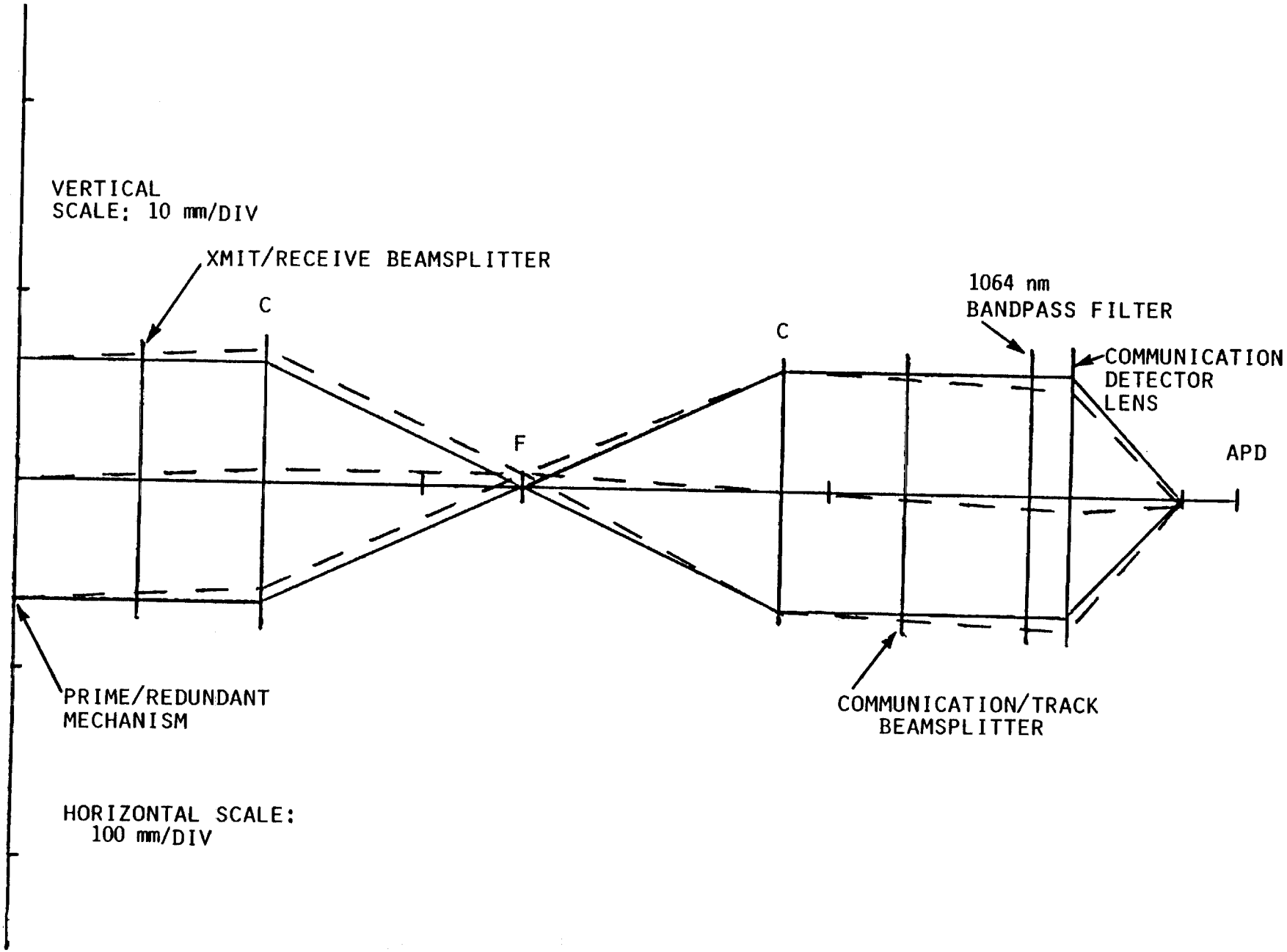

FIGURE 12 EARTH (BROADBAND) TRACKING THIN LENS LAYOUT

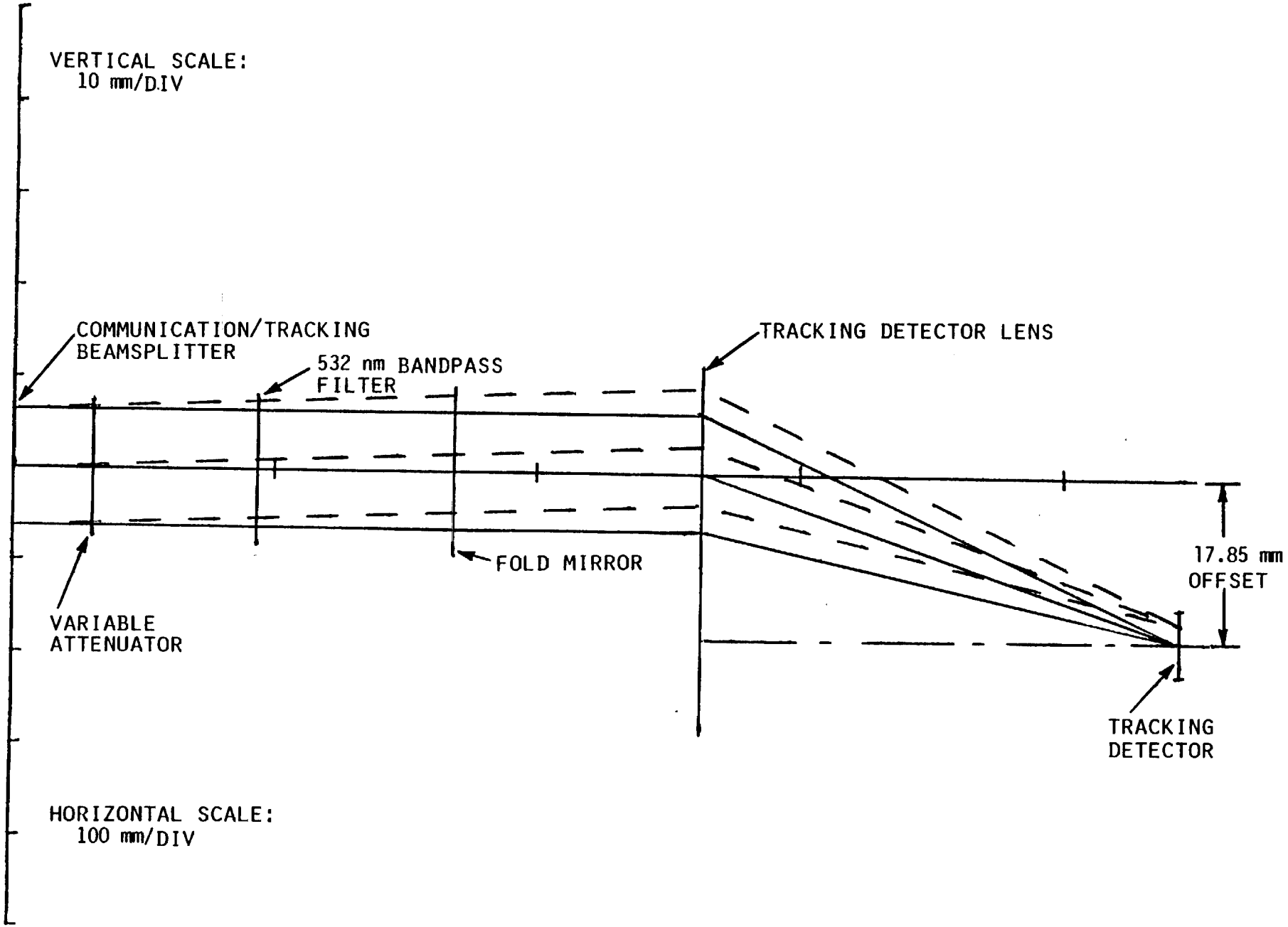

FIGURE 13 OFFSET (532 NM) TRACKING THIN LENS LAYOUT

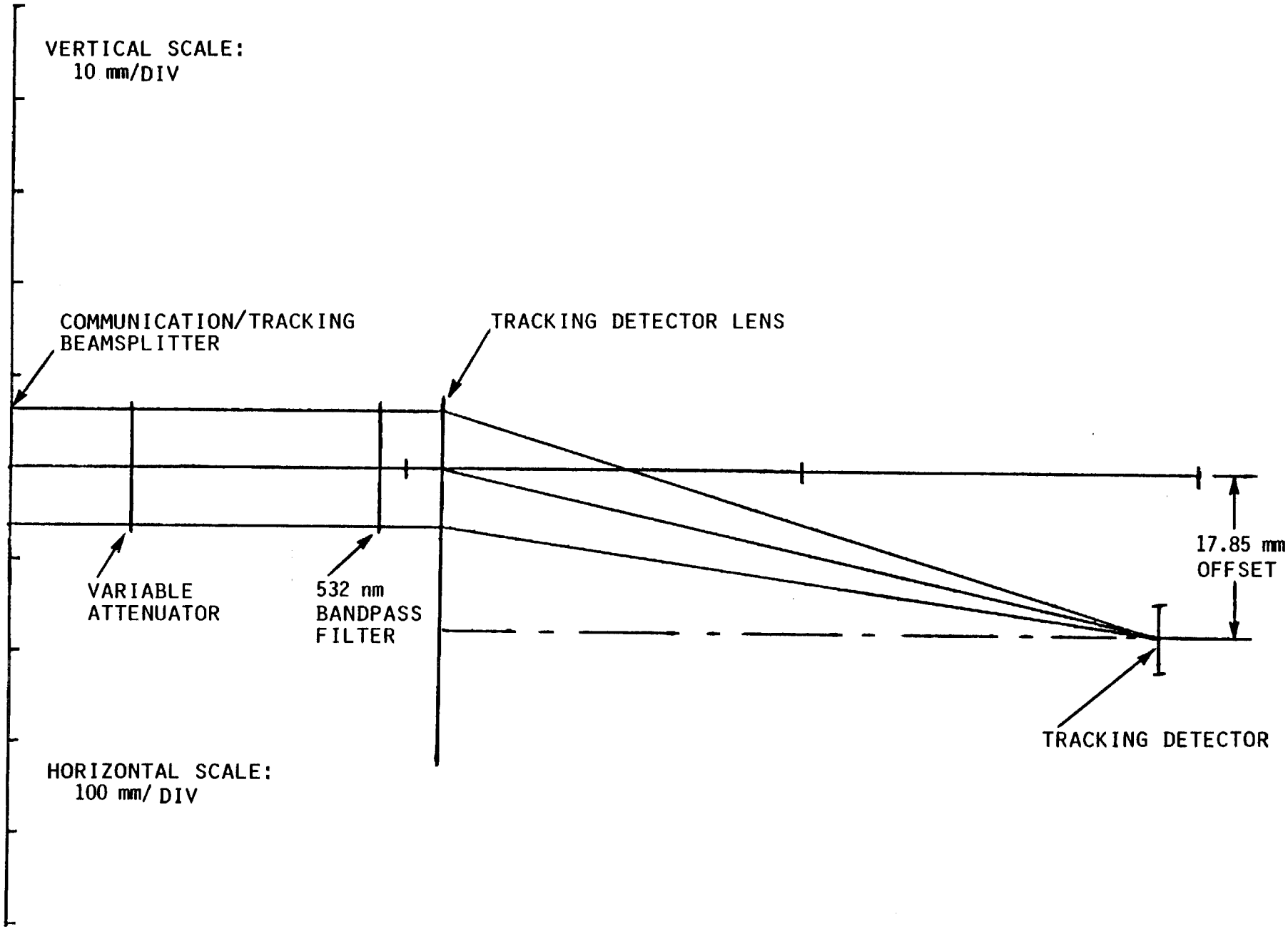

OPTRANSPAC
OPTICAL ISOMETRIC VIEW

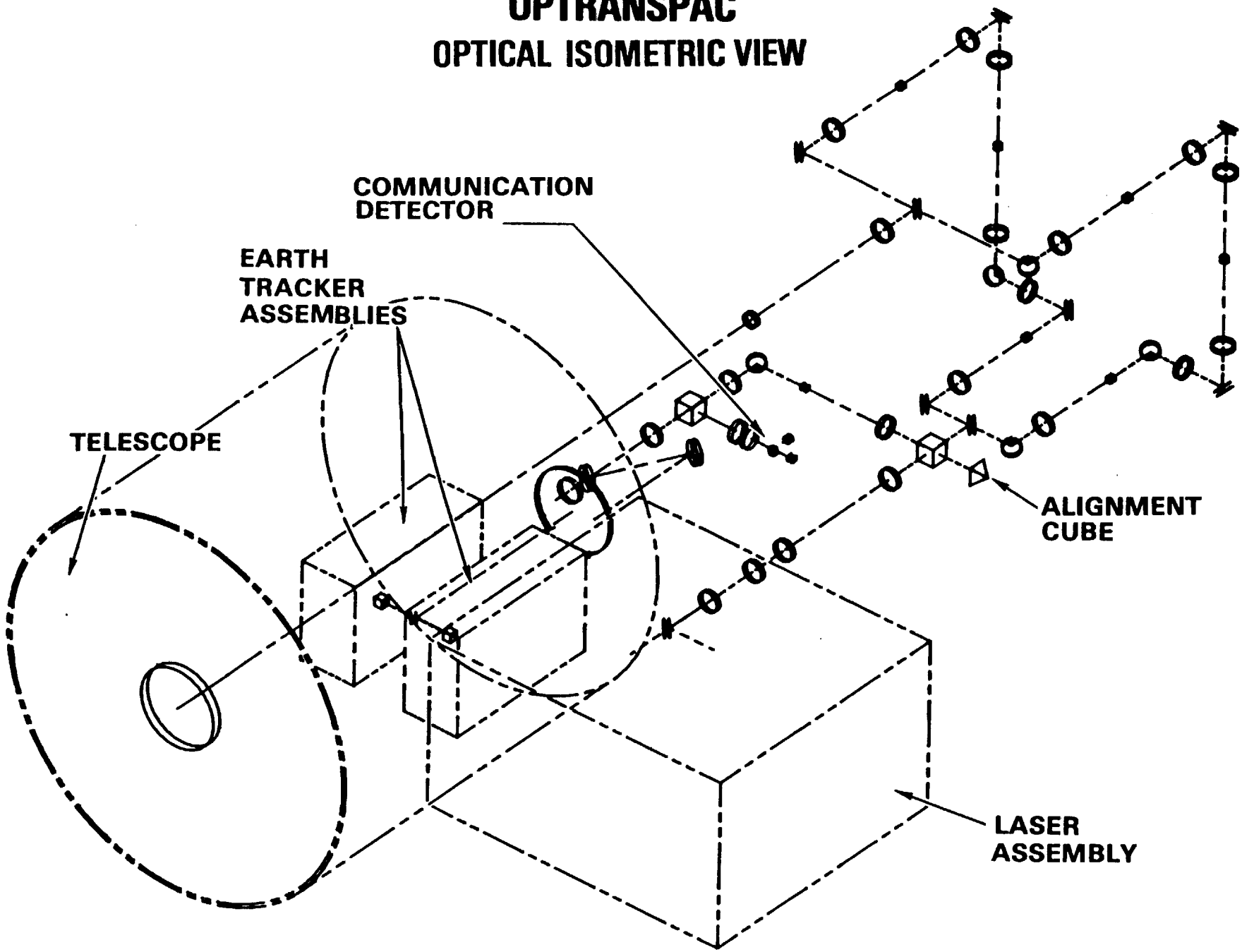

FIGURE 14

FIGURE 15 A

OPTRANSPAC

ORTHOGRAPHIC

TOP VIEW

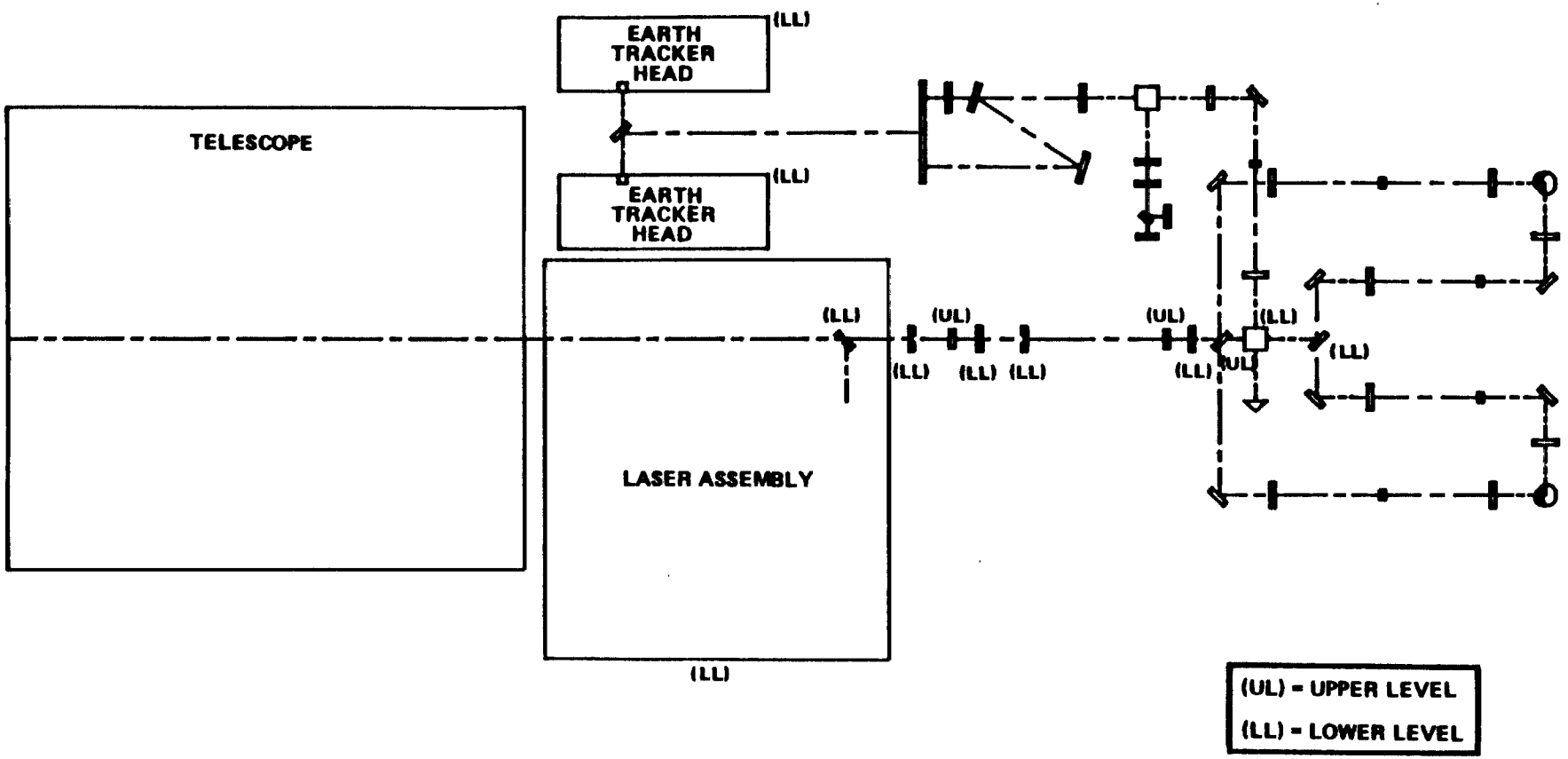

FIGURE 15 B

OPTRANSPAC

ORTHOGRAPHIC

SIDE VIEW

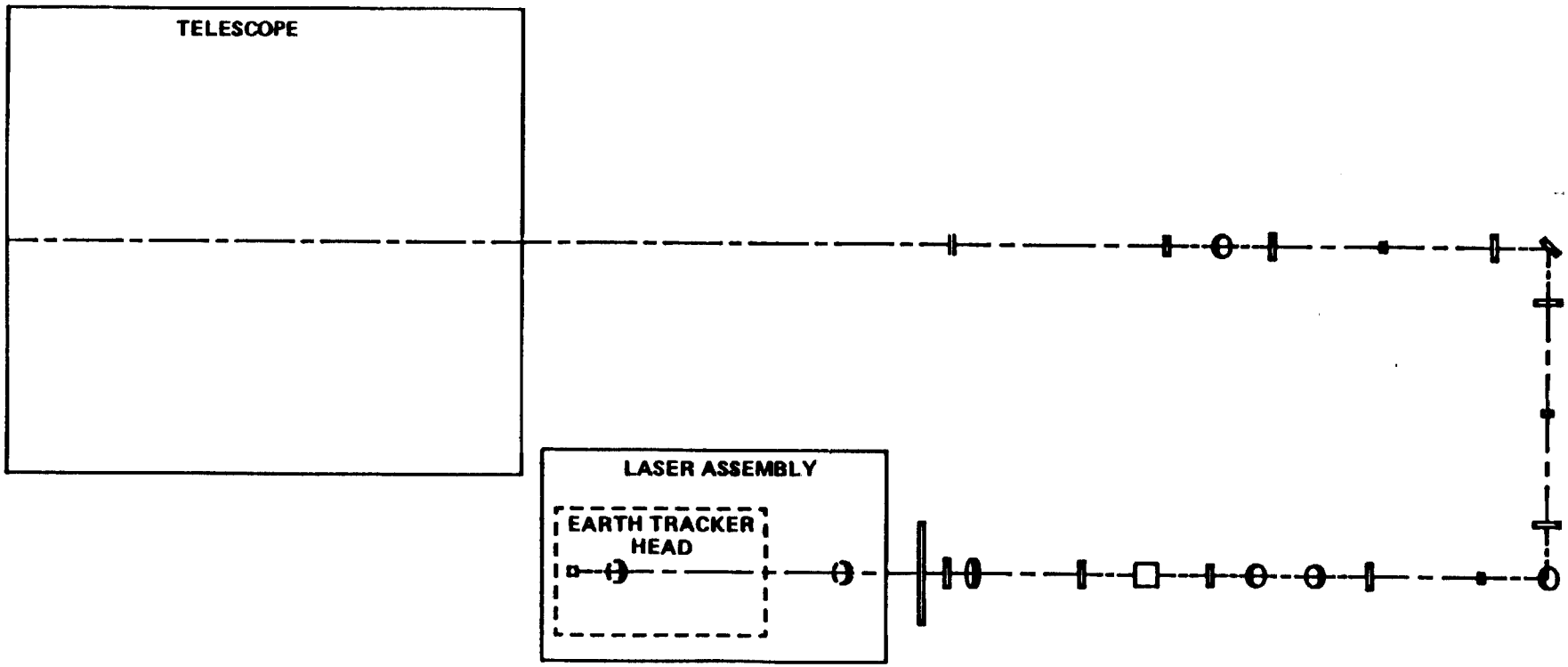

OPTRANSPAC
ISOMETRIC VIEW

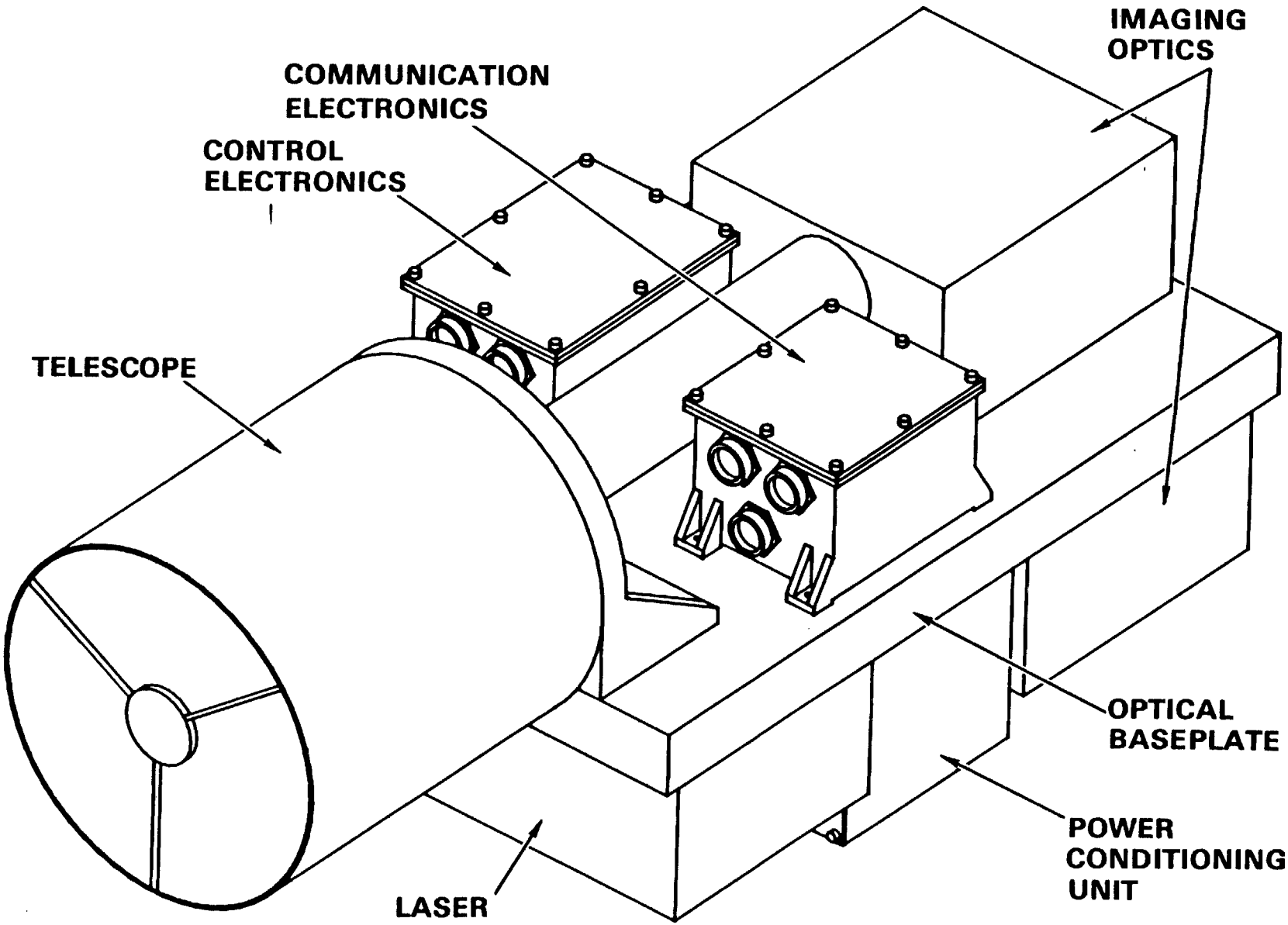

FIGURE 16

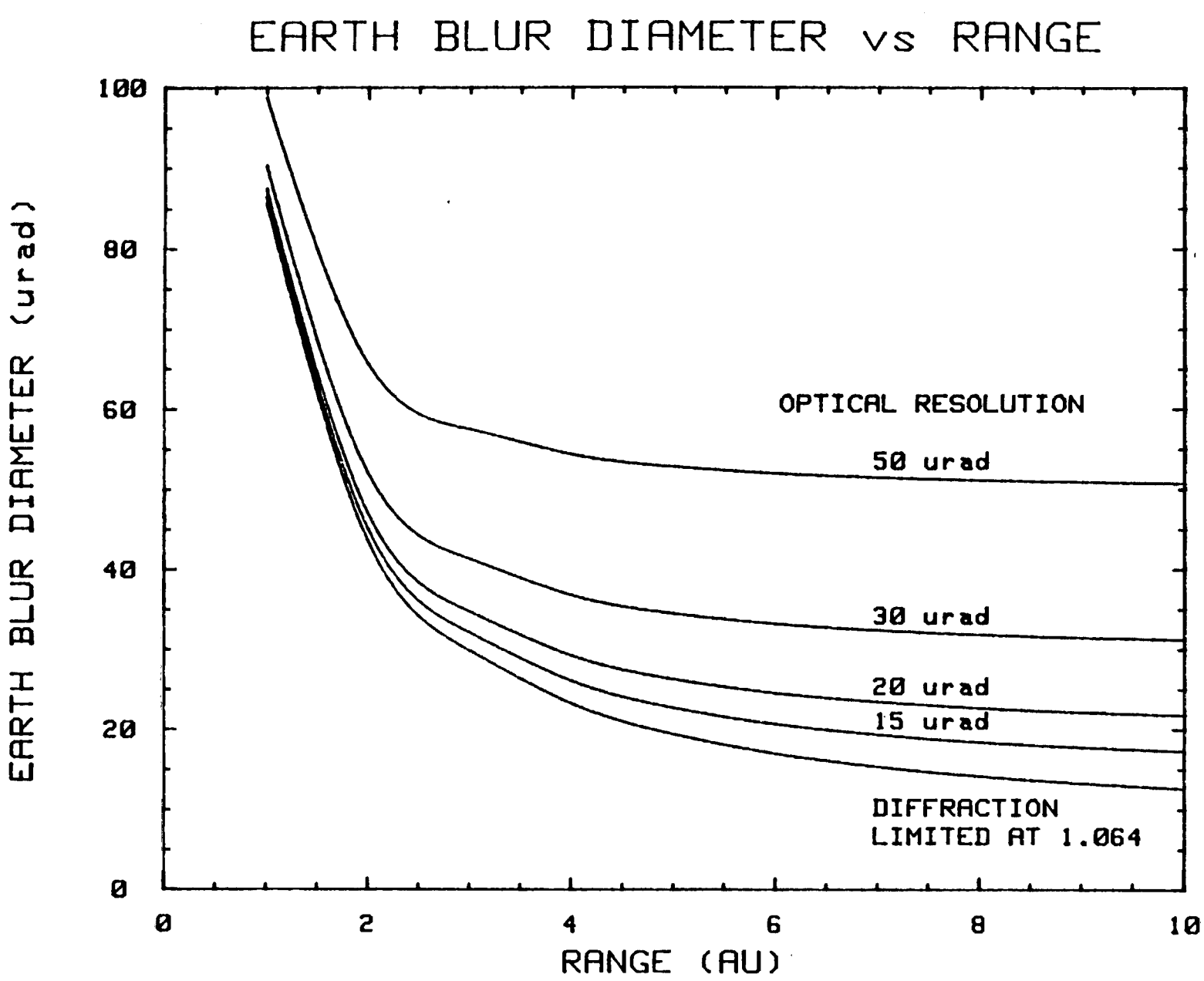
EARTH BLUR DIAMETER vs RANGE
EARTH BLUR DIAMETER (urad)
100
80
60
40
20
0
0
2
4
6
8
10
RANGE (AU)
OPTICAL RESOLUTION
50 urad
30 urad
20 urad
15 urad
DIFFRACTION
LIMITED AT 1.064

FIGURE 17

TABLE 1 OPTRANSPAC OPTICAL SYSTEM REQUIREMENTS

• APERTURE	11" (279.4 MM) DIAMETER
• FIELD-OF-VIEW	1 MRAD FOR TRACKING AND COMMUNICATION
• ANGULAR STEERING RANGE	± 2 MRAD (4 MRAD TOTAL)
• WAVELENGTH	RECEIVE - 400-1100 NM TRANSMIT - 532 NM
• RESOLUTION	RECEIVE SPOT SIZE ≤ 25 μ RAD TRANSMIT DIFFRACTION LIMITED TO λ/14 RMS OVER ±2 MRAD ANGULAR FIELD
• TRANSMISSION (EOL)	RECEIVE TRACK: ≥ 20% RECEIVE COMM.: ≥ 41% TRANSMIT: ≥ 66%
• REDUNDANCY	NO SINGLE POINT FAILURE - REDUNDANT ACTIVE DEVICES - >10 YEAR LIFE

TABLE 2A OPTRANSPAC TELESCOPE REQUIREMENTS

• APERTURE SIZE	11" (279.4 MM). SYSTEM MAPS 11" BUNDLE TO 0.5" (12.7 MM) BUNDLE IN IOA
• FIELD-OF-VIEW	4 MRAD
• OBSTRUCTION RATIO	22% (DIAMETER RATIO)
• BEAM STEERING	FIXED FIELD-OF-VIEW. COARSE POINTING BY SPACECRAFT. FINE POINTING DONE BY IOA.
• WAVELENGTH OF OPERATION	400-1100 NM
• TRANSMISSION (EOL)	BROADBAND VISIBLE - $\geq$ 80% 532 NM TRANSMIT - $\geq$ 90% 1064 NM RECEIVE - $\geq$ 90%
• IMAGE QUALITY	RECEIVE - SPOT SIZE $\leq$ 18 μ RAD (GUARANTEED BY MEETING TRANSMIT REQUIREMENTS) TRANSMIT - DIFFRACTION LIMITED TO λ/20 RMS OVER 4 MRAD FOV
• SIZE, WEIGHT, AND POWER	SIZE - $\leq$1'x1'x2.3' (305 MM x 305 MM x 732 MM) WEIGHT - 18 LBS (39.6 KG) POWER - NONE (UNLESS ACTIVE HEATING OF TELESCOPE STRUCTURE NEEDED TO MAINTAIN IMAGE QUALITY)

TABLE 2B OPTRANSPAC IMAGING OPTICS REQUIREMENTS

• APERTURE SIZE	ACCEPTS 0.5" (12.7 MM) BUNDLE FROM TELESCOPE. INTERFACES DETECTORS AND LASER TO TELESCOPE.
• FIELD-OF-VIEW	COVERS $\pm$ 44 MRAD
• ANGULAR STEERING RANGE	COVERS $\pm$ 44 MRAD
• WAVELENGTH OF OPERATION	400-1100 NM
• TRANSMISSION (EOL)	BROADBAND VISIBLE - $\geq$ 25% 532 NM TRANSMIT - $\geq$ 46% 1064 NM RECEIVE - $\geq$ 73%
• IMAGE QUALITY	RECEIVE - SPOT SIZE $\geq$18 µRAD TRANSMIT - DIFFRACTION LIMITED TO λ/20 RMS OVER FIELD-OF-VIEW
• SIZE, WEIGHT, AND POWER	SIZE - $\leq$ 1'x1.5'x2.4' (305 MM X 457 MM X 732 MM) WEIGHT - 13.5 KG (29.7 LBS) POWER - 2W CONTINUOUS (TMBS PAIR IN USE ONLY). POWER NEEDED FOR PRIME/REDUNDANT MECHANISM SWITCHING BUDGETED ELSEWHERE. REQUIREMENTS WILL BE MORE IF ACTIVE THERMAL CONTROL REQUIRED.

TABLE 3 TELESCOPE PRESCRIPTION
EXAMPLE RITCHEY CHRETIEN WITH CORRECTOR LENSES

BASIC LENS DATA

SURF	RD	TH	MEDIUM	RN	DF
0	0.000000	.785700E+10	AIR		
1	0.000000	13.593396	AIR		
2	-32.5919597	-13.593396	REFL		
3	-6.785295	13.049691	REFL		
4	-1.309862	.271874	SILICA	1.452590	-52.364
5	-91.157784	.259634	AIR	1.452590	-52.364
6	-.619316	.543737	SILICA	1.452590	-52.364
7	-.808265	0.000000	AIR		
8	2.395433	.419493	SILICA	1.452590	-52.364
9	-4.736221	3.520722	AIR		
10	0.000000	-4.885582	AIR		
11	0.000000	0.000000	AIR		

REFRACTIVE INDICES

SURF	N1	N2	N3	N4	N5
4	1.452590	1.000000	1.000000	1.000000	1.000000
6	1.452590	1.000000	1.000000	1.000000	1.000000
8	1.452590	1.000000	1.000000	1.000000	1.000000

CC AND ASPHERIC DATA

SURF	CC	AD	AE	AF	AG
2	-.10214E+01				
3	-.25397E+01				

CLEAR APERTURES AND OBSTRUCTIONS

SURF	TYPE	CAY	CAX
1	CIRCLE	5.4999	
1 (OB)	CIRCLE	.9868	
2	CIRCLE	5.4999	
2 (OB)	CIRCLE	.9428	
3	CIRCLE	.9868	
6	CIRCLE	.4321	
7	CIRCLE	.6168	
8	CIRCLE	.6796	
9	CIRCLE	.6824	

REF OBJ HT	REF AP HT	OBJ SURF	REF SURF	IMG SURF
-.157700E+08 (.12 DG)	5.49990	0	1	11

EFL	BF	F/NBR	LENGTH	GIH
145.4814	-4.8856	10.39	18.0652	.2920

WAVL NBR	1	2	3	4	5
WAVELENGTH	.53200	1.06400	.83500	0.00000	.00000
SPECTRAL WT	1.0000	1.0000	1.0000	1.0000	1.0000

NO APERTURE STOP

LENS UNITS ARE INCHES

EVALUATION MODE IS FOCAL

TABLE 4
OPTICAL SCHEMATIC KEY

NUMBER	OPTICAL PATH	COMPONENT DESCRIPTION
1	TELESCOPE	CASSEGRAIN PRIMARY MIRROR
2	TELESCOPE	CASSEGRAIN SECONDARY MIRROR
3	TELESCOPE	FIELD CORRECTION GROUP
4	COMMON (PRIME & REDUNDANT)	COLLIMATOR
5	COMMON (PRIME & REDUNDANT)	REDUNDANT SELECT MECHANISM ("POP MIRROR")
6, 8, 9	COMMON (PRIME)	COLLIMATOR-FIELD LENS-COLLIMATOR GROUP ("CFC")
10	COMMON (PRIME)	TORQUE MOTOR BEAM STEERER (TMBS)
11, 12, 13	COMMON (PRIME)	CFC GROUP
14	COMMON (PRIME)	TMBS
15, 16, 17	COMMON (PRIME)	CFC GROUP
18	COMMON (PRIME & REDUNDANT)	REDUNDANT SELECT MECHANISM ("POP MIRROR")
7A, 7B, 19	COMMON (REDUNDANT)	CFC GROUP
20	COMMON (REDUNDANT)	TYPICAL FOLD MIRROR
21,22,23	COMMON (REDUNDANT)	CFC GROUP
24	COMMON (REDUNDANT)	TMBS
25, 26, 27	COMMON (REDUNDANT)	CFC GROUP
28	COMMON (REDUNDANT)	TMBS
29, 30, 31	COMMON (REDUNDANT)	CFC GROUP
32	COMMON (REDUNDANT)	TYPICAL FOLD MIRROR

TABLE 4

OPTICAL SCHEMATIC KEY
(CONTINUED)

NUMBER	OPTICAL PATH	COMPONENT DESCRIPTION
33, 34, 35	COMMON (REDUNDANT)	CFC GROUP
37	COMMON PATH (PRIME & REDUNDANT)	TRANSMIT/RECEIVE BEAMSPLITTER (DICHROIC) CUBE (TRANSMITS 532 NM)
36	STATIC ALIGNMENT	STATIC ALIGNMENT RETROREFLECTOR
38, 39, 40	RECEIVE	CFC GROUP
41	RECEIVE	TRACKING/COMMUNICATION BEAMS SPLITTER (DICHROIC) CUBE (REFLECTS 1064 NM)
42	COMMUNICATION	1064 NM BANDPASS FILTER
43	COMMUNICATION	COMMUNICATION DETECTOR FOCUSSING LENS
44	COMMUNICATION	PRIME/REDUNDANT COMM DETECTOR SELECT MECHANISM ("POP MIRROR")
45	COMMUNICATION	COMMUNICATION DETECTOR (APD)
46	TRACKING	VARIABLE ATTENUATION FILTER (INCLUDES SELECTION MECHANISM)
47	TRACKING (AND STATIC ALIGNMENT)	532 NM BANDPASS FILTER (PASS 532 NM AND REFLECT OUTSIDE PASSBAND)
48	TRACKING	MIRROR FOR EARTH TRACKING CHANNEL
49	STATIC ALIGNMENT	WEDGE (DEVIATES RETROREFLECTED TRANSMIT BEAM TO OFFSET POSITION OR TRACKING DETECTOR
50	TRACKING	TRACKING FOCUSSING LENS
51	TRACKING	PRIME/REDUNDANT TRACKING DETECTOR SELECT MECHANISM ("POP MIRROR")

TABLE 4

OPTICAL SCHEMATIC KEY
(CONTINUED)

NUMBER	OPTICAL PATH	COMPONENT DESCRIPTION
52	TRACKING	TRACKING DETECTOR
53, 54	TRANSMIT	TRANSMIT BEAM EXPANDER
55, 56	TRANSMIT	ACTIVE FOCUS UNIT
57	TRANSMIT	PRIME/REDUNDANT LASER SELECT MECHANISM ("POP MIRROR")
58	TRANSMIT	LASER

TABLE 5 OPTRANSPAC TELESCOPE ASSEMBLY

ELEMENT	FOCAL LENGTH/ RADIUS OF CURVATURE	DIAMETER	SPACING TO NEXT ELEMENTS/ENDPOINTS
① PRIMARY MIRROR	488.95/977.9	279.4	-389.0/①-②
② SECONDARY MIRROR	-121.21/-242.42	58.7	571.4/②-③
③ TELESCOPE FIELD LENS	600./ -	11.2	127.0/③-④
④ TELESCOPE COLLIMATOR	127.0/ -	23.7	30.48/④-⑤
⑤ PRIME-REDUNDANT SELECT POP MIRROR	- / ∞	12.7 @ 45°	30.48/⑤-⑥ OR ⑤-⑦

NOTE: ALL DIMENSIONS IN MILLIMETERS

TABLE 6 OPTRANSPAC COMMON PATH

ELEMENT	FOCAL LENGTH/ RADIUS OF CURVATURE	DIAMETER	SPACING TO NEXT ELEMENTS/ENDPOINTS
⑤ PRIME-REDUNDANT SELECT POP MIRROR	- / ∞	12.7 @ 45°	30.48/⑤-⑥
⑥ COLLIMATOR	65.5/ -	15.4	63.5/⑥-⑧
⑧ FIELD LENS	61.05/ -	5.6	63.5/⑧-⑨
⑨ COLLIMATOR	63.5/ -	15.4	30.48/⑨- ⑩
⑩ TMBS	- / ∞	12.7 MM	30.48/ ⑩ - ⑪
⑪ - ⑭	REPEAT OF ⑥- ⑩		30.48/ ⑭ - ⑮
⑮ - ⑰	REPEAT OF ⑥-⑨		30.48/ ⑰ - ⑱
⑱ PRIME-REDUNDANT SELECT POP MIRROR	- / ∞	12.7 @ 45°	30.48/ ⑱ - ㊲
㊲ TRANSMIT/RECEIVE BEAMSPLITTER	- / ∞		30.48/ ㊲ - ㊳ OR ㊲ - ㊸

NOTE: ALL DIMENSIONS IN MILLIMETERS

TABLE 7 TRANSMIT PATH SECTION

ELEMENT	FOCAL LENGTH/ RADIUS OF CURVATURE	DIAMETER	SPACING TO NEXT ELEMENTS/ENDPOINTS
(37) TRANSMIT/RECEIVE BEAMSPLITTER	- / ∞	15.0	30.48/ (37) - (53)
(53) BEAM EXPANDER OUTPUT LENS	63.5/ -	15.0	88.5/ (53) - (54)
(54) BEAM EXPANDER INPUT LENS	25/ -	6.0	30.48/ (54) - (55)
(55) ACTIVE FOCUS OUTPUT LENS	25/ -	6.0	25 (VARIABLE)/ (55) -, (56)
(56) ACTIVE FOCUS INPUT LENS	25/ -	6.0	30.47/ (56) - (58)
(58) LASER INPUT PLANE	- / ∞	6.0	(PENDING DEFINITION OF LASER INTERFACE CHARACTERISTICS)

NOTE: ALL DIMENSIONS IN MILLIMETERS

TABLE 8 OPTRANSPAC COMMUNICATION RECEIVE PATH

ELEMENT	FOCAL LENGTH/ RADIUS OF CURVATURE	DIAMETER	SPACING TO NEXT ELEMENTS/ENDPOINTS
㊲ TRANSMIT/RECEIVE BEAMSPLITTER	- / ∞	13.4	30.48/ ㊲ - ㊳
㊳ COLLIMATOR	63.5/ -	14.0	63.5/ ㊳ - ㊴
㊴ FIELD LENS	61.05/ -	5.6	63.5/ ㊴ - ㊵
㊵ COLLIMATOR	63.5/ -	12.7	30.48/ ㊵ - ㊶
㊶ BEAMSPLITTER	- / ∞	13.4	30.48/ ㊶ - ㊷
㊷ BANDPASS FILTER	- / ∞	14.0	10.0/ ㊷ - ㊸
㊸ COMM DETECTOR LENS	27.27/ -	14.3	27.8/ ㊽ - ㊺
㊹ POP MIRROR	- / ∞	≈ 8 @ 45°	MIDWAY BETWEEN ㊸ AND ㊺
㊺ COMM DETECTOR	- / ∞	0.8	—

NOTE: ALL DIMENSIONS IN MILLIMETERS

TABLE 9 TRACKING RECEIVE PATH

ELEMENT	FOCAL LENGTH/ RADIUS OF CURVATURE	DIAMETER	SPACING TO NEXT ELEMENTS/ENDPOINTS
(46) VARIABLE ATTENUATION FILTER	- / ∞	15.5	62.72/ (46) - (47)
(47) 532 NM BANDPASS FILTER	- / ∞	17.0	75.26/ (47) - (48)
(48) FOLD MIRROR	- / ∞	18.5	94.07/ (48) - (50)
(49) WEDGE	- / ∞	17.25	12.5/ (49) - (50)
(50) TRACKING DETECTOR LENS	181.82/ -	61.0	181.82/ (50) - (51) OR (52)
(51) OR (52) TRACKING DETECTOR	- / ∞	5.12x5.12	—

NOTE: ALL DIMENSIONS IN MILLIMETERS

NOTE: OFFSET BETWEEN EARTH TRACKING CHANNEL AND GREEN CHANNEL IS 35.7 MM ALSO CENTER LINE OF TRACKING DETECTOR LENS LIES MIDWAY BETWEEN ABOVE CHANNELS.

NOTE: SEPARATION 47 - 49 ≅ 15.7 MM

TABLE 10 OPTRANSPAC TRANSMISSION BUDGET

CONTRIBUTER	532 NM TRANSMIT	1064 NM RECEIVE	BROADBAND VISIBLE RECEIVE	532 NM OFFSET TRACK
• TELESCOPE TOTAL	0.93	9.93	0.82	-
• IMAGING OPTICS BREAKDOWN				
A. COMMON PATH	0.81	0.79	0.46	-
B. TRANSMIT PATH	0.97	-	-	0.97
C. COMMUNICATION RECEIVE	-	0.62	-	-
D. TRACKING RECEIVE	-	-	0.59	-
E. OFFSET TRACKING RECEIVE	-	-	-	0.0031
• IMAGING OPTICS TOTAL	0.79	0.49	0.27	0.0030
• TOTAL BOL TRANSMISSION (TELESCOPE & IMAGING OPTICS)	0.73	0.46	0.22	0.0030
• ESTIMATED TOTAL EOL TRANSMISSION (TELESCOPE & IMAGING OPTICS)	0.66	0.41	0.20	0.0029

TABLE 11 TELESCOPE MISALIGNMENT SENSITIVITIES

- PRIMARY MIRROR TILT SENSITIVITY = 0.64 λ RMS/MRAD λ = 532 NM
  (MOTION OF 0.078 MRAD WOULD TAKE ENTIRE 0.05 λ RMS BUDGET)

- SECONDARY MIRROR TILT SENSITIVITY = 0.13 λ RMS/MRAD λ = 532 NM
  (MOTION OF 0.38 MRAD WOULD TAKE ENTIRE 0.05 λ RMS BUDGET)

- PRIMARY/SECONDARY DECENTER SENSITIVITY = 1.32 λ RMS/MM λ = 532 NM
  (MOTION OF 38 μM WOULD TAKE ENTIRE 0.05 λ RMS BUDGET)

- PRIMARY/SECONDARY DESPACE SENSITIVITY = 17.1 λ RMS/MM λ = 532 NM
  (MOTION OF 3. μM WOULD TAKE ENTIRE 0.05 λ RMS BUDGET)

THIS PAGE INTENTIONALLY LEFT BLANK

APPENDIX D

INTERFACE DOCUMENT

OPTRANSPAC INTERFACE REQUIREMENTS

OPTRANSPAC STRUCTURE

- Defined in Figures 1 through 10

LOOK DIRECTION AND FIELD-OF-VIEW

- System pointed nominally towards earth ± 2 mrad
- Minimum unobstructed FOV: ± 2 mrad

MASS PROPERTIES

- Total weight less than 115 lbs. (see Figure 11)
- Center of Gravity defined in Figure 1
- Moving Parts
  - Torque Motor Beam Steerers (4)
    - Moment of Inertia: $\leq 5 \times 10^{-5}$ oz-in-sec^2
    - Maximum Angular Acceleration: $\leq 2 \times 10^5$ rad/sec^2
    - Control Loop Bandwidth: 20 Hz

INSTALLATION

- Mount: 3-point
- Mounting Surface Finish: see Figure 1
- Mounting Surface Flatness: see Figure 1

ALIGNMENT

- Installation Alignment: $\leq \pm$ 0.17 mrad
- Alignment Stability: $\leq \pm$ .60 µrad, variations assumed slow. Use of auto collimators to indicate drift errors. Biases removed by control system.

ELECTRICAL POWER INTERFACES

- For details not given here, see OPTRANSPAC Design Note, "OPTRANSPAC Electronics", by H. J. Mingo
- Bus Power: 28±6 volts direct current
- Total Power Requirement: 57 watts (see Figure 11)
- Telemetry - Analog, Serial, and Bi-level
- Command Control Data - Discrete and Serial
- Communication Data - $\leq$100 Kbps Pulse Position Modulation (PPM)

THERMAL CONTROL

- S/C Interface - Adiabatic
- Operating Temperatures

	Median Operating Temperature	Variation From Median
Electronics	$30^{o}C$	$\pm 40^{o}C$
Electro-optics	$20^{o}C$	$\pm 3^{o}C$

- Survival Temperatures (Non-operating)

	Survival Temperatures
Electronics	$35^{o} \pm 90^{o}C$
Electro-optics	$0^{o} \pm 35^{o}C$

- Heat Rejection

Subassembly	Power Dissipated (Watts)
Electro-optics	6.0
Detectors	5.0
Electronics	46.0

OPTRANSPAC
ISOMETRIC VIEW

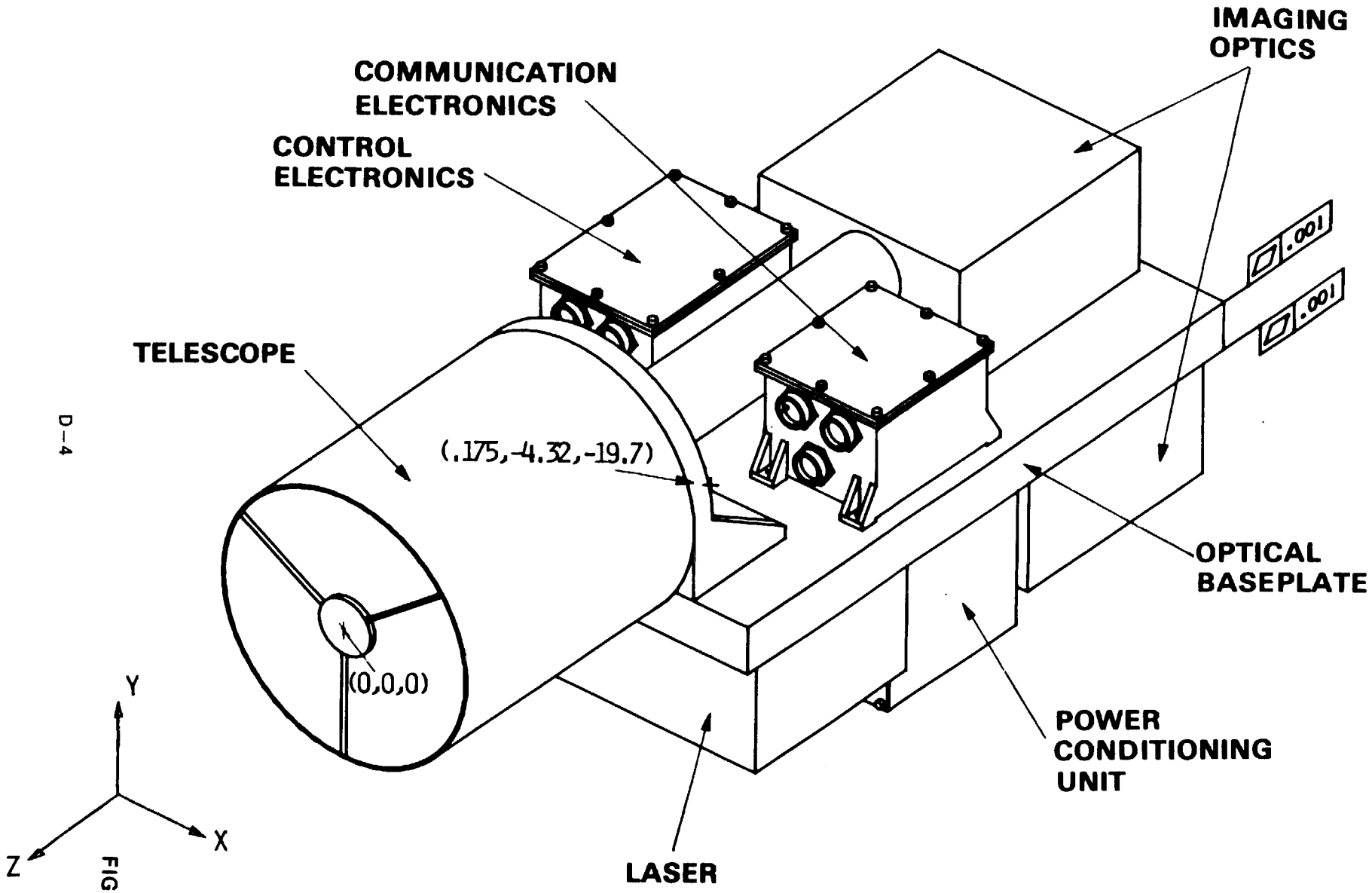

FIGURE 1

OPTRANSPAC
OPTICAL ISOMETRIC VIEW

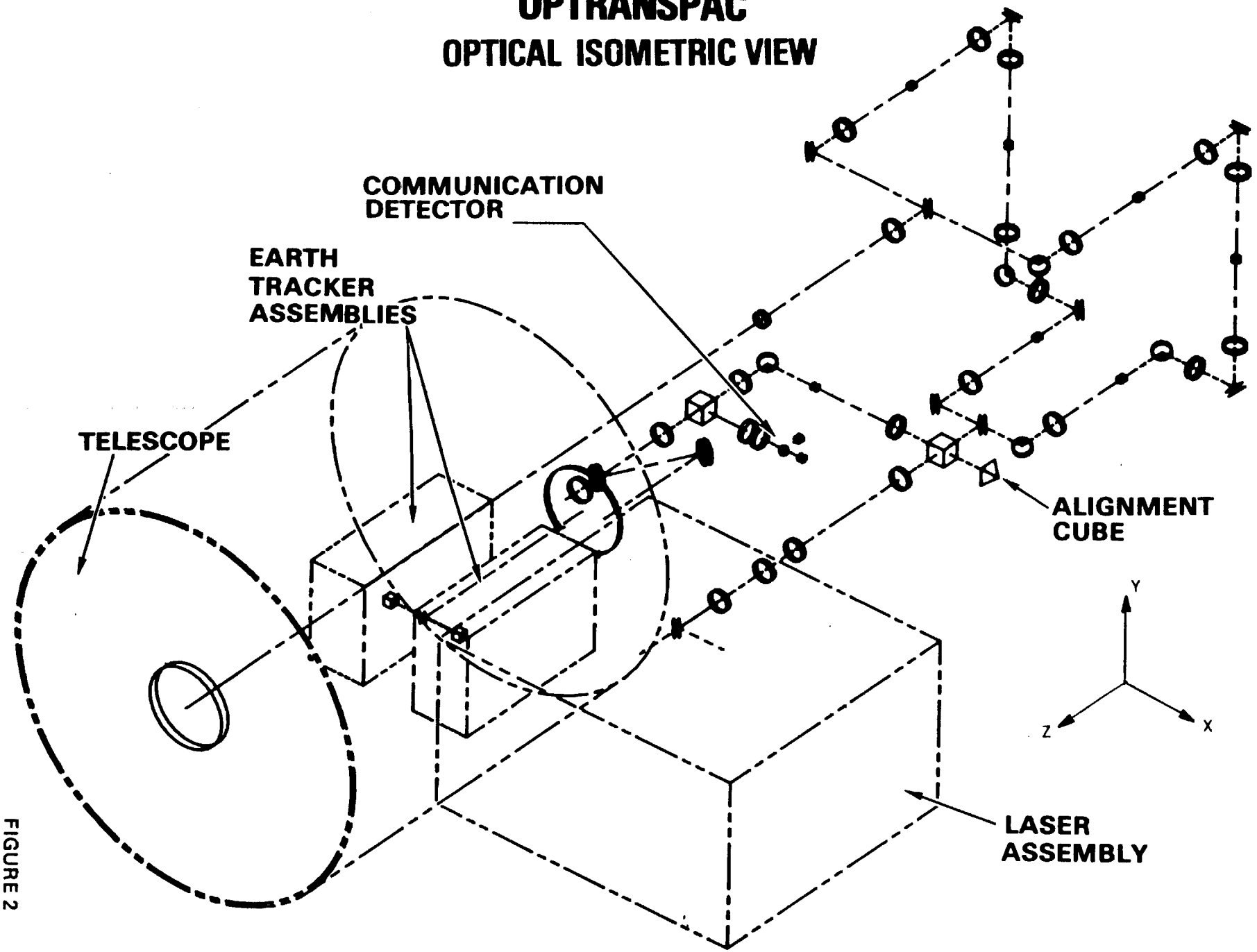

FIGURE 2

OPTRANSPAC
ORTHOGRAPHIC
SIDE VIEW

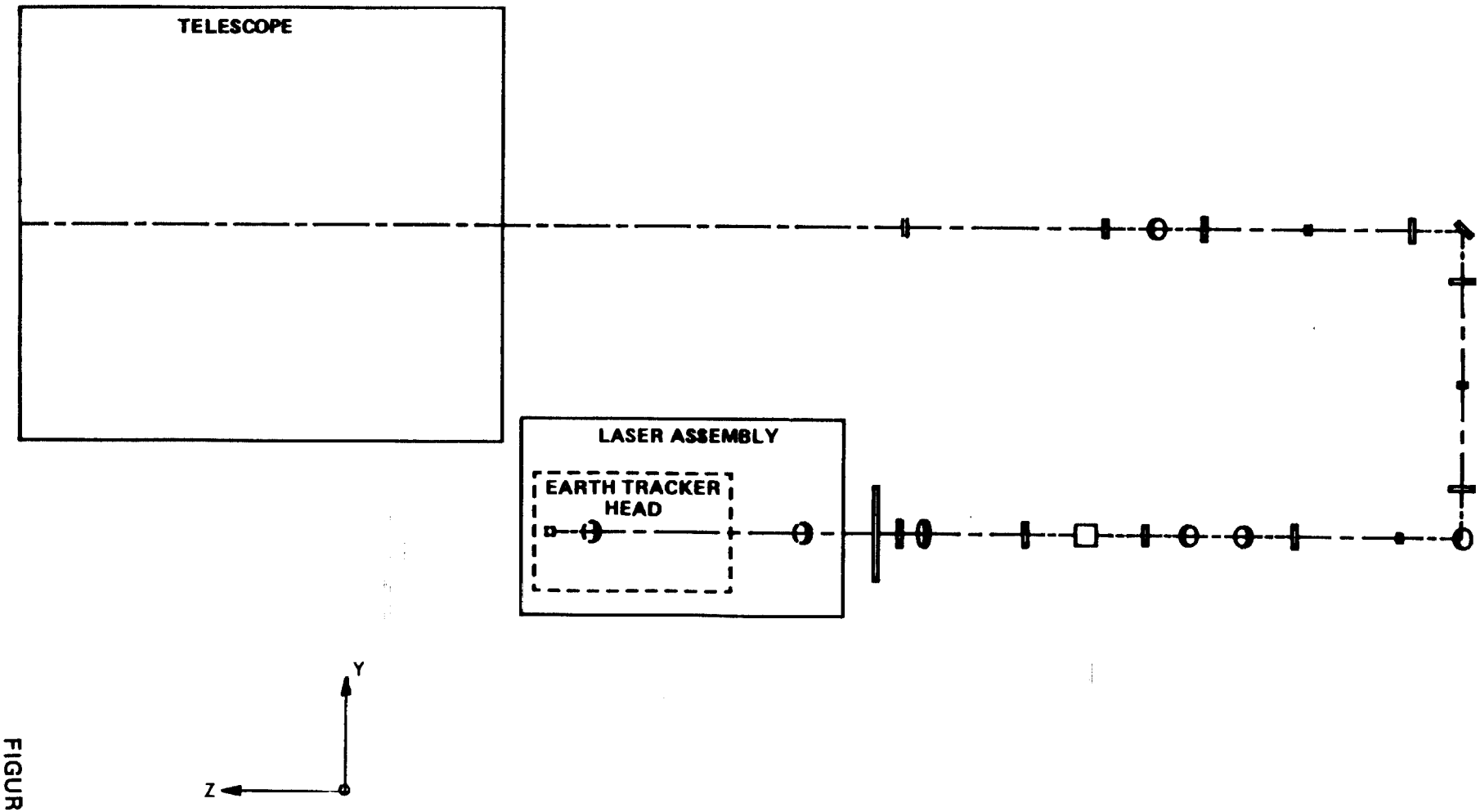

FIGURE 3

OPTRANSPAC
ORTHOGRAPHIC
TOP VIEW

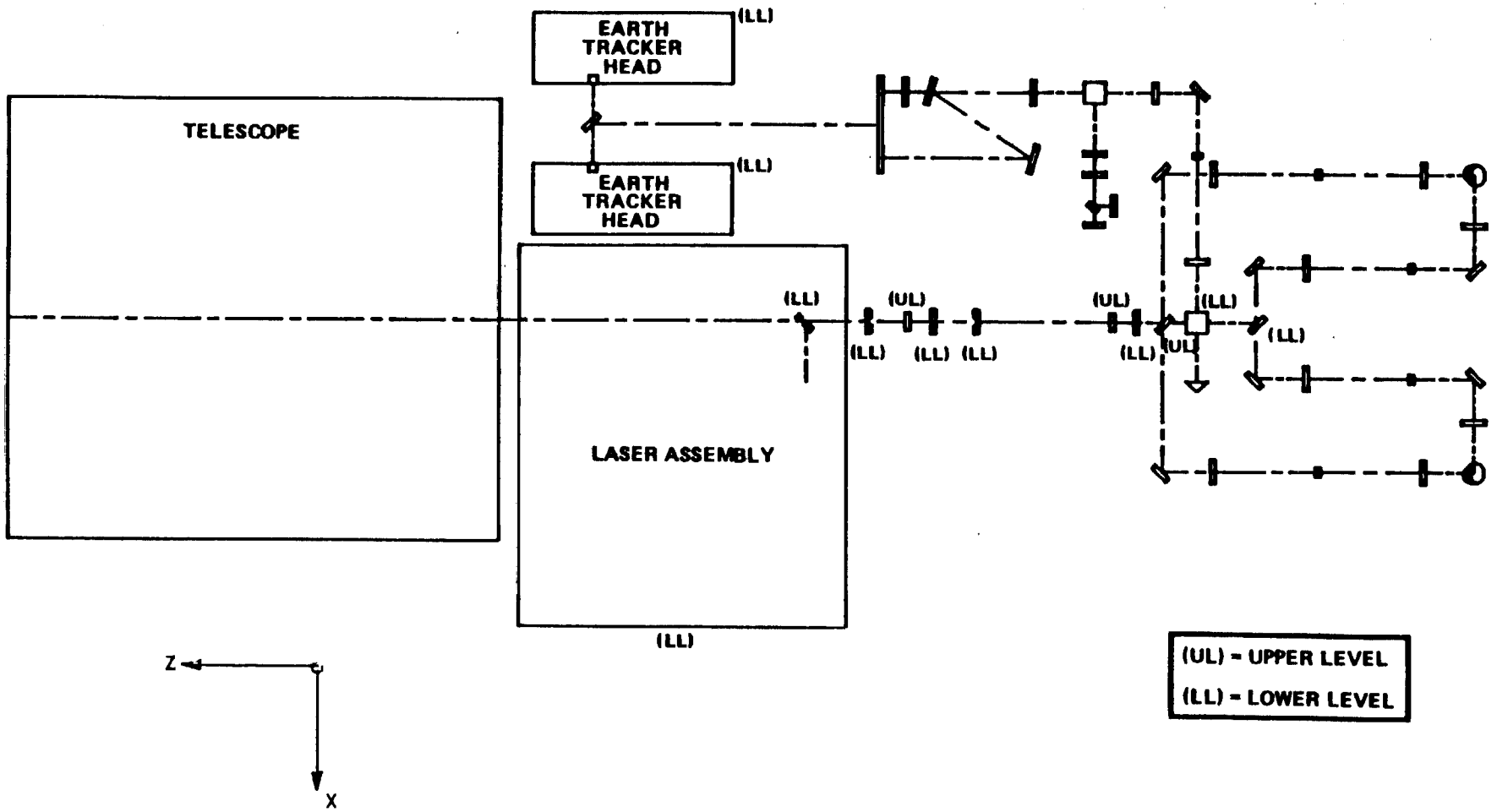

FIGURE 4

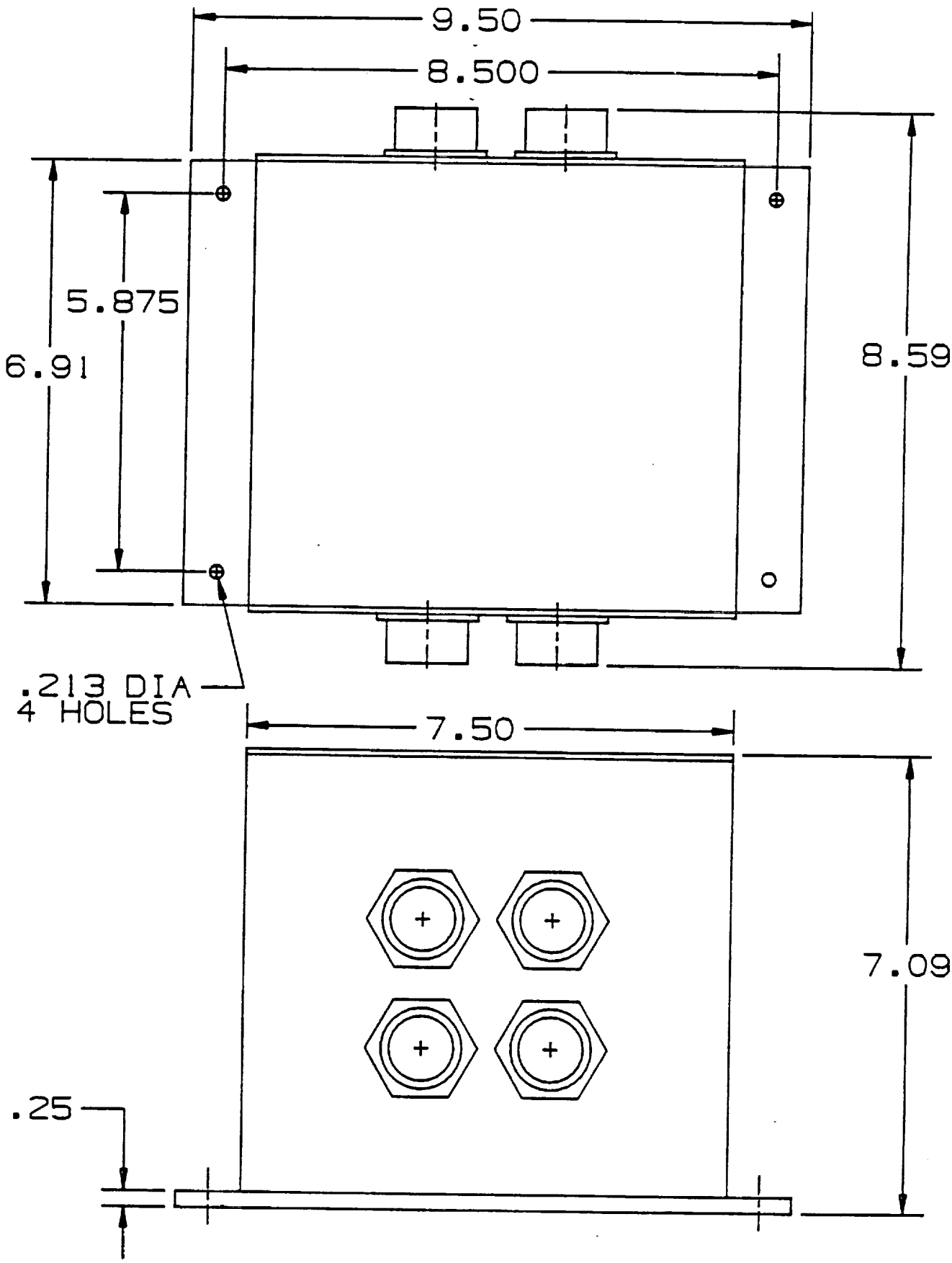

POWER CONDITIONING UNIT

FIGURE 5

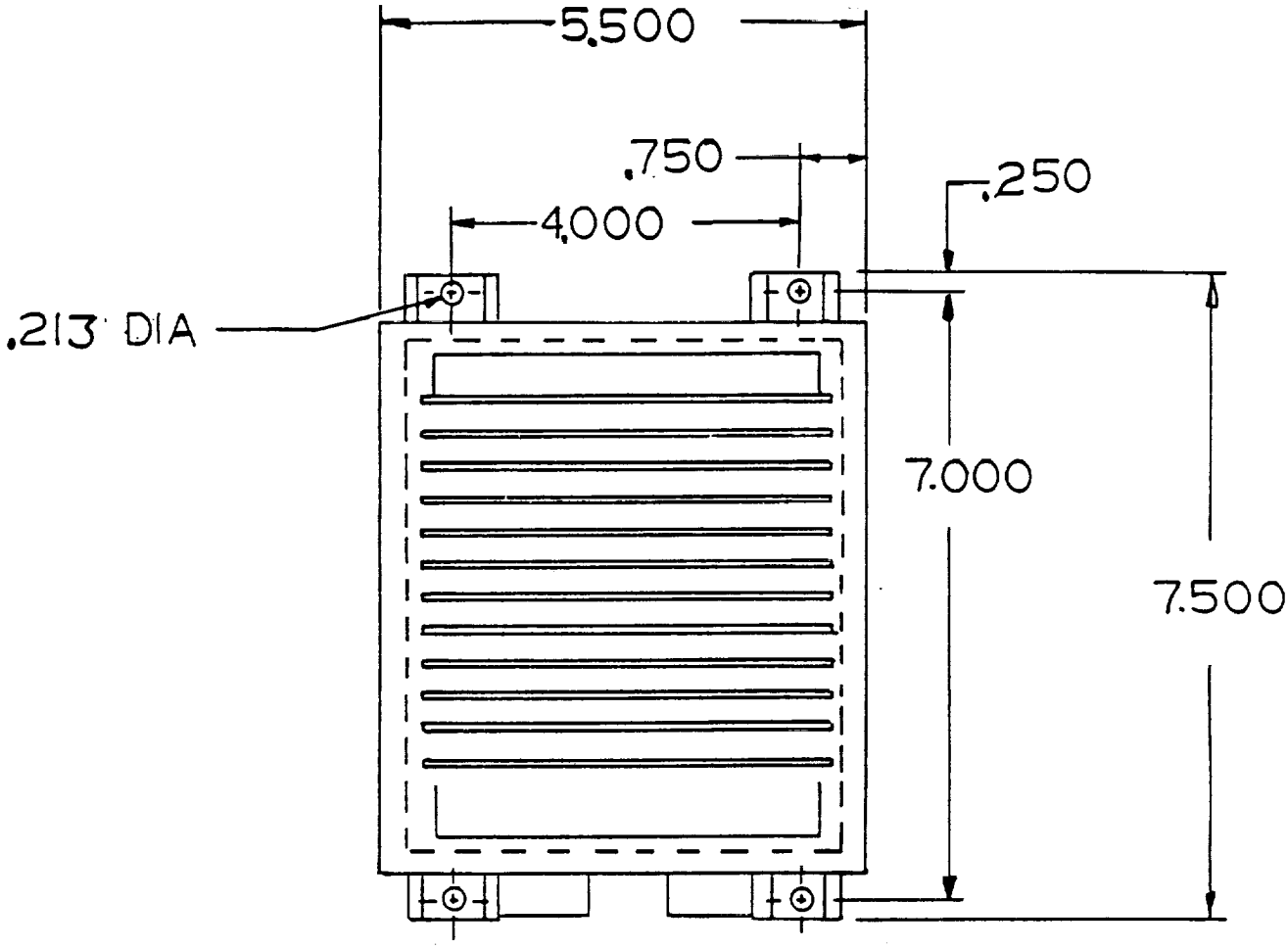

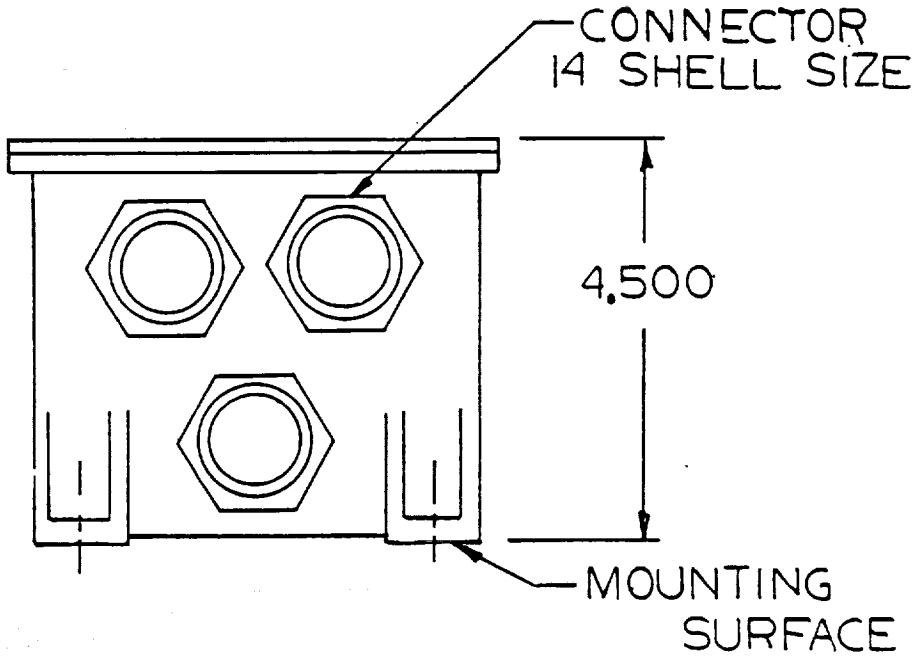

COMMUNICATIONS ELECTRONICS

FIGURE 6

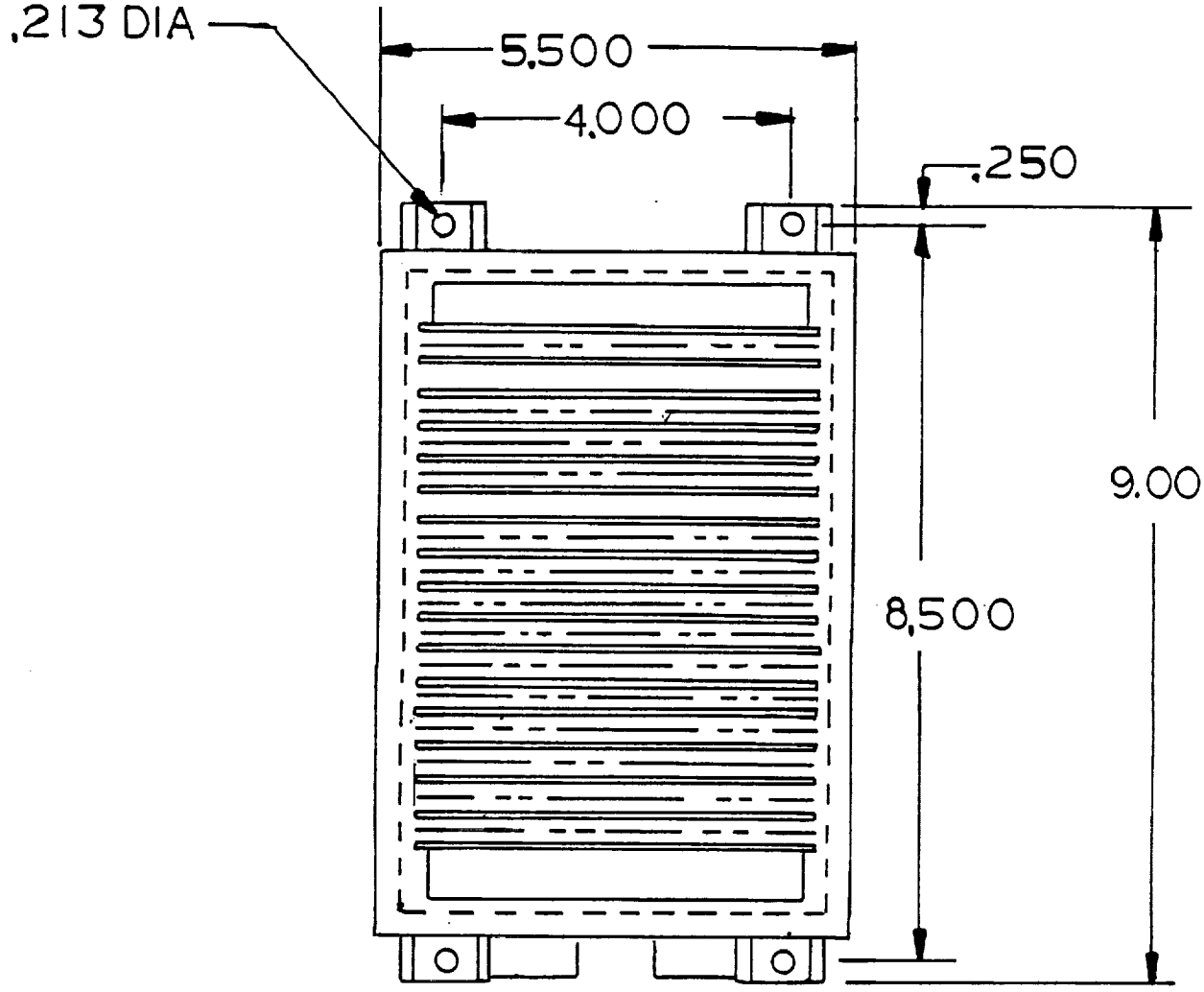

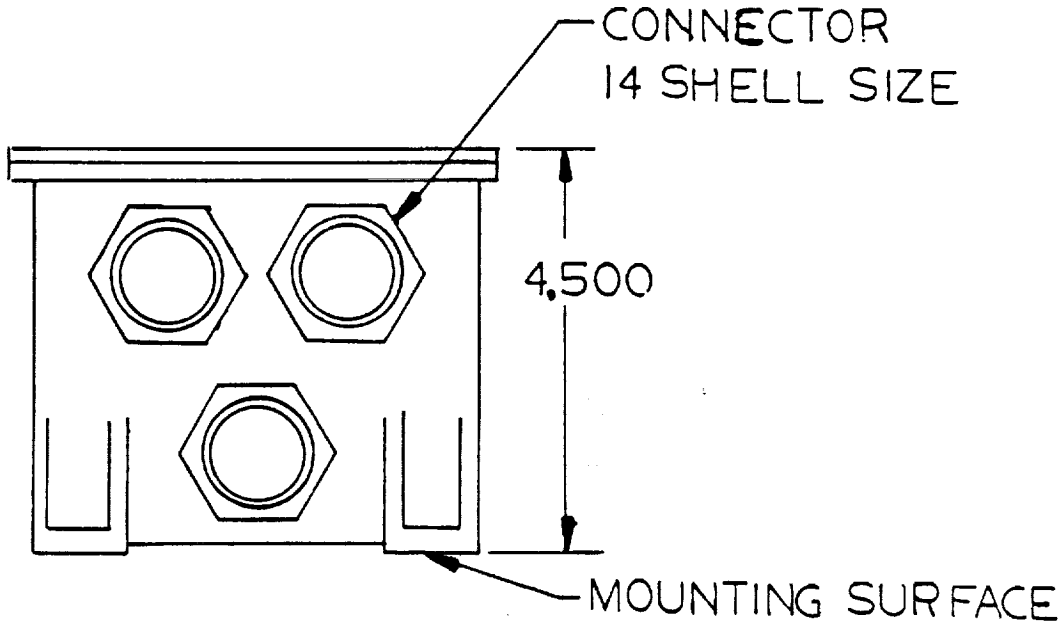

CONTROL ELECTRONICS

FIGURE 7

POWER CONDITIONING UNIT ISOMETRIC

FIGURE 8

FIGURE 9

COMMUNICATION ELECTRONICS ISOMETRIC

FIGURE 10

WEIGHT AND POWER SUMMARY

ITEM	WEIGHT (LBS.)	POWER (WATTS)
• ELECTRO-OPTICS ASSEMBLY	(57.0)	(11.0)
TELESCOPE (11 IN)	18.0	-
IMAGING OPTICS ASSEMBLY	13.5	2.0
LASER ASSEMBLY	20.0	4.0
DETECTOR ASSEMBLY	1.0	.4
EARTH TRACKER	4.5	4.6
• ELECTRONICS	(41.0)	(39.3)
COMMUNICATIONS ELECTRONICS	9.0	7.7
CONTROL ELECTRONICS	12.5	14.5
POWER CONDITIONER UNIT	19.5	17.1
• STRUCTURE/WIRE/MISC	(17.0)	(6.7)
TOTAL	115.0	57.0

FIGURE 11

 APPENDIX E

PATENT CONTRACT
(1) EXECUTED ___ DATE ___
EXCEPTIONS YES ___ NO ___
(2) EXECUTED ___ DATE ___
EXCEPTIONS YES ___ NO ___
(3) EXECUTED ___ DATE ___
EXCEPTIONS YES ___ NO ___

PRINT OR USE TYPEWRITER

MCDONNELL DOUGLAS CORPORATION

PATENT DEPT DOCKET NO

ASSIGNED TO:

EMPLOYE DISCLOSURE RECORD

(THIS FORM AND ACCOMPANYING DRAWING AND DESCRIPTION SHEETS (FORM MDC 136-2 (01 JUL 69) TO BE COMPLETED FOR EACH ITEM AND PROMPTLY FORWARDED TO THE PATENT DEPARTMENT)

SHORT TITLE OF ITEM (THREE WORDS OR LESS)

A CONTINUOUS LASERCOM OPTICAL ALIGNMENT DEVICE

FULL NAME(S) OF EMPLOYE(S) INVENTOR(S) (FIRST) (MIDDLE INITIAL) (LAST)	HOME ADDRESS(ES)	LOC/DEPT	CLOCK OR EMP NO	PHONE EXT
1) William L. Casey	Rt. 1, Box 124, Marthasville, MO 63357	101A/231 E413	064552	234-8445
2)				
3)				

INFORMATION AND DATES CONCERNING THIS ITEM

NEEDED IN THE EVENT OF A CONTEST OF PRIORITY OF INVENTION IN THE U.S. PATENT OFFICE. ALL RECORDS CITED SHOULD BE DATED AND SIGNED BY RESPONSIBLE EMPLOYE(S), AND DATED AND SIGNED BY TWO INDEPENDENT WITNESSES WHO HAVE READ AND UNDERSTAND THE MATERIAL.

ON WHAT DATE DID YOU FIRST THINK OF THIS INVENTION OR ITEM? (WHAT RECORDS SHOW THIS?
08 Feb 1985 - Monthly Status Report MDAC-STL to CIT/JPL OPTRANSPAC Study - Attachment (1)

GIVE DATE OF AND IDENTIFY EARLIEST SKETCH OR DRAWING
Illustrated in above Monthly Status Report

WHEN WHERE AND TO WHOM DID YOU MAKE THE FIRST DISCLOSURE TO OTHERS OF THE ITEM EITHER ORALLY OR IN WRITING?
In above Monthly Status Report

DESCRIBE DETAILS OF ANY WORK OR TESTS DONE TO PRODUCE OR OPERATE THE ITEM GIVE DATES AND WITNESSES (USE OTHER PAGES IF NECESSARY)
Filter technology/alignment of laser to receive path and use of galvanometer driven mirrors for alignment and point-ahead go back many years in Lasercom.

DESCRIBE AND GIVE DATES OF ANY OTHER SKETCHES, DRAWINGS OR REPORTS PERTINENT TO THIS ITEM
Only sketches in above Monthly Status Report

SALE OR PUBLICATION

NEEDED TO ESTABLISH THE DATE OF ANY PRINTED PUBLICATION, PUBLIC USE OR SALE, SINCE NO PATENT APPLICATION MAY BE FILED AFTER ONE YEAR FROM SUCH DATE

IF A DEVICE HAS BEEN SOLD OR USED FOR PROFIT, WHEN AND TO WHOM DELIVERED OR WHEN AND HOW USED?
Not yet sold or delivered

HAS A PRINTED DESCRIPTION OF THIS ITEM BEEN MADE AVAILABLE TO PERSONS OUTSIDE THE COMPANY? IF SO HOW AND WHEN AND WAS USE RESTRICTED?
Yes - To CIT/JPL in above referenced Monthly Status Report

POTENTIAL MARKET INFORMATION

NEEDED FOR POSSIBLE MARKETING INVESTIGATIONS AND AS AN AID TO POTENTIAL LICENSING TO OTHERS

DESCRIBE ANY POTENTIAL OR EXISTING MARKET FOR SALE OR LICENSE OF THIS ITEM:

A GOVERNMENT: In Lasercom systems for space/air

B COMMERCIAL: In Lasercom systems for space/air

C IDENTIFY ANY KNOWN FIRMS OR VENDORS WHO MAY BE INTERESTED IN THE ITEM

CONTRACT INFORMATION

NEEDED TO ASSESS THE PARTICULAR RIGHTS OF VARIOUS PARTIES IN THE INVENTION OR ITEM

IF THIS ITEM WAS FIRST CONCEIVED OR CONSTRUCTED IN CONNECTION WITH:

A. A GOVERNMENT CONTRACT GIVE GOVERNMENT CONTRACT NUMBER AND SHOP ORDER

B AN IRAD OR COMPANY PROJECT GIVE PROJECT IDENTIFICATION NUMBER

C NEITHER A NOR B, EXPLAIN CIT/JPL Contract No. 957601 for Design and Analysis Study of a Spacecraft Optical Transceiver package.

D ARE TIME RECORDS AVAILABLE TO VERIFY THE ABOVE STATED CONTRACT OR SHOP ORDER? Yes

I (WE) HEREBY ASSIGN MY (OUR) ENTIRE INTEREST IN THE ABOVE ENTITLED ITEM OR INVENTION, AS SHOWN AND DESCRIBED ON THE ACCOMPANYING SHEET(S), TO MCDONNELL DOUGLAS CORPORATION.

SIGNATURE(S) OF EMPLOYE(S) INVENTOR(S): (USE BLACK INK)

(1) William L. Casey (2) ___ (3) ___

DATE 19 July 1985 DATE ___ DATE ___

SOCIAL SECURITY NO 192-20-6621 SOCIAL SECURITY NO ___ SOCIAL SECURITY NO. ___

NOTE: ANY OMITTED INFORMATION BECOMING AVAILABLE AT A LATER TIME SHOULD THEN BE PROVIDED TO THE PATENT DEPARTMENT

PRINT OR USE TYPEWRITER

MCDONNELL DOUGLAS CORPORATION

PATENT DEPT DOCKET NO

EMPLOYE DISCLOSURE RECORD

(DRAWING AND DESCRIPTION SHEET)

PROVIDE THE FOLLOWING INFORMATION CONCERNING THE DISCLOSED ITEM AND IN THE INDICATED SEQUENCE:

1. DISCUSS THE PROBLEMS WHICH THE ITEM IS DESIGNED TO SOLVE, REFERRING TO ANY PRIOR DEVICES OF A SIMILAR NATURE WITH WHICH YOU MAY BE FAMILIAR.
2. STATE THE ADVANTAGES OF THE ITEM OVER PRESENTLY KNOWN DEVICES, SYSTEMS OR PROCESSES.
3. SPECIFICALLY DESCRIBE THE ITEM AND ITS OPERATION. YOU MAY USE AND ATTACH COPIES OF SKETCHES, PRINTS, PHOTOGRAPHS, AND ILLUSTRATIONS, WHICH SHOULD BE SIGNED, WITNESSED AND DATED. USE NUMBERS AND DESCRIPTIVE NAMES IN DESCRIPTIONS AND DRAWINGS.
4. LIST ALL KNOWN AND OTHER POSSIBLE USES FOR THE ITEM.
5. LIST THE FEATURES OF THE ITEM THAT ARE BELIEVED TO BE NOVEL.

USE AS MANY OF THESE SHEETS AS NECESSARY AND ATTACH TO COMPLETED FORM MDC 136-1 (01 JUL 69)

1. In Lasercom systems, the narrowness of the transmit laser beam requires that the laser needs to continuously be coaligned to the track detector in the presence of thermal/ structural bending. If continuous realignment is not performed, the transmit laser beam divergence must be increased to accommodate the maximum misalignment between the track detector boresight and the laser. If this is not done, the laser beam may be misdirected and the peak laser power will not impinge on the lasercom terminal to which the laser beam is directed. Conventional quadrant detectors are capable of only one track point so two beams cannot be tracked simultaneously. Option D of Attachment (1) illustrates the operation of conventional realignment techniques as follows; when not tracking another terminal, the shutter in front of the alignment cube is pulled out of the way and laser energy is then reflected from the beamsplitter to the cube and retroreflected back through the beamsplitter toward the tracker. The tracker, a quadrant detector receives the laser signal and supplies error signals to the align/point-ahead beam steering mirrors to null the track point. When it is necessary to provide a point-ahead function, the point-ahead beam steerers (TMBSs) are driven to the calculated position which offsets the laser beam to compensate for the velocity aberration of light. When the realignment is complete, the shutter is closed and the terminal may function as a transceiver. Another realignment cannot be performed until tracking is discontinued.

2. The proposed device offers the following advantages:
   a. Continuous alignment is possible even when the receive wavelength is very close (20 angstroms) to the transmit laser wavelength. If polarization isolation is used, continuous alignment should still be possible since polarization separation can be performed at the device instead of spectral separation.

SIGNATURE(S) OF EMPLOYE(S)/INVENTOR(S):	DATE:	WITNESSED, READ AND UNDERSTOOD BY:	DATE:
(1) William L. Casey	7/22/85	Stephen D. Lambert	7/22/85
(2)		Richard A. Kobylinski	7/22/85
(3)			7-22-85

(EACH SHEET MUST BE SIGNED, DATED AND WITNESSED. USE BLACK INK.)

MCDONNELL DOUGLAS CORPORATION

PATENT DEPT DOCKET NO

EMPLOYE DISCLOSURE RECORD

(DRAWING AND DESCRIPTION SHEET)

PROVIDE THE FOLLOWING INFORMATION CONCERNING THE DISCLOSED ITEM AND IN THE INDICATED SEQUENCE:

1. DISCUSS THE PROBLEMS WHICH THE ITEM IS DESIGNED TO SOLVE, REFERRING TO ANY PRIOR DEVICES OF A SIMILAR NATURE WITH WHICH YOU MAY BE FAMILIAR.
2. STATE THE ADVANTAGES OF THE ITEM OVER PRESENTLY KNOWN DEVICES, SYSTEMS OR PROCESSES.
3. SPECIFICALLY DESCRIBE THE ITEM AND ITS OPERATION. YOU MAY USE AND ATTACH COPIES OF SKETCHES, PRINTS, PHOTOGRAPHS, AND ILLUSTRATIONS, WHICH SHOULD BE SIGNED, WITNESSED AND DATED. USE NUMBERS AND DESCRIPTIVE NAMES IN DESCRIPTIONS AND DRAWINGS.
4. LIST ALL KNOWN AND OTHER POSSIBLE USES FOR THE ITEM.
5. LIST THE FEATURES OF THE ITEM THAT ARE BELIEVED TO BE NOVEL.

USE AS MANY OF THESE SHEETS AS NECESSARY AND ATTACH TO COMPLETED FORM MDC 136-1 (01 JUL 69)

b. An alignment shutter/drive is not required since continuous alignment is performed and the alignment cube may be continuously utilized.

c. Weight, size, power and complexity should be reduced.

d. Continuous alignment is possible when wide band sources are tracked since the laser wavelength is "sliced out" of the wide band with only minor transmission loss

e. Diffraction limited optical quality beams can be accommodated with only minor degradation.

3. The device works as follows, referring to Figure 1: Collimated energy of wavelengths λ_1 and λ_2 enter the device at point (A), pass through the block and reach the filter (B) where the two wavelengths are spectrally separated. Lambda 1 is transmitted through the filter (B) and λ_2 is reflected from the filter (B) toward the mirror (C). Mirror (C) reflects the λ_2 energy at an angle that is not parallel to the λ_1 optical axis. This angular offset permits λ_1 and λ_2 to be tracked at two separate points on the CCD detector (F). The amount of angular separation determines the physical track point offset x and is a function of system requirements. Lambda two energy, following reflection from mirror (C) exits the block at point (D). Both λ_1 and λ_2 pass through the lens (E) and are imaged onto the CCD track detector (F). With a polarization separation of orthogonal linear polarizations a polarization beam splitter cube or equivalent polarization element replaces the filter but the device functions the same as for spectral separation. The CCD tracker track points for the two signals can be extracted for alignment and/or point-ahead functions.

SIGNATURE(S) OF EMPLOYE(S)/INVENTOR(S):	DATE:	WITNESSED, READ AND UNDERSTOOD BY:	DATE:
(1) William L. Casey	7/22/85	Stephen D. Lambert	7/22/85
(2)		Richard A. Rykowski	7/22/85
(3)		R. Fox	7-22-85

(EACH SHEET MUST BE SIGNED, DATED AND WITNESSED. USE BLACK INK.)

PAGE ___ OF ___

PRINT OR USE TYPEWRITER

MCDONNELL DOUGLAS CORPORATION

PATENT DEPT DOCKET NO

EMPLOYE DISCLOSURE RECORD

(DRAWING AND DESCRIPTION SHEET)

PROVIDE THE FOLLOWING INFORMATION CONCERNING THE DISCLOSED ITEM AND IN THE INDICATED SEQUENCE:

1. DISCUSS THE PROBLEMS WHICH THE ITEM IS DESIGNED TO SOLVE, REFERRING TO ANY PRIOR DEVICES OF A SIMILAR NATURE WITH WHICH YOU MAY BE FAMILIAR.
2. STATE THE ADVANTAGES OF THE ITEM OVER PRESENTLY KNOWN DEVICES, SYSTEMS OR PROCESSES.
3. SPECIFICALLY DESCRIBE THE ITEM AND ITS OPERATION. YOU MAY USE AND ATTACH COPIES OF SKETCHES, PRINTS, PHOTOGRAPHS, AND ILLUSTRATIONS, WHICH SHOULD BE SIGNED, WITNESSED AND DATED. USE NUMBERS AND DESCRIPTIVE NAMES IN DESCRIPTIONS AND DRAWINGS.
4. LIST ALL KNOWN AND OTHER POSSIBLE USES FOR THE ITEM.
5. LIST THE FEATURES OF THE ITEM THAT ARE BELIEVED TO BE NOVEL.

USE AS MANY OF THESE SHEETS AS NECESSARY AND ATTACH TO COMPLETED FORM MDC 136-1 (01 JUL 69)

4. Known or possible uses for the device include:
   a. Continuous alignment of two narrow wavelength sources in a lasercom system.
   b. Continuous alignment of a wideband source with a narrow wavelength source embedded in it in a lasercom system.
   c. Continuous separation of more than two sources by cascading two or more devices and imaging onto a single CCD for a lasercom system.
   d. Continuous alignment for laser systems other than lasercom.
   e. Continuous alignment of polarization isolation lasercom systems by use of polarization separation in lieu of spectral separation.
   b. Separation/alignment continuously in a lasercom system or elsewhere when two sources are as close as 20 angstroms spectrally.

5. Features believed to be novel:
   a. Continuous alignment of a lasercom system.
   b. Close spectral separation (20 angstroms) alignment of a lasercom system.
   c. Continuous point-ahead function with closed loop correction. Implementation is normally open loop based on calculated values.
   d. Continuous alignment of a lasercom system using polarization isolation.
   e. Continuous alignment of a lasercom system where the transmitter wavelength is embedded in a broadband track signal such as an earth-tracker.
   f. Any of the above not in a lasercom system.

SIGNATURE(S) OF EMPLOYE(S)/INVENTOR(S):	DATE:	WITNESSED, READ AND UNDERSTOOD BY:	DATE:
(1) William L. Casey	7/22/85	Stephen D. Lambert	7/22/85
(2)		Richard A. Rhoylinski	7/22/85
(3)			7-22-85

(EACH SHEET MUST BE SIGNED, DATED AND WITNESSED. USE BLACK INK.)

PAGE ___ OF ___

MCDONNELL DOUGLAS CORPORATION

PRINT OR USE TYPEWRITER

PATENT DEPT DOCKET NO

EMPLOYE DISCLOSURE RECORD

(DRAWING AND DESCRIPTION SHEET)

PROVIDE THE FOLLOWING INFORMATION CONCERNING THE DISCLOSED ITEM AND IN THE INDICATED SEQUENCE:

1. DISCUSS THE PROBLEMS WHICH THE ITEM IS DESIGNED TO SOLVE, REFERRING TO ANY PRIOR DEVICES OF A SIMILAR NATURE WITH WHICH YOU MAY BE FAMILIAR.
2. STATE THE ADVANTAGES OF THE ITEM OVER PRESENTLY KNOWN DEVICES, SYSTEMS OR PROCESSES.
3. SPECIFICALLY DESCRIBE THE ITEM AND ITS OPERATION. YOU MAY USE AND ATTACH COPIES OF SKETCHES, PRINTS, PHOTOGRAPHS AND ILLUSTRATIONS, WHICH SHOULD BE SIGNED, WITNESSED AND DATED. USE NUMBERS AND DESCRIPTIVE NAMES IN DESCRIPTIONS AND DRAWINGS.
4. LIST ALL KNOWN AND OTHER POSSIBLE USES FOR THE ITEM.
5. LIST THE FEATURES OF THE ITEM THAT ARE BELIEVED TO BE NOVEL.

USE AS MANY OF THESE SHEETS AS NECESSARY AND ATTACH TO COMPLETED FORM MDC 136-1 (01 JUL 69)

FIGURE 1

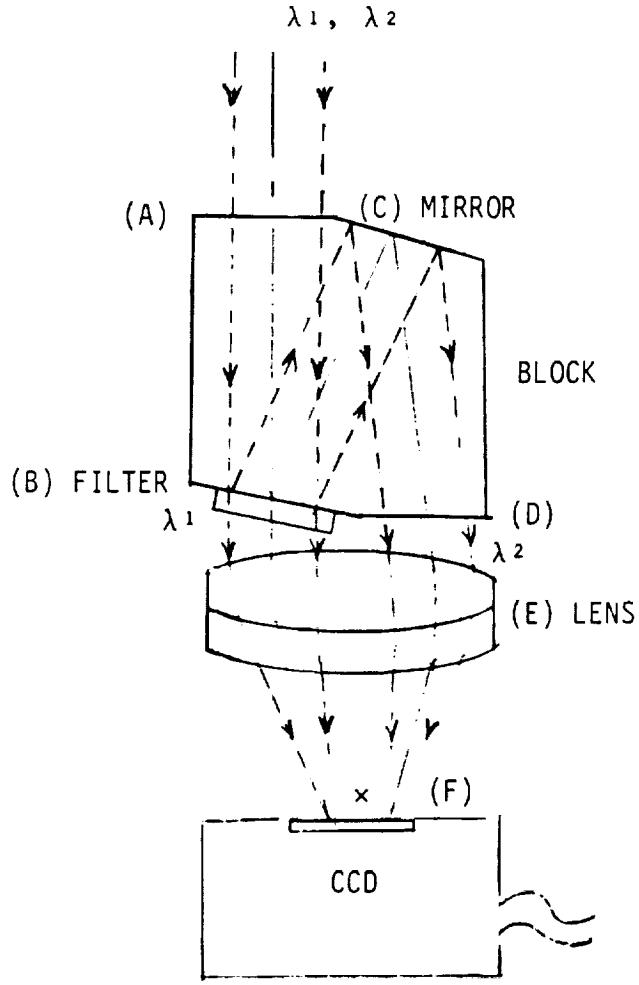

SIGNATURE(S) OF EMPLOYE(S)/INVENTOR(S):	DATE:	WITNESSED, READ AND UNDERSTOOD BY:	DATE:
(1) William L. Casey	7/22/85	Stephen D. Lambert	7/22/85
(2)		Richard A. Kolodziej	7/22/85
(3)		Russ Lowe	7-22-85

(EACH SHEET MUST BE SIGNED, DATED AND WITNESSED. USE BLACK INK.)

PAGE ___ OF ___

THIS PAGE LEFT INTENTIONALLY BLANK

APPENDIX F
ACRONYM LIST

Al	Aluminum
APD	Avalanche Photodiode
AU	Astronomical Unit
BER	Bit Error Rate
CCD	Charge Coupled Device
CID	Charge Injection Device
cm	centimeter
dB	decibel
EORS	Earth Orbiting Relay Station
FWHM	Full Width Half Maximum
Hz	Hertz
IOA	Imaging Optics Assembly
JPL	Jet Propulsion Laboratory
KBPS	Kilobits per second
Kg	Kilograms
Km	Kilometers
KPPS	Kilopulses per second
KRADS	Kilorads
LSI	Large Scale Integrated
MeV	Mega Electron Volt
MHz	Megahertz
mm	millimeters
msec	millisecond
µsec	microsecond
mW	milliwatts
NASA	National Aeronautics and Space Administration
NASA-JSC	NASA Johnson Space Center
Nd:YAG	Neodymium Yttrium Aluminum Garnet

APPENDIX F
ACRONYM LIST

nm	nanometer
NRZ	Non-Return to Zero
OPTRANSPAC	Optical Transceiver Package
PCU	Power Conditioning Unit
PMT	Photomultiplier Tube
PPM	Pulse Position Modulation
PPS	Pulse Per Second
RMS	Root Mean Squared
RS	Reed-Solomon
RSS	Root Sum Squared
sec	second
Si	Silicon
SNR	Signal To Noise Ratio
TMBS	Torque Motor Beam Steerer
VLSI	Very Large Scale Integrated

REFERENCES

1. "Orbital Measurements Of The Earth's Radiation Budget During The First Decade Of The Space Program", William R. Bandeen, Earth Radiation Science Seminars, NASA Conference Publication 2239, June 1980 to October 1981.

2. "Lasercom Background Noise Sources", Informal Memo, S. D. Simmons, McDonnell Douglas Astronautics Company - St. Louis Division, 3 Nov 1982.

3. "PPM Demodulation For Reed-Solomon Decoding For The Optical Space Channel", D. Divsalar, R. M. Gagliardi, And J. H. Yuen, TDA Progress Report 42-70, May - June 1982.

4. "Spacecraft Attitude and Articulation Control Systems for Future Planetary Missions," L. F. McGlinchey (JPL) and R. E. Rose (TRW), AIAA, 79-1717.

5. "Space Optical Communication With The Nd:YAG Laser", M. Ross, etal, Proceedings of the IEEE, Vol. 66, No. 3 March 1978.

6. "An Advanced Tracker Design For Pointing And Control Of Space Vehicles Using The Charge Injection Device", C. Jones, J. Kollodge, Annual Rocky Mountain Guidance and Control Conference, January 30 - February 3, 1982.

THIS PAGE LEFT INTENTIONALLY BLANK